

*Design of a component that learns dynamic driving behavior
and vehicle characteristics, in known situations, for a later
fuel consumption prediction on roads that have not been
driven before*

Dissertation

der Mathematisch-Naturwissenschaftlichen Fakultät
der Eberhard Karls Universität Tübingen
zur Erlangung des Grades eines
Doktors der Naturwissenschaften
(Dr. rer. nat.)

vorgelegt von
Adrien H. J. Marquette
aus Meaux (Frankreich)

Tübingen
2013

Tag der mündlichen Qualifikation:

30.05.2014

Dekan:

Prof. Dr. Wolfgang Rosenstiel

1. Berichterstatter:

Prof. Dr. Wolfgang Rosenstiel

2. Berichterstatter:

Prof. Dr. Thomas Kropf

Acknowledgements

This work was conducted within the Core function development team of the Robert Bosch Car Multimedia GmbH in Hildesheim, and was advised by Prof. Dr. Rosenstiel, Dean of the Faculty of Science at the University of Tübingen (Germany).

First of all, I want to deeply thank Prof. Dr. Rosenstiel for his supervision, patience and confidence in me all along my university career.

I would also like to thank Prof. Dr. Kropf (Senior Vice President of the Bosch Car Multimedia GmbH and Professor for Computer Science at the University of Tübingen) for his willingness to supervise this thesis as second reviewer. I'm very grateful.

I thank all my colleagues of CM-AI/PJ-CF for valuable comments on my work and for supporting me. A special thank to Guido Müller and to Dr. Andreas Engelsberg for being my tutors within the company, to Ulrich Kersken for initializing my PhD project, and Dr. Werner Poehmueller, Bjoern Hornburg, and Guido Stuebner for the interesting discussions and their support.

To Christian Ruzicka and Christian Stresing for the exciting discussions about technologies. Another special thank to Dr. Alexander Weber for his support and recommendations during my last year in Hildesheim, to Andreas Vogel for the mathematical background explanation and his kindness, and finally to Ralph Behrens for being such a pleasant boss during my time in Hildesheim.

Most of all, I would like to thank my family, and especially my wife Johanna and my grandparents, who continuously supported me during the years of hard work and who pushed me towards the end of this thesis.

"A thought is like a thing. Everything you have and do began with a thought."
Graeme "The Flying Scotsman" Obree

"The more we study the major problems of our time, the more we come to realise that they cannot be understood in isolation. They are systemic problems, which means that they are interconnected and interdependent."
Fritjof Capra

Table of contents

Table of contents	9
List of Abbreviations.....	12
1 Introduction	13
1.1 Motivation	13
1.2 State of the Art	14
1.2.1 EcoRouting and EcoRoute	14
1.2.2 Fuel Consumption Prediction Today.....	16
2 Goals and Challenges of this Work	18
3 Theory and Background.....	22
3.1 Vehicle Influences on the Fuel Consumption	22
3.1.1 The Internal Combustion Engine (ICE)	23
3.1.2 Generator	24
3.1.3 The Transmission	25
3.2 Forces that Affect the Moving Vehicle.....	25
3.2.1 Non-conservative Forces.....	26
3.2.1.1 Air Resistance	26
3.2.1.2 Wheel Resistance	28
3.2.2 Conservative Forces	33
3.2.2.1 Grade Resistance	33
3.2.2.2 Acceleration, Deceleration and the Force of Inertia	33
3.3 Driver Impact on Fuel Consumption	34
3.3.1 Fuel Consumption Variations Related to the Driving Style.....	36
3.3.2 Driving Behavior: Impact of the Use of Auxiliary Consumers	38
3.4 Existing Models for Driving Style Explanation.....	39
3.5 Situation-dependent Driving Style	41
3.5.1 Acceleration	42
3.5.2 Braking Maneuvers	42
3.5.3 Chosen Speed of Travel	42
3.5.4 Gear Selection	44
3.5.5 Other External Influences on the Driving Style.....	44
3.6 Parameters Classification According to their Impact on the Fuel Consumption and their Potential Variation	47
4 Available Information for Understanding the Interactions Between Vehicle, Driver and Surroundings.....	50

4.1	Information Available from Satellites.....	50
4.2	Sensor Network Integrated to the Vehicle	52
4.3	Telematics.....	53
4.4	Navigation Database.....	53
4.5	Proposed Solution.....	54
5	Concept and Realization.....	56
5.1	Concept Presentation and Use Cases	56
5.1.1	Use Case: Route Calculation.....	56
5.1.2	Use Case: Vehicle is Moving Without a Calculated Route	57
5.1.3	Use Case: Vehicle is Moving With a Calculated Route.....	58
5.1.4	Simulation and Learning Component	58
5.2	Realization of the Vehicle Specific Concept Part.....	58
5.2.1	The Engine Map.....	58
5.2.1.1	Relevant Input:.....	59
5.2.1.2	Filling Strategy.....	59
5.2.1.3	Use Strategy	63
5.2.1.4	Exception: Cold Start	65
5.2.2	Transmission Ratio.....	66
5.2.2.1	Relevant Input:.....	66
5.2.2.2	Filling Strategy.....	67
5.2.2.3	Use Strategy	69
5.2.3	Remaining Vehicle Characteristics	69
5.2.3.1	Calculating the Torque	69
5.2.3.2	Vehicle Characteristics Needed to Compute the Torque	70
5.2.3.3	How the Vehicle Characteristics are Learned	71
5.3.1	Relation between Surrounding Characteristics and the Driving Style.....	75
5.3.1.1	Available Surrounding Influences Description.....	75
5.3.1.2	Splitting a Route into Situations.....	76
5.3.1.3	Splitting a Route into Phases.....	78
5.3.2	Driving Style Mapping.....	78
5.3.2.1	Differentiating a Stabilization Phase from a Transition Phase	79
5.3.2.2	Mapped Driving Style	81
5.3.3	Generating a Driving Style for a Given Route.....	84
5.4.1	Summing Up the Fuel Prediction:.....	86
5.4.2	Adaptation to Electric Vehicles (EV):	87
5.4.3	Summing Up the Prototypical Learning:	88
6	Results and Analysis	89
6.1	Results – Vehicle Part	90
6.1.1	Results – Engine Map	90
6.1.1.1	Engine Map Input Data Filter.....	90
6.1.1.2	Engine Map Resolution and Quality After X Kilometers	90
6.1.1.3	Lambda Sensor and the Engine Control Unit (ECU).....	95
6.1.2	Results – Simulation.....	96

6.1.2.1	First Simulation Test	98
6.1.2.2	Second Simulation Test.....	98
6.1.2.3	Third Simulation Test.....	99
6.1.3	Results of the Vehicle Parameters Estimation	100
6.1.3.1	Transmission Filter Results	100
6.1.3.2	Transmission Ratio.....	101
6.1.3.3	Torque Calculation.....	103
6.1.3.4	Remaining Vehicle Characteristics	104
6.1.4	Prototype Quality Approximation: The Vehicle Part.....	115
6.1.5	Fuel Consumption Curves	117
6.2	Results – Driver Part	119
6.2.1	Track Preparation	119
6.2.1.1	First Step: Track Extraction out of the Navigation System Map Database	119
6.2.1.2	Second Step: Database Logs Correction	119
6.2.1.3	Third Step: Test Track Splitting into Situations and Phases	120
6.2.1.4	Fourth Step: Chronological Attribute Variation Representation for Input into Simulation	121
6.2.2	Driving Style Learning Results	122
6.2.3	Driving Style Prediction.....	122
6.2.4	Prototype Quality Approximation: Adding the Driving Style	123
6.2.4.1	Prototype Quality Testing Strategy and Hi01 Test Track Splitting into Two Halves	123
6.2.4.2	Presentation and Analysis of the Prototype Fuel Consumption Prediction Results:	124
6.3	Results Comparison with the State of the Art	127
6.3.1	Comparison with Mean Consumption (Onboard Cluster)	128
6.3.2	Comparison with today’s EcoRoute.....	128
6.3.3	Comparison with Online Fuel Consumption Estimation	129
7	Summary and Conclusion	131
	References	137
	ANNEX A: The Stuttgart Bosch-FKFS Dataset	151
	ANNEX B: The Hildesheim ‘Original’ Dataset.....	156
	ANNEX C: The Hildesheim ‘Mass & Air’ Dataset.....	159
	ANNEX D: The Hildesheim ‘Double Loop’ Dataset.....	163
	ANNEX E: Analysis of the Driving Style and the Database Characteristics that Influences the Fuel Consumption	166
	ANNEX F: Vehicle Database Used to Compute the Forces that Influence a Moving Vehicle Depending on the Speed of Travel	174

List of Abbreviations

ACC	<i>Autonomous Cruise Control</i>
ADAS	<i>Advanced Driver Assistance Systems</i>
AT	<i>Automatic Transmission</i>
BMEP	<i>Brake Mean Effective Pressure</i>
CAN	<i>Controller Area Network</i>
CFD	<i>Computational Fluid Dynamics</i>
CPU	<i>Central Processing Unit</i>
CVT	<i>Continuously Variable Transmission</i>
DCT	<i>Dual Clutch Transmission</i>
DSG	<i>Direct Shift Gearbox</i>
ECU	<i>Engine Control Unit</i>
ESP	<i>Electronic Stability Programme</i>
EV	<i>Electric Vehicle</i>
FTP	<i>Federal Test Procedure</i>
FWD	<i>Front Wheel Drive</i>
GPS	<i>Global Positioning System</i>
HEV	<i>Hybrid Electric Vehicle</i>
ICE	<i>Internal Combustion Engine</i>
MOST	<i>Media Oriented Systems Transport</i>
NDS	<i>Navigation Data Standard</i>
NHTSA	<i>National Highway Traffic Safety Administration</i>
NEDC	<i>New European Driving Cycle</i>
OBD	<i>On-Board Diagnostics</i>
RPM	<i>Revolutions Per Minute</i>
RWD	<i>Rear Wheel Drive</i>
SRTM	<i>Shuttle Radar Topography Mission</i>
TMC	<i>Traffic Message Channel</i>
TPMS	<i>Tire Pressure Monitoring System</i>
TPS	<i>Throttle Position Sensor</i>
WGS84	<i>World Geodetic System 1984</i>

1 Introduction

In the last three decades, discussions about the role of carbon dioxide in global warming became more frequent. While the influence of the CO₂ level on the observed weather and natural changes are still being discussed, it is undeniable that the CO₂ production increased with the worldwide industrialization that is occurring. In an attempt to regulate the worldwide pollution and to motivate industries to invest into cleaner technologies, some of the world-leading countries agreed, in the 1997 Kyoto Protocol, to cut down 5.2% on carbon dioxide production between 2008 and 2012 (compared to the level of 1990).

The amount of CO₂ produced can be approximated mathematically but hardly measured accurately. Furthermore, the production level associated to specific areas or industries varies from country to country and over the years. It is assumed that in 2010, in Germany, transport was responsible for 20% of the global CO₂ production, passenger cars being responsible for half of it [DATG11]. On this account, and beside other proposals, the European commission submitted a proposal for a regulation reducing the emissions of passenger cars to 120g CO₂/km [KeuG07], which initiated an ecologically innovative thrust. Engine downsizing, hybrid and electrical powertrains, or start-stop systems, are some of the well-known resulting examples, but there have been more than that.

1.1 Motivation

Considering that personal vehicles consumed a total of 45401 Million liters of fuel on German roads in 2008 [BuVe10], even a small percentage of improvement for each vehicle is important. When it comes to the CO₂ produced by a vehicle, the emitted gas is directly linked to the consumed fuel, which can be reduced by building more efficient cars, but that is not the only way. Based on the work of Durth [Durt74] and Donges [Dong78], driving can be described as a three-component model composed of a driver, a vehicle, and the dual-system interacting with the world surrounding it. Therefore, beside the vehicle itself, the driver and the surroundings are also influencing the fuel consumption, and indirectly the CO₂ production. Based on this, EcoDriving and EcoRouting were born.

While EcoDriving functionalities concentrate on the driver, analyzing his behavior and/or providing him feedback about his driving skills related to fuel consumption, EcoRouting concentrates on the surroundings.

EcoRouting have become a common alternative to fast and short route in modern high-end navigation systems. While the short route and the fast route propose the shortest and the fastest path (based on the projected speed of travel) in the road network graph that makes up the navigation system database, the EcoRoute, on the other hand, concentrates on fuel or energy consumption. The objective is to find the most economical path between a start and a destination, and therefore indirectly reduce the CO₂ production related to the travel.

The impact such a technology can have on the fuel consumption is variable and depends on the surroundings themselves. High variable parameters such as traffic have to potential to contrast the difference between ecological and the short or fast path. Also, the road network itself doesn't always offer alternative routes, so that it is sometimes possible to have a route which is the fastest, the shortest and the most economical at the same time. Nevertheless, during the development of the EcoRoute, the Robert Bosch Car Multimedia GmbH measured an average 9% less fuel consumption while driving the EcoRoute, compared to the fast route [Bosch10]. A study conducted in Lund (Sweden) for 100 test routes, and taking live traffic information into account, measured a 4% fuel consumption improvement [ErBr06]. These results, which may be enhanced with the prognosticated increase of the traffic, show how relevant and effective EcoRouting is when it comes to reducing CO₂ emissions.

Increasing vehicle sensors and computing power in the navigation systems have created a new basis for new generation *Advanced Driver Assistance Systems* (ADAS) capable of

understanding part of the driver-vehicle-surrounding interactions, and provide a better support. EcoRoute is one of them.

The last ten years witnessed the emergence of *Hybrid Electric Vehicle* (HEV), one of the first important sale volumes, and probably the most famous is the Toyota Prius. In the last few years, there's also been more and more *Electric Vehicle* (EV) available for sale. Beside the upper class vehicles build by Tesla Motors, which have proven that the technology is mature enough to sustain the company, compact cars like the Nissan Leaf (2010), the Chevrolet Volt (2010)¹ and the Opel Ampera (2011) have found their ways to international roads. However, the electric technology isn't clean enough to renounce EcoRouting. Spicher points out in [Spic12] that the use of personal vehicles produced 105 million tons of CO₂ in 2010, and the production of electricity 320 million tons of CO₂ during the same year. The whole electrical energy produced was 600 TWh, which is a 530 g CO₂/kWh. This value takes into account the German energy mix made of 40% emission-free (so-called "green" energies, atom energy) and 60% fossil fuels (coal, kale, gas). Considering the personal vehicle CO₂ production in relation to the yearly driving distance of circa 600 milliard km and the reference vehicles (8,5 l/100 km gasoline, 6,2 l/100 km diesel – with a 70:30 distribution) fuel consumption, then, the CO₂ emissions are found out to be 323 g CO₂/kWh in average. Even if EV might not be as green as they are often supposed to be, this calculation is only valid for the actual share of green energies in the energy production. Vehicles using alternative powertrains should become the standard in the near future. Therefore, during the concept phase, the compatibility to hybrid and electric vehicle became an important topic, and with it, the possibility to use the prototype described in this work for an electric vehicle range prediction.

1.2 State of the Art

Information about EcoRoute and fuel consumption prediction that are state of the art have been collected during the preparation of this work and are presented in this sub chapter. Despite the attempt to provide a full state of the art overview, algorithms describing the EcoRoute and fuel consumption prediction functionalities are rarely described. Therefore, the presentation here will be reduced to a few well-described examples that illustrate the common solutions available.

1.2.1 EcoRouting and EcoRoute

EcoRouting is the functionality that finds the EcoRoute: the most fuel-efficient path between the start and destination. The road network is mapped in the navigation system database as a graph of links and nodes. The shortest, fastest and most efficient path can be found using the A* ("A Star") algorithm, an extension of Edsger Dijkstra's 1959 algorithm. In the case of EcoRouting, the links and nodes are weighted with the expected amount of fuel needed.

Although they are good enough to find an economical alternative path, EcoRoute functionalities rarely display their fuel consumption prediction. For example, Kang and Associates describe the results of a link-based model without absolute fuel consumption prediction [KaMa11]. The main problem is that the fuel consumption linked to a route is subject to variations that cannot be saved in a simple form.

Bosch used a slightly different approach [Bosch10]. In the case of longer travel distance, a driver might not be willing to accept reduced fuel consumption at the cost of a considerable travel time increases. Therefore, the first generation EcoRoute was implemented as a

¹ Chevrolet Volt and Opel Ampera are considered electric vehicles although they have a range extender combustion engine that can charge the battery, but also can be switched directly to the transmission.

statistical mix of short and fast route. The second, and actual, generation is much more complex and based on a functional road class analysis. It considers the number of road crossings and the cities that are being driven through. In a second step, typical vehicle consumption for given speed and acceleration are used to compute a fuel consumption for the possible routes and find the optimal path using all that data.

Navteq (part of the Nokia group), one of the leading navigation map database provider worldwide, defines EcoRouting as follows [NavGreen10]:

“Eco-routing calculates routes that incorporate multiple factors, including start-and-stop sequences, acceleration and deceleration, and hills which impact fuel efficiency. Digital maps and traffic information enable routing applications to calculate paths, which minimize these factors by identifying the locations of specific road conditions in order to:

- *Avoid changes in speed along routes, including speed limits and upcoming dangerous situations, e.g. railway crossings*
- *Avoid start-and-stop situations such as traffic lights and stop signs*
- *Avoid sharp curves and steep hills*
- *Avoid roads with known traffic congestion”*

Again, the EcoRoute functionality is limited to the search of an optimal path between two points, considering database attributes that generally have an influence on the fuel consumption, but without making any fuel consumption prediction.

Garmin, one of the leading GPS handheld unit producers, introduced in 2010 a new device called Nüvi 3790T with EcoRouteHD functionality. The GPS handheld units and mobile phones are limited to the information they obtain from the navigation database, and, in the best case, the few signals transmitted over an OBD2 (*On-Board Diagnostics*) connector. During a review, the Garmin marketing department was asked about the way EcoRouteHD works. Garmin explained that the component uses an average consumption curve, and that the OBD2 signals are used to find out how the driver’s driving style is [Heise11].

Using an EcoRoute technology based on location dependent multi-source historical and real-time traffic information, Boriboonsomsin and colleagues found out that around 25% fuel could be saved on a route starting from Los Angeles Airport to downtown Los Angeles which avoids traffic jams [BoBa10].

Actual Limits of EcoRouting

The main general limitations of EcoRouting are the static consumption curves or static weights on the road links, which are used to find the EcoRoute. For example, the Bosch actual EcoRouting implementation is based on a proprietary database and needs the typical fuel consumption curves for constant speed and acceleration, which have to be provided from the car manufacturers for each vehicle. Because of the planned switch to NDS (*Navigation Data Standard* – a new database standard that has been widely adopted in the automotive world), and because of the complexity of getting precise consumption information for each vehicle variant, it was decided to remodel the EcoRouting functional component.

Depending on the car manufacturer, the consumption curves were more or less accurate; and sometimes it wasn’t even possible to obtain any. Ideally, the information needed from the car manufacturer had to be replaced with self-generated information. Also, the number of attributes available for evaluation during the route calculation was very limited. With the switch to NDS, the amount of information available about the route during the route calculation will potentially increase, providing data that allows a more precise fuel consumption prediction.

Navteq implementation of the EcoRoute uses only the navigation database, disregarding the vehicle or the driver type. It doesn't have the possibility to compute any fuel prediction for these routes.

Garmin's approach will never be able to compute an accurate fuel consumption because the fuel injection value on the CAN (*Controller Area Network*) bus isn't available over OBD2.

The last presented solution based on traffic historical data is only as good as the data quality is, and as long as the periodicity of traffic pattern is true.

In conclusion, most of the solutions don't consider the vehicle or the driver specificity at all, and only few of them try to take them into consideration with generalized consumption curves.

1.2.2 Fuel Consumption Prediction Today

Independently from EcoRouting, there are two possibilities to compute a fuel consumption prediction. The first one is using location dependent information related to the database links and nodes, and the second is using location independent models.

Location Dependent

Due to the strong variations between different vehicle configurations, and the need of a link to the CAN bus to get the live fuel injection values, no location dependent memorization of the fuel consumption has been developed so far.

Location Independent

In 2011, Ben Dhaou [Dhao11] described a fuel estimation model for EcoDriving and EcoRouting based on Willan line scaling techniques for ICE (*Internal Combustion Engine*). The fuel estimation model takes into account the number of stops, the average speed, the efficiency of the gearbox, the air-drag coefficients, and the engine parameters available from the automaker. The results showed that the proposed solution was able to distinguish between a low fuel consumption and high fuel consumption route, and therefore the EcoRoute functionality seemed to be valid. The fuel estimation was computed for 14 routes using three solution variations. The average estimations quality was measured with a -26.63%, -37.25% and -21.39% deviation from the measured consumption.

The U-embedded Convergence Research Center of the Korea Electronics Technology Institute described a method of fuel consumption prediction that uses vehicle information transmitted over OBD2 [GJPY11]. Two tests were conducted on a 5km test route. The first test uses the relation between engine RPM and fuel consumption, and the second one the relation between the throttle position and fuel consumption. The test vehicle was a Hyundai Grandeur TG Q270, which hands over the amount of fuel consumed over OBD2. This isn't a standard feature in Europe and only very few manufacturers hand over this value. The correlation coefficients were found out to be 76% (engine RPM based) and 88% (*Throttle Position Sensor* (TPS) based).

The Garmin EcoRouteHD functionality described above is highly likely to use general TPS curves.

Actual Limits of Fuel Consumption Prediction

To provide a wide coverage, location dependent data is often composed of a mix of collected data from different drivers in different vehicles. This makes it possible to recognize general tendencies, but not to consider specific driver and vehicle properties.

The high complexity of the interactions between the driver, vehicle and surroundings makes it difficult to find a simple model, like the Willan lines, that is accurate enough to display the fuel consumption estimation. Additionally, information regarding the vehicle (e.g.

aerodynamic properties and vehicle mass), which are subject to strong variations from vehicle to vehicle, are needed to generate the Willan lines.

2 Goals and Challenges of this Work

Based on the identified limitations, the following goals were defined:

- (1) Design a prototype that is able to make a fuel consumption prediction for every route, even if it hasn't been driven before, based on the information available in the navigation database and the telematics inputs and data that had been learned.

The solution must take into account that:

- (2) The prototype has to work without any vehicle specific input from the car manufacturer.
- (3) The energy consumption prediction has to be as precise as possible. It is expected that, similar to travel time prediction, the acceptance for erroneous prediction will be low. The acceptable margin of error should be defined according to the standard deviation observed during the multiple drives on a mixed route.
- (4) The energy consumption prediction has to be computed onboard. Complex calculations can be made on an online server, but a data connection would be needed in this case. Because there's no guarantee that a data connection is available, the whole system should be able to run onboard.

Obviously:

- (5) The prediction provided has to be more accurate than actual offline (and if possible online) solutions.

An additional request was formulated for practical reason:

- (6) Generate consumption curves compatible with the actual EcoRoute implementation.

And lastly, during this work it has been taken into account that, as far as possible, the designed solution should consider a future upgrading for EV compatibility. The prototype, if possible, has to provide some solid basis for a range prediction function component. Because of the lack of EV data, it wasn't possible to scientifically prove that the prototype works with an electric powertrain. Therefore, the description of this work concentrates on ICE. However, the future adaptation needed for an EV will be mentioned. Even though the lack of available data didn't allow proofing scientifically that the prototype solution works for EV, the results obtained so far in the context of the project OpEneR² (whose range prediction component is partially based on the described system) seems to indicate that it is valid.

The navigation system function component prototype (later referenced as 'prototype') presented in this work has as its goal to assist the infotainment system (which the navigation system is part of), to reduce the needed amount of fuel for a given trip.

Therefore, the subject of this work was defined to be:

Design a component that learns characteristics of the dynamic driving style and of the vehicle, in known situations, for a later fuel consumption prediction on roads that haven't been driven before.

There are three possible approaches to use past information for future predictions.

² <http://www.fp7-opener.eu/index.php/project.html>

First, and similar to historical traffic data, the system can save information related to a particular geo-location. This information can be coupled with other information (e.g. Time and Date). In this case, an important amount of recordings are needed to reach a statistical accuracy. The complexity of the situation description is often reduced to a few characteristics to keep the amount of data needed for statistics low. A driver specific statement is often neglected for non-specific driver predictions, which are based on the supposition that the observed driving style at the particular location is very similar for the selected situation characteristics. It implicates that the driving style is mainly determined by the surroundings. Because it is geo-located, driver and vehicle are unspecific, and the amount of needed recording is too high, this solution wasn't considered for this work.

The second approach is a statistical analysis of the recordings linked to a set of predefined characteristics that describe the situation. For example: the analysis of the speed of travel according to the speed restriction, the weather condition, and the time of the day. This statistics can then be used for other routes when a similar condition exists.

While this approach can generate driver-specific statistically based predictions for a route that hasn't been driven before, there is still a problem. Because the needed amount of recording for statistical accuracy is proportional to the number of possible situations that have been defined, the complexity of the real world must be generalized to a very few characteristics. The result is that according to the low number of characteristics chosen, a low prediction quality is expected because of the strong generalization and little amount (or outdated) of recordings used to make such a statistical prediction.

The third alternative is the most complex, because it requires an understanding of the real world that isn't needed in a statistical approach. First of all, according to the kind of prediction that must be made, factors that influence the fuel consumption must be found, understood, and sorted. Then, it is possible to make a simulation approach that can be tested and corrected against the real world. This alternative is only as good as the identification and understanding of the factors with influence, and, as the simulation.

Layout of this Work and Leading Thought

To decide if either the statistical approach or the simulation should be considered, the relevant parameters that have a direct and indirect influence on the fuel consumption have been analyzed. In a second step, the available system information has been reviewed to find out which fuel-influencing parameters can be recognized during the drive, and which ones can be predicted during the route calculation. After that, a solution proposal was made according to the theoretical understanding of the problem. Test cases were defined and the prototypical implementation results discussed.

This work is based on the three-stage model proposed in 1974 by W. Durth [Durt74] that describes the interactions between a driver, his vehicle and his surroundings. In 1982, Donges [Dong82] described the driving task as a three-stage model made of 'Navigation', 'Trajectory guidance (track and speed)' and 'Vehicle stabilization'. He updated his model [Dong09] with Rasmussen's [Rasm83] three-stage task performance model in 2009 (Figure 1). The driving task is described as the interaction between a driver, his vehicle and the surroundings, with a main focus on the human behavior.

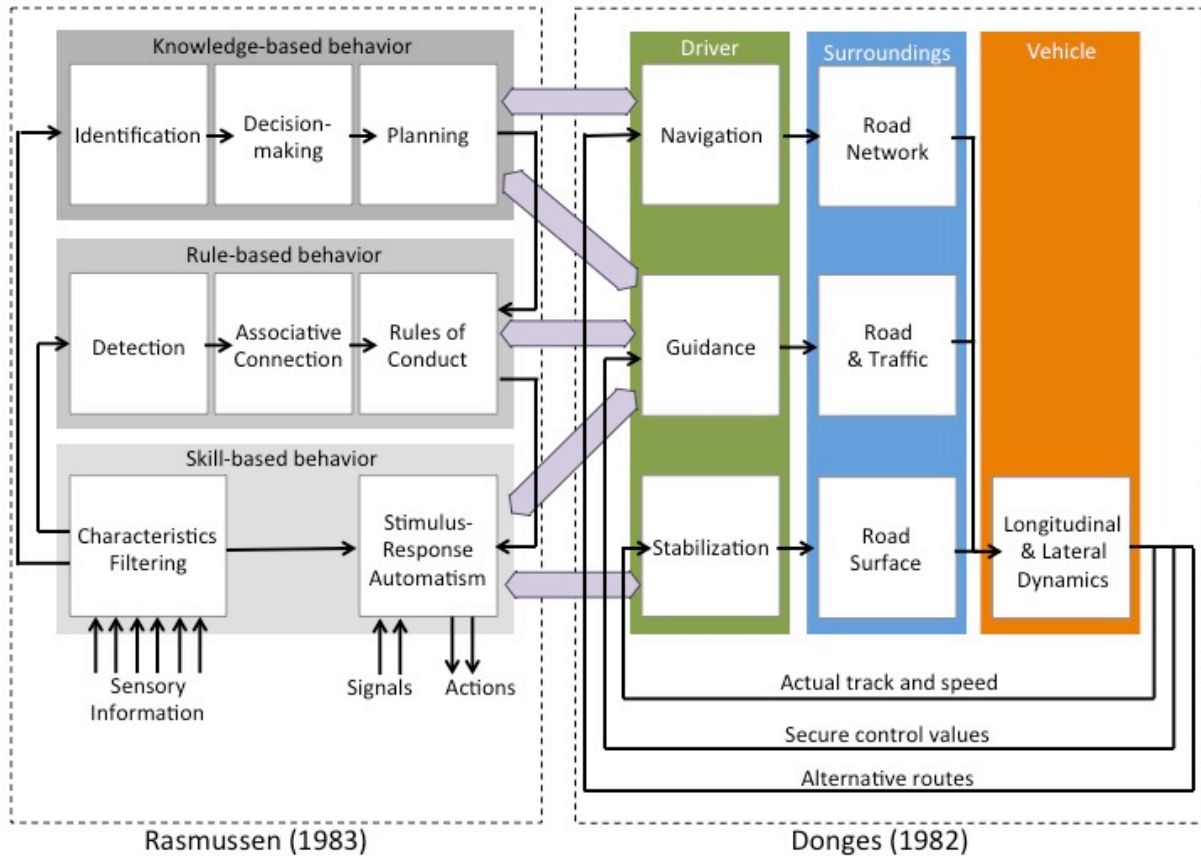


Figure 1: Donges Three-stage Model Extended with Rasmussen's Three-stage Task Performance [Dong09]

More recently, this model has been used for example in the project ecoSmartDriving [EiSu10]. In the use case description, experts propose matrix-linking driving decisions (acceleration / deceleration / idle / speed / gear selection) to surrounding characteristics (traffic / road / weather – environment), to the driver himself, and to his vehicle.

Based on those models, this work uses a fuel consumption-oriented model which is split into four parts (Figure 2):

- The first part links the fuel consumption to the vehicle
- The second part describes the interaction between the surroundings and the vehicle.
- The third part describes the interaction between the driver and the vehicle.
- The last part describes the interaction between the surroundings and the driver.

The first two parts are referred to as ‘vehicle part’ and the last two parts as the ‘driver part’.

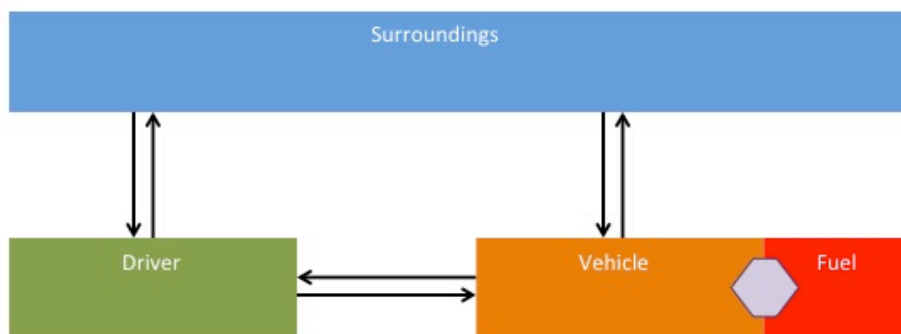


Figure 2: Basic Model Proposition for an Understanding of the Influences on Fuel Consumption

Since the interactions between driver, vehicle and surroundings will be only evaluated in the next chapter, the arrows indicate a supposed action and reaction, despite the fact that the reaction might not be highly relevant to the fuel consumption.

3 Theory and Background

This chapter is an introduction to the vehicle-related characteristics that are directly or indirectly responsible for fuel consumption ('Vehicle Part'), and then measures the impact of the driving style on fuel consumption and investigates the characteristics that influence it ('Driver Part').

3.1 Vehicle Influences on the Fuel Consumption

Based on Figure 2, and with the exception of the oxygen level in the air, the vehicle influence on the fuel consumption is basically a closed circuit within the vehicle and is limited to the highlighted elements in this simplified model:

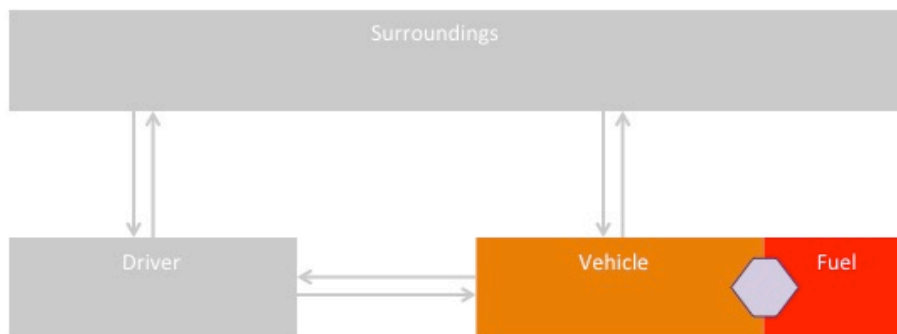


Figure 3: Technical Influences on the Fuel Consumption Highlighted in the Proposed Model

There are three categories of vehicle characteristics that influence the fuel consumption:

- The engine characteristics: The engine uses fuel mixed with oxygen to induce a chemical reaction and produce a mechanical movement (Figure 2: described as 'Fuel' – in red).
- The transmission characteristics: The transmission converts and transfers the engine rotational movement to the vehicle wheels, and is subject to energy losses (Figure 2: the connection between 'Fuel' and 'Vehicle' – in orange and purple).
- The forces that apply on a moving vehicle vary according to some vehicle characteristics (Figure 2: the arrow from 'Surroundings' to 'Vehicle' – Chapter 3.2).

This energy is used to overcome the driving resistances, and/or to store energy in the vehicle. Energy can be saved in the form of kinetic energy when the vehicle is accelerating, and in the form of potential energy when the vehicle drives uphill (Figure 2: the arrow from 'Vehicle' to 'Surroundings').

Additionally, the generator converts parts of the mechanical movement into electricity, which is used for the auxiliaries.

A study conducted in Germany in 2011 [RuBa11], measured the vehicle energy in real situations using test vehicles full of sensors. The test route was defined to match the average distribution of road types (from highway to city roads). It was measured that:

- 67% of all the fuel energy had been transformed into heat during the energy transformation process
- 8% had been used for the auxiliary units:
 - 2% for the air conditioner compressor
 - 2% for the power steering wheel
 - 2% for the generator (which had a measured average efficiency of 64%)
 - The remaining auxiliaries used the remaining 2%
- 2% had been lost to friction in the drive train
- 23% had been used for the moving of the vehicle:
 - 6.5% because of the rolling resistance

- 8% because of the drag resistance
- 8.5% because of energy loss while braking

These values are similar to the ones usually found in the literature (e.g. [Huch98]), and illustrate the significance of the engine role in the fuel consumption.

3.1.1 The Internal Combustion Engine (ICE)

As estimated during the German study mentioned before [RuBa11], today's gasoline engine efficiency is under 40 %, and under 43% for personal vehicles diesel engines [Goll05]. Volkswagen [VWir10] gives the following ranges as indicators for personal vehicle engine efficiency:

- 25 to 30% for common engines running on gasoline
- Up to 35% for gasoline direct fuel injection engines
- 35 to 40% for common engines running on diesel
- Up to 45% for diesel direct fuel injection engines

Even for a single engine, the efficiency is often mentioned as a range due to the variations observed.

Diesel and gasoline engines are used to convert the chemical energy found into fuel into mechanical energy. They initiate a fuel-air reaction (particularly with the oxygen) with the help of compression (pressure and temperature augmentation), and an external source of ignition in the case of gasoline engines (spark plugs). Engines have a variable efficiency defined by the ratio between the amount of fuel energy used and mechanical energy produced. For these reasons, the fuel and air properties and compression ratio variation, controlled by the throttle and regulated by the *Electronic Control Unit* (ECU), are responsible for an ICE efficiency variation. Additionally, the efficiency may vary according to engine speed (because of the engine internal friction losses).

Influence of Fuel Type and Additives on the ICE Efficiency

The consumed fuel volume V_K (in m^3) is defined as:

$$V_K = \left(\frac{b_e \cdot P_e \cdot t}{1000} \right) \cdot \frac{1}{\rho} \quad [\text{EiK108}]$$

Where

- b_e Engine specific fuel consumption in g/kWh
- P_e Engine induced performance in kW
- t Time in hour
- ρ Fuel density in kg/m^3

Based on the previous equation, the fuel density, whose legal limits are defined in DIN EN 228:2008-11 ($720kg/m^3 < \text{Allowed fuel density at } 15^\circ\text{C} < 775kg/m^3$), has a direct influence on the volume of fuel consumed.

According to the Aral fuel technical sheets (Extract in Table 1), the fuel properties vary not only according to the fuel type, but also according to the season. The fuel properties are adapted to the temperatures changes between summer and winter, enabling the ICE to run in an optimal way.

The DIN EN 228:2008-11 set the following legal limits for fuel steam pressure according to the season:

- 45kPa < Allowed fuel steam pressure (RVP) in summer < 60kPa
- 60kPa < Allowed fuel steam pressure (RVP) in winter < 90kPa.

In addition to that, high-end fuels are mixed with additives that increase the fuel efficiency. They work as cleaning substance concentrates, friction modifiers, ignition accelerators, lubricants and stabilizers [Bass08] [Aral10] and influence the engine efficiency.

	Method	Aral SuperPlus98	Aral Ultimate 102
Density at 15°C	DIN EN ISO 12185	747.8 kg/m ³	742.2 kg/m ³
ROZ	DIN EN ISO 5164	98.5	102.0
MOZ	DIN EN ISO 5163	88.6	89.8
Steam pressure	DIN EN 13016-1		
01.05-30.09		55.7 kPa (Summer)	57.6 kPa (Summer)
01.10-15.11		64.8 kPa (Transition)	62.9 kPa (Transition)
16.11-15.03		76.8 kPa (Winter)	68.5 kPa (Winter)
16.03-30.04		65.9 kPa(Transition)	59.7 kPa(Transition)

Table 1: Fuel Properties of Aral SuperPlus98 and Ultimate 102 [ArSu10] [ArUI10]

Influence of Air Filter and Air Pressure on the ICE Efficiency

Shannak and Alhasan [ShAl01] measured the air capacity and the fuel consumption of a four-cylinder four-stroke petrol engine for:

- Engine speeds between 1000 and 4000 rpm
- An atmospheric altitude between 600 and 850 m above the sea level
- At pressure between 0.9 and 0.95 bar.

They found out that, a 200 m change on the altitude, corresponding to a change in atmosphere pressure of about 3000 Pa, has a very strong effect on the engine. The efficiency, and therefore the fuel consumption, increased 10% at low and middle engine speed, and about 40% at high engine speed. The tests were conducted without an air-fuel ratio feedback loop.

The study of Shannak and Alhasan leads to the following explanation: The air/fuel ratio is known as the stoichiometric mixture when enough air is provided to completely burn all of the fuel. Vehicles using an oxygen sensor (cars less than 30 years old) or another feedback loop that controls the air/fuel ratio (usually by controlling fuel volume), will compensate for the changes in the fuel's stoichiometric rate automatically by measuring the exhaust gas composition, and adapting to match the stoichiometric mixture. For this reason, measurement on a modern vehicle differs from the previously introduced results.

Zervas [Zerv11] compared the fuel consumption of gasoline passenger cars at 700m and 2200m altitudes. He measured a circa 5% decreased consumption on the NEDC (*New European Driving Cycle*) and FTP (*Federal Test Procedure*) driving cycles at higher altitudes, while he measured a 5% increase during a highway drive test.

The effects of intake air filter condition on vehicle fuel economy were analyzed in 2009 [NoHu09]. It was showed that clogging the air filter has no significant effect on the fuel economy of the newer vehicles, because they are able to adapt the fuel injection depending on the analysis of the exhaust emission of the previous combustion cycle.

Influence of Cold Start on the ICE Efficiency

When the engine is cold, the injected fuel does not easily vaporize and tends to drop on the cylinder wall. Therefore, and until the engine is warm, a so-called 'rich mixture' with a noticeable fuel volume increase is injected. It guarantees the presence of enough fuel vapors for a normal explosion despite the low temperature. After a few minutes (depending on the engine, the temperature, the fuel, and the engine use), the engine reaches the minimum needed temperature to maintain the fuel vaporized, and regulates the fuel injection down to the normal mode of operation.

Furthermore, oil viscosity depends on its temperature [CaGa10]. It means that as long as the oil is cold, the viscosity is low and the friction with the moving parts of the engine are strong.

3.1.2 Generator

Personal vehicles include a generator, which converts the rotating movement produced by the engine into electricity. The electricity supplies primary electrical consumers (e.g. fluid pumps), as well as secondary electrical consumers controlled by the driver (e.g. air condition).

The generator efficiency depends on the rotational speed and the load [ScTh07], and while the typical efficiency is circa 70% to 74%, it should reach up to 80% in the near future [Schr10].

3.1.3 The Transmission

A transmission provides the connection between the engine and the wheel. It is made of a clutch, connecting the engine to the gearbox, which is connected to an axle or prop shaft. The shaft is often connected over a differential to the drive shaft.

The worst efficiency is measured when the clutch is open and the engine is running. In this case, the vehicle is not moving, and fuel is still being consumed. This situation can be avoided with a Start-Stop system, which shut off the engine when the vehicle isn't moving, and was measured to save an average of 4.2% fuel in Western Europe [Fiat10].

According to the Robert Bosch GmbH [Bosc02], manual transmission efficiency, when the clutch is closed, depends on friction in the gearbox, axle conversions and respective bearings. The efficiency range is 91 to 95% for *Front Wheel Drive* (FWD) vehicles and 88 to 92% for *Rear Wheel Drive* (RWD) vehicles.

One of the main parts of the transmission is the gearbox, whose efficiency varies depending on the selected gear used. There are multiple kinds of automatic gearbox technologies available today, the most important beside the classical AT (*Automatic Transmission*) is the DCT (*Dual Clutch Transmission*) sometimes called DSG (*Direct Shift Transmission*). The following values are mentioned by Volkswagen [Volk08] to characterize the efficiency of their gearboxes:

- 83% for a 6 gear conventional automatic transmission (max torque 320Nm)
- 85% for a 6 gear DSG (*Direct-Shift Gearbox* - max torque 350Nm)
- 91% for a 7 gear DSG (max torque 250Nm)

That is less than the values published by Naunheimer and Bertsche in their book "*Fahrzeuggetriebe, Grundlagen, Auswahl, Auslegung und Konstruktion*" [NaBe07]: 90% to 95% for AT and DCT. They also mention a less usual kind of gearbox named CVT (*Continuously Variable Transmission*) that can change through an infinite number of gear ratios that vary between maximum and minimum values. In this case, the gearbox efficiency varies between 87 and 93%.

3.2 Forces that Affect the Moving Vehicle

Based on Figure 2, and with the exception of acceleration, the interaction of the surroundings and the vehicle that influences the fuel consumption is limited to the highlighted elements in the simplified model:

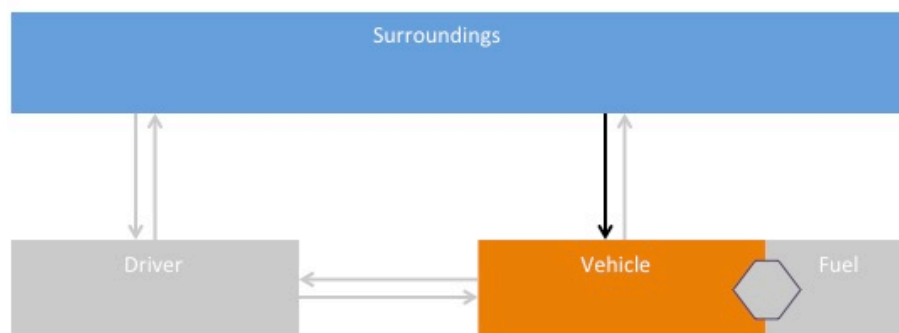


Figure 4: Surrounding Influences on the Vehicle that Lead to Changes in Fuel consumption

Back in 1687, Sir Isaac Newton formulated three of the most important laws in modern mechanics. The three laws, published in *Philosophiae Naturalis Principia Mathematica*,

define the connection between the energy that the vehicle produces to rotate the wheels and the forces that apply to the moving vehicle.

Newton's three laws of motion are:

First Law:

Every object in a state of uniform motion tends to remain in that state of motion unless an external force is applied to it.

Second Law:

The relationship between an object's mass m , its acceleration a , and the applied force F is $F = ma$.

Acceleration and force are vectors; in this law the direction of the force vector is the same as the direction of the acceleration vector.

Third Law:

For every action there is an equal and opposite reaction.

The forces that apply on a moving vehicle can be divided in two categories:

- The non-conservative forces, which, according to the first law of motion, slow down the vehicle
- The conservative forces, which, inter alia, include the acceleration as described in the second law of motion.

Then, according to the third law of motion, the sum of all the forces that apply on the moving vehicle are equal to the propulsion force measured on the wheel, but in an opposite direction.

3.2.1 Non-conservative Forces

The non-conservative forces are usually reduced to two main forces: the air resistance and the rolling resistance.

3.2.1.1 Air Resistance

The air resistance force is defined as:

$$F_{Air} = \frac{1}{2} \cdot \rho \cdot c_{Air} \cdot A \cdot v^2 \quad [MiWa04] \text{ and } [Fial06]$$

Where

- ρ The air density, which depends on barometric pressure, altitude over sea level, and air temperature.
- c_{Air} The air drag coefficient of the car, which depends on the vehicle geometry
- A The cross section of the car in driving direction, which depends on the vehicle geometry
- v Speed in m/s

and

$$\rho = \frac{p}{R_f \cdot T}$$

Where

- p is the current air pressure in Pascal ($J \cdot kg^{-1}$), which depends on altitude over sea level and climatic conditions
- T is the current temperature in Kelvin
- R_f is the gas constant of humid air in $J \cdot kg^{-1} \cdot K^{-1}$, which depends on relative humidity and temperature.

According to DIN 1946-3: 2006–07, the temperature may vary between –45 and 55 degree Celsius all over the world. For normal conditions at sea level, the air pressure is assumed to be 1013.25 hectopascal, the temperature 15 degree Celsius, the air gas constant 287.1 J/kg K, and the air density 1225 kg/m³ [Bohl80].

Vehicle Characteristics: The Vehicle Cross-section and the Drag Coefficient

The vehicle cross section, in m², is the flattened surface observed while facing the vehicle. It is derived from the height and the width of the vehicle, but not from its length.

The drag coefficient c_{Air} is a digital representation of the aerodynamic properties of the vehicle. It must be estimated using CFD (*Computational Fluid Dynamics*) programs or experiments in wind tunnels. For the estimation of the mechanical energy required to drive a typical test cycle, this parameter is assumed to be constant [GuSc05].

According to [Huch98], the vehicle body causes approximately 65% of the aerodynamic resistance. The rest is due to wheel housings (20%), exterior mirrors, eave gutters, window housings, antennas (approximately 10%), and engine ventilation (approximately 5%). Over the years, the average personal vehicle drag coefficient has evolved; from 0.453 with a scattering of 0.0425 in 1974 while today’s vehicle have a drag coefficient between 0.25 and 0.35 [MiWa04] [Fial06].

Some vehicles have variable aerodynamic properties. A car can be equipped with automated spoilers that are speed activated (e.g. Volkswagen New Beetle). BMW sometimes has active grille shutters that increase the aerodynamic flow when the engine doesn’t need to be cooled down. The Audi Q7 can lower the suspension from 180 Millimeter to 145 Millimeter when driving faster than 160 km/h, which reduces the fuel consumption of 0,3 Liter/100km [ÖrRü09].

The driver can also influence the aerodynamic properties when he opens the windows, the rooftop or the convertible top. The drag coefficient of convertibles varies very much depending on if the top is open or closed:

	Open	Closed
Opel Tigra TwinTop	0.40	0.35
Mercedes-Benz SLK 200K	0.37	0.32
Mercedes Benz SL 500	0.34	0.29
Audi A4 Cabrio	0.34	0.31
Mercedes E350 Convertible (2011)	0.33	0.28
Maserati GranCabrio (2010)	0.39	0.35

Table 2: Convertible Drag Coefficient (Source: [NaBe07], Mercedes, Maserati)

In the case of a convertible, the vehicle cross section should remain almost unchanged. Additionally, the driver can mount a roof box or ski racks on the top of his car, augmenting the vehicle cross section and modifying the vehicle aerodynamic properties (drag coefficient increase as indicated in Table 3).

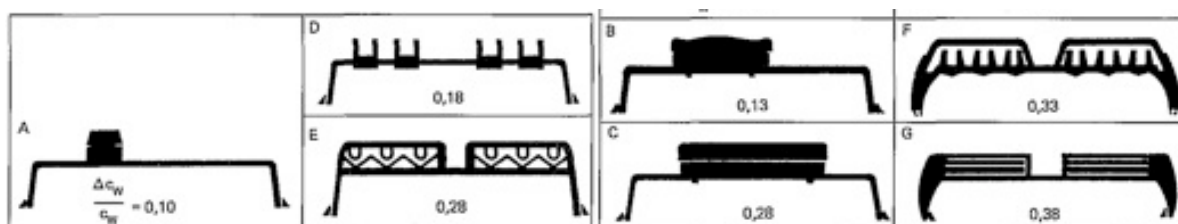


Table 3: Drag Coefficient Changes Depending on the Rack Geometrical Form [Huch05]

The special case of a trailer increases not only the drag resistance but also the weight and the rolling resistance. Because of the modeling complexity, the decision was made not to consider this special (and rare) case during this work.

Besides that, the wind has a variable influence on the air resistance depending on the vehicle shape and the wind direction. Mitschke and Wallentowitz [MiWa04] propose the following curves describing the relation between drag coefficient and the angle of incidence for three kind of vehicle shapes:

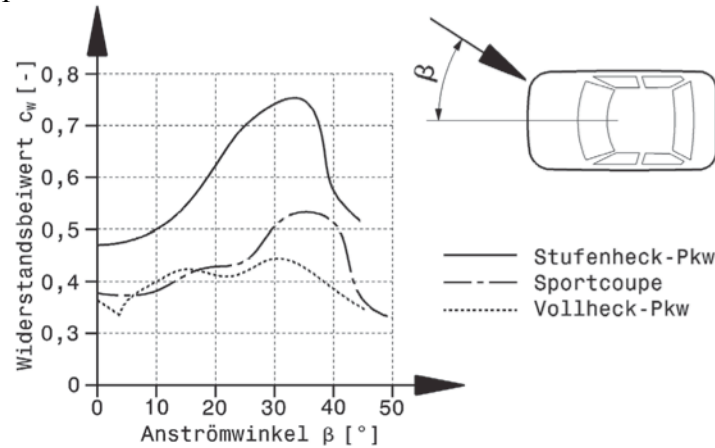


Table 4: Relation Between Drag Coefficient and Wind Angle of Incidence According to [MiWa04]

Then, the incidence of wind on air resistance can be approximated with the following formula:

$$F_{Air} = \frac{1}{2} \cdot \rho \cdot c_{Air|Wind} \cdot A \cdot (v_{effective})^2$$

$c_{Air|Wind}$ The air drag coefficient of the car considering the wind angle of impact

$v_{effective}$ The effective speed considering the wind flow velocity

This can be simplified to:

$$F_{Air} = \frac{1}{2} \cdot \rho \cdot c_{Air} \cdot A \cdot (v + v_{Wind})^2$$

v_{Wind} Wind speed share in m/s on the axe of vehicle travel. May be negative if the wind is blowing in the direction of travel.

3.2.1.2 Wheel Resistance

Another non-conservative force applied on the moving vehicle is the wheel resistance. It is the global resistance caused by the wheels, and is subdivided in smaller specific resistances as described here:

$$F_{Wheels} = F_{Roll} + F_{Surge} + F_{Bearing} + F_{Toe-in} + F_{Curve} + F_{Suspension} \quad [MiWa04]$$

Where

- F_{Roll} Deformation of tires and surface
- F_{Surge} Apply when wheels have to displace water on the road surface
- $F_{Bearing}$ Friction in wheel bearings
- F_{Toe-In} Slip and deformation of front wheels due to toe-in
- F_{Curve} Wheel deformation and slip in curves
- $F_{Suspension}$ Losses because of wheel suspension

For simplification, the wheel bearing friction ($F_{Bearing}$), the slip and deformation of the front wheels due to toe-in (F_{Toe-In}) and the losses because of wheel suspension ($F_{Suspension}$), are often considered constant and assimilated to the deformation of tires and surface: F_{Roll} .

F_{Roll}: The Deformation of Tires and Surface

The rolling resistance F_{Roll} depends on four factors and is defined as:

$$F_{Roll} = c_{Roll} \cdot m \cdot g \cdot \cos \alpha$$

Where

- c_{Roll} is the rolling friction coefficient (see below);
- m is the vehicle mass (with passengers and load);
- g is the acceleration of earth's gravity which depends on latitude and altitude. The mean value is $g = 9.81 \text{ ms}^{-2}$. At the poles g is 0.23 % higher and at the equator 0.3 % lower; the reduction in 5000 m altitude is circa 0.16 %.
- α is the gradient angle.

Similar to the drag coefficient, the rolling friction coefficient is a vehicle-specific (in this case tire-specific) value created to represent the tire properties in a mathematical way. Guzzella and Sciarretta [GuSc05] describe c_{Roll} in their book 'Vehicle Propulsion Systems: Introduction to Modeling and Optimization' as follow:

“The rolling friction coefficient c_r depends on many variables. The most important influencing quantities are vehicle speed v , tire pressure p , and road surface conditions. The influence of the tire pressure is approximately proportional to $\frac{1}{\sqrt{p}}$. A wet road can increase c_r by 20% and driving in extreme conditions (for example, sand instead of concrete) can easily double that value. The vehicle speed has a small influence at lower values, but its influence substantially increases when it approaches a critical value where resonance phenomena start.”

ISO 8767, ISO 18164 and ISO 28580, specifies methods for measuring the rolling resistance, under controlled laboratory conditions, for tires designed for use on passenger cars, trucks, buses and motorcycles. However, the rolling resistance varies with the speed. The reason is not only the friction between the surface of the tire and the street; it's also the deformation of the tire. According to email interviews with Bridgestone [Brid10] and Michelin [Mich03], every time a tire is rolling it also tumbles. In that case a bulge is building up in the front of the contact zone between tire and road. Therefore, c_{Roll} should be described in a speed dependent way, for example as Mitchke and Wallentowitz [MiWa04] did:

$$C_{r_{speed}} = C_r + 0,001 \cdot C_r \cdot \frac{v(\text{km/h})}{100(\text{km/h})} + 0,022 \cdot C_r \cdot \left(\frac{v(\text{km/h})}{100(\text{km/h})} \right)^4$$

where 'v' is the speed in km/h.

In a similar way, Jazar [Jaza08] also proposed an approximation for average tires with:

$$C_{r_{speed}} = C_0 + C_1 v_x + C_2 v_x^4$$

where $C_0 = 9.91 \times 10^{-3}$, $C_1 = 1.95 \times 10^{-5}$ and $C_2 = 1.76 \times 10^{-9}$

To determine if there are tire characteristics that may be used as an indicator of the rolling friction coefficient, the results of an independent rolling resistance measurement from the TÜV Automotive GmbH in 2002 have been analyzed. The measurements were made at a constant speed of 80km/h on a drum test rig. The largest tested winter tires were 205/55 R16 with a $c_{Roll} = 1.066\%$ average, while the widest tested summer tires were 225/45 R17 with a $c_{Roll} = 1.311\%$ average rolling resistance [StRa04]. The measured rolling friction coefficients (in %) for different kind of tires (S for Summer / W for Winter / G for All-Year) and different widths, are represented by red dots in the following graphic:

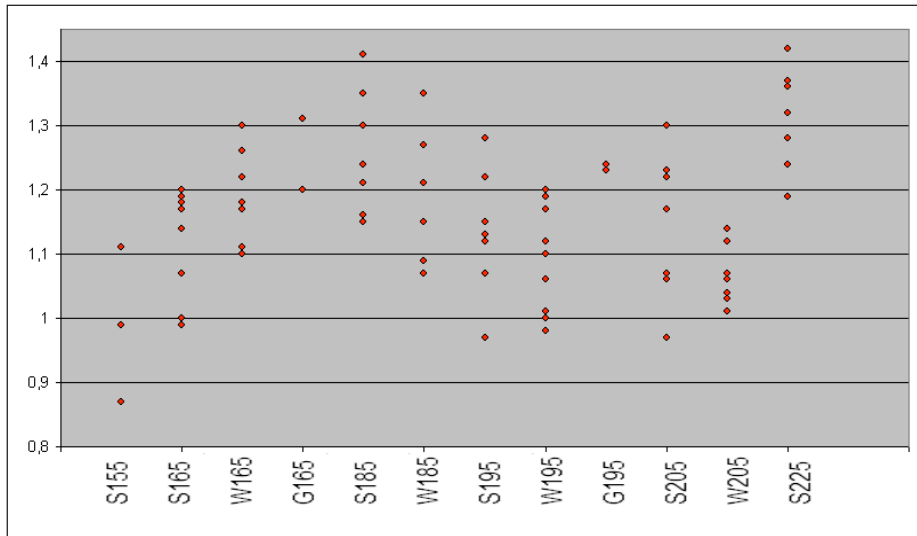


Figure 5: Rolling Friction Coefficient Sorted by the Kind of Tire and their Widths

It seems that there is a very limited difference between winter and summer tires for personal cars that can barely be generalized. This could be due to the fact that the measurements were all made at a speed of 80km/h, where the tires show similar kind of properties. Also, since the most economical tire was one of the narrowest, and one of the widest tires was measured to have the highest rolling resistance, the tire width seems to have little repercussion on the rolling resistance, but there is no identifiable general trend.

Furthermore, the age and the shape of the tire have an influence on its properties. According to Michelin, the tire gum degrades over its use, reducing the structure depth and therefore the gum volume that can be deformed. The more the tire tread is degraded, the less rolling resistance will be measured. Additionally, over time (10 year horizon), the gum tends to stiffen, which also reduces the deformation and therefore the resistance [Mich10] [Mich03].

Tire pressure was also found out to have a noticeable influence on the tire rolling property. For example, a study of the Continental AG shows that rolling resistance increases of 20% and fuel consumption of 4% at constant speed if the tire pressure is dropped from 2.0 Bar to 1.4 Bar [StRa04]. Figure 6 (left) is an approximation of the typical relation between rolling resistance and tire pressure.

The temperature of the tire and the gas filling it, inter alia, are responsible for the observed pressure variation during a cold start as represented by the curve (right) in Figure 6.

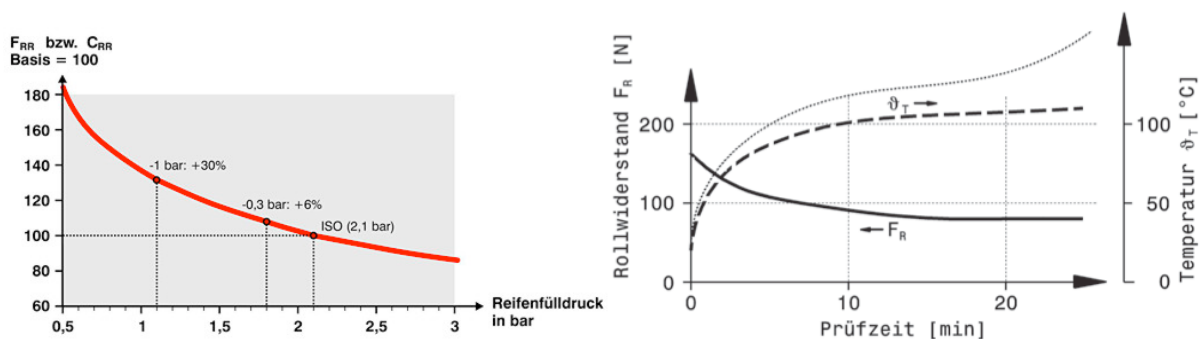


Figure 6: Left: Variation of the Rolling Resistance Coefficient (in %) According to the Tire Pressure (in bar)
Source: Michelin [Mich03]

Right: Variation of the Rolling Resistance Coefficient (in %) According to the Temperature (in °C)
Source: [Trze10]

This effect is responsible with the engine cold start setting for increased fuel consumption when the vehicle is moved while being cold.

Jazar [Jaza08] mention that the following equation has been suggested to show the effects of pressure and load on the rolling friction coefficient:

$$c_{Roll} = \frac{K}{1000} \cdot \left(5.1 + \frac{5.5 \cdot 10^5 + 90 \cdot F_{LoadVeh}}{p} + \frac{1100 + 0.0388 \cdot F_{LoadVeh}}{p} \cdot v^2 \right)$$

Where:

K : is equal to 0.8 for radial tires and 1.0 for non radial tires

p : the tire pressure in Pa

$F_{LoadVeh}$: the force linked to the load in Newton

V : the speed in m/s

Beside the tire, the second component involved in the rolling resistance is the road. The FKA (Forschungsgesellschaft Kraftfahrwesen mbH Aachen) built a trailer equipped to measure tire characteristic variation in real conditions. They found out that the road surface has an impact on the tire friction and therefore the rolling resistance [HuBa11].

Table 5 regroups typical values found in available written works:

Roadway (Rigid)	μ_0	Roadway (soft)	μ_0
Asphalt	0.010 / 0.012	Forest path (good)	0.045 / 0.040
Concrete (smooth)	0.011 / 0.013	Forest path (loose)	0.160
Concrete (rough)	0.014	Sand	0.150 to 0.300
Road and Pavement Condition		μ_0	
Very good concrete		0.008 - 0.1	
Very good tarmac		0.01 – 0.0125	
Average concrete		0.01 – 0.015	
Very good pavement		0.015	
Very good macadam		0.013 – 0.016	
Average tarmac		0.018	
Concrete in poor condition		0.02	
Good block paving		0.02	
Average macadam		0.018 – 0.023	
Tarmac in poor condition		0.023	
Dusty macadam		0.023 – 0.028	
Good stone paving		0.033 – 0.055	
Good natural paving		0.045	
Stone pavement in poor condition		0.085	
Snow shallow (5 cm)		0.025	
Snow thick (10cm)		0.037	
Unmaintained natural road		0.08 – 0.16	
Sand		0.15 - 0.3	

Table 5: Typical Rolling Friction Coefficient Values Depending on the Ground Properties
Source: [Bosc95] [Jaza08] [MiWa04]

The general observable trend is that the harder and smoother the surface is, the less is the rolling resistance. Beside that, the road surface characteristics can increase the rolling friction up to a factor 5, and therefore have an immense influence on the rolling resistance.

F_{Surge}: Force that Apply when Wheels have to Displace Water on the Road Surface

Beside F_{Roll}, F_{Surge} and F_{Curve} are the two most variable and potentially important components of the rolling resistance. In addition to the road characteristics influencing the rolling resistance, water can be present on the road surface, modifying the friction between tire and road surface. According to Mitschke and Wallentowitz, F_{Surge} can be approximated with the following equation:

$$F_{Surge} = \frac{Width}{100} \cdot \left(\frac{v}{10 \cdot X(H)} \right)^{Y(H)} \quad [MiWa04]$$

Where

Width The tire width in mm

v The speed in km/h

X(H) and Y(H) are dependent from the water film thickness on the road surface:

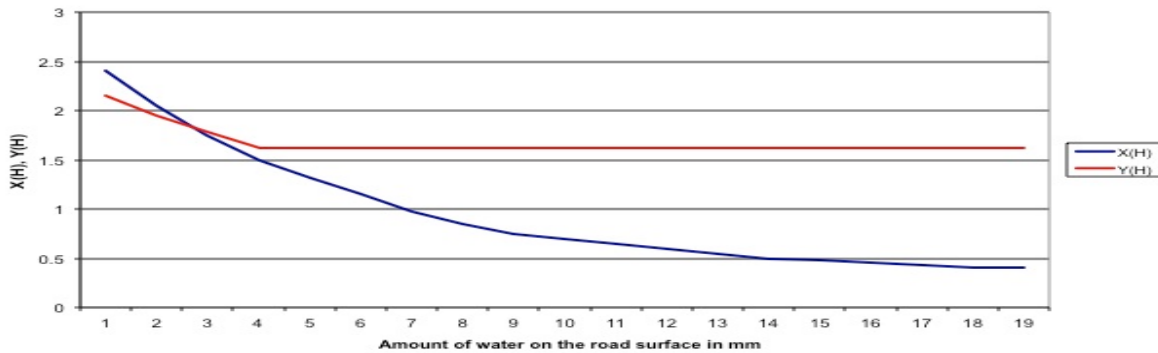


Figure 7: X(h) and Y(H) Values in Relation to the Amount of Water on the Road Surface (in mm)

How relevant this force is, has been calculated for different tire width at different speeds, in relation to the amount of water on the road.

In red: tire width is 215mm

In purple: tire width is 205mm

In green: tire width is 195mm

In blue: tire width is 185mm

From top to bottom, the four series are for a speed of 200km/h, 160km/h, 100km/h, 60km/h

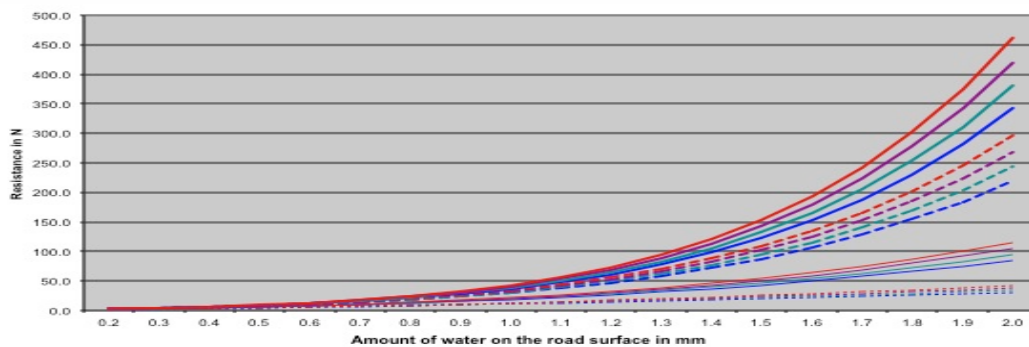


Figure 8: Water Friction Resistance in Newton for Different Tire Width at Different Speeds

For example, according to the equation, a 215mm wide tire, at 160km/h on a road with a 2mm water film, is responsible for an additional 300N resistance. As an indication, this is the maximum torque produced by a Golf MK4 V6 2.8l engine.

F_{Curve}: Wheel Deformation and Slip in Curves

While driving in a curve, the tire’s friction on the road is modified, adding a lateral component to the longitudinal one. An energy loss results from this, which can be approximated for average tires with

$$F_{Curve} = k_{\alpha} \cdot F_{LoadVeh}$$

Where

k_{α} is a slip angle dependent slip resistance coefficient that can take the following values:

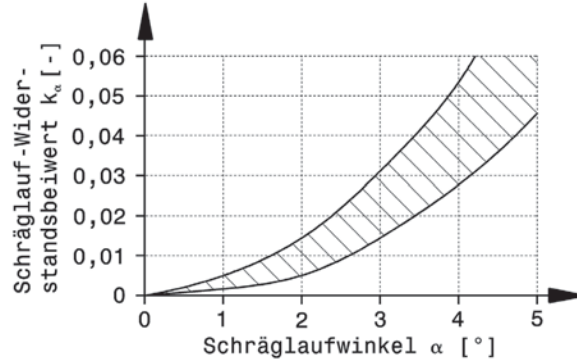


Figure 9: Relation Between Slip Angle and Slip Resistance Coefficient [MiWa04]

Obviously, the amount of energy lost in a curve is very dependent from its angle and increases exponentially.

The importance of the non-conservative forces is discussed at the end of this chapter in order to create a fuel consumption prediction-specific simulation.

3.2.2 Conservative Forces

Beside the non-conservative forces, conservative forces apply on a moving vehicle. These forces are usually reduced to the grade (or slope) resistance and the acceleration, which is linked to the force of inertia.

3.2.2.1 Grade Resistance

The grade resistance can be calculated with:

$$F_{Grade} = m \cdot g \cdot \sin \alpha \quad [\text{Fial06}]$$

Where

- m is the actual vehicle mass including load and passengers.
- g is the gravitational acceleration constant,
- α is the degree of grade in degree

With

$$\alpha = \arctan\left(\frac{q}{100}\right)$$

Where q is the slope in %.

The force is called ‘conservative’ because the energy used to move the vehicle uphill makes it possible that the vehicle can drive downhill using the force of gravitational attraction instead of fuel to get back to the same height level. When driving uphill, ‘ $\sin \alpha$ ’ takes a positive value; and when driving downhill, ‘ $\sin \alpha$ ’ is negative.

3.2.2.2 Acceleration, Deceleration and the Force of Inertia

Based on Jeongwoo Lee’s description of the acceleration force [Lee05]:

$$F_{acc} = F_{accT} + F_{accR}$$

Where

$$F_{accT} = m \cdot a \quad \text{and} \quad F_{accR} = \left(m_{Veh} + \frac{\theta_R + i^2 \theta_M}{r^2} \right) a = \lambda \cdot m_{Veh} \cdot a$$

and

- m_{Veh} The vehicle mass
- m The vehicle load mass
- a The acceleration in m/s^2
- i The gear specific transmission ratio
- θ_M The engine mass moment of inertia
- θ_R The wheels mass moment of inertia
- r The tire radius
- λ The rotational inertia factor

Then:

$$F_{acc} = (\lambda \cdot m_{Veh} + m_{Load}) \cdot a$$

Michael Safoutin gives the following description of the rotational inertia factor λ :

„The rotational inertia factor estimates the inertia invested in rotating powertrain components, such as engine pistons and crankshaft, transmission components, driveshaft, and wheels. This inertia affects energy and power demand similarly to the mass of the vehicle, but mass only accounts for translational inertia. When inertia is calculated, the rotational inertia factor is applied to the vehicle mass to artificially increase mass enough to account for rotational inertia.“ [Safo03]

Typical λ values can be found in the literature. For example, Haken [Hake07] lists the following ranges for a five-gear gearbox:

- Gear 1: $1.25 < \lambda < 1.50$ Gear 3: $1.04 < \lambda < 1.11$ Gear 5: $1.03 < \lambda < 1.05$
- Gear 2: $1.06 < \lambda < 1.21$ Gear 4: $1.04 < \lambda < 1.06$

The Robert Bosch GmbH [Bosc95] describes a relation between the gear ratio and the rotational inertia factor as shown in Figure 10:

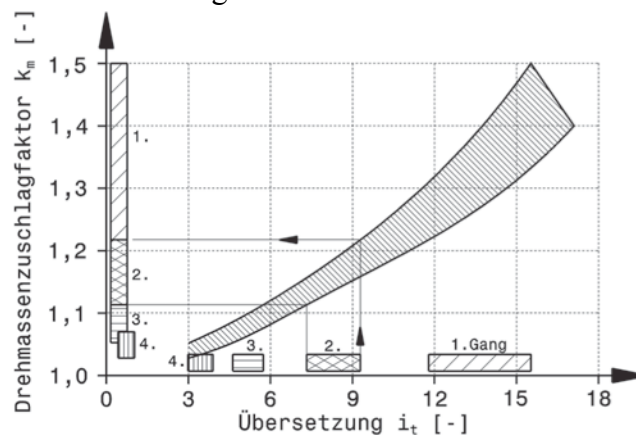


Figure 10: Robert Bosch GmbH Relation Between λ and Gear Ratio [Bosc95]

Despite that the figure is only valuable for a four-gear gearbox, it is interesting to see that the rotational inertia factor converges towards 1 for higher gears. This observation was used to make an approximation of the test vehicle gear 5 and 6 factors.

The acceleration can take negative values in the case of a deceleration. In this case, and similar to the grade resistance, the force is negative and therefore propels the vehicle in driving direction.

3.3 Driver Impact on Fuel Consumption

Besides the technical influences on the fuel consumption listed in chapter 3.1 and the forces that apply on a moving vehicle described in chapter 3.2, the driver himself influences the way

the vehicle in moving. This relation is highlighted in Figure 11, representing the simplified interaction model used in this work.

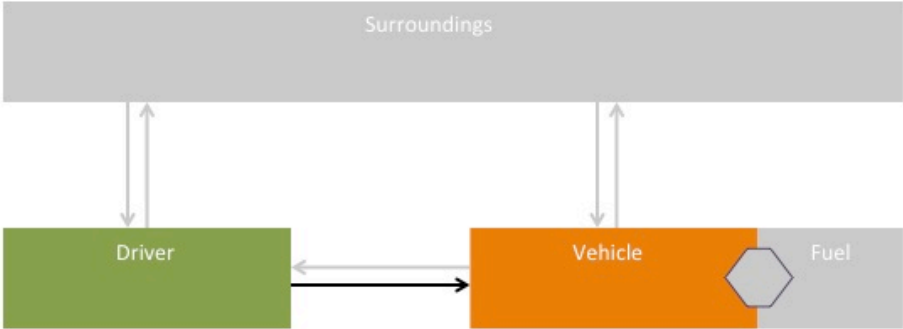


Figure 11: Driver Influences on the Vehicle that Leads to Changes in the Fuel Consumption

In the different publications analyzing the interaction between a driver and his vehicle, the words ‘driver type’, ‘driving behavior’ and ‘driving style’ are often used with no distinguishable limits, sometimes even misused. Therefore, to bring some uniformity, it was decided to use the definitions proposed by Köhler [Köhl09] and depicted in the following graphic:

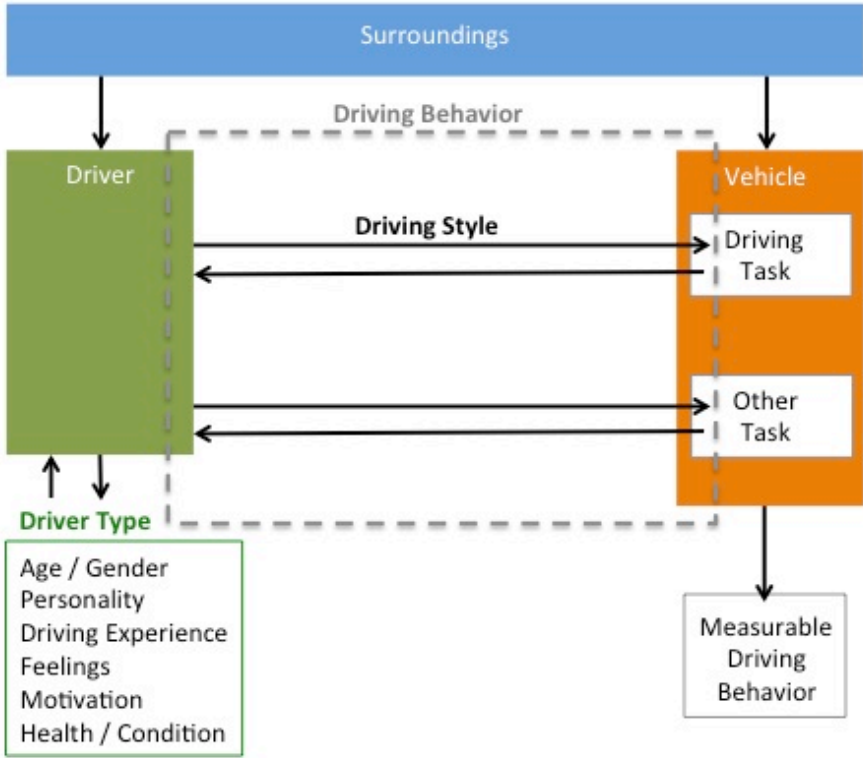


Figure 12: Differences Between Driver Type, Driving Style and Driving Behavior [Köhl09]

The driver type describes the driver itself, in a more psychological than technical way, and is often used to compare different drivers, or to regroup them into categories. The driving style concentrates on the driving tasks, while the driving behavior regroups the driving style and the non-driving related tasks. Such tasks can be the use of a navigation system, or the activation of the air conditioning system, for example.

In this work, the learning concentrates on the driving style. Recognizing that the driver type has been researched before to improve the automated comfort and electronic settings, it is supposed that this information should be later made available to the other vehicle components. Because the use of the auxiliaries is not part of the navigation, the forecast of the

driving behavior part that is not driving task-related should be generated in a separated component independent from the navigation system.

3.3.1 Fuel Consumption Variations Related to the Driving Style

A survey using recordings on a representative track around Stuttgart (Germany) [BaRu10] showed that, with a conventional vehicle, the driver has an average influence of 6.5% on the total amount of fuel needed to drive around the track. The maximum driver responsible variation observed was measured to be 32%. This variation was found out to be road-type dependent. For inner city, an average variation of 9.6% with a maximum of 50% was recorded, while the variation outer city was 6.7% with a maximum deviation of 27%.

This level of variation indicates that the driver might be a very important factor when it comes to fuel consumption prediction. Therefore, to confirm this supposition, the recordings of the test drives made for this work were analyzed. Each dataset (see Annex A, B, C, D on pages 151, 156, 159, 163) is assigned one specified route, with one selected vehicle, during the same season. Therefore, it is reasonable to presume that the fuel consumption variation recorded in the different datasets is mainly related to the driving style.

	Mean Amount of Fuel Consumed	Minimum Amount of Fuel Consumed	Maximum Amount of Fuel Consumed	Standard Deviation
Dataset A - 30 Drivers - 63km route - 86 logs	4.9922 Liter	4.5603 Liter (-8,6%)	5.6789 Liter (+13,7%)	0.2461 Liter (4,9%)
Dataset B - 4 Drivers - 63km route - 117 logs	4.2952 Liter	3.7565 Liter (-12%)	4.7684 Liter (+11%)	0.1923 Liter (4,5%)
Dataset D - 3 Drivers - 78km route - 20 logs	5.3573 Liter	5.0386 Liter (-6%)	6.1793 Liter (+15%)	0.3646 Liter (6,8%)
Dataset E - 2 Drivers - 39km route - 10 logs	2.7316 Liter	2.4821 Liter (-9%)	3.0879 Liter (+13%)	0.18120 Liter (6,6%)

Table 6: Fuel Consumption Variations Related to the Driving Style (The Four Datasets are Introduced in the Annex of this Work)

- Regarding the results of the recordings analysis, following observation were made:
- The variations amplitude seems to depend on the vehicle type, the route, the traffic conditions, and probably other non-recorded factors.
 - The difference between minimum and maximum is around 20%, so the driving style is responsible for up to 20% variation in the fuel consumption.
 - The standard deviation is around 5% (Datasets D and E small amount of recordings have a negative influence on the standard deviation).

The results have been confirmed by the published values. It has been shown that the driver responsibility in the fuel consumption, depending on the car and the environment, is circa an average 25%, and in extreme situations over 30% [DATG11] [FKAa09] [FedS10].

Also, tests were conducted on a route defined to match the statistical percentage repartition of route types driven in Germany, with a selection of German population representative test

drivers (over age and sex). The driver related fuel consumed standard deviation was measured to be +/-6.5 % with a maximum deviation of 33% [RuBa11].

Regarding the fuel consumption reduction measured while EcoDriving, the following observation have been made:

- As part of the Fiat Eco:Drive, which concentrates on the driving style, 428 000 routes were driven from 5.697 drivers in 5 countries in 150 days. It was shown during this study that EcoDriving saves up to 16% fuel. The maximum potential was found out to be in gear selection and deceleration [Fiat10].
- Johansson et. al. [JoFa99] compared a group of EcoDriving trainees before and after their training on a 10 km route. The fuel usage was reduced by 10.9 % average in their test runs.
- Using an anticipatory driving assistance for energy efficient driving, 12.97% savings were realized [BaKo11].
- During tests with a Smart EV, the difference between driving in a moderate manner and more aggressively was measured to be 30% more in energy consumption [BiWa11].
- At the Fleet World MPG (*Miles Per Gallons*) Marathon, United Kingdom's longest-running economy driving event, 53% improvement were achieved in a V8-powered Vauxhall VXR8 driven by two EcoDriving experts, on separate routes covering 350 miles of countryside including a mixture of A and B roads and motorway driving [Vaux11]. During the 2012 edition, the Citroen C1 1.0 VTR achieved an improvement of 28.92%, and the Ford Fiesta EConetic 27.07% [Ford12].

It is very likely that the engine properties define how much influence a driver could potentially have on fuel consumption, and that bigger engines have bigger potential.

- Tests made in Belgium in 1999 using nine different popular cars showed that aggressive driving was responsible for fuel consumption increase of up to 40% depending on road type and technology. The driving style had a greater influence on petrol-fueled than on diesel-fueled cars [VIKe00].

In sum, variation of circa 20% between two extreme drivers has often been measured, and even more in special situations, depending on the route and the surroundings. During EcoDriving studies, improvements of 10 to 30% have been observed. According to these values, a realistic quality goal (Goal (3) in chapter 2) should be to make a fuel consumption prediction with a maximum deviation of around 10%.

After the influence of the driving style on fuel consumption has been estimated and found out to be important, the global influence has been split into the driving tasks. Analyses based on the dataset ST01 (Annex A – page 151) have been performed (Annex E – page 166). This dataset has the most different drivers, and therefore it is particularly interesting to compare EcoDrivers to HFC-Divers (*High Fuel Consumption*).

In a standard vehicle, the driver will control the car using:

- The pedals: gas, brake and clutch. The sensor information was available in the ST01 database for gas and brake. The gear information was not available, but the engine speed was, which allows us to extrapolate the selected gear (the engine rotation to speed ratio is gear specific).
- The steering wheel: the wheel angle sensor information was available.

Additionally, the driver will activate or deactivate some of the electric auxiliaries in the car (there was no information about the auxiliaries use available in the database ST01).

This means that, except for the use of electrical auxiliaries and the gear selection (that is semi-relevant in the case of ST01 because the vehicle was equipped with an automatic gearbox),

there was enough sensor information to decide what is actually important when it comes to fuel consumption. The detailed results are regrouped in Annex E (page 166).

The results showed that:

- The number and length of stops (vehicle engine idle)
- The way the driver accelerates and decelerates or brakes
- The time spent with the engine running at high rpms

had the most influence on the fuel consumption.

Confirming observations made in various studies can be found for:

- The influence of the acceleration:

In comparison of the fuel consumption of a constant driver compared to a nervous driver that was made using the New European Driving Cycle (NEDC), the use of the gas pedal may be responsible for up to 24% increase (5.35liter to 6.61liter) [RaMa08].

- The driving at high speed and/or high rpm:

According the eCoMove project, excessive speed may be responsible for 11% fuel waste [VrMa10].

- The deceleration and the brake pedal use:

Studies as part of the eCoMove project showed that inefficient deceleration and lack of anticipation might be responsible for 22% fuel waste [VrMa10].

A Volkswagen study on a 32.3km test route measured a fuel efficiency improvement of 13% due to deceleration optimization [DoJu12].

In the case of a deceleration from 100 to 50km/h, fuel savings up to 65% have been measured [Dorr03].

- The selected gear:

Using the NEDC, Rabl and Makarenko calculated a 3.5% fuel consumption reduction for early shifting to higher gears (5.35liter to 5.16liter), and a 12% increase when using lower gears (5.35liter to 6.02liter) [RaMa08].

- The steering wheel use:

Electric steering saves an average 0.25 Liter/100km fuel [ÖrRü09]. This means that the curviness of the route has an indirect influence on the fuel consumption.

3.3.2 Driving Behavior: Impact of the Use of Auxiliary Consumers

The use of auxiliary consumers was identified in the early phase of the work as a very complex topic requiring driver identification combined with knowledge about the driver habits, and conditions according to the microscopic (in-vehicle) and macroscopic (vehicle in the surroundings) situation. For this reason, it was decided that the use of auxiliary consumers should be separated from the navigation. Nevertheless, it is noticeable, that the uses of auxiliaries have a remarkable influence on the fuel consumption.

Lunanova [Luna09] lists usually observed power consumption ranges:

Power Consumption [Watt]			
	Minimum	Average	Maximum
Air condition	200	3000	8000
Generator	500	1200	6500
Power steering	100	300	7000
Coolant pump	50	400	1700
Drive unit fluid fan	50	500	4500

Table 7: Typical Power Consumption According to Lunanova [Luna09]

Looking at the average values, it is clear that the use of the air conditioning system, a typical driver behavior that has nothing to do with the driving style, is responsible for the most of the

energy use. However, the quoted numbers might be a little exaggerated compared to information that could be found in two other publications.

Rabl and Makarenko evaluated the consumption increase due to the use of electrical auxiliary (1900Watt with a 1000Watt Air condition) on the NEDC around 20%. The fuel consumption increased from 5.35 Liter to 6.38 Liter [RaMa08].

While describing a new air condition technology developed for the BlueOn EV (vehicle based on the i10), Hyundai measured the energy consumption of a classical air conditioner [LeKw12]. It was found out to be between 2 and 2.5kW when a 0°C outside temperature applies, and the vehicle has to be heated to 23°C. The consumption was dependent on the number of vehicle climate zones that had to be heated (driver only to whole vehicle). Also, the energy consumption was measured to be between 0.8 and 1kW when the outside temperature was 35°C and the vehicle was cooled down to 23°C.

3.4 Existing Models for Driving Style Explanation

Now that the significance of the driver's influence on fuel consumption has been determined, it is necessary to understand why a driver acts, or reacts, the way he does. Before discussing the influence of the driver's surroundings on his driving style, it might be significant to explore the actual psychological explanation of the driving task.

In chronological order:

According to the “**Field of Safe Travel**”, from Gibson and Crooks (1938) [Cacc07], a driver perceives a space around him, in which he can move safely. This space is limited by the traffic, the route, and surrounding object properties that are perceived as being potentially dangerous. In this space, there is a minimum stopping zone, whose size is proportional to the driving speed.

In the “**Driving as a Self-paced Task Governed by Tension/Anxiety**”, from Taylor (1964) [Cacc07], the driving style is described as an auto-regulated system based on tension. If the driver anxiety rises, so does his tension, and the driving style is regulated to lower them. If the driver is feeling too comfortable, he might adjust his driving style to maintain a certain tension to keep him alert

In 1974, Durth presented a **Three-stage model** [Durt74], which this work is based on. The model includes surroundings composed by traffic, weather, route and optical guidance properties that influence the driver and the vehicle as presented in Figure 13.

The surroundings are perceived over the sense organs, and the driving tasks executed with the body muscles, which leaves room for external effects on perception and action. A feedback loop from the vehicle to the sense organ is included to allow a correction of the driving task.

The “**Zero-risk Model**”, proposed by Naatanen and Summala (1974) [Cacc07] strengthens the feeling regulation theory and proposes that, according to his perception, his cognitive ability and his motivation, a driver will adapt his driving style to lower the potential risks towards zero. Two years later, the theory was extended with the notions of time pressure, effort avoidance, the seeking for a determined speed, the remaining distance to the destination and the pleasure of driving. The pleasure of driving was also mentioned beside risk by Rothengatter in 1988 in his “**Risk and the Absence of Pleasure**” theory.

The “**Decision-Theory Model of Danger Compensation**”, from O'Neill (1977) [Cacc07], is a model that is based on an observation made in 1974. O'Neill showed that U.S. race drivers are statistically more often subjected to being implicated in an accident, and to get speeding tickets than the casual driver. He proposes that the driver makes decisions according to his goals, which then influences his driving behavior. Some decisions increase risk (for example an acceleration made for overtaking) and are then regulated by the fear of an accident or punishment.

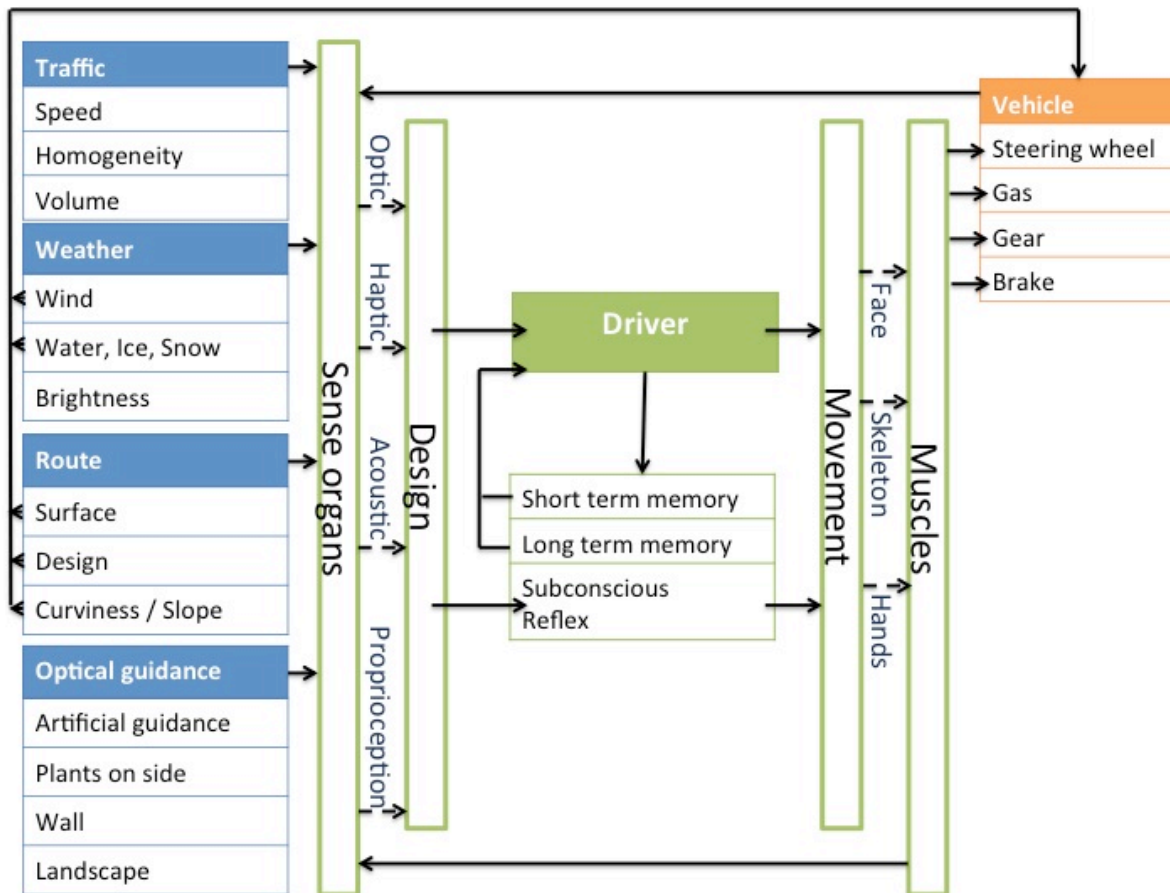


Figure 13: Three-stage Model According to Durth [Durt74]

Another risk-based theory was presented in 1982 from Wilde and is referred to as “**Risk Homeostasis**” [Cacc07]. According to this theory, the driver behavior is regulated depending on his tolerated level of risk. Observation made on taxi drivers driving vehicles with and without ABS, as well as the overtaking of cyclists with and without helmets, seems to confirm the theory. In the “**Threat-Avoidance Model**”, Fuller (1984) [Cacc07] said that the driving behavior for a given situation depends on the rewards and penalty linked to the several alternatives.

In the nineties, the theories proposed were more specific, and the elements influencing the driving style more detailed. In 1993, Hancock and Caird [HC93] mentioned the influence of time and time pressure on the driving style. A driver, and therefore his driving style, is seen to be more and more influenced when the time pressure increases.

Similar to the tension-based regulation; the “**Sensation Seeking**” theory proposed by Zuckerman in 1994 [Cacc07] supposes that every driver has an optimal excitement level. This excitement level is regulated by the provocation or the avoidance of various situations.

In 1999, Ahmed [Ahme99] proposed that the desired speed of travel is defined as the speed a driver wants to maintain after considering the factors of the speed limit of the section he is traveling, the vehicle mechanical capability, the effect of surrounding traffic, the roadway, the weather conditions, and the geometry of the roadway section.

In 2000, Fuller extended the models of Wild and of Naatanen in his “**Task Difficulty**” model [Cacc07]. He added that the complexity of a driving task is a speed-dependent value, but the estimation of an accident probability is not speed dependent as long as the driver has the ability to control the situation.

The “**Drivability**” model from Bekiaris, Amditis and Panou (2003) [Cacc07] describes the following influential factors on the driving task regrouped in five categories:

Driver state:

- Social state
- Psychological state
- Mental state
- Physical state

Knowledge:

- about the vehicle
- about the driving task
- about the route
- about security

Surroundings:

- The route
- The vehicle type
- The weather
- The traffic
- The line of sight

The risk awareness:

- How the risk is perceived
- How much vehicle electronic are operating
- The driver concentration
- ...

The driver tasks:

- Navigation system, telephone use
- Discussion with a passenger

Sakakibara und Tagushi (2005) [ST05] tested the level of Chromogranin A found in saliva (as an indicator of tension) of test persons during a drive. They pointed out a relation between tension and the quality of the execution of the driving tasks. In the same year, Furugori, Yoshizawa, Iname und Miura [FYI05] found out that the level of fatigue was observed to have an influence on the driving behavior.

Complementary Findings

- In a general way, the driver can only drive the way he wishes to if the traffic makes free circulation possible [TrKe10] & [Sand04].
- Young drivers are more influenced by their surroundings, the light condition (day or night drive), the weather, the road condition, the vehicle and the trip motivation [Coms95] & [Shop06].
- In a NHTSA (USA) study in 2002, people were asked to tell the five most important factors that influence their driving behavior [Oecd07]. The weather condition, their self-estimation of the appropriate speed, the speed limits, the traffic condition and the route familiarity were the most often mentioned. The average speed of the surrounding traffic, the risk of being punished and the time pressure were considered to influence their driving style as well.

In summary, the driving style seems to be regulated by the driver tension and the feeling of risk produced by the perception of their surroundings. Also, the traffic condition and the notion of time pressure seem to influence the driver to act in certain ways.

3.5 Situation-dependent Driving Style

As it was found in the previous chapter, the driving style seems to be mostly influenced by the surroundings (on the microscopic and macroscopic level). Therefore, a further analysis of the state of knowledge about the driving style in relation to the surroundings was made.

In a general way, a consortium of Swiss industry companies analyzed the driving style of different drivers [BAFU06] in relation to their surroundings. They started with the following road characteristics grid definition:

- Highways: number of lanes, longitudinal tilt, average velocity, traffic properties (freight proportion), traffic volume (vehicle/h), road work
- Roads outside urban areas: road width, longitudinal tilt, curviness, traffic properties (freight proportion), traffic volume (vehicle/h)

- Roads inside urban areas: operational mode (e.g. right of way, traffic lights), building density, location (e.g. city center), kind of use (e.g. industrial zone), traffic functionality (e.g. main road, side road), number of lanes, separated road/one way, traffic volume (vehicle/h)

They then compared the measured driving style properties of the different categories to keep only the significant ones. They found out that the following grid is sufficient to analyze a situation-dependent driving style:

- Highway: number of lanes, longitudinal tilt (only $> \pm 4\%$), speed limits, traffic volume (vehicle/h), road work
- Roads outside urban areas: curviness defines the base speed, longitudinal tilt, traffic volume (vehicle/h)
- Roads inside urban areas: operational mode (e.g. right of way, traffic lights), building density, road width, and curviness.

Focusing on the fuel consumption, the driving task was split into acceleration, braking maneuvers, speed of travel and gear selection to find out which surroundings characteristics have an effect on the fuel consumption relevant driving tasks.

3.5.1 Acceleration

Besides being limited by the vehicle engine capabilities and the driver anxiety, the acceleration is often assigned to two categories. Ahmed called them the ‘car following model’ and the ‘free flow acceleration model’ [Ahme99]. The first category is limited by the surrounding traffic while the second one corresponds to the driver’s wish or the vehicle capabilities.

3.5.2 Braking Maneuvers

In a similar way, there are two kind of braking maneuvers. The first one happens to prevent a collision with another vehicle while driving in the car following model. The free flow braking is a response to some surroundings characteristics identified by Volkswagen as: speed regulation signs, city boundary signs, stop signs, crossings and sharp curves [DoJu12].

In the case of traffic lights, the distance of the vehicle to the stopping line when the lights turn from green to orange and the driver decides to stop [BeWe07] have a direct influence on the braking intensity.

3.5.3 Chosen Speed of Travel

The vehicle velocity was often seen as the most responsible for accidents, and therefore examined with a particular attention over the year.

Besides speed limits, which obviously regulate the chosen speed of travel [FiCa10], the following characteristics were found out to have an influence on the speed of travel:

The Lane Width:

A relation between the lane width for straight road section [FiCa10] and the speed of travel was analyzed. It was measured that a reduction of the lane width from 8.5m to 5.5m leads to a speed reduction of on average 13% [KöBo79]. Besides that, roads have been often classified according to their width; and the limit for two classes has been frequently defined to be 6m [Trap74] [Lipp97].

According to Ebersbach [Eber06], the influence of the road width depends on the driving style. Sport drivers noticeably reduced their speed according to the road width. The normal driver reacted to the road width depending on the curviness (increased reaction with an

increased curviness) while the relaxed driver didn't show any noticeable reaction to the road width.

The Roadside Development:

Roadside developments classified as commercial, park residential, or school have been linked to speed variations [FiCa10].

The Traffic Condition:

Sandkuehler describes traffic-induced driving situation classes [Sand04]. The situations were divided in two main groups for low speed and high speed (limit was set between 60-70km/h). The low-speed group was composed by situations rearranged in 'stopping', 'following' and 'starting', while the high-speed group was sub-divided into 'approaching', 'accelerating', 'following' and 'free flow'.

Analysis of recordings made in Germany and Netherlands showed a direct relation between the traffic density (number of cars per kilometer and per lane) and the average driven speed [TrKe10]:

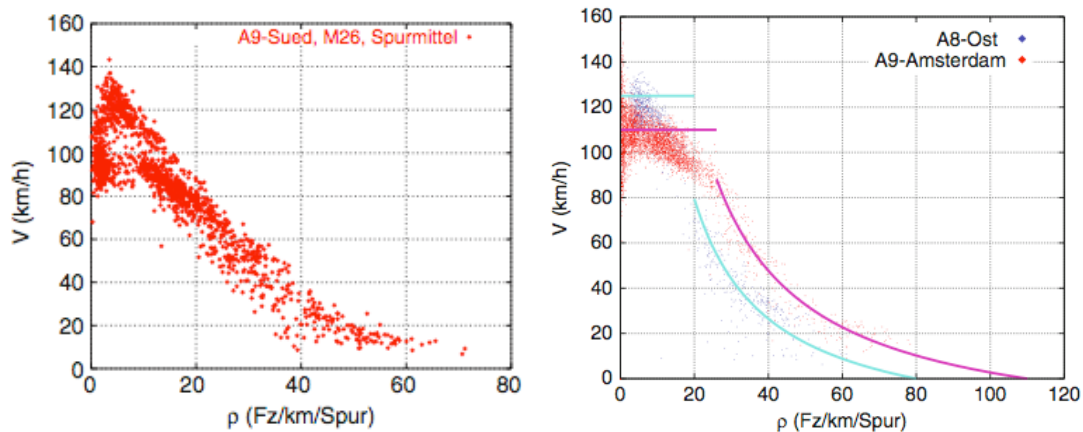


Figure 14: Influence of Traffic Density on the Average Speed of Travel [TrKe10]

Left: measurements on Highway A9 from Nürnberg to München

Right: measurement on A9 from Haarlem to Amsterdam (Netherlands) and A8-Ost around Irschenbergs (Germany)

X-Axis: number of vehicles per kilometer per lane

Y-Axis: observed speed in km/h

Free flow was found out to be possible only for very low traffic density. The relation between traffic density and driven speed resemble a logarithmic distribution.

The Line of Sight:

The influence of sight was almost always merged with the influence of curviness, so that unambiguous findings could not be made with only the line of sight.

The Curviness and Radius:

The road curviness was proven to have an influence on the chosen speed of travel. Curves with a radius up to 350m have a strong influence, while a radius over 500m has no more influence [KöBo79] [Buck92] [FiCa10] [Appe98] [Soso01] [Baka03]. It was noticed, that the definition of the curve extremities and therefore the observed length have a huge importance on the computation of the curviness factor. Disregarding the type of driver (e.g. eco, sport), the radius has an influence on the driven speed. This generally decreases with the radius [Eber06]. Furthermore, the relevance of curviness on the speed of travel seems to be tightly coupled with the change of direction angle [Lamm73] [MeGe75].

The direction of the curve was also found out to influence the speed of travel. Left curves (left driven vehicle) could be ‘cut’ and the visibility was better than for right curves, therefore the speed was observed to be up to 10% faster [DuLi93] [SpBe98].

Despite that the curviness seems to have an influence on the chosen speed of travel, different observations were made on similar curves, indicating that there could be other relevant properties [Lamm73] [Schl76] [Baka03] [Eber06].

The Slope:

While it was shown in the past that slope has an influence on the speed of travel [KöBo79] [Buck92] [Diet65], a more recent study shows that with the augmentation of the engine power, the observation seems to be inaccurate for smaller slopes [Lipp97]. This kind of speed regulation might be mainly due to limited vehicle power.

Other Drivers:

Different studies over the years have shown that excessively speeding drivers motivate other drivers to adopt excessive speeding [CoAb93].

Law Enforcement:

As it was supposed in psychological models, the likelihood of being caught and fear of the penalty defines the chosen speed of travel as well [ShKn85] [ShSt86] [WaRo94]. Therefore, the presence or visibility of law enforcement has an influence on the chosen speed of travel.

Age:

Fildes and Rumbold [FiRu91] reported that young male drivers (<25 years) are most likely to exceed the speed limit. Additionally, two studies [BaMa90] [CoSi92] pointed out that younger drivers tend to drive faster than older drivers and violate traffic laws more often than any other group.

3.5.4 Gear Selection

While speed has been studied over the year to understand and reduce the number of road accidents it has been responsible for, the use of gear hasn't. Gear selection might be adapted during acceleration or deceleration (engine brake), or while driving a slope to run the engine in a powerful way.

3.5.5 Other External Influences on the Driving Style

The Degree of Familiarity

A study of the Köln University and the Universitätsklinikum Essen in Germany showed that the attention and the response time are worse on well-known routes [BrGi10].

The driving style in curves was observed during a study ordered by the Continental AG. It shows that the tension drops while driving in well-known curves, and rises in unknown curves, influencing the acceleration and the uses of the brakes [ElSt03].

The degree of familiarity also applies to the vehicle-driver relation. It was found out that vehicle owners tend to drive faster with their vehicle, as opposed to drivers that are not the owner [EwEb09].

However, it was not researched if the behavior observed is due to the familiarization phase between driver and vehicle, which is necessary to adjust the feelings for the feedback as mentioned in Figure 13.

Previous Speed Restriction

The last valid speed restriction might have an unconscious influence on the driven speed. It was observed, that after driving at 70km/h for three minutes, and driving in a 30km/h zone

after that, the driven speed was 5 to 15km/h higher than the one observed for people who didn't drive at 70km/h before [Dent80]. A more general observation made seven years later measured the average speed of vehicle coming from German highways and Bundesstrassen to be higher than the one of vehicles heading from the city to the functional road classes [CaLu87].

The Traffic

According to the study of Mustyn and Sheppard [MuSh80], over 75% of drivers claim they adapt their speed to the traffic and weather conditions.

In Belgium, nine popular passenger cars (the selection of these cars was based on information supplied by the Belgian Institute of Statistics and the car importers) were tested to find out the influence of traffic on fuel consumption. Traffic condition effect on fuel consumption was measured to be between 20 and 200% [VIKe00]. For city driving, intense traffic increased fuel consumption by 20 to 45%. During rush hours on ring roads, the increases were measured to be between 10 and 200%.

In Canada, a survey mentioned that 52% of the respondents think that it is more important to adapt the speed to the traffic than to the speed limits [Ekos05]. Similar answers were made in Great Britain [Orci05].

It was found out that some Australian drivers chose to drive faster as they wish to prevent some uncomfortable aggressive driving of the other drivers surrounding them [MiZi03].

Rain

While it was raining, a speed decrease of 35km/h in a 375m-radius curve, and of 10km/h maximum on a straight route portion has been measured [HiKn89]. On the other side, Lippard observed a speed increase of 4km/h while it was raining [Lipp94]. Thoma [Thom94] measured the speed of travel and defined three raining classes: 0.5 to 0.9 mm/h; 1.0 to 2.9 mm/h and >3.0 mm/h. He could observe a reduction of the speed of travel in the last defined category. This was confirmed by another study, which measured a maximum 8km/h reduction for sporty drivers. They were showing stronger reduction than 'normal' and 'relaxed' drivers [Eber06].

Older studies ([Hoff84] [Hawk88] [DuBi83]) are no longer relevant because of the distribution of ABS and ESP technologies, which support the driver while driving on wet roads.

Time

Thoma [Thom94] noticed a speed increase in the early morning (5:00AM) of 7km/h, which could be due to the light traffic condition or the time pressure. At night, a little speed increase (up to 1km/h) was observed in all the tests during a five tests series [Eber06].

Alcohol, Drugs and Medications

According to a survey [Hess93], circa one-third of the 17-year-olds take medication. The proportion is similar for adults. Currently taken medications are:

- Headache medicine (66%)
- Pain killer (51%)
- Sleeping pills (21%)
- Stimulants (16%)

All these medications have an influence on the driving behavior [Haur06].

Additionally, feelings [Dvr02], the vehicle type [Alls95], the passengers [EnGr08], and probably other factors were proven to influence drivers.

In summary, based on Dillings three-component model, the driving task can be summarized in the following figure:

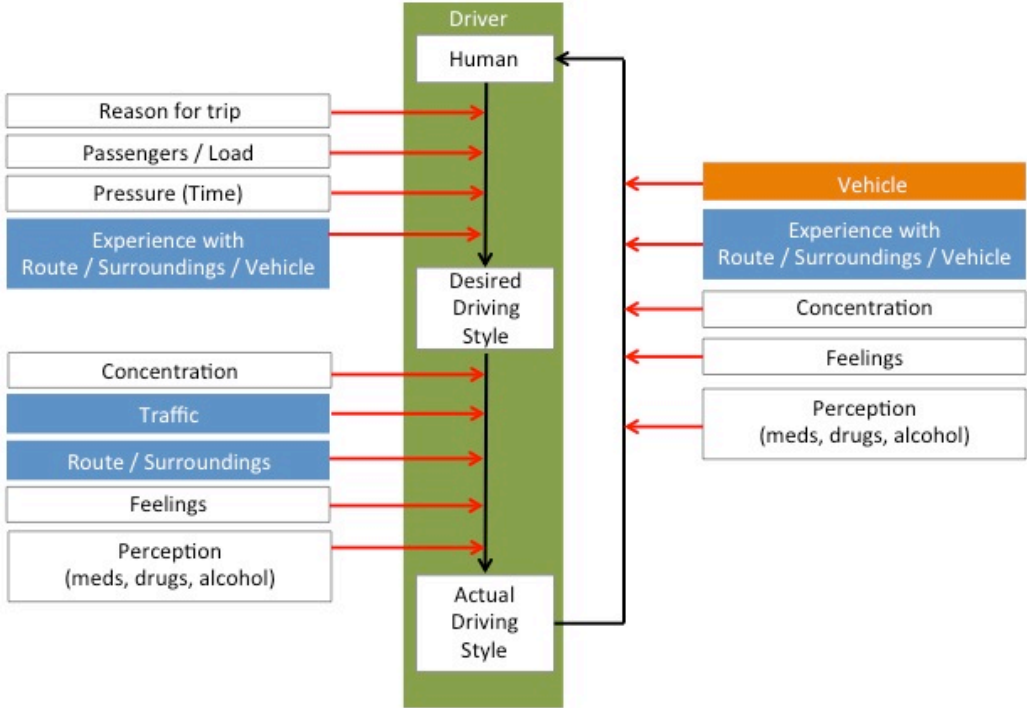


Figure 15: Abstract of the Driving Task Parameters

There are probably more parameters that have an influence on the driver, but studies have been financed and conducted only for limited fields of interests, often related to safety, and for parameters that can be measured.

The Driver’s Degree of Freedom:

During the analysis of the Hi01 data (Annex B – page 156), it was observed that the four drivers, while driving the same vehicle on the same route section at different times, were adapting their speed in a similar way. While the acceleration, deceleration, and chosen speed of travel remain slightly different, it looks like there were unpronounced limitations, producing some rough patterns. In the following figure, the speed variation of the four drivers over the distance is represented in four different colors:

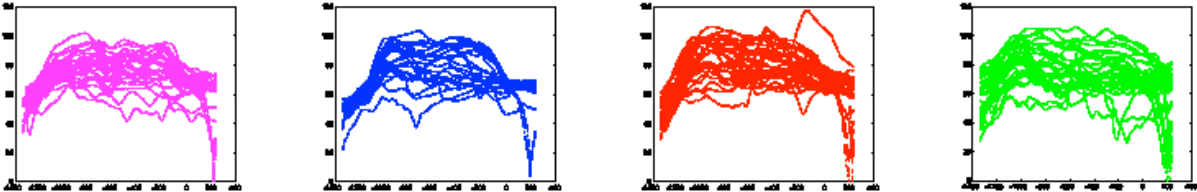


Figure 16: Driver's Degree of Freedom

X-Axis: Distance in meter for a small route section
 Y-Axis: Speed in km/h

There was a traffic light at the end of the selected route section, forcing the drivers to brake sometimes. Otherwise, a minimum speed was always maintained on the segment, while a maximum speed (that does not correspond to vehicle limitation) was never exceeded. The acceleration was limited by the driven vehicle and maybe by the surrounding traffic, while the braking maneuver was sometimes due to the traffic light switching to red. The similarity in the patterns show that a driver has a limited degree of freedom while driving the vehicle, and

therefore, shows us how important the matching of the driving style to the surroundings is for a future prediction.

3.6 Parameters Classification According to their Impact on the Fuel Consumption and their Potential Variation

The vehicle, driver and surrounding characteristics presented in Chapter 3 have been summed up in an overview in Figure 17. Due to the complexity level and in order to make a fuel consumption prediction, the vehicle and driver characteristics have been sorted into three categories:

- The characteristics that are known
- The characteristics that should be learned
 - o No constant value / subject to high variation.
 - o The influence on fuel consumption is important.
 - o The variation frequency is high enough to not consider them as constant.
- The characteristics that should be simplified to constant values or can be ignored.

The collected knowledge presented in Chapter 3 has been used to sort the vehicle and driver characteristics and the results are summed up in Table 8 and Table 9.

The fuel properties and the kind of additives mixed in it are subject to changes every time the fuel tank is filled. Even if the variations are delimited by ISO standards, the engine efficiency may be affected and therefore should be updated in a high frequency to map the influence of the fuel changes, making it possible to consider fuel and additives together. The transmission efficiency includes the gear dependent efficiency of the gearbox, the axle, the differential and the wheels. This value cannot be isolated out of the vehicle sensors recordings, and is relatively constant for higher gears, making an approximation with a constant value possible. The rotational inertia factor must be approximated in a similar way due to the same reasons.

Vehicle Characteristics			
	Is known	Should be learned	Should be approximated (constant)
Vehicle aerodynamic properties		X	
Vehicle rolling and friction resistance		X	
Vehicle mass		X	
Auxiliaries		X	
Fuel type / additives			X
Transmission efficiency			X
Transmission ratio		X	
Engine efficiency		X	
Engine cold start properties		X	
Rotational inertia factor			X

Table 8: Overview of the Vehicle Characteristics that Have an Influence on the Fuel Consumption

It only makes sense to learn what can be recognized in a sufficient resolution and later predicted in the same resolution with enough accuracy. The driver reaction to the weather conditions should be approximated because of the high complexity of weather prediction and variation. Coupled to the complex reaction of a human, the time needed to learn could be longer than that of the vehicle life cycle.

Driver Related Properties			
	Is known	Should be learned	Should be approximated
Acceleration		X	
Deceleration / Braking		X	
Driven speed		X	
Selected gear		X	
Psychological influences	No sensor information available		
Medication / Drugs / Alcohol	No sensor information available		
Time / Trip duration	X		
Drivers reaction to weather conditions			X

Table 9: Overview of the Driver-related Properties that Have an Influence on Fuel Consumption

Additionally, the following surroundings parameters have been found out to be relevant and should be considered while performing a fuel consumption prediction:

- The traffic condition on the route
- The road type / the speed limit / the situations that leads to a stop / the road surface
- The temperature / the air pressure / the wind speed and direction / the amount of water on the road
- The curves and slope on the route

4 Available Information for Understanding the Interactions Between Vehicle, Driver and Surroundings

The following chapter is an overview of the relevant information recorded or available during this work, and the presentation of their sources.

4.1 Information Available from Satellites

GPS stands for *Global Positioning System* and is often misused to describe positioning and navigation devices. The GPS technology was developed by the US army in the 1970s, became fully operational in the 1990s, and was made accessible to the public with partial accuracy.

The satellites send signal continuously, so that a receiver can extrapolate his position based on the position of the emitting satellites (sphere center) and the time needed to receive the message (sphere radius). Considering all the spheres in the same system of coordinates, the receiver is located on the cross section of the spheres. For this reason, at least four satellites are needed to provide a single location point. Then the date and time, as well as the latitude, longitude and elevation, can be extracted from the GPS information.

The signal quality varies depending on the GPS receiver, the possible reflections (e.g. from buildings), and the interruption (e.g. because of a tunnel). Therefore, a navigation system will apply a logical process based on previous speed and direction on the raw GPS data to predict where the vehicle is expected to be and avoid a position accuracy decrease. This process is called ‘dead-reckoning’.

During this work, the GPS position was recorded with an external GPS receiver without dead reckoning functionality and therefore subject to some errors. The following screenshots represents two GPS position recordings coupled to satellite photos (accessed on Google Maps):



Figure 18: GPS Position Without Dead Reckoning and Technical Problems

On the left screenshot, a GPS position accuracy decrease that might be related to the trees along the route, thereby interrupting the signal, is visible. On the right screenshot, a data loss is visible. It is supposed that either the receiver lost satellite reception, or a connection between the recording computer and GPS receiver was interrupted. Regardless, the lack of data and the defective recordings influenced the values extracted from the GPS signal such as speed of travel (and acceleration) and slope.

Extracting the Slope

Navteq (a Nokia brand) and Tele Atlas (a TomTom brand) are the two main data providers for navigation systems in Europe. They both provide databases that includes slope information for the main roads in Germany, and more precisely: on ADAS roads [NavRDF10]. ADAS roads are the roads whose quality and attributes are good enough to allow the operation of the

Advance Driver Assistance System (ADAS) that uses the navigation database. Sadly, slope, even though it might have been available in the navigation system (it is discarded in some navigation database conversions), wasn't recorded during the test drives. Only GPS and CAN signals were recorded. For this reason, slope was extracted out of the GPS_Z (height) logs. The unfiltered GPS_Z signal was available at 1Hz with a resolution of one meter. Because the rest of the data has been synchronized to 10Hz for more accuracy, the slope was extrapolated to the same frequency. On the other side, the height information had to be smoothed to avoid artifacts as displayed in the following figure:

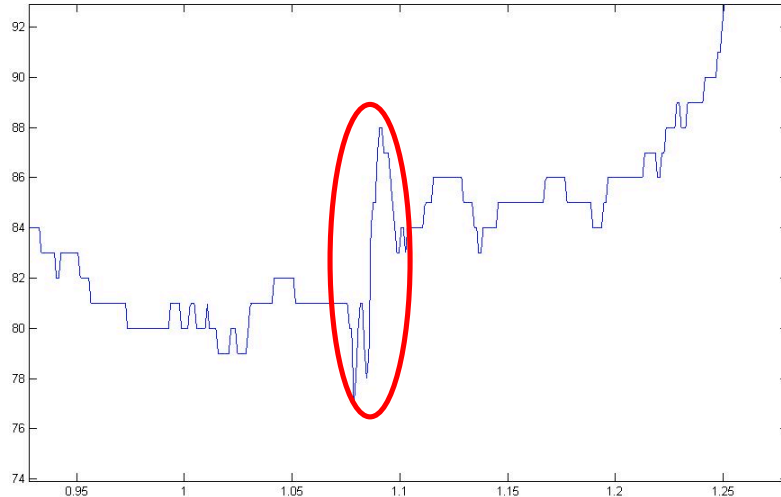


Figure 19: Recorded Height Over a Six Minute Time Period

X-Axis: time in 10^3 sec

Y-Axis: height in meters

Marked in red: potential error that had to be smoothed

Two approaches were considered:

- Smooth the height, extract the slope (at 1Hz) and then extrapolate the values to 10Hz, or
- Extrapolate the height to 10Hz, smooth it and then calculate the slope.

Both of the transformations are similar, just the sequence isn't the same, so therefore the results are expected to be similar. It was decided to use the second option, using a simplified Kalman filter. The Kalman filter was preferred to other filters because of its use (in a more complex form) during the position determination process to counter positioning errors.

The implemented filter was based on the Kalman principle and simplified to following specification:

$$\vec{x} = \begin{pmatrix} z \\ \beta \end{pmatrix}$$

where:

z: the height per second

$\beta \sim \text{slope} = \Delta z$

That implicates $\vec{x}_{n+1} = \begin{pmatrix} z_{n+1} \\ \beta_{n+1} \end{pmatrix}$

$$z_{n+1} = z_n + v_n \times \beta + \text{noise}$$

$$\beta_{n+1} = \beta_n + (x \times v_n + \text{noise})$$

where:

V_n : speed in m/s

We define:

$$A_n = \begin{pmatrix} 1 & v_n \\ 0 & 1 \end{pmatrix}$$

$$Q_n = \begin{pmatrix} noise^2 & 0 \\ 0 & v_n^2 \times x_n \end{pmatrix}$$

$$H = (1 \mid 0)$$

$$R = (\text{var}(gps))^2$$

where:

var(gps)= 2,7595m/s (measured)

Noise was simplified to 0

x_n: slope in degree ~1°/m

Then:

$$x_{n+1} = A \times x_n + Q_n = \begin{pmatrix} 1 & v_n \\ 0 & 1 \end{pmatrix} \begin{pmatrix} z \\ \beta \end{pmatrix} + \begin{pmatrix} 0 & 0 \\ 0 & v_n^2 \times x_n \end{pmatrix}$$

$$z_n = H \times x_n + R$$

The produced slope information over time (in red) is compared to the original data (in blue) in the following figure. After comparing the average values, the standard deviations and the extreme values, the produced slope was found out to be satisfying in quality, and used during this work.

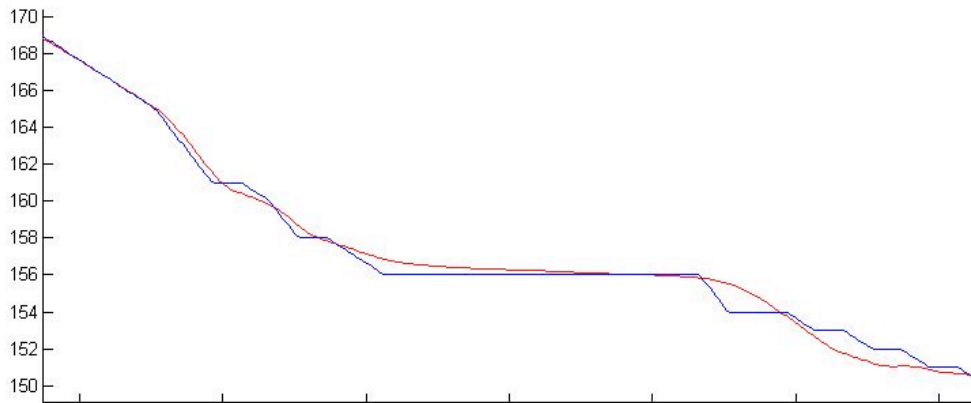


Figure 20: Height Over a Thirty Second Period

X-Axis: time in 10³sec

Y-Axis: height in meters

Blue: original recorded height (GPS_Z)

Red: smoothed height (with pseudo-Kalman filter)

As an alternative, external data such as the one collected during the *Shuttle Radar Topographic Mission* (SRTM) could be mapped to the roads and the slope extracted for all the roads. Similar data could be extracted out of the elevation information used for three dimensional map displays. This would require a lot of computing time but could be done during the map database compilation process.

4.2 Sensor Network Integrated to the Vehicle

CAN bus (*Controller Area Network*) and MOST (*Media Oriented Systems Transport*) are two standards of networks used in the automotive industry to allow a communication between sensors and the entire vehicle electronics. The CAN bus technology is available as part of the OBD2 standard in all the vehicles sold in Europe since 2001 for gas engines (1996 in the USA) and 2004 for diesel engines, and was available in the vehicles used for testing during this work. The recorded signals are listed in the annex that describes the test drives (mainly in Annex A & B).

One of the recorded sensor information was the acceleration, which turned out to be easily distorted, probably due to the vehicle vibrations. For this reason, the acceleration recordings

were swapped with the one calculated out of the speed (based on the wheel sensor), which didn't show distortion.

Acceleration (10Hz) was defined as:

$$Acceleration_t = \frac{Speed_{t+1} - Speed_t}{0.1}$$

Then smoothed:

$$FinalAcceleration_t = \frac{sum(Acceleration_{t-4} : Acceleration_{t+4})}{9}$$

The computed acceleration (in red) is compared to the original recordings (in blue) in the following figure.

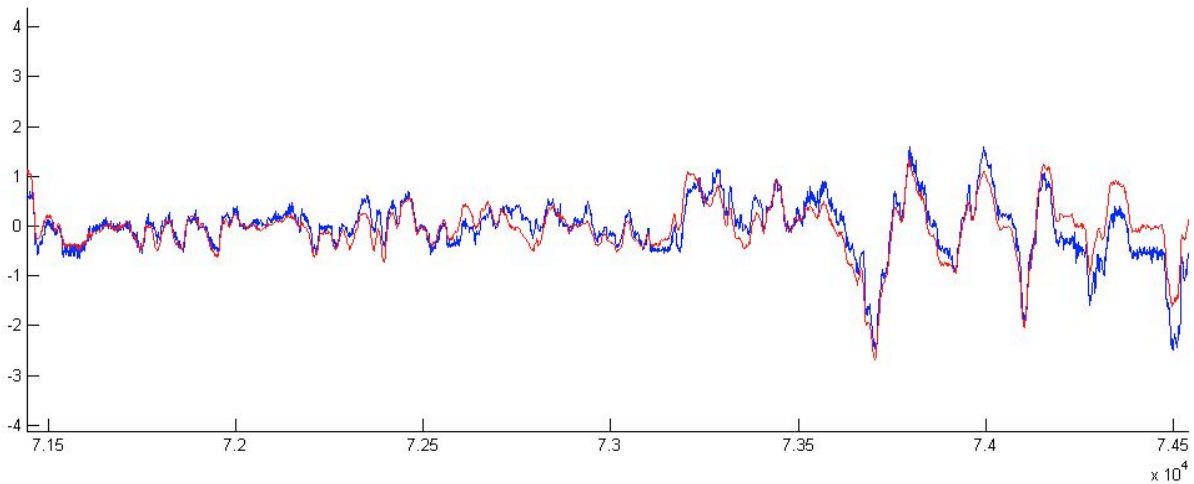


Figure 21: Acceleration signal computation versus the original signal
X-Axis: time in 10^3 sec (5 minutes displayed)
Y-Axis: acceleration in m/s^2
Blue: original recorded longitudinal acceleration sensor
Red: computed and smoothed acceleration from the recorded speed

The deviation between original recordings and computations visible at the end could be explained by a possible lack of resynchronization to zero while driving downhill, but cannot be confirmed.

4.3 Telematics

TMC (*Traffic Message Channel*) and XM Satellite Radio are two technologies for delivering traffic and general information to vehicles. While TMC is available over radio waves, XM uses satellite technology. The services are liable for costs, and while the live traffic state is described in a simplified form for the main roads, traffic state predictions are not available. For example, XMTraffic defines 8 traffic flow states. Seven of them are in the form 'Traffic congestion, average speed of X km/h', where X takes values between 10km/h and 70km/h in 10km/h steps, and a 'traffic flowing freely' informative message.

4.4 Navigation Database

Navteq and Tele Atlas are the two main database suppliers for European and US American navigation databases. The data provided is based on the recordings of a special fleet in charge of collecting accurate geo-positions, road descriptions and video recordings, coupled with information recorded by truck drivers, taxis, mobile phones and other portable devices. The quality of the information and their number varies according to the country and the regions. As mentioned while describing the slope, the best available quality is described as ADAS and is available on the main roads in Germany. According to the Navteq Green Streets sheet

[Walsh10], absolute height and slope, speed limits (on FRC1-4), signals and stop signs, and traffic patterns are available.

Curvature information is not available, but the digitalized knots should be enough to approximate it.

In 2008, Navteq European traffic patterns were limited to the United Kingdom and Germany with a limited availability [Navt08] and often available in a very simplified form, representing general cyclic observation more than actual predictions.

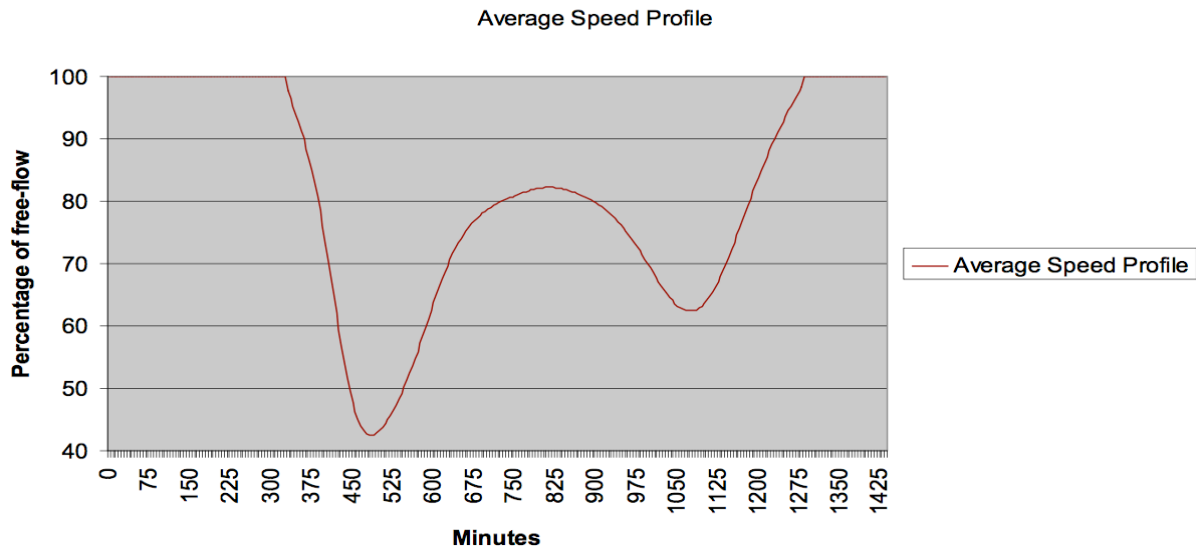


Figure 22: Average Speed Profile Example [TeAt08]

X-axis: change in time over a 24-hour period

Y-axis: percentage value of the freeflow speed for a Transportation Element

Source: [TeAt08]

The pattern doesn't take non-cyclic events as weather variations, road works or holidays (with some exceptions) into account.

Additionally, country-specific (e.g. Russia, China, and India) and Open Source (e.g. Open Street Map) alternatives are available. The number and quality of the attributes needed for navigation is expected to be similar in the best cases.

4.5 Proposed Solution

The main goal of this work is to provide a solution able to learn some of the driver and vehicle characteristics, to later make a fuel consumption prediction. For this reason, characteristics that cannot be recognized or classified during the learning and characteristics that cannot be predicted should be dismissed.

The Weather Conditions:

The temperature should be taken into account since it is often measured by one of the vehicle sensors and predictions are available over the telematics inputs (e.g. XM). The quantity of water on the road and the wind direction are not measurable while driving and were not available for prediction. For these reasons, and despite the fact that the equation was incorporated into the final solution (but commented out), the system performance was not tested to include these two parameters.

The traffic Conditions:

While it is proven that traffic influences the driving style and therefore the fuel consumption, the traffic state prediction is a field of high complexity computations and rarely are precise

predictions available. Since the traffic influences not only the consumption but also the travel time, driver stress and the driving maneuvers, it is expected that online services providing traffic forecasting will increase in quality in the near future, providing a solid base that could not only be used for navigation purposes, but also for macroscopic simulations that make it possible to compute a fuel consumption prediction. The traffic state was neither available nor recorded during the test drives.

The Auxiliaries:

The secondary tasks, including the use of electrical consumers (e.g. air conditioning systems), are very complex to predict and simulate, as pointed out by Lunanova [Luna09].

Because it is not navigation relevant, a prediction using historical data, a driver profile and the sensor information should be developed separately. This decision was later reinforced by a similar decision in the OpEneR project³.

Proposed Solution:

Despite the complexity, the decision was made to build a fuel consumption-oriented simulation capable of learning vehicle and driver characteristics, and to make specific fuel consumption predictions based on the information about the route available during a route calculation.

For the previous mentioned reasons, the proposed solution will not provide an auxiliary instruments usage (e.g. air conditioning usage) prediction, nor will it make a traffic state prediction, but expect the following information to be available from other future distinct sources.

Weather and road description will be incorporated as far as they are available in the actual vehicle sources of information.

³ <http://www.fp7-opener.eu/>

5 Concept and Realization

This chapter describes the solution-setting proposition and realization developed to solve the fuel consumption prediction problem. First, the interaction use cases of the solution prototype with the rest of the navigation system are presented. After which, the details and implementation of every component and database is described. In conclusion an overview of the implemented system prototype is given.

5.1 Concept Presentation and Use Cases

The vehicle and driver characteristics we need to pay attention to, the kind of information that is available to describe these characteristics, and the way they are linked to another has been established. The next logical step is the description of the prototype interaction with the navigation system, and the description of the learning process of the vehicle characteristics values.

There are the three different use cases that can be encountered while navigating:

- The first use case is a classical route calculation. It consists into finding a route between the starting point (usually the actual position) and a destination. This part is done in the navigation system route searching function component. In this case, it is assumed that the vehicle is not moving.
- The second use case describes a moving vehicle without active route guidance. In this case, the prototype learns out of the route segments that have been driven without giving feedback to the navigation system. This use case has a limited application because of the development of the electronic horizon. The electronic horizon is a collection of permanent updated possible paths, and will interact with the fuel prediction component as the route searching does, even if the guidance is not active. That leads to the third use case.
- The last use case is a vehicle moving with an active guidance or a navigation system with an electronic horizon. In this case the system works similar to the second use case, but gives feedback when needed.

5.1.1 Use Case: Route Calculation

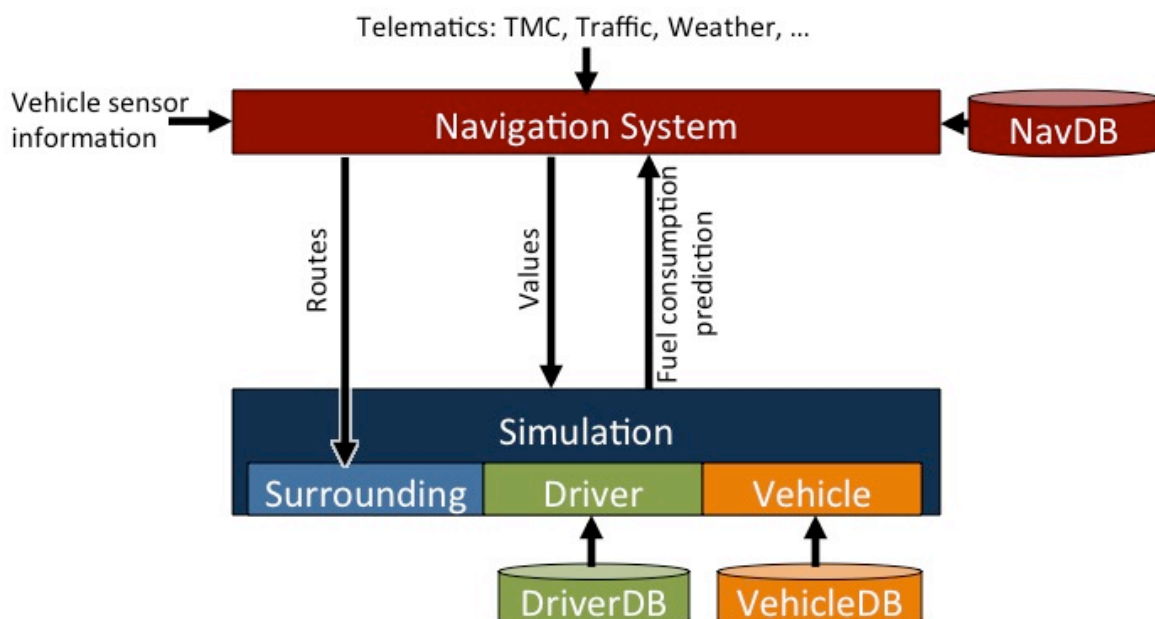


Figure 23: Interaction Between Simulation (Part of the Prototype) and the Navigation System
Use Case: Route Calculation

Blue: Simulation Part of the Prototype

Red: Part of the Navigation System

In the case of EcoRouting, the route-searching component would send the following information to the prototype:

- The route segments sequences with all the available attributes (from the navigation database)
- The actual telematic information available describing the actual surrounding world state
- The actual CAN sensor information describing the vehicle state

This information and the effective driver and vehicle characteristics will then be fed into a simulation (part of the prototype) that computes a fuel consumption prediction for each route and sends the results back to the route-searching component (part of the navigation engine). After that, the route-searching component is able to choose the most economical route for this driver-vehicle combination. Figure 23 above is a graphic representation of the use case.

5.1.2 Use Case: Vehicle is Moving Without a Calculated Route

Although, in the future this use case might be rare, as it is expected that the electronic horizon becomes a standard feature in the navigation system, it is a good introduction to the third use case, which will be presented in the next chapter.

While the vehicle is moving, the prototype receives all available data describing the driver’s interaction with the vehicle and the current vehicle state. In addition, it gets the route segment and surrounding descriptions. Similar to the first use case, it is able to compute the fuel consumption for the last driven segment (using the recorded driver interaction with the vehicle). This time it won’t be sent back to the navigation system, but to a learning component (part of the prototype), that will compare the computed value with the recorded one. If there’s a difference, then the vehicle characteristics database must be updated. The learning component must then decide which characteristic must be updated (Chapter 5.4).

The learning use case is illustrated in the following figure:

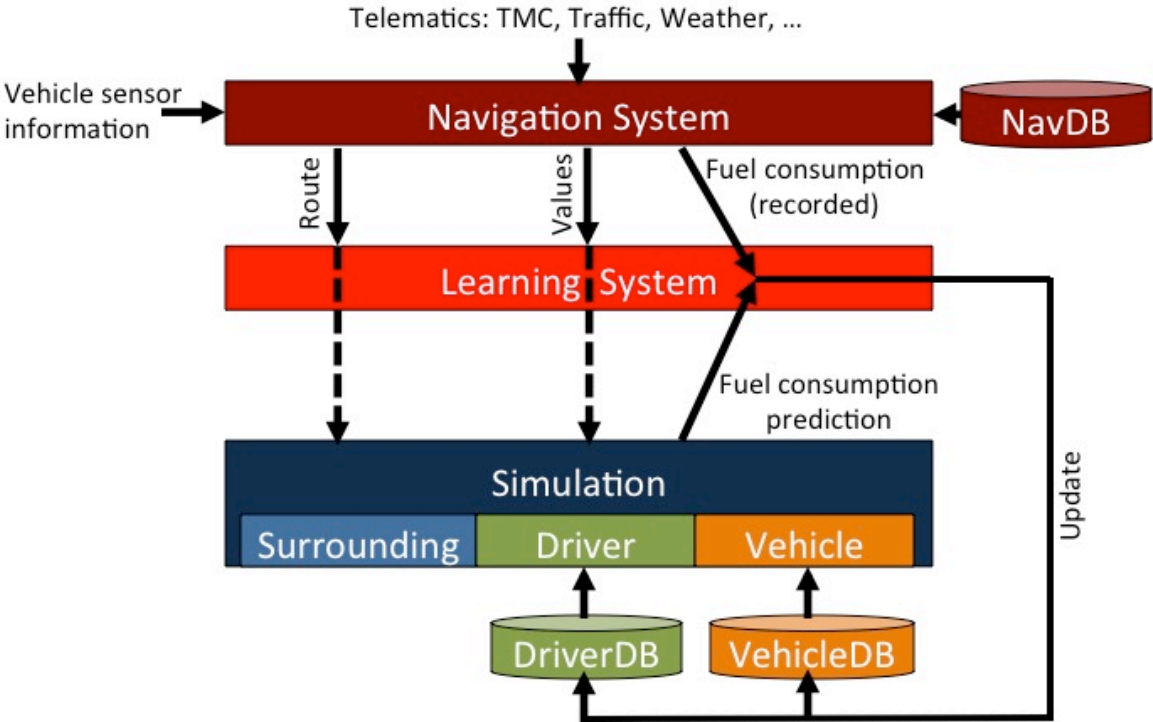


Figure 24: Interaction Between the Prototype and the Navigation System Use Case: Vehicle Moves Without Guidance

Blue: Simulation part of the prototype
 Red (bright): Learning part of the prototype
 Red (dark): part of the navigation system

5.1.3 Use Case: Vehicle is Moving With a Calculated Route

Because of the electronic horizon functionality, this use case is expected to be the ‘standard’ use case when the vehicle is moving. It is a combination of the first and second use cases:

- The prototype updates the database if needed (as described in the second use case)
- The electronic horizon or another component of the navigation system asks for some fuel consumption predictions for different routes (as described in the first use case).

5.1.4 Simulation and Learning Component

According to the use cases, the prototype solution should be made of a simulation and a learning component.

One solution might have been to use the vehicle’s recorded reaction to the driver and the surroundings to find a fitting mathematical function. In this case it would have been difficult to guarantee the quality of the results on roads that have never been driven before. On top of this, some vehicle characteristics that might be important for other system components would have been missing.

For these reasons, the decision was made to go for another solution: a simulation that describes the vehicle, as it is known from the standpoint of physics and mechanics. Besides that, a learning component that uses the same simulation to adapt the learned vehicle and driver characteristics will be implemented. This way, any small simulation inaccuracies will be balanced by the learned characteristics, and a fuel consumption prognostic would still be accurate.

5.2 Realization of the Vehicle Specific Concept Part

In this chapter, the implementation of the ‘vehicle part’ according to the graphical representation in Figure 3 and Figure 4 is described.

It describes the simulation and how the learning component uses it to update the vehicle characteristics database.

The simulation consists of:

- An engine map that connects the fuel consumption to the engine torque and rotations.
- A transmission that links the engine rotations to the vehicle speed.
- An equation that transforms the surroundings influence and forces applying on the vehicle into a torque value..

5.2.1 The Engine Map

The Engine Map represents a simplification of the whole energy conversion process: from fuel to the rotational movement with a moment of a torque.

The impacts of: fuel characteristics, temperature, fuel pump, amount of oxygen in the air, engine characteristics, compressor (turbo or supercharger), cold start, engine efficiency, ECU, λ -sensor, charging pressure, oil and engine frictions, and so on, are represented in this engine map as long as they are relevant.

Sensor Values Available on CAN:

- Engine rotations per minute: this information is needed because it impacts the engine efficiency, the way the compressor (turbo or supercharger) works, the friction with oil and the engine internal friction.
- Torque in Newton/meter: this information is crucial for similar reasons as the engine rotation speed is. A classical engine map describes the relation between engine speed in rpm, engine load (Brake Mean Effective Pressure) and the engine efficiency in percent.

According to [Rajp05]:

“Mean effective pressure is defined as hypothetical pressure which is thought to be acting on the piston throughout the power stroke. [...] Based on B.P. it is called brake mean

effective pressure ($B_{m.e.p.}$ or P_{mb}). [...] The torque and mean effective pressure are related by the engine size.”

and

“Brake power (B.P.). The power developed by an engine at the output shaft is called brake power:

$$B.P. = \frac{2\pi NT}{60 \times 1000} .kW$$

Where, N = engine speed in r.p.m., and T = torque in Nm.”

Because, for a given engine, torque and BMEP are related, an engine map with torque instead of BMEP is also possible.

5.2.1.1 Relevant Input:

The following signals were available:

- Engine rotational speed in rounds per minute
- Torque output in Nm, calculated out of engine sensor
- Incremented consumed Fuel in μ -liter
- Date
- Time elapsed since logging start: for cold start identification
- Engine/Oil Temperature in $^{\circ}$ C: for cold start identification
- Gas pedal pressure
- GPS X Signal (altitude): only available information about oxygen level in the air
- Car identification number

Note: since the altitude didn't vary much during our tests, and the used car remains the same, the GPS_X signal and car ID were ignored.

The following wanted signals were missing:

- Air temperature
- Engine pressure
- Fuel type
- Humidity
- Oxygen level in the air
- Compressor function (turbo charging or supercharging)
- Air / fuel ratio

5.2.1.2 Filling Strategy

Step 1: Import and Synchronization:

Because of the high delivery frequency of CAN message with engine status, it was possible to synchronize the dataset at 10Hz. To do so, three alternatives were considered:

- An extrapolation based on the last recorded two values
- An interpolation based on the last recorded value and the next one.
- Last available value is overreached.

While the first solution offers a precise approximation of the consumed fuel in 0.1sec, the mean engine speed and the mean produced torque in case of a uniform value changing, will fail in case of strong changes.

The second solution has the following problem: there is no way to predict when the next information will be available and, in the worst case, the system could wait forever.

The accuracy of the third solution depends on the update frequency of the CAN messages. If the elapsed time between the last received message and the time stamp considered for synchronization is too long, the last available value may not be valid anymore.

The database that was used during this work provides CAN messages with engine information at a high frequency, and the fuel consumption sensor had an accuracy of 10 μl . Considering that the test vehicle had an idle fuel consumption of 35 $\mu\text{l}/0.1\text{s}$, it means that the error range (30 $\mu\text{l}/0.1\text{s}$ rounded to 35 and 40 $\mu\text{l}/0.1\text{s}$ rounded to 35) was almost 15% in the worst case.

Since there is no torque sensor in the vehicle, torque must have been calculated out of ECU (*Electronic Control Unit*) information (e.g. intake air amount), and seems to have been smoothed since there is no noise observation. It means that the computed torque may also vary from the actual value. Since BMW doesn't communicate on their torque calculation, it isn't possible to estimate the quality of this information, but according to [FFG07] it should be 2-5% deviation at least.

To provide a maximum quality, because the synchronization was running offline and because it was possible to predict when the data stream ends, the decision was taken to implement the second solution (interpolation).

Step 2: Fuel Decomposition:

After synchronization, the consumed fuel was still in an incremented form. The next step was to decompose these values in the amount of fuel consumed during 0.1sec.

- In the database Hi01, Hi02 and Hi03 (see Annex B, C, D), the incremented amount of fuel was stored in an unsigned long integer u32 (value is between 0 and 4294967295), it means that the maximum cumulated fuel value allowed was a bit less than 4295 liters.

- In the database ST01 (Annex A), the fuel value was stored in an u16 (value between 0 and 65535). In this case, a special case of re-initialization (**fuel(i-1) > fuel (i)**) must be considered. The following graphic displays the incremented fuel consumed value over the time. The re-initialization occurs when the value is over 65535 μl .

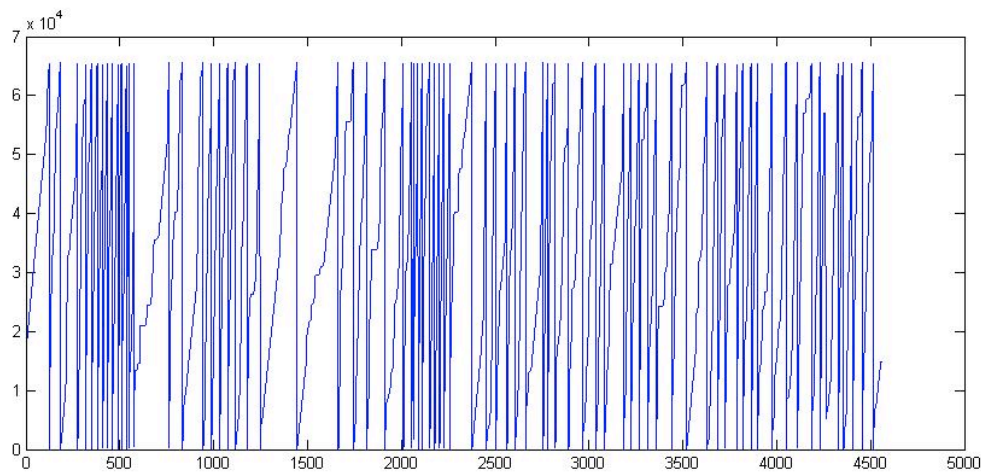


Figure 25: incremented Fuel Value over the Time (ST01 - Driver 15 - First Drive)

X-Axis: time in sec

Y-Axis: fuel volume in μl

In this particular case of a re-initialization, the fuel consumed in 0.1sec won't be equal to **fuel(i)-fuel(i-1)** but to **fuel(i) + [65535 - fuel(i-1)]**.

Step 3: Error Filter:

The dataset may contain some incorrect values. Mostly during the startup phase and sometimes while driving, sensors may return invalid values or no values at all. For example, the following figure shows the fuel injection sensor not responding (the value is not being updated):

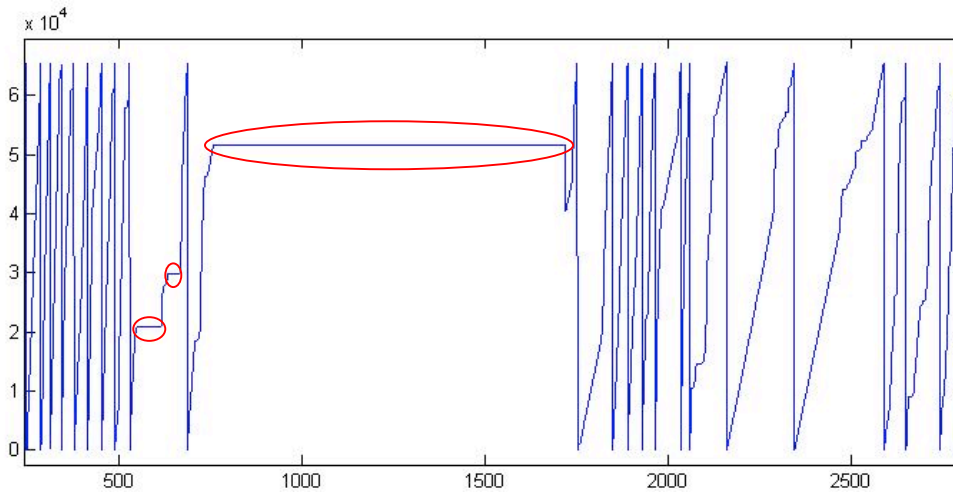


Figure 26: Incremented Fuel Value over the Time (ST01 - Driver 15 - Aborted)
X-Axis: time in sec
Y-Axis: fuel volume in μl
Marked in red: fuel injection is not updated (error)

There are two kinds of possible error filter strategies:

- Define authorized minimum and/or maximum values. This option works only for known engine characteristics.
- Find out which minimum and/or maximum should be allowed with the help of statistics

The following solution was implemented:

- Fuel injection / 0.1sec:

Because there is no energy recuperation in the test vehicles, the minimum value allowed is set to zero. The maximum value depends on the engine properties and has to be found out. The maximum injected fuel can be recorded while the gas pedal pressure is 100%, torque at the maximum and engine speed at the maximum. Because there is no guarantee that this constellation will ever be recorded, another solution was considered.

A normal distribution of fuel injection values for each single combination of torque and engine speed is expected, therefore the three sigma rule can be applied to decide if the last recorded fuel value is valid or not.

For:

- fuel_{REC} : the last recorded fuel injection value associated to a torque ($\text{Torque}_{\text{REC}}$) and an engine speed ($\text{EngSpd}_{\text{REC}}$).
- fuel_{DB} : the mean value of the ten last recorded fuel injection for a given torque ($\text{Torque}_{\text{DB}}$) and a given engine speed ($\text{EngSpd}_{\text{DB}}$).
- fuel_{STD} : the standard deviation calculated out of the ten last recorded fuel injection values for a given torque ($\text{Torque}_{\text{DB}}$) and a given engine speed ($\text{EngSpd}_{\text{DB}}$).

```

find  $\text{fuel}_{\text{DB}}$  for  $\text{EngSpd}_{\text{DB}} == \text{EngSpd}_{\text{REC}}$  &&  $\text{Torque}_{\text{DB}} == \text{Torque}_{\text{REC}}$ 
if  $\text{fuel}_{\text{REC}} > \text{fuel}_{\text{DB}} + 3 * \text{fuel}_{\text{STD}}$  ||  $\text{fuel}_{\text{REC}} < \text{fuel}_{\text{DB}} - 3 * \text{fuel}_{\text{STD}}$ 
then do not use  $\text{fuel}_{\text{REC}}$ 
else: use  $\text{fuel}_{\text{REC}}$  to calculate new  $\text{fuel}_{\text{DB}}$ 

```

- Torque in Nm:

Since there is no energy recuperation, the fuel injection shut off sensor information is a good indicator to determine the minimum relevant entry in the engine map. There is no need to keep record of fuel values equal to zero; it is sufficient to mark the negative torque limit (that changes depending on the engine speed) to recognize the zero fuel injection zone in the engine map.

The maximum torque possibility delivered varies with the engine speed. Because the torque is not measured but calculated, the value can be assumed to be filtered and therefore used as it is.

- Engine speed in rpm: The minimum allowed value is set as the mean engine speed in idle (cold start excluded). Every engine speed record less than zero is ignored. The maximum engine speed can be calculated out of the maximum driven speed recorded and the motor rpm to speed ratio of the highest gear. This ratio is one of the vehicle characteristics that are learned. In a second step, isolated entries (highest entry – second to last >100) and entries higher than 10.000 rpm are erased.

- Engine and oil temperature in Kelvin
Negative temperatures are erroneous and should be ignored. The maximum allowed temperature is not relevant for the engine map. The temperature is used as an indicator to identify a cold start phase if the signals ‘Engine Status WARMUP’ and ‘Engine Status WARM’ are not available.

- Time in seconds
Time should be a positive value, which is greater than the last received time stamp.

Step 4: Resolution:

The following data resolution was available and therefore should be considered as highest possible resolution of the engine map:

- Fuel injection: accuracy of 25 µl
 - Torque: accuracy of 0.5 (ST01 database) or 1 Nm (HI databases)
 - Engine speed: accuracy of 1 rpm
- As described in [GrAn09]:

$$P_B = T \times \omega = T \times 2\pi \times N$$

With:

P_B: Brake power

T: torque

ω: rotational speed in radians / unit time

N: rotational speed in revolutions / unit time

This is equal to:

$$P_B (Watt) = \frac{T(Nm) \times 2\pi \times N(rpm)}{60}$$

The power produced by the engine is related to the amount of power released by the explosion of fuel injected into the engine; therefore, the torque and the engine speed have a similar action to the quantity of fuel injected. The axis of the engine map (torque and engine speed) should have a similar resolution.

Because of that five sets of resolutions were defined:

- Torque rounded off to the nearest 100 rpm and engine speed rounded off to the nearest 20 Nm (in Figure 27 on the right side)
- Torque rounded off to the nearest 50 rpm and engine speed rounded off to the nearest 10 Nm
- Torque rounded off to the nearest 20 rpm and engine speed rounded off to the nearest 5 Nm
- Torque rounded off to the nearest 10 rpm and engine speed rounded off to the nearest 2.5 Nm
- Torque rounded off to the nearest 5 rpm and engine speed rounded off to the nearest 1 Nm (in Figure 27 on the left side)

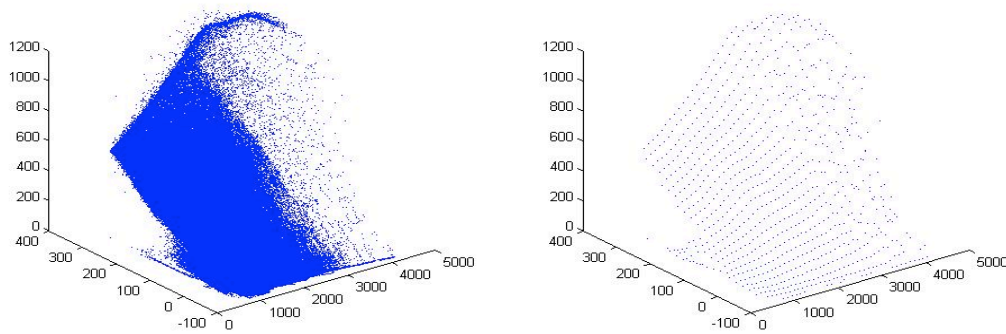


Figure 27: Engine Maps with Two Different Resolutions

X-Axis: engine speed in rpm
Y-Axis: torque in Nm
Z-Axis: injected fuel in $\mu\text{l}/0.1\text{s}$

Step 5: Filling:

The engine map can now be filled with the synchronized and cleaned data. There are three main strategies to fill the engine map:

- Every new input replaces the old value saved in the engine map. In this case, the engine map reacts rapidly to changes (e.g. oxygen ratio, engine failure), but errors that haven't been filtered have a strong negative impact on the engine map quality.

- For each entry in the engine map, the last X-inputs are considered, computed into a mean value and saved into the engine map. This solution is more resistant to errors, but needs more memory (depending on the engine map resolution) and more time to adapt to new engine characteristics. On the other hand, the engine is expected to be relatively stable, and the engine region that is often used should be updated fast.

- For each entry in the engine map, every past input is considered; computed into a value coupled to a factor and saved into the engine map. Memory use stays low, but the engine characteristics evolve very slowly. On the other side, this might be the more resistant option to errors, even though their (low) effect on the calculated value will last forever.

Because of the limited amount of data recorded (compared to a vehicle expected life cycle), the second and the third solution are similar. The datasets were recorded during a short time (a few days to a few months), so it is possible to assume that there was no important engine characteristics change. For this reason the third solution was implemented, and every single input had the same weight.

5.2.1.3 Use Strategy

Within the scope of the vehicle simulation, the engine map provides an amount of fuel consumed in 0.1s for a given torque and a given engine speed.

Case 1: [torque; engine speed] Combination Exists

If the requested torque ($Torque_{WANTED}$) and engine speed ($EngSpd_{WANTED}$) combination is linked to a stored fuel value in the engine map, then the stored value will be returned.

Case 2: [torque; engine speed] Combination is Nonexistent

If ($Torque_{WANTED}$; $EngSpd_{WANTED}$) is nonexistent in the engine map, then there are different options.

As mentioned previously:
$$P_B (Watt) = \frac{T(Nm) \times 2\pi \times N(rpm)}{60}$$

The power is proportional to the torque and the engine speed, it means, if ($Torque_{WANTED}$; $EngSpd_{WANTED}$) is missing in the engine map, it is still possible to approximate the wanted

fuel injection volume using the next match. For example, the fuel injection volume in 0.1s with $Torque_{WANTED}=150$ and $EngSpd_{WANTED}=1960$ is wanted but not available in the engine map (with a resolution of 10Nm and 40rpm). It is possible to approximate the wanted value using the available combinations [150; 1920] and [150; 2000], or the combinations [140; 1960] and [160; 1960] as displayed in the following figure.

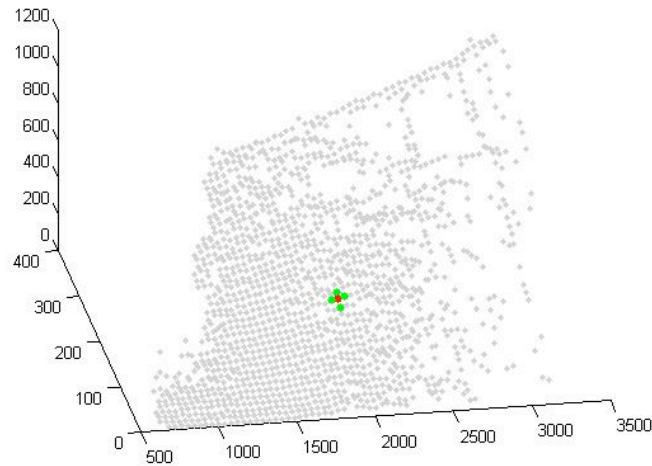


Figure 28: Interpolation in Engine Map (Resolution 10Nm / 40rpm)
X-Axis: engine speed in rpm
Y-Axis: torque in Nm
Z-Axis: fuel injected in $\mu\text{l}/0.1\text{s}$
Red: the wanted combination ($Torque_{WANTED}$; $EngSpd_{WANTED}$) which is not available in the engine map
Green: two possible combinations that can be used to approximate the wanted value

It is always possible to approximate the fuel injection with an interpolation as long as:

- There are two combinations available with:
(Torque < torque_{WANTED}; Engine speed == EngSpd_{WANTED})
&&
(Torque > torque_{WANTED}; Engine speed == EngSpd_{WANTED})

or

- There are two combinations available with:
(Torque == torque_{WANTED}; Engine speed < EngSpd_{WANTED})
&&
(Torque == torque_{WANTED}; Engine speed > EngSpd_{WANTED})

Otherwise, the fuel injection can be approximated with an extrapolation.

Because the fuel injection evolution is not perfectly linear (Figure 29 - combustion engine have a variable degree of efficiency), the approximation quality may vary depending on the used data.

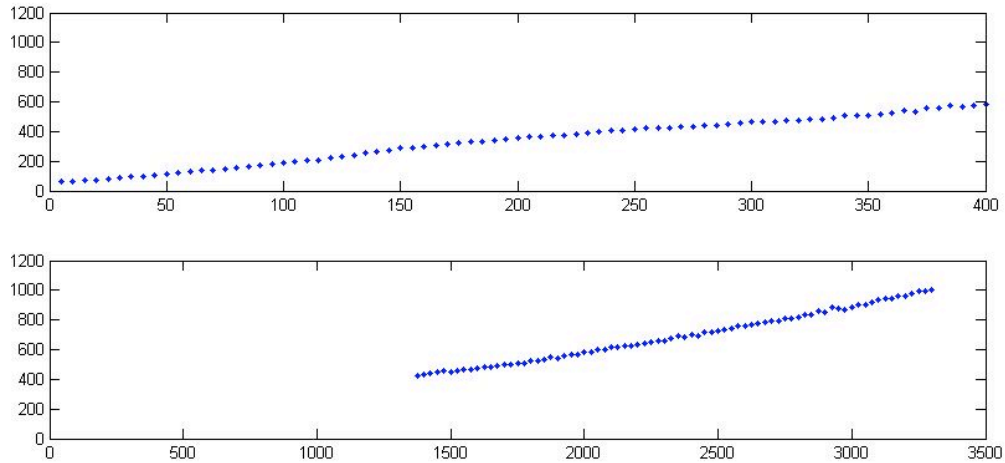


Figure 29: Fuel Injection Volume over Torque and over rpm

Subgraph 1: Fuel Injection Volume over Torque for a Constant Engine Speed of 2000rpm

X-Axis: torque in Nm

Y-Axis: Injected fuel volume in $\mu\text{l}/0.1\text{s}$

Subgraph 2: Fuel Injection Volume over Engine Speed for a Constant Torque of 400Nm

X-Axis: engine speed in rpm

Y-Axis: Injected fuel volume in $\mu\text{l}/0.1\text{s}$

Results are presented and discussed in chapter 6.

5.2.1.4 Exception: Cold Start

A cold start is an engine start while the engine and the fluids have not reached operating temperature. Therefore, the injection timing and injected fuel amount must be adapted to guarantee a proper combustion. The injected fuel amount highly increases during this phase. Ideally, the CAN signals ‘Engine state run’ and ‘Engine state cold start’ are available and indicate without a doubt whether the vehicle is in a cold start phase or not. These signals were not available in the recorded databases. A backup solution is to use the engine, or at least the oil temperature CAN signal coupled with the engine running time since start to determine whether the vehicle is in a cold start phase or not.

The engine temperature is available in degrees Kelvin, so that it is possible to compute the recorded mean engine temperature and standard deviation. For the analysis in this work, it was decided to set the limit to mean recorded engine temperature minus recorded standard deviation and to end the cold start phase the first time the recorded temperature crosses it.

For example (results displayed in Figure 30):

(Based on a test drive recorded on 02.09.11 at 11: 32GMT with the BMW E91 vehicle)

Runtime total: around 1 hour

Measured mean engine temperature: 361.28 Kelvin = 88.13°C

Measured standard deviation: 1.72°C

Limit between cold start phase and normal engine run: 86.41°C

Cold start duration: 170 sec = 2min 50sec since start of recording (it is unknown but unlikely that the records start with the vehicle ignition).

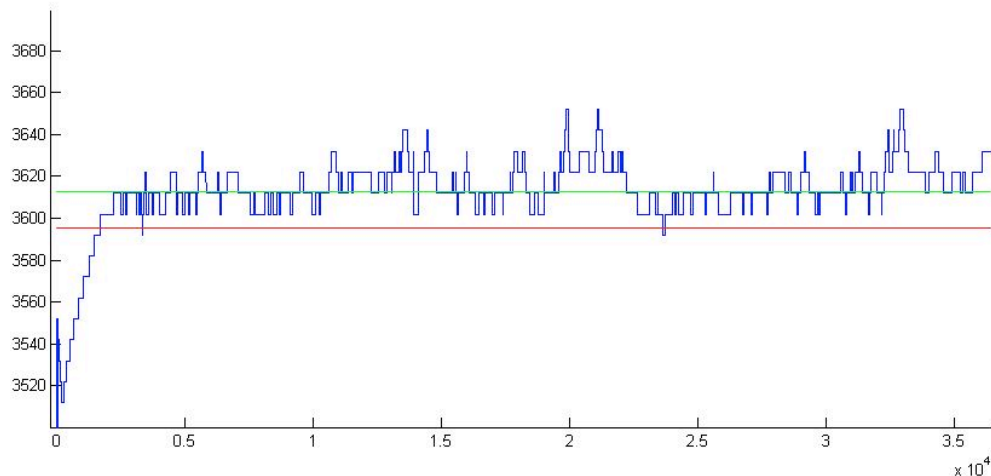


Figure 30: Engine Temperature Variation over the Time (with Cold Start Phase)

X-Axis: time in 0.1sec

Y-Axis: temperature in Kelvin*10⁻¹

In green: the measured mean engine temperature

In red: the limit between cold start phase and normal engine run

Instead of filling a new engine map, the idea is to save cold start phase offsets (the difference between the ‘normal’ fuel injection amount and the ‘cold start’ fuel injection amount) in the existing engine map. The expectation was to observe similar proportional properties as in the engine map, so that a deduction of the cold start fuel injection amount for some engine map area that have not been used during a cold start phase could be made.

The test drives used in this work have been strictly timed, so that the vehicle was almost always moving during the day. The few cold starts that were recorded were early in the morning; however, the vehicle was often on the factory premises for some data check-up or software update. Therefore, and because the cold start phase is short, there is not enough data available to make a quality analysis on the results.

5.2.2 Transmission Ratio

For this work, a transmission is defined as a combination of a clutch, a gearbox, a propulsion shaft, a differential, a drive shaft and a wheel with a tire. The transmission ratio is the relation between the number of engine rotations and the distance the vehicle traveled in meters. This ratio is gear specific and doesn’t evolve over time (unless one of its parts is changed). Wheel sizes (including tire) are considered constant for momentum, although the wheel size might change a little over time depending on:

- Used or new tires: the ratio should adapt to this slow change
- Tire pressure: the pressure augments in the case of a cold start phase and then stabilizes. Tire pressure sensors (The European Commission decided that *Tire Pressure Monitoring Systems* (TPMS) should be available in every new car from 2014 [EU661/2009]) and can be an indicator to adjust the ratio.
- Winter and summer tires may have a minimal difference in size; therefore, the system should recognize a tire change on the traction axle of the vehicle to calibrate the ratio.

Note: The test vehicles both had automatic gearboxes.

5.2.2.1 Relevant Input:

Available:

- Engine rotational speed in round per minute
- Selected gear (and gearbox state: P-N-D)
- Gas pedal pressure

- Speed in m/s
- Longitudinal acceleration in m/s²
- Car identification number

Not available:

- Gearbox state: differential lock front
- Gearbox state: differential lock rear
- Tire pressure

5.2.2.2 Filling Strategy

Step 1: Import and Synchronization:

The importance and synchronization of the data is similar to the engine map part. The data quality varies depending on the wheel rotation sensor accuracy, and is used to calculate the speed. Alternatively, the actual driven speed can be calculated based on the GPS position but the accuracy will vary with signal quality, the number of used satellites and the actual driven speed. For this reason, it was decided to use the vehicle sensor based speed.

Step 2: Data Filter:

The actual driven speed calculated out of the vehicle sensor doesn't match the speed displayed on the speedometer. According to the Economic Commission for Europe:

“Power-driven vehicles having at least four wheels and used for the carriage of passengers” and “Vehicles used for the carriage of passengers and comprising not more than eight seats in addition to the driver's seat” belong to the vehicle category M1 [ECEWP39], and the following rules then apply:

“The production shall be deemed to conform to this Regulation if the following relationship between the speed indicated on the display of the speedometer (V_{speedo} ⁴) and the actual speed (V_{real} ⁵) is observed“:[ECERE39]

$$0 \leq (V_{speedo} - V_{real}) \leq 0.1 \times V_{real} + 6 \text{ km/h}$$

At this point, it is ambiguous if the value available on CAN is V_{speedo} or V_{real} .

Because of the observation made while analyzing the driving style, it can be assumed that the value available in the test vehicle (BMW E91) is V_{real} . This observation can't be generalized; therefore in case the available value is V_{speedo} , it should be converted to V_{real} .

- Selected gear information:

Note: Continuously Variable Transmissions (CVT) and manual transmissions couldn't be tested and will therefore be ignored. However, based on the theory, it is expected that both systems would actually work with the simulation as long as:

- The CVT logic is known or can be deduced (expectation is that the CVT tries to maintain the constant optimum engine rpm).
- Manual transmission: the clutch pedal status (pressed or not) and the selected gear must be available on CAN.

Both test vehicles had an automatic gearbox; unfortunately, the selected gear information wasn't available on the BMW E60 (ST01 – Annex A), so that the observed results must be limited to the gearbox that was used in the second test vehicle. The BMW E91 gearbox is made by the ZF Friedrichshafen AG and is a classical planetary gearbox similar to other automatic gearboxes provided to car manufacturers. Therefore, it is very probable that the observation made can be transferred to other gearboxes.

⁴ In original text: “V1”

⁵ In original text: “V2”

Depending on the driver, the driven speed and the gear, strong variations of the computed transmission ratio were observed. One possible logical explanation is that the sensor information (Engine rpm and driven speed) is not synchronic, and/or that the calculated driven speed is false or needs some time to adjust after strong acceleration or deceleration. Two different filters were tested, depending on the available sensor information:

- In the first alternative filter (no gas pedal pressure information available), the following entries were dismissed:

$$t_{Gear-shift} - 1sec \leq \dots \leq t_{Gear-shift} + 1sec$$

$$Longitudinal_acceleration \leq -0.2m/s$$

$$Longitudinal_acceleration \geq 0.2m/s$$

$$Lateral_acceleration \leq -0.15m/s$$

$$Lateral_acceleration \geq 0.15m/s$$

- In the second alternative filter, the following entries were dismissed:

$$GasPedal_pressure > 0$$

Step 3: Filling:

The particular example display below is based on following drive:

Database: Hi01

Driver: R.

Date: 05 September 2011

Time: 10:30am

There were 22953 entries with following characteristics: {engine rotational speed in rpm; speed in m/s; selected gear; longitudinal acceleration; gas pedal use} after the 10Hz synchronization.

Figure 31 (left) shows all the recorded 22953 entries.

Figure 31 (middle): after applying filter alternative one the entries were reduced to 3488.

Figure 31 (right) alternative filter two: the entries then are reduced to 3814

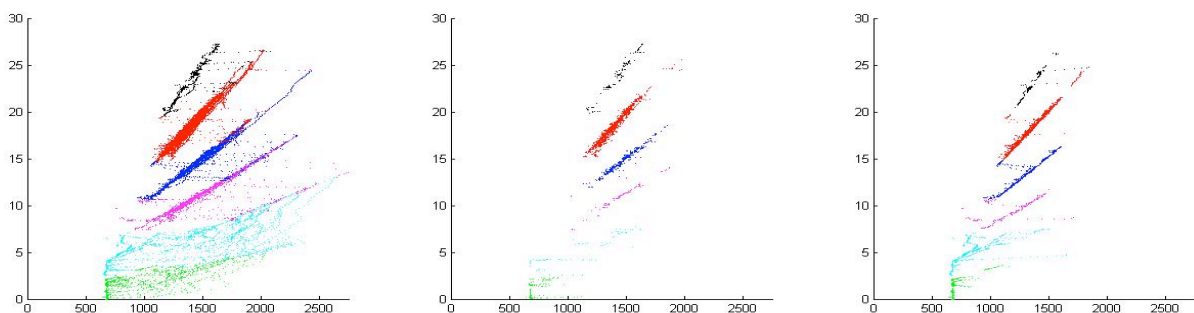


Figure 31: Speed in m/s in Relation to the Number of Engine Rotations per Minute

Hi01 – driver R – 05 September 2011 – 10:30am

X-Axis: Engine rotation per minute

Y-Axis: Speed in m/s

First gear: green

Second gear: cyan

Third gear: magenta

Fourth gear: blue

Fifth gear: red

Sixth gear: black

Expected are six distinguished lines representing each gear ratio. Results are discussed in chapter 6.

5.2.2.3 Use Strategy

A gear specific coefficient can now be calculated out of the remaining entries. Those coefficients link the driven speed to the number of engine rotation per minute for each single gear. Because the driving style is described with driven speeds, selected gears and typical longitudinal acceleration; the missing links to convert this information into engine revolution, and thereby use of the engine map, is now available.

5.2.3 Remaining Vehicle Characteristics

To be able to use the engine map and therefore make a fuel consumption prediction, two inputs are needed:

- The number of engine rotations, which can be derived out of the prognosticated speed and selected gear using the transmission ratio.
- The moment of torque that lasts on the engine in Newton per meter.

In the following subchapter, a way to calculate the engine torque out of the external forces that applies to a moving vehicle is presented.

5.2.3.1 Calculating the Torque

According to Newton's third law of motion:

For every action, there is an equal and opposite reaction

It means in the case of a moving vehicle that:

The force needed to move the car: $F_{\text{wheel_force}}$ is equal to the sum of the forces that apply on the moving car. The most important forces are listed in the theoretical part of this work and can be reduced to:

- Air resistance (Chapter 3.2.1.1): F_{air}
- Rolling resistance (Chapter 3.2.1.2): F_{roll}
- Acceleration (Chapter 3.2.2.2): F_{acc}
- Slope resistance (Chapter 3.2.2.1): F_{slope}

In Summary:

$$F_{\text{wheel_force}} = F_{\text{air}} + F_{\text{roll}} + F_{\text{acc}} + F_{\text{slope}}$$

The power the engine has to provide is related to $F_{\text{wheel_force}}$, and therefore $F_{\text{air}} + F_{\text{roll}} + F_{\text{acc}} + F_{\text{slope}}$, over the whole transmission. In addition, the electric generator, which is powered by the engine, is responsible for an extra resistance.

In rotational systems (the rotating engine), power is defined as:

$$P_{\text{engine}} = T \cdot \omega$$

With:

P: the power output of the machine

T: the torque Nm

ω : rotational speed in radians per seconds

It means:

$$P_{\text{engine}} = T \cdot 2\pi \cdot \frac{\omega}{60} \quad \text{and} \quad T = \frac{P_{\text{engine}}}{2\pi \cdot \frac{\omega}{60}}$$

With:

P: the power output of the machine in Watts

T: the torque in Nm

ω : rotational speed in rpms

In mechanical systems (the vehicle on the road), power is defined as:

$$P_{\text{vehicle}} = F_{\text{wheel_force}} \cdot v$$

With:

P: the power at the wheel in Watts (because 1 Watt = 1Nm/1sec)

F_{wheel_force} : in N

v: the velocity in m/s

Because P_{engine} and $P_{vehicle}$ are linked together over the transmission (with loss μ in percent) and the power needed for the generator as to be added:

$$P_{engine} = \frac{P_{vehicle}}{\mu} + P_{generator}$$

Therefore:

$$T = \frac{\frac{F_{wheel_force} \cdot v}{\mu} + P_{generator}}{2\pi \cdot \frac{\omega}{60}} = \frac{\frac{(F_{air} + F_{roll} + F_{acc} + F_{slope}) \cdot v}{\mu} + P_{generator}}{2\pi \cdot \frac{\omega}{60}}$$

The prediction of $P_{generator}$ for energy consumption prediction has a high complexity because it is dependent on where, when and who drives, or rather what electric consumer the driver will choose to activate. It has been decided that a special component dedicated to $P_{generator}$ forecast is necessary; therefore it has been simplified to a constant value $T_{generator}$ for this work. Despite the fact that the value is engine rotation dependent, the mean of the recorded torque while the vehicle isn't moving was extracted and used. The previous equation can be simplified to:

$$T = \frac{(F_{air} + F_{roll} + F_{acc} + F_{slope}) \cdot v}{2\pi \cdot \frac{\omega}{60}} + T_{generator}$$

With:

T: the torque in Nm

$F_{air} + F_{roll} + F_{acc} + F_{slope}$: the forces that apply on the moving car in Newton

v: the vehicle speed of travel in m/s

μ : the transmission loss in percent $\sim 90\%$ in the case of an automatic gearbox (see theory chapter)

ω : rotational speed in rpms

$T_{generator}$: an approximation of the needed torque to run the generator

5.2.3.2 Vehicle Characteristics Needed to Compute the Torque

Starting from the previous equation, $F_{air} + F_{roll} + F_{acc} + F_{slope}$ must be calculated to find the torque that applies on the engine. Referring to chapter 3.2:

- The air resistance is approximated with $F_{air} = \frac{\theta}{2} \cdot c_w \cdot A \cdot v^2$

While ' θ ' can be approximated and ' v ' is known, ' $c_w \cdot A$ ' is unknown and therefore must be learned.

- The rolling resistance is approximated with $F_{roll} = c_{r-speed} \cdot m \cdot g$

Where ' v ' and ' g ' are known values. The vehicle mass ' m ' is unknown and therefore must be learned.

- The acceleration force is approximated with $F_{acc} = \lambda \cdot m \cdot a$

While the acceleration 'a' is given from the recorded CAN, and λ (rotational inertia factor) is approximated, the vehicle mass 'm' is unknown and therefore must be learned.

- The grade resistance is approximated with $F_{slope} = m \cdot g \cdot \sin \alpha$

The gravitation force 'g' is approximated (9,81m/s) and 'sin α ' computed out of the route segment slope database value.

The vehicle mass 'm' is unknown and therefore must be learned.

To sum up: The vehicle characteristics missing to solve the previous equation are:

- The air drag coefficient multiplied with the vehicle front surface. The value out of this product is called 'air resistance coefficient' in the rest of this work.
- The speed dependent rolling resistance coefficient of the tires.
- The vehicle mass.

5.2.3.3 How the Vehicle Characteristics are Learned

The learning phase (when activated, see chapter 5.1.2 and chapter 5.1.3) is used to update the engine map, the transmission ratio and the three previously defined vehicle characteristics, if needed.

It is based on multiple comparisons between predictions out of the simulation and recorded values. These comparisons are then used to decide what part should be updated if necessary.

If $fuel_{predicted} \neq fuel_{recorded}$:

- With: $rpm_{predicted} = rpm_{recorded}$ and $torque_{predicted} = torque_{recorded}$ then, the engine map must be updated.

- With: $rpm_{predicted} \neq rpm_{recorded}$ then, the transmission ratio must be updated.

- With: $torque_{predicted} \neq torque_{recorded}$ then, at least one of the three vehicle characteristics must be updated.

Because the simulation is only an approximation and the origin of the recorded data is not always reliable, a certain level of error can be tolerated (e.g. to avoid a constant learning and therefore reduce the onboard CPU load). Because there was no system load restriction for the prototype, it was decided to go for a zero tolerance strategy, which leads to continuous learning.

While an engine map and transmission ratio constant update is not a problem, it is not always possible to update the vehicle characteristics. Most of the time, it's not possible to distinguish the one characteristic that should be updated from the others.

Therefore, some special use cases where only a few of the four forces (F_{air} , F_{roll} , F_{acc} , F_{slope}) are relevant were defined. Then it was possible to isolate one or two of the vehicle characteristics (C_{air} , $C_{roll-speed}$, and Vehicle mass) and update them.

Three use cases were defined; one for each vehicle characteristic, and then a prototypical dispatcher whose function is to filter the recorded data was implemented. The dispatcher recognizes the use cases, and adapts the selected vehicle characteristic, or if not possible, discards the recorded information.

Updating the Rolling Resistance Coefficient (First Use Case):

First, it is necessary to sort the situations, where the vehicle mass and the air resistance coefficient influences on the fuel consumption are reduced to their minimum. The dispatcher looks for recorded data with a slope and a vehicle acceleration that are almost equal to zero.

In this case it is reasonable to assume that: $F_{air} + F_{roll} + F_{acc} + F_{slope} \approx F_{air} + F_{roll}$

At this point, the main problem was to separate the rolling resistance force from the drag force. Because the two forces always apply on the moving car, it is impossible to separate them. One solution would have been to create a new speed dependent coefficient that would have represented a mix of the two forces, but then the influences of rain, road surface and so on could not have been approximated with the known physical equation anymore. For this reason, it was decided to express the drag force according to the rolling resistance force. Later, the drag force will be updated dependent from the actual rolling resistance coefficient value to balance the possible error due to the first approximation.

Based on the equations introduced in the third chapter, and the characteristics of a selection of 188 BMW vehicles (described in Annex F), analysis regarding the percentage representation

of $\frac{F_{roll}}{F_{roll} + F_{air}}$ over the speed has been made.

The results are displayed in the following figure:

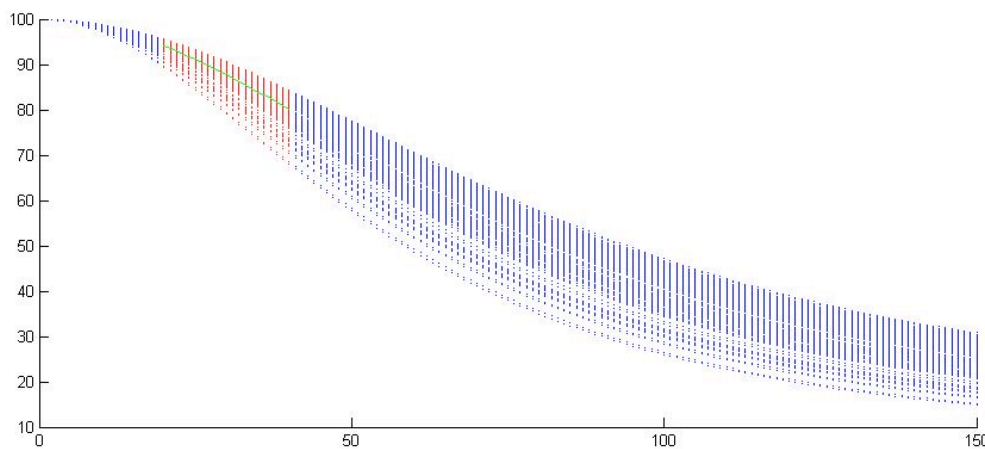


Figure 32: Selection of 188 BMW Rolling Resistance Percentages Depending from the Vehicle Speed

The 188 BMW are Listed in Annex F

X-Axis: Speed in km/h

Y-Axis: percent

Blue: Percentage representation of $F_{roll}/(F_{roll}+F_{air})$ over the speed of travel

Red: Speed ≥ 20 km/h & ≤ 40 km/h selection

Green: mean values of the percentage representation of $F_{roll}/(F_{roll}+F_{air})$

Based on this distribution, it seems that it is possible to find a speed dependent coefficient to express F_{air} according to F_{roll} at low speed. The speed between 0 and 20 km/h is not considered because of the variable transmission degree of efficiency while the gear is engaged (Hydraulic automatic gearbox fluid's influence).

The dispatcher selection to update the rolling resistance coefficient is defined as:

$$(5\text{m/s})18\text{km/h} \leq \text{recorded speed} < (15\text{m/s})54 \text{ km/h}$$

$$-0.2\text{m/s}^2 \leq \text{recorded acceleration} \leq 0.2 \text{ m/s}^2$$

The Matlab function `polyfit` was used to make an approximation of the mean values of the

percentage representation of $\frac{F_{roll}}{F_{roll} + F_{air}}$ with $-0.7077 \cdot v(\text{km} / \text{h}) + 108.6678$

Therefore:

$$F_{air} \approx 1 - \left(\frac{-0.7077 \cdot v + 108.6678}{100} \cdot F_{roll} \right)$$

Then, according to F_{roll} formula and the engine torque formula:

$$C_R = \frac{(T_{CAN} - T_{generator}) \cdot \mu \cdot 2\pi \cdot \frac{(-0.7077 \cdot v + 108.6678)}{100}}{\left(100 + 0.04 \cdot \left(\frac{v}{100 \text{ km/h}}\right) + 15 \cdot \left(\frac{v}{100 \text{ km/h}}\right)^4\right) \cdot m \cdot g \cdot X_{Transmission} \cdot 60}$$

With:

C_R : Rolling resistance coefficient

v : Vehicle speed in km/h

m : Vehicle mass in kg

g : Gravitational acceleration in m/s²

$X_{Transmission}$: The relation between speed in m/s and engine rpm (Chapter 5.2.2)

T_{CAN} : The recorded torque available over the CAN bus

$T_{generator}$: The torque resulting out of the use of electrical components in the vehicle

μ : The transmission efficiency in percent

Updating the Air Resistance Coefficient⁶ (Second Use Case):

Similar to adjusting the rolling resistance coefficient, the dispatcher looks for recorded data with a slope and a vehicle acceleration that is almost equal to zero where it can be assumed that: $F_{air} + F_{roll} + F_{acc} + F_{slope} \approx F_{air} + F_{roll}$

According to the observations made in **Figure 32**, the drag force is much greater than the rolling resistance force at high speed. Therefore, to isolate the air resistance coefficient as far as possible, the dispatcher must consider high speed of travel.

The dispatcher selection to update the air resistance coefficient is defined as:

(30m/s)108km/h <= recorded speed

0m/s² <= recorded acceleration <= 0.15 m/s²

In this case, slope has been extended from -0.2° to -1° and from 0.2° to 1° because the highway part of the Hi01 track would not have been selected to adapt the air resistance coefficient.

According to F_{air} formula and the engine torque equation formula, and assuming that:

$$\theta = 0,349 \cdot \frac{1013,15 - \frac{h_m}{8}}{T_{\circ C} + 273,15}$$

θ : The air density in g/l

h_m : The height in meter

$T_{\circ C}$: The surrounding temperature in °C

Then:

$$A \cdot c_w = \frac{\frac{(T_{CAN} - T_{generator}) \cdot \mu \cdot 2\pi}{X_{Transmission} \cdot 60} - F_{Roll}}{\frac{1}{2} \cdot 0,349 \cdot \frac{1013,15 - \frac{h_m}{8}}{T_{\circ C} + 273,15} \cdot v^2}$$

With:

$A \cdot c_w$: The air resistance coefficient

v : Vehicle speed in m/s

⁶ air drag coefficient multiplied with the vehicle front surface

The rest is identical to the rolling resistance coefficient formula.

Updating the Vehicle Mass (Third Use Case):

The vehicle mass is needed to compute F_{roll} , F_{acc} and F_{slope} . At a first glance there is no reason to use the dispatcher to select only a part of the input, but due to the approximations that have been made so far, it is recommended to discard some special cases.

To compute F_{acc} , an approximation of the rotational inertia factor is used.

As described in chapter 3.2.2.2, the potential error lowers in the higher gears. And as described in chapter 3.2.2.1, the slope has been computed from the GPS data and smoothens out. The slope quality is not expected to be good enough to be used, so for this reason, situations with slope converging to zero will be preferred.

Because of the engine brake side effect, it was decided to discard all the decelerations and situations where the brake pedal was used.

Because of the exponential increase of the drag force and rolling resistance force at high speed, it was decided to limit the maximal allowed speed to adapt the vehicle mass to 90 km/h (when the system starts to adapt the air resistance coefficient).

All this restriction can possibly be optimized to allow the use of more data and increase the speed of the learning effect.

To sum up, the dispatcher selection to update the vehicle mass is defined as:

$$\begin{aligned} 0.2\text{m/s}^2 &\leq \text{recorded acceleration} \\ \text{Gear} &= 4 \mid 5 \end{aligned}$$

Then, according to the forces equations formula and the engine torque equation formula:

$$m = \frac{(T_{CAN} - T_{generator}) \cdot \mu \cdot 2\pi - (F_{air} + F_{roll})}{\frac{X_{Transmission} \cdot 60}{e_i \cdot a}}$$

v : The recorded speed in km/h

e_i : The gear dependent rotational inertia factor

a : The acceleration in m/s²

The other parameters are identical as in the rolling resistance coefficient formula

Updating the Vehicle Characteristics:

The three vehicle characteristics may vary over time. For example, the air resistance coefficient will vary if an active spoiler is activated. However, this kind of change is likely to be communicated over CAN and the system could be prepared. In the case a roof box is mounted on the top of the vehicle, the system has no way to find out, but should recognize the change and adapt to it. Analog changes that are not documented on the CAN may influence the rolling resistance and the vehicle mass.

For this reason, it is important to use the last learned vehicle characteristic values to guarantee the adaptation to newly made modifications.

On the other side, the learning part of the prototype uses the simulation part to approximate the vehicle characteristics. Due to the imprecision of the simulation and the very limited amount of surrounding effects on the vehicle the system is aware of, the learned vehicle characteristics may be subject to strong variation. Therefore, a history of learned vehicle characteristics should be used to compute the mean values, and use these for the fuel consumption prediction.

So the dilemma is: to adapt as fast as possible to change observed in the last recorded values, but on the other hand, consider the history because of the learned noise, and therefore avoid strong variation.

5.3 Realization of the Driver-specific Concept Part

This chapter describes the implementation of the ‘driver part’ as described in Chapter 3.4 and Chapter 3.5. In the Three-stage model, it represents the influence of the surroundings on the driver and its output to the vehicle as highlighted in the following figure.

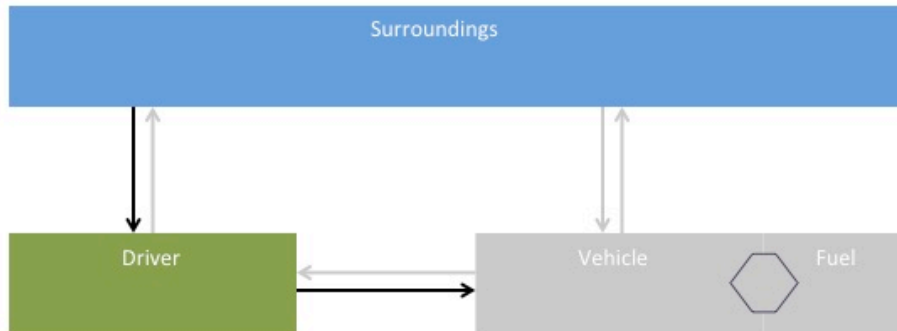


Figure 33: The 'Driver Part' in the Three-stage model

5.3.1 Relation between Surrounding Characteristics and the Driving Style

As mentioned in Chapter 3.4 and Chapter 3.5, it is supposed and partially proven, that several surrounding characteristics have an influence on the driver, his behavior and his driving style. The prototype is supposed to get the torque needed for auxiliary consumers computed from another system component. Therefore, the focus is on surrounding influences on the driving style.

The prototype's first and main objective is to make a fuel consumption prediction for a given route that hasn't been driven before. In this case, the prototype can access the vehicle and driver database, the weather prediction, the traffic state prediction, and the route description according to the database.

It is important to accent the difference between actual weather and traffic information and their predictions. While planning a trip, the driver is not interested in an actual traffic jam that will be gone by the time he will drive into the area.

5.3.1.1 Available Surrounding Influences Description

Although knowledge and formulas that approximate the weather influence on the fuel consumption are available, they couldn't be tested with the test drives recorded during this work. For this reason, and as mentioned in chapter 4, the weather part in the implementation (water and wind influences) was deactivated.

The traffic prediction is a very complex subject that is rarely available as of this date. The live traffic information, on the other hand, wasn't recorded for the few segments of the test tracks even though it might have been available. Therefore, it was also not considered for the rest of this work. The expectation is that, because of the subject complexity, this field will undergo a massive evolution with the generalization of server-based services.

What remains is the description of the route according to the navigation database, and some parameters that can be assumed like daytime and luminosity.

The logical consequence of the observations made previously in Chapters 3.4 and 3.5, is to associate driving style characteristics to 'situations'. In this work, 'situations' are defined as the following:

a combination of surroundings characteristics that have a significant influence on the driving style.

For example, a simple situation could be ‘driving on a highway’, and a precise situation could be ‘driving on a road, outside the city, with two lanes, at night, with three passengers in the vehicle, in a traffic jam, 20 kilometers away from the destination’.

5.3.1.2 Splitting a Route into Situations

Before the prototype starts with the route splitting into situations, these have to be defined. There are two possible ways to define situations: in a static or automatic way.

The static definition of situations requires a fundamental knowledge about the relevance of the different surrounding characteristics to avoid situations with no recorded driving style match. Also, it presumes that different drivers react to the same surrounding characteristics. The problem with this kind of definition is that there is no way to guarantee that all the defined situations will be filled with recorded information. For example, the situation ‘road with a speed limit of 80 km/h’ is defined but the driver has never been on such a road in the past. An error will occur when a new route suggestion guides through a road segment with an 80km/h limited speed.

The automatic definition of situations takes care that the prototype will never be confronted with empty situations. It starts with one situation defined: ‘the vehicle is moving’, and will automatically split the situation when enough information has been collected. For example: someone driving only in the city could have ‘speed limit is less than 50km/h’ and ‘speed limit is more than 51 km/h’. Another driver working in the city and living outside could have: ‘Inner City’ and ‘Outer City’.

In this theory, the automatic solution is the better option. But, because the driving style may vary (e.g. seasonal influence or negative crash experience), and evolve over time (e.g. from vehicle discovery phase to well-known), the database should be able to ‘forget’. This means that old data should be erased, with the condition that some data remains. That erased old data then might implicate a new redefinition of certain situations (e.g. the driver relocates). Therefore, all the information from the past might be saved and the system should compute the new situation splitting from time to time. This implicates a high memory use and high computation power. Such a solution might be outsourced on a server, raising the question of data privacy.

In addition to that, the amount of data recorded by a single driver on different routes to test such a concept, and prove that it might work wasn’t available. For this reason, and because the test track was known and therefore the filling of the defined situations with driving style description assured, it was decided to start with a static situation definition. Only three categories were defined:

- ‘drives on a highway’
- ‘drives on a road outside the city’
- ‘drives on a road in a city’

The second step is based on the findings in Chapters 3.4 and 3.5, and the few road attributes available in the navigation system database. It was assumed that the desired speed of travel was essentially based on the authorized speed. Therefore the typical driven speed should be matched to the speed restriction.

In summary, situations were defined as a combination of road type and speed restriction (e.g. {Highway;120}, {City;50}, ...). In the case a driving style wasn’t available for a given speed restriction, it could be presumed that the driver’s driving style was similar to the one saved in the most similar situation description. Figure 34 illustrates the two-step splitting process for the Hi01 test track (Annex B):

- First, a given route (top) is split into the three categories (middle) -

- Then, there is a second split based on the speed restriction (bottom) -

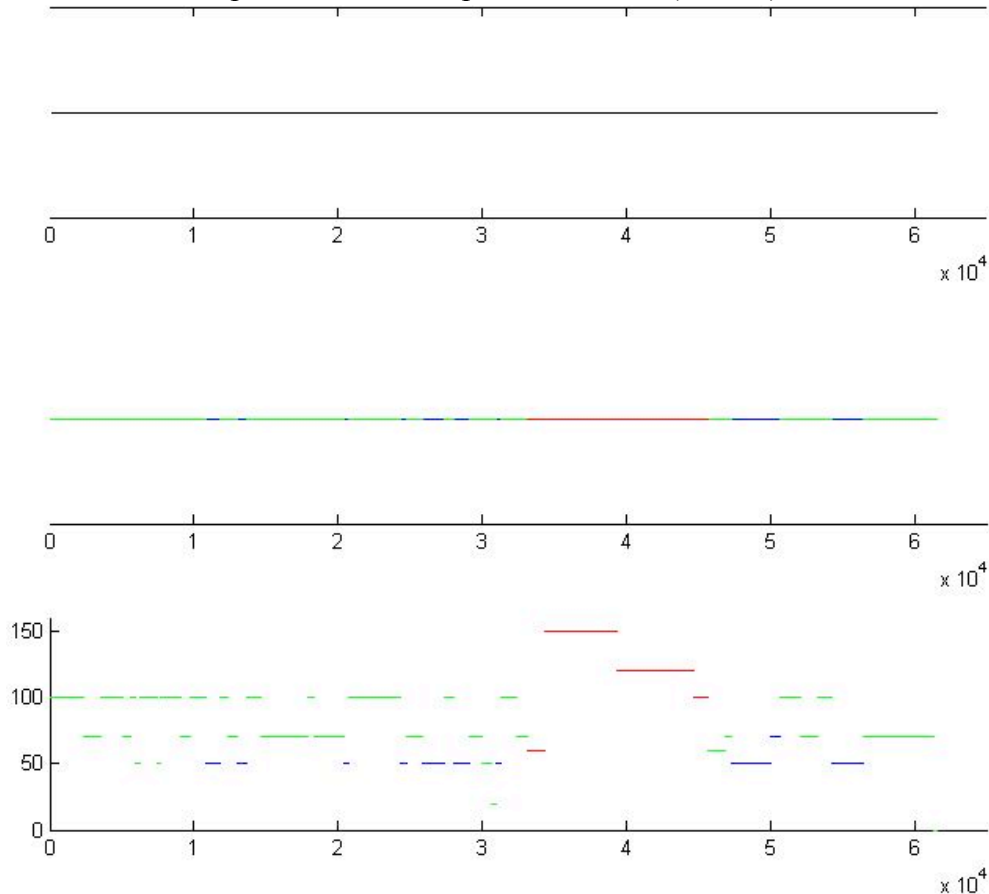


Figure 34: First part of the Route Splitting Process

Test Track Used: recorded Hi01 with speed restriction from video log

X-Axis: Distance in meters

Y-Axis third graph: speed restriction in km/h

Blue: In the city

Green: Outside the city

Red: Highway

Note: the highway part without a speed limit has been replaced with a 150km/h speed restriction for visualization. There was a speed limit of 60km/h on another part of the highway due to roadwork.

For this example, at the end of the splitting process, 47 situations (start and stop included) have been defined. In the best case, the splitting accuracy can only be as good as the database it is based on.

The road type is part of the standard attribute set that is recorded when a road is digitalized and therefore is available for every digitalized road. This attribute won't change often, unless a new settlement is built around the road.

The speed restriction attribute is one of the classical road segment attributes. It is available for every main road in Europe, and almost every secondary road. The attribute quality is defined as 'the number of speed signs that does match the database value'. It varies depending on the roads, the region, the country and the time since the last database update. Although there's no published quality analysis, it is commonly supposed that the quality in Germany, on side roads, with a two-year-old database is between 85-95%. Because of the increasing ADAS that requires a high accuracy of speed signs matching the database, automated speed limit sign recognition solutions have appeared in the last few years. These solutions might help to improve the accuracy in the near future.

Recorded historical speed patterns like ‘Navteq Traffic Pattern’ or ‘Tele Atlas Historical Traffic Speeds’ could be an alternative to speed limits. At this time, there is no known quality or availability analysis for this however.

5.3.1.3 Splitting a Route into Phases

Besides the splitting into database-related situations, another kind of route splitting was considered. With focus on the driver, and based on the background presented in Chapter 3.3.1, it was demonstrated that the acceleration and deceleration maneuver between two situations has an important impact on fuel consumption. Therefore, it was decided to divide the route into two kinds of phases:

- A stabilization phase, when the driver tries to maintain the vehicle at a constant speed
- A transition phase, when the driver adapts their speed of travel to a new situation.

For the example used in Figure 34, 47 transition phases (Figure 35– top - in magenta) have been defined to the 46 stabilization phases (Figure 35– top - in black).

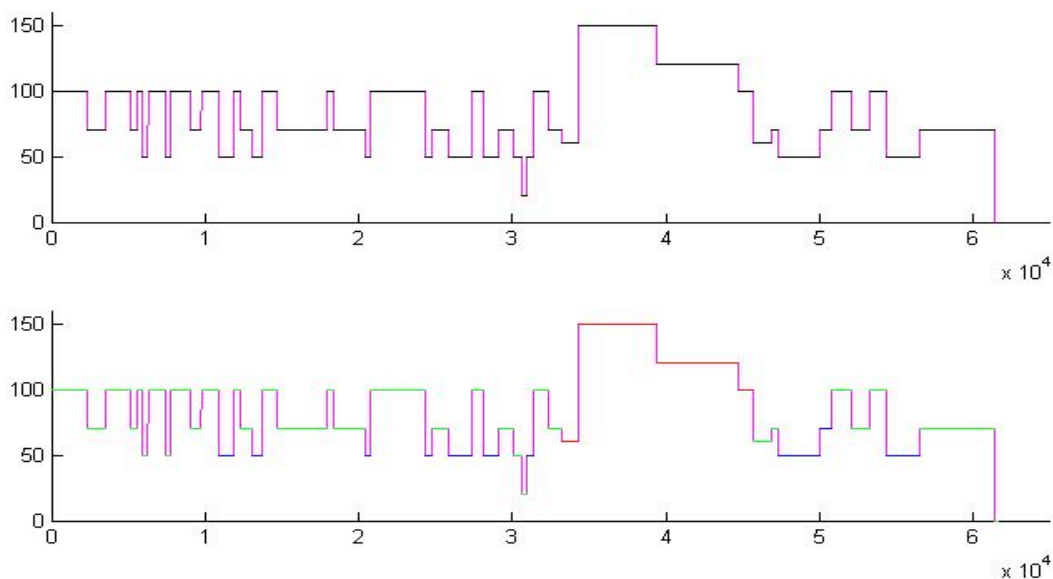


Figure 35: Second Part of the Route Splitting Process

Test track used: recorded Hi01 with speed restriction from video log

X-Axis: Distance in meters

Y-Axis: Speed restriction in km/h

Black: Stabilization phase

Magenta: Transition phase

Blue: In the city

Green: Outside the city

Red: Highway

Summing up (Figure 35– bottom): there are 46 transition phases, and 47 different stabilization phases according to their speed restriction, and road type.

5.3.2 Driving Style Mapping

The route is now divided into situations. To make a fuel consumption prediction, driving style specific to these situations must be learned. This means:

- While the vehicle is moving, the prototype should differentiate the transition phase from the stabilization phase, and in the best-case scenario, without using the database information because this might be false.

- The driving style characteristics that have to be learned (e.g. typical acceleration) must be linked to the road type and the driven speed.

5.3.2.1 Differentiating a Stabilization Phase from a Transition Phase

The test drive analysis of the four test driver's driving styles on the test track Hi01 (Annex B) brings similar results: the vehicle was almost never moving at a perfect constant speed, and the distance driven while accelerating (longitudinal acceleration is >0) is comparable to the distance driven while decelerating (longitudinal acceleration is <0). Therefore, two limits must be set to isolate transition from stabilization without using the navigation database information.

$$\text{Transition} < \text{Deceleration limit} \leq \text{Stabilization} \leq \text{Acceleration limit} < \text{Transition}$$

One solution that might be apparent is to use a recorded mean acceleration value as a limit. The mean positive acceleration for the three defined road types is displayed in the first row of the following figure.

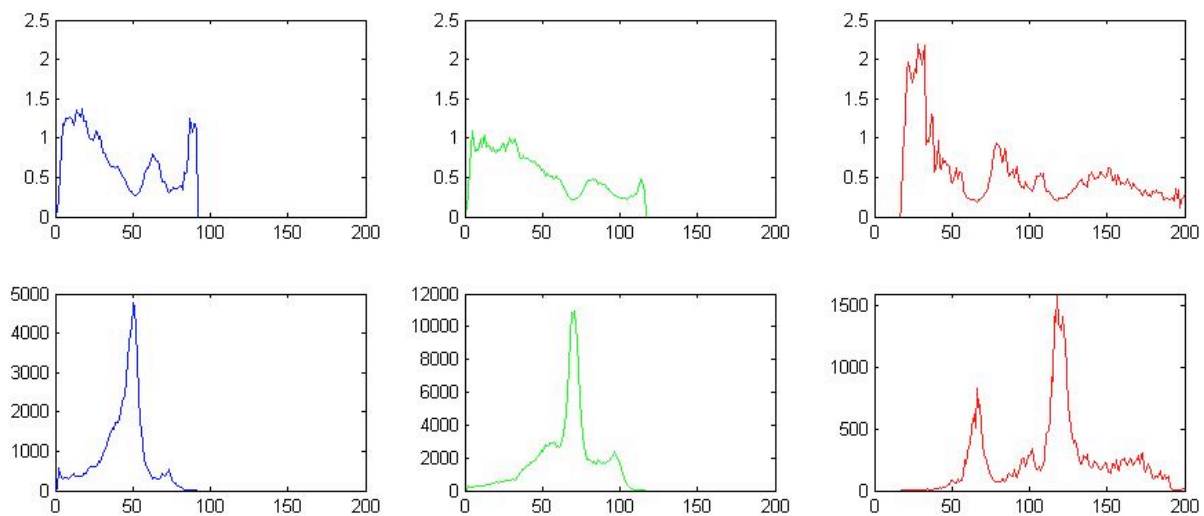


Figure 36: Driver B. (Hi01) Acceleration Analysis for the Three Defined Road Types

X-Axis: Speed in km/h (1km/h resolution)

First Row:

Y-Axis: Mean recorded acceleration for a given speed

Second Row:

Y-Axis: Amount of data available to compute the mean acceleration displayed in the first row

Blue: In the city

Green: Outside the city

Red: Highway

Data: Driver B (Hi01)

Similar results as the one depicted in Figure 36 have been recorded for the other drivers.

It is obvious that the amount of data available (in the second row) is related to the speed restriction:

- 50km/h in the city
- 70 and 100 km/h outside the city
- 60 and 120 km/h on the highway (60 due to road work)

On the other side, the mean recorded acceleration (in the first row) seems to be influenced by the amount of used data. Focused on 20km/h speed ranges, the more data available for a given speed (the more the vehicle was stabilized at this speed), the smaller the mean recorded acceleration at this speed.

This means that a filter can't be simplified to:

$$\text{Transition} < \text{mean deceleration} \leq \text{Stabilization} \leq \text{mean acceleration} < \text{Transition}$$

because the experienced speed restriction during the learning phase would have a huge influence on the selection.

In the preceding example, an acceleration of 0.5m/s^2 at 40km/h or 60km/h would be classified as stabilization, but the same acceleration at 50km/h would be classified as transition.

Taking this problem into account, the following solution has been implemented in the prototype:

- 1- First, a maximum speed value of 200km/h was set. All the recordings over that value will be dismissed.
- 2- The recorded speed resolution has been lowered. The speed values were rounded to the next integral number, so that a statistical approximation was possible.
- 3- The data has been split into the three road type categories: 'in the city', 'outside the city', and 'highway'. A road segment is either classified 'highway' or 'outside the city' and can't be both. Priority is on 'highway'.
- 4- Mean and maximum acceleration was calculated for every integral speed value between 1km/h and 200km/h, respecting their road type. The same procedure was done for deceleration. At the end, there were twelve typical curves: three mean acceleration curves and three maximum acceleration curves, one for each road type category. Similarly, there are six curves for typical deceleration.
- 5- To handle the problem described in Figure 36, a coefficient defined as the following was used:

$$C_{mean2max} = \frac{\overline{a_{InCity}} + \overline{a_{OutCity}}}{\overline{\max(a_{InCity})} + \overline{\max(a_{OutCity})}}$$

With:

$\overline{a_{InCity}}$: mean of the accelerations in the city

$\overline{a_{OutCity}}$: mean of the accelerations outside the city

$\overline{\max(a_{InCity})}$: mean of the maximum accelerations in the city

$\overline{\max(a_{OutCity})}$: mean of the maximum accelerations outside the city

Highways have not been used because of the low amount of data available compared to the two other road type categories.

The coefficient is then used to lower the maximum acceleration curve to the level of the mean acceleration. The results are displayed in following graph:

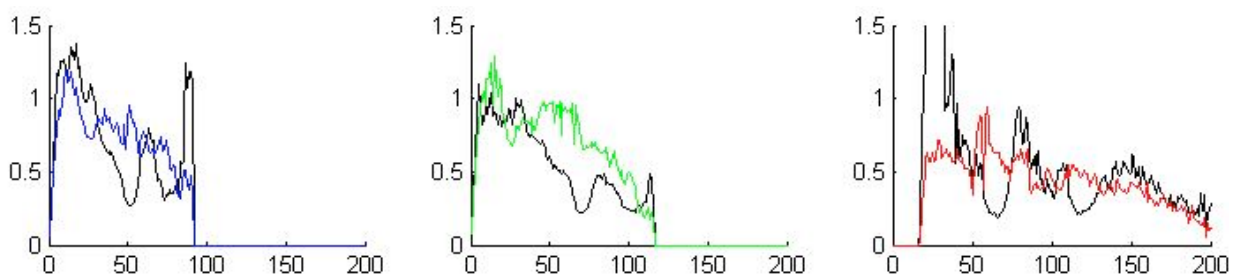


Figure 37: Acceleration Limits for each Road Type Category

X-Axis: Speed in km/h (1km/h resolution)

Y-Axis: Mean acceleration in m/s²

Blue: Lowered maximum acceleration in the city

Green: Lowered maximum acceleration outside the city

Red: Lowered maximum acceleration on the highway

Black: Computed mean acceleration as seen in Error! Reference source not found.

Data: Driver B (Hi01)

The benefit of this computation is that the distortion observable in the mean acceleration curves is dampened. It is possible to reduce the noise with a Kalman filter or similar, but that is not obligatory. As tests later showed, a smoothing over 5km/h range was good enough.

Similar computation has also been done for the deceleration.

6- The next step consists of associating the recorded data momentum with acceleration, deceleration, or stabilization.

Before the acceleration and deceleration limits are used, there are two simple tests:

- If the pressure on the brake pedal is more than zero, then the vehicle is considered to be decelerating.
- If the pressure on the gas pedal is equal to zero, then the vehicle is considered to be decelerating.
- The filter then uses the computed limits displayed in Figure 37 follows:

Transition <= deceleration limit < Stabilization < acceleration limit <= Transition

After that, every input data is associated with one of the three phases (the transition phase is sub-divided into acceleration and deceleration).

7- To correct the isolated transition and stabilization, the system must make a second data analysis and harmonize the results. Assuming that acceleration or deceleration lasts for more than one second, two second ranges were considered and harmonized as follows:

- Number of stabilizations >= number of accelerations & >= number of decelerations

Then: the two seconds range is considered to be at stabilization.

- Number of accelerations >= number of stabilizations & >= number of decelerations

Then: the two seconds range is considered to be at acceleration.

- Number of decelerations >= number of accelerations & >= number of stabilizations

Then: the two seconds range is considered to be at deceleration.

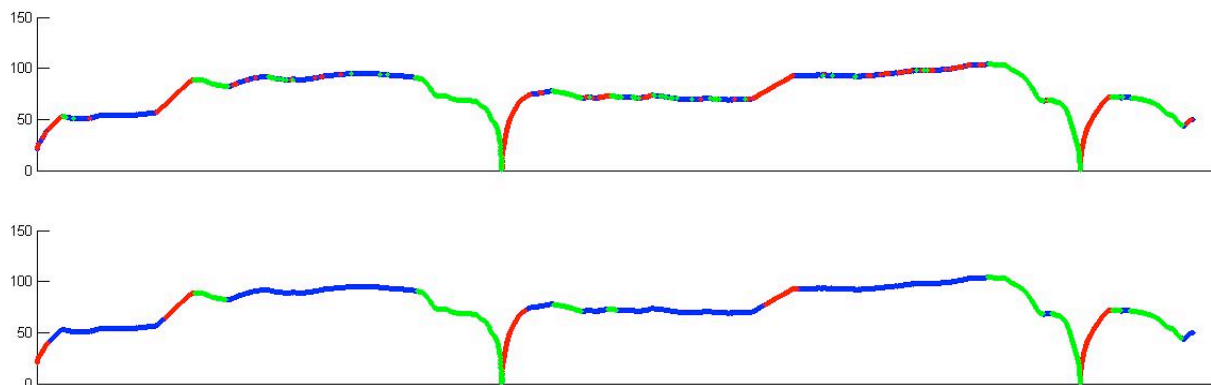


Figure 38: Example of a Situation Split on a Five Minute Recording Section

Data: Driver B (Hi01), test drive on 06.09.2011 at 09:38

X-Axis: 5 minute range

Y-Axis: Recorded speed in km/h

Blue: Stabilization phase

Green: Transition phase (deceleration)

Red: Transition phase (acceleration)

Figure 38 is an example of a 5-minute data range filtered as described, before (first row) and after (second row) harmonization.

The filtering could possibly be enhanced with the use of the navigation system database. In this case, transitions would only be allowed in the vicinity of a situation switch, as described in Figure 35. However, some potential problems are linked to database use, i.e. a transition phase assimilated to stabilization because a speed restriction is not updated. For this reason, and because the results seem to already have sufficient accuracy, a database was not used in the prototype implementation.

5.3.2.2 Mapped Driving Style

The system is now able to divide a given route into situation-induced stabilization phases linked with transition phases. It is also able to recognize when a driver is currently in a

transition or stabilization phase. The last needed part is the storage of the driving style characteristics specific to those phases and situations, which later allows making a driving style prognostic for a given route.

The recorded driving style is saved in four different categories that describe the typically observed: acceleration, deceleration, speed of travel and gear selection strategy, according to the parameters that have been chosen to define the situations of speed restriction and road type.

The Typical Acceleration and Deceleration in a Transition Phase

In this case, only the values recorded during a transition phase are evaluated, and all the recordings over 200km/h are dismissed. The data has been split into the same three road type categories used to define the situations. Then, the speed values are rounded to the next integral number to facilitate the statistical analysis. The mean acceleration is calculated for every integral speed value between 1km/h and 200km/h, respecting their road type. The same procedure is done for deceleration.

To provide an acceleration approximation for speeds without associated recorded acceleration, a polynomial interpolation of 15 degrees is computed. The interpolation is then corrected to avoid negative accelerations and positive decelerations (values set to zero).

The results are displayed in the following graph:

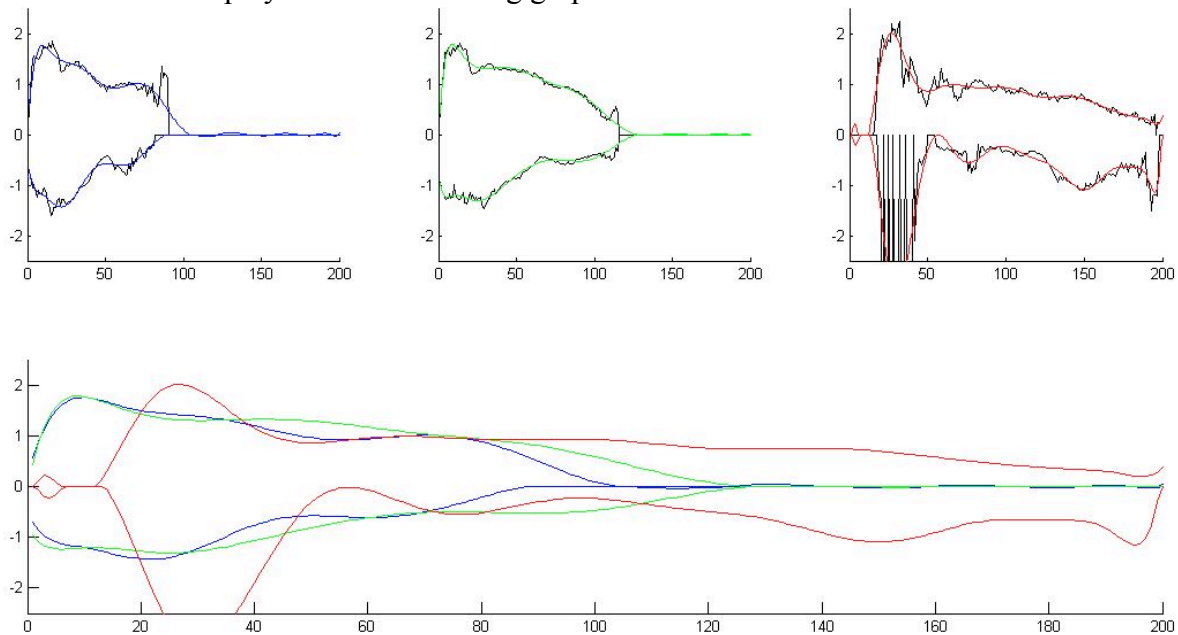


Figure 39: Typical Acceleration and Deceleration during a Transition Phase

X-Axis: Speed in km/h (1km/h resolution)

Y-Axis: Mean acceleration in m/s²

Blue: Smoothed typical acceleration and deceleration in the city during a transition phase

Green: Smoothed typical acceleration and deceleration outside the city during a transition phase

Red: Smoothed typical acceleration and deceleration on the highway during a transition phase

Black: Computed mean acceleration and deceleration during a transition phase

Data: Driver B (Hi01) - identical as in Figure 37

The extrapolation of missing deceleration is clearly recognizable for highway deceleration (first row on the right) in the speed range of 25 to 40 km/h. Another observation is that the typical acceleration and deceleration values for in the city and outside the city seem to be very similar (second row). However, this observation should be tested for other test tracks, and the split into road type might still be relevant when it comes to typical driven speed.

Typical Acceleration and Deceleration in a Stabilization Phase:

The exact same calculation as in the transition phase is made for the typical acceleration and deceleration in the stabilization phase.

Typical Speed in a Stabilization Phase

The original idea was to represent the typical driven speed and its small variations with a sinusoidal curve. The mean driven speed and its standard deviation define the axe of symmetry and the amplitude of such a curve. The typical acceleration and deceleration during the stabilization phase are used to define the frequency. This approach has a hidden complexity due to the consideration of the engine capacity during the sinusoidal approximation. The curve has to be corrected during its generation according to the engine capabilities.

Because of the pressure of time, and the satisfying results with a typical driven speed simplified to the mean recorded speed difference to the speed limit, the original idea was discarded. The typical driven speed is saved in the form of the difference between the mean recorded speed and the speed restriction for each possible speed restriction. For example, if the mean recorded speed for stabilization situations outside the city with a speed restriction of 70km/h was 74,5km/h, then, the variation of '+4,5km/h' is linked to this speed restriction.

Gear Selection

All the test vehicles had an automatic gearbox; therefore, gear change logic could be extracted. The gear change programming seems to be dependent from the engine rpm and the engine torque. The following figure shows the recorded gearshift behavior and a simplification of it:

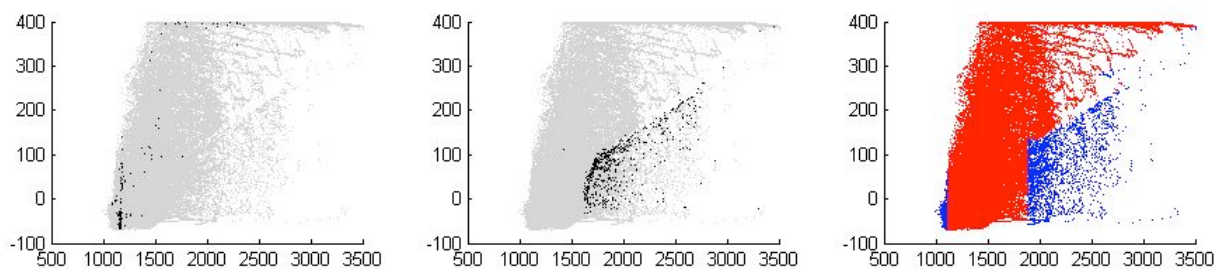


Figure 40: Fifth Gear Shift Logic Representation in an Engine Map (Automatic Gearbox)

X-Axis: Engine rotation per minute

Y-Axis: Engine torque in Nm

Grey: Recorded values while the fifth gear was selected

Black: Decision points. Last recorded value before the gear was changed.

Blue: Gearshift zone approximation

Red: Gear validation zone

Data: BMW E91 and Driver B (Hi01)

According to the left figure, it seems that the downward shift (Gear Five to Four) zone is only defined by the engine rpm. On the other side, the maximum authorized engine rpm before up shift (Gear Five to Six) seems to vary according to the engine torque (figure in the middle). These findings are summed up in the right graph in the form of three zones: a confidence zone (in red) where the selected gear remains unchanged, and two shift zones (in blue) where the gear has to be adapted.

While it is presumable that such a pattern might be recognized in vehicles with an automatic gearbox, it is improbable that manual gearbox use presents the same strong characteristics. The introduction of such gearshift logic implies the following problem: to make the decision if the gear should be shifted at a given momentum, the engine rpm and torque for this momentum have to be computed. The problem in this case is that the selected gear is an input needed to calculate the engine rpm and the torque. The solution is then to compute those values for every possible gear and make a selection afterwards.

These are the reasons that initiate the decision to renounce the torque refinement and implement a similar strategy as for the acceleration and deceleration. The gearshift logic was represented by a gear selection statistic related to the speed and to either stabilization or transition.

5.3.3 Generating a Driving Style for a Given Route

To make a fuel consumption prediction, the vehicle simulation part of the prototype needs a driving style input generated for a given route. This chapter describes the process of generating a driving style according to the route segment attributes.

Route Input and Splitting

The route is a sequence of road segment descriptions extracted from the navigation system database. It is provided from the route search function component.

After the prototype receives the route, it is divided into situations and phases as described in Chapters 5.3.1.2 and 5.3.1.3.

Stops Insertion

Because of the high influence of acceleration and braking on fuel consumption, the situations where the vehicle has to stop must be considered. Therefore, the next step consists of inserting stops in the generated frame. This was done based on the description in the navigation system database as follows:

- Only the road types 'In City' and 'Outside City' were updated. Stops were not allowed on highways.
- In case the street name changed, it is supposed that a turn was required and inserted a stop.
- In the city, a stop was inserted for every intersection with a least 4 segments.

Generating the Driving Style

The driving style generation is done in two steps. First, the accelerations and decelerations are generated for the next one to two situations at the transition points. Then the accelerations and decelerations are put together, and shortened or extended with the stabilization speed to match the segment length if needed. Basically, acceleration is always generated starting from a transition, and deceleration is always ending at a transition.

The driving style generation occurs chronologically. After a segment generation is completed, the new driving style is added to the styles already generated, and the acceleration and deceleration arrays are emptied.

The following steps have been implemented into the prototype with:

- $Speed_{ACTUAL}$ is the last valid prognosticated speed. Per default, the whole route starts with a non-moving vehicle, therefore a $Speed_{ACTUAL}$ is equal to zero.
- $SPLimit_{ACTUAL}$ describes the actual speed restriction + variation as defined in Chapter 5.3.2.2. In the case there is no variation available for a given speed restriction, the variation from the next best match is applied.
- $SPLimit_{FUTURE}$ describes the speed restriction + variation of the next situation. At stops, a speed restriction + variation equal to zero is set.
- $Segment_{LENGTH}$: is the total length of the actual stabilization segment.

Then:

1 **If** $Speed_{ACTUAL} < SPLimit_{ACTUAL}$

A typical acceleration is generated starting from $Speed_{ACTUAL}$ until the $SPLimit_{ACTUAL}$ is reached. This acceleration timeline is saved in an acceleration container for later use.

2 **If** $Speed_{ACTUAL} > SPLimit_{ACTUAL}$
 & $SPLimit_{FUTURE} > 0$

A typical deceleration is generated starting from $Speed_{ACTUAL}$ until the $SPLimit_{ACTUAL}$ is reached. This deceleration timeline is saved in a deceleration container for later use.

```
3   If  $Speed_{ACTUAL} > SPLimit_{ACTUAL}$ 
    &  $SPLimit_{FUTURE} == 0$  (stop)
```

In this case, the vehicle has to stop at the next transition. For this special case, a forced deceleration is defined, whose value is the deceleration needed to stop the vehicle from moving within the segment length. In case the segment length is over 250m, then the forced deceleration is computed for 250m. This kind of deceleration reproduces the deceleration due to the traffic lights that are not completely driver related.

```
3-1 If  $Speed_{ACTUAL} > SPLimit_{ACTUAL}$ 
    &  $SPLimit_{FUTURE} == 0$  (stop)
    &  $Segment_{LENGTH} < 250m$ 
```

The needed deceleration to stop the vehicle is adapted to the segment length.

```
3-2 If  $Speed_{ACTUAL} > SPLimit_{ACTUAL}$ 
    &  $SPLimit_{FUTURE} == 0$  (stop)
    &  $Segment_{LENGTH} > 250m$ 
```

A typical deceleration is generated starting from $Speed_{ACTUAL}$ until the $SPLimit_{ACTUAL}$ is reached and saved as Part One. Then, a forced deceleration is computed for 250m from $SPLimit_{ACTUAL}$ to 0 and saved as Part Two.

- If the length needed for Part One and Two is more that the segment length, then the two parts are replaced with a forced deceleration. This is calculated starting from $Speed_{ACTUAL}$ until the vehicle is not moving for the exact segment length.

- If the length needed for Part One and Two is less that the segment length, then the gap between Part One and Two is filled with $SPLimit_{ACTUAL}$.

```
4   If  $Speed_{ACTUAL} < SPLimit_{ACTUAL}$ 
    &  $SPLimit_{FUTURE} == 0$  (stop)
```

Similar to 3-1 and 3-2, depending on the segment length, typical deceleration or forced deceleration are computed, but because the $Speed_{ACTUAL}$ is smaller than $SPLimit_{ACTUAL}$, the deceleration needed to stop is calculated starting from $SPLimit_{ACTUAL}$.

```
5   If  $Speed_{ACTUAL} < SPLimit_{FUTURE}$ 
    &  $SPLimit_{ACTUAL} > SPLimit_{FUTURE}$ 
```

Because $SPLimit_{ACTUAL} > SPLimit_{FUTURE}$, the segment is expected to end with a deceleration; therefore a typical deceleration is prepared and saved in a deceleration container. But in this particular case, a problem might be that the vehicle acceleration isn't enough to reach the minimum speed defined as $SPLimit_{FUTURE}$ at the end of the segment. In this case, there will be no intersection between the acceleration and the prepared deceleration curve.

For this reason, the deceleration and acceleration container are erased, and replaced with a deceleration starting from $Speed_{ACTUAL}$ to $SPLimit_{FUTURE}$. The acceleration and deceleration have been generated if needed and saved into specific containers:

- $ACC_{timeline}$: Describes the acceleration evolution of speed, acceleration, and distance over the time until targeted speed is reached.

- $DCC_{timeline}$: Is similar to $ACC_{timeline}$ for a deceleration.

The next step is to merge the computed timelines into the stabilization. Acceleration is always generated starting from a transition and deceleration is always ending at a transition, therefore a stabilization segment can hold a single acceleration or a single deceleration, or both together.

```
6   If  $ACC_{timeline} > stabilization\ phase\ length$ 
then  $ACC_{timeline}$  is shortened to the segment length.
```

```
7   If  $DCC_{timeline} > stabilization\ phase\ length$ 
then  $DCC_{timeline}$  is shortened to the segment length.
```

```
8   If  $ACC_{timeline} < stabilization\ phase\ length$ 
    & there is no  $DCC_{timeline}$ 
```

then the end of ACC_{timeline} is extended with a constant speed equal to $SPLimit_{\text{ACTUAL}} + \text{variation}$ until the segment length is reached.

9 If $DCC_{\text{timeline}} < \text{stabilization phase length}$
 & there is no ACC_{timeline}

then the beginning of DCC_{timeline} is extended with a constant speed equal to $SPLimit_{\text{ACTUAL}} + \text{variation}$ until the segment length is reached.

10 If there is a ACC_{timeline} and a DCC_{timeline}
 & $ACC_{\text{timeline}} + DCC_{\text{timeline}} < \text{stabilization phase length}$

then the gap between ACC_{timeline} and DCC_{timeline} is filled with a constant speed equal to $SPLimit_{\text{ACTUAL}} + \text{variation}$ until the segment length is reached.

11 If there is a ACC_{timeline} and a DCC_{timeline}
 & $ACC_{\text{timeline}} + DCC_{\text{timeline}} > \text{stabilization phase length}$

then the entry with the highest speed in ACC_{timeline} or DCC_{timeline} is deleted and the distance checked against the stabilization phase again. This part is repeated until $ACC_{\text{timeline}} + DCC_{\text{timeline}} = \text{stabilization phase length}$.

After this is done, ACC_{timeline} and DCC_{timeline} are emptied and the next route segment is processed until the whole route has been done. At the end, the selected gear probability is added to the chronological sequence completing the driving style input needed for vehicle simulation.

5.4 Concept Summation

5.4.1 Summing Up the Fuel Prediction:

(Starting from Chapter 5.1.1).

1

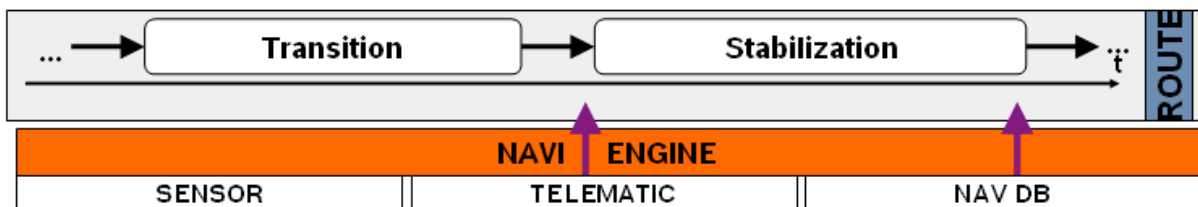


Figure 41: Summing Up the Route Division Process

Starting from the bottom of the previous figure:

The navigation system engine has selected at least one route in the form of a sequence of route segments with attributes and the actual telematic information related. This route description is transferred for fuel consumption prediction to the prototype. First, the route is divided into situations and phases.

2-

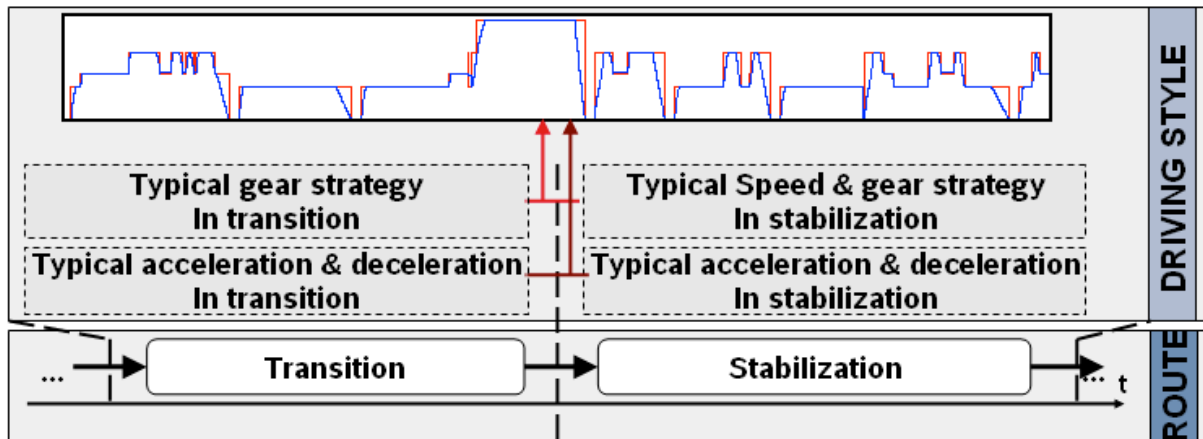


Figure 42: Summing Up the Driving Style Generating Process

Starting from the bottom of the previous figure -

A sequence of transition and situation phases describing situations is transferred from the prototype route part to the driver part. Then the typical driving style with speed, acceleration, deceleration and selected gear is matched in the route describing sequence.

3-

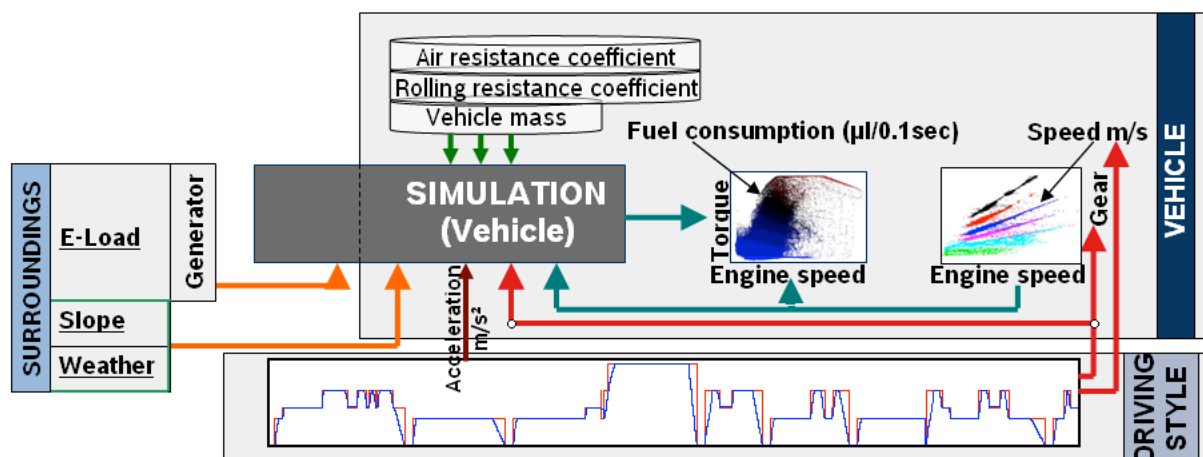


Figure 43: Summing Up the Fuel Prediction Process

To compute the engine torque, the vehicle simulation uses:

- The generated driving style (bottom - in the 'driving Style' part)
- The surrounding information (left - in the 'surroundings' part)
- The navigation system database route description (left - in the 'surroundings' part)
- The updated vehicle parameter database (top - in the 'vehicle' part)
- The engine speed that has been calculated out of the driving style's prognosticated speed and gear (right - in the 'vehicle' part).

Then the sequence of engine torque and engine speed is converted into a sequence of fuel consumption for 0.1sec with the help of the engine map (in the middle of the 'vehicle' part).

5.4.2 Adaptation to Electric Vehicles (EV):

The status in 2013 is that EVs are built similarly to combustion engine vehicles. The combustion engine is replaced with one or more electric engines. Each electric engine powers an axle or a wheel.

Therefore, like the aforementioned sequence for combustion engine vehicles:

- 1- The route splitting remains identical. The situation definition might be adapted to route attributes that are especially relevant for EVs.
- 2- The typical driving style remains identical and might be simplified if the electrical vehicle has no gearbox. This is made possible by the high torque availability range and high engine rpm maximum of electrical engines. It is also common on small city vehicles that have a limited top speed to save on weight.
- 3- In case there is more than one engine, an extra logic component that calculates the torque repartition on the engines has to be implemented. Such a component might be integrated in the EV in the same way as it is in the Mercedes SLS AMG electric drive. In this particular case, the AMG Torque Dynamics (a torque vectoring logical unit) controls the torque available on the two motors connected to one gearbox with two independent gears.

Instead of fuel volume, the engine map is filled with the electricity amount. In the negative torque part of the engine map, electricity recuperation can be saved in the form of a “negative consumption”. In this case, the prototype can take energy recuperation into account while it makes an energy consumption prediction.

5.4.3 Summing Up the Prototypical Learning:

(Starting from Chapter 5.1.3).

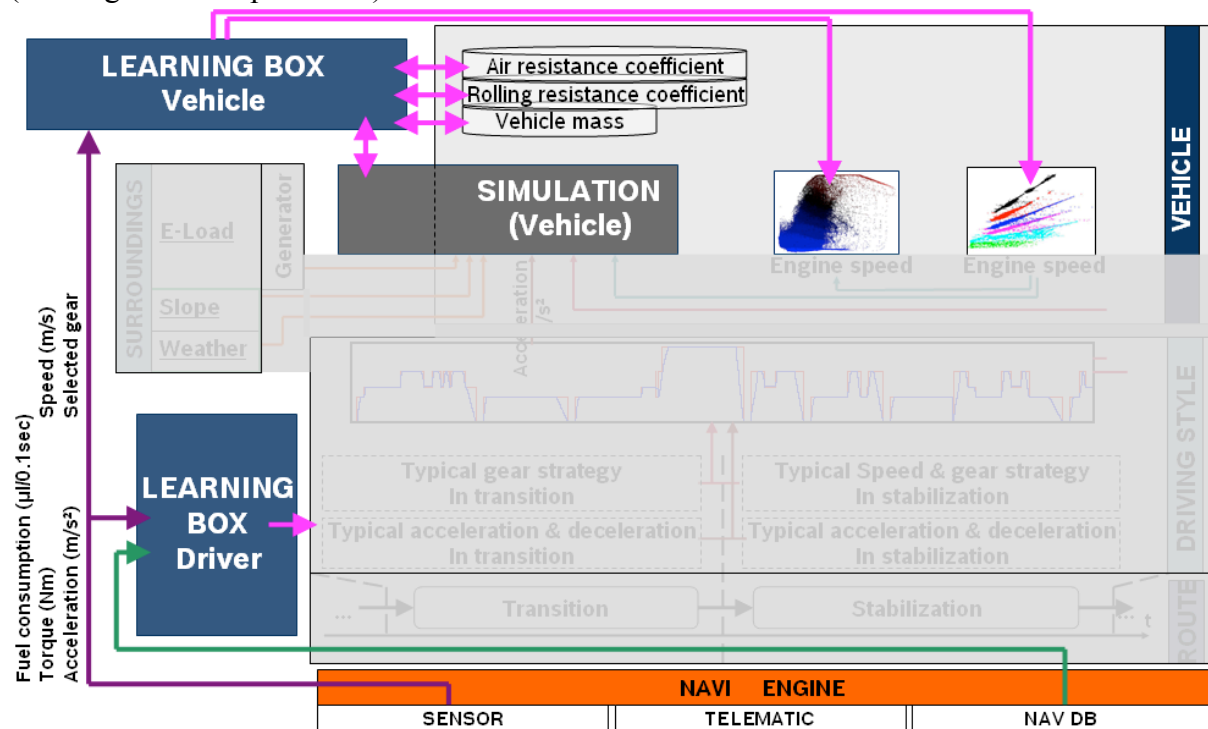


Figure 44: Summing Up the Prototypical Learning Process

While the vehicle is moving, the prototype constantly updates the databases:

- The driving style uses the navigation database inputs to sort the recorded data into the defined categories (e.g. road type or speed restriction). Then, the sensor data is used to update the driver's driving style descriptions.
- In the vehicle part, when the dispatcher recognizes predefined conditions, some of the vehicle parameters are updated with the help of the vehicle simulation. The engine map and transmission ration are constantly fed with the last recorded data.

6 Results and Analysis

This chapter regroups all the results computed by the solution prototype, as it is described in Chapter 5, and their analysis. The results are arranged into the two main categories that were used in the previous chapter and are based on the three-stage model:

- The vehicle-related part
- The driver-related part

Finally, the prototype's results are compared with today's available solutions to measure the reached quality of estimation.

The third part of the three-stage model, the surroundings, has been tested in a limited way because of the lack of sensors and available information. Also, the amount of needed data would have dramatically increased to provide as many combinations as possible. Therefore, plenty of records of identified drivers on a defined route are needed. Driving repeatedly on a defined route provides a well-known test area, and may, at the end, reduce the influence of side effects like traffic, daytime, fatigue, while the database characteristics remains identical.

For this reasons, the decision was taken to use the data recorded in Hi01 (Annex B - all four drivers) and Hi03/Hi04 (Annex D - only driver D1 and D2 had the minimum required amount of recorded data) for the main analysis.

The database Hi02 (Annex C) was later used during the vehicle subchapter, to check the capability of the prototype to recognize changes in the car characteristics, but couldn't be used for the driver part because the amount of data (related to a single driver) was insufficient.

The use of database St01 (Annex A) was limited to the illustration of differences between drivers in the same vehicle on the same test-track because of the missing gear information.

The data was split into two sub databases:

- First, a database that was used to learn - called the "Learning Database". It is made of all the Hi01 recordings except four randomly selected laps for each driver, and of all the Hi03 recordings.

The Learning Database was made of:

- Driver 1 (previously Driver B in the Hi01 database): 1257.86 recorded kilometers.
- Driver 2 (previously Driver D1 in the Hi03 database): 842.19 recorded kilometers.
- Driver 3 (previously Driver K in the Hi01 database): 1839.89 recorded kilometers.
- Driver 4 (previously Driver D2 in the Hi03 database): 1795.74 recorded kilometers (1121.52 Kilometers on Highway).
- Driver 5 (previously Driver R in the Hi01 database): 1726.02 recorded kilometers.
- Driver 6 (previously Driver V in the Hi01 database): 1908.32 recorded kilometers.

- Secondly, a database that was used to compare the recorded results to the learning results. It is later referenced as the "Evaluation Database" in this work. This database is made of the four random selections per driver (a total of 16 laps), and the Hi04 (Annex D) recordings.

The Evaluation Database was made of:

- Driver 1: 4 randomly selected lap logs (at ~63km)
- Driver 2: 5 lap logs (at ~39km)
- Driver 3: 4 randomly selected lap logs (at ~63km)
- Driver 4: 6 lap logs (at ~39km)
- Driver 5: 4 randomly selected lap logs (at~63km)
- Driver 6: 4 randomly selected lap logs (at ~63km)

The quality of the prototype estimations were measured by comparing the fuel consumption predictions with the recorded amount of fuel needed. In order to isolate the sub-components

as much as possible, the quality analysis started with the last prototype elements involved into the fuel consumption prediction, and enlarged the amount of implicated elements from test to test until running the full prototype. The quality was analyzed in each step so that the variations observed between the two tests could be related to the last added prototype element. The sequence is similar to the one described in Chapters 5.2 and 5.3.

6.1 Results – Vehicle Part

The first part of the prototype was analyzed, and the last part, used in a fuel consumption prediction, was the vehicle-related part implementation.

6.1.1 Results – Engine Map

First, the filtering results were evaluated, then the produced engine maps were compared and the possible reasons that could lead to the quality variation are discussed here.

6.1.1.1 Engine Map Input Data Filter

The Learning Database is filled with a total of 9370 kilometers recordings, subdivided in six drivers, and took 148 hours 27 minutes 40 seconds to record. During this time, 259 entries (at 0.1sec) were filtered and dismissed.

- In 143 cases, the recorded fuel was over the set limit.
- In 72 cases, the engine rpm was found too low
- In 44 cases, the engine rpm was found too high.

In summary, a total of 26 seconds erroneous data were filtered. This is a 0.0048% error rate.

An identified error doesn't mean that it is sourced from the CAN bus since an elaborate platform of hardware and software was used to intercept and record some of the CAN messages. The log files were saved into JSON files, and the information available in those files was later extracted into a Matlab compatible format. In a last step, the data was synchronized as described in Chapter 5.2.1. All those steps could be responsible for the established errors.

Since a 0.0048% rate is judged acceptable, further analysis on the error origin was not conducted.

6.1.1.2 Engine Map Resolution and Quality After X Kilometers

The following chapter regroups the analysis and observations of the generated engine maps.

General Impressions:

The engine map displayed in Figure 45 was generated out of the 9370 kilometer recordings of a BMW E91 (using all the data available in the learning database and disregarding the drivers).

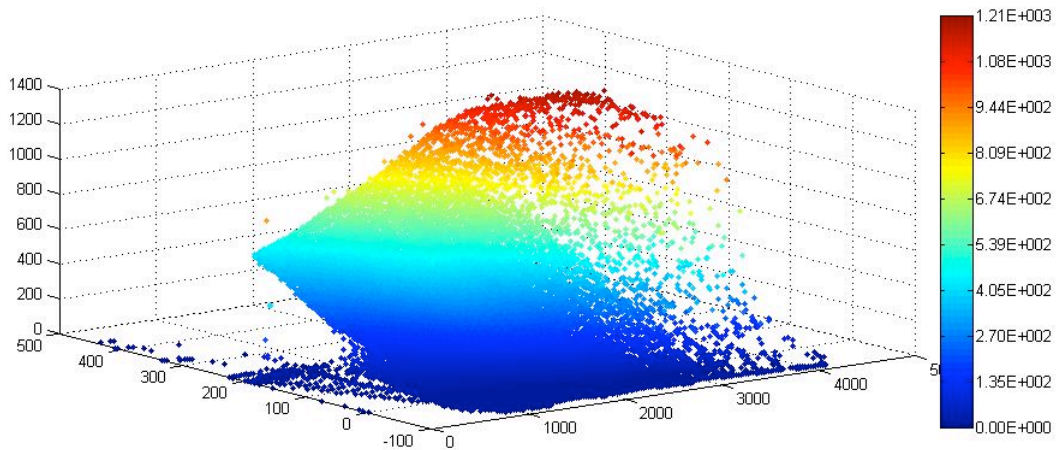


Figure 45: Engine Map of a BMW 325d (E91) after 9368km

X-Axis: Engine speed in rpm

Y-Axis: Engine torque in Nm

Z-Axis: Fuel injection volume in $\mu\text{l}/0.1\text{sec}$

Color: The color varies depending on the fuel injected volume according the bar on the right side

Following observations can be made:

- The engine torque varies between -100 and 400Nm, with a few isolated exceptions over 400, mainly at a really low rpm with no fuel injection, which may suggest that this occurs during the engine ignition.
- The engine speed varies from 0 to over 4000rpms. Some values have been recorded between 0 and the engine idle rpm with no fuel injection and a positive torque. These values seem to be related to the engine ignition as well. A value over 4000rpms would represent a speed of 239.04 or 248.42km/h (calculated transmission ratio versus official transmission ratio) in the sixth gear. The maximum recorded speed with the test vehicle was slightly over 210km/h, therefore it is presumable that this engine range has been recorded while driving in a lower gear during a typical 'kick down' acceleration phase.
- The injected fuel volume varies between zero (fuel injection shutoff) and around 1210 $\mu\text{l}/0.1\text{sec}$ \sim 43.5liters/hour. This value is recorded for an engine speed of \sim 3500rpm \sim 211.5km/h (sixth gear). It means a fuel consumption of 20.5liter/100km/h when the vehicle is moving at 210km/h in the sixth gear. There are no official consumption values available for high speed driving, but based on the fuel injection values observed in the cluster instrument while driving, this seems to be accurate.
- Because there are no important gaps, the engine map filling seems to be satisfying. The range between the engine's idle speed and 3000rpms is densely filled; this may indicate that the automatic gearbox switches to the next higher gear at 3000rpms. The fuel injection volume over torque and over engine speed seems to be almost linear, as described in Figure 29. This characteristic is required for an optimal fuel consumption prediction.

Number of Recorded Entries:

Since the fuel consumption is recorded and saved for every 100 milliseconds, the engine map is time dependent and not distance dependent. For this reason, it is possible that the number of entries for two identical vehicles on the identical test track differs according to the driven speed, and therefore the time needed to drive the test track. It also means that it is not possible to guarantee a minimum quality only based on the driven distance.

Engine Map Filling Range:

The engine map range depends mainly on the driver. The way he accelerates/decelerates, his chosen speed of travel, and the gear he selects while driving have a direct impact on the engine speed and the torque. Some extreme cases of engine map filling ranges are displayed in 'Figure 46' below. The 90 test drives of the ST01 database were sorted according to their fuel consumption, and four of the most representing examples picked on the extremes are displayed.

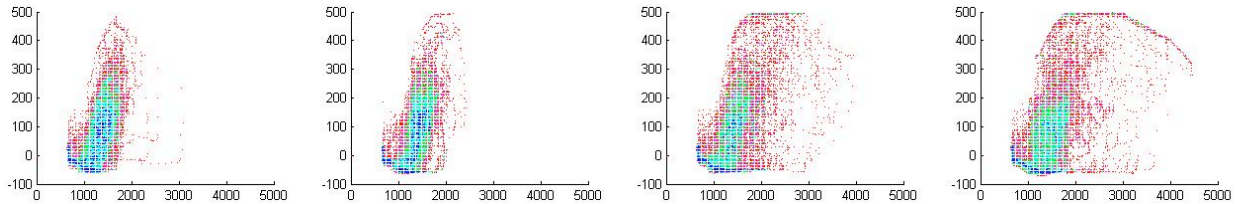


Figure 46: Engine Map of Eco-drivers and High Fuel Consumption Drivers

Engine map resolution 25rpm / 5Nm

X-Axis: Engine speed in rpm

Y-Axis: Engine torque in Nm

Red: Less than 2 entries

Magenta: Between 2 and 5 entries

Green: Between 5 and 12 entries

Cyan: Between 12 and 30 entries

Blue: More than 30 entries

On the left side are the two engine maps generated out of two of the most economic lap logs, and on the right side are two of the least economic lap logs. There are two main differences between the two types of drivers:

- Eco-drivers don't drive at a high engine speed. It means lower speed, but also an early shift to the next higher gear.
- Eco-drivers drove more often in the 100Nm/1250rpm area which is characteristically the more efficient engine area.

Therefore, the engine map filling is expected to be very dependent on the driver's driving style.

Engine Map Resolution and Driver Influence on the Quality of the Engine Map:

Step 1: Generating Engine Maps with Various Resolutions out of the Learning Database:

Five engine maps resolutions have been defined, from low to high definition. The steps have been chosen so that torque and engine rpms have a similar resolution and are defined as follows:

100rpm/20Nm | 50rpm/10Nm | 20rpm/5Nm | 10rpm/2.5Nm | 5rpm/1Nm

For each one of the six drivers available in the learning database, five engine maps in the defined resolution have been produced. Additionally, five engine maps using the total 9370.02 recorded kilometers were generated.

At the end, a total of 35 engine maps were produced to analyze the influence of drivers and engine map resolution on the quality of the engine map.

Step 2: Preparing the Evaluation Database:

The recorded torque and engine speed over time was extracted from the recordings that composed the evaluation database. This database wasn't used to generate the engine maps for this test.

The torque and engine speed timelines (Timeline_[torque; engine speed]) of the 27 evaluation database recordings were then converted into fuel injection timelines (Timeline_{Fuel}) using the

35 generated engine maps. For every single $\text{Timeline}_{\text{Fuel}}$, the sum of all the entries is equal to the total amount of fuel consumed.

A total of 945 fuel consumption predictions was produced, and for each one of them, the deviation to the original recorded fuel consumption was then calculated.

The following table regroups the mean deviation in percentage between the computed fuel consumption and the related original recordings. In this particular case, the engine maps generated out of the driver-specific part of the Learning Database were used. This should be the most common case (an identified driver using his own car).

	Driver-specific Engine Map				
	100rpm/20Nm	50rpm/10Nm	20rpm/5Nm	10rpm/2.5Nm	5rpm/1Nm
D1: 4 randomly selected lap logs (@~63km)	-1.64	-1.58	-1.70	-1.46	-1.45
D2: 5 lap logs (@~39km)	-2.04	-2.00	-1.97	-1.86	-1.67
D3: 4 randomly selected lap logs (@~63km)	-1.12	-0.80	-0.79	-0.70	-0.43
D4: 6 lap logs (@~39km)	-3.68	-3.59	-3.49	-3.25	-2.81
D5: 4 randomly selected lap logs (@~63km)	-0.70	-0.79	-0.72	-0.69	-0.63
D6: 4 randomly selected lap logs (@~63km)	-1.70	-1.66	-1.52	-1.25	-1.14

Table 10: Engine Map Resolution Influence on the Fuel Prediction Quality: Mean Deviation in Percentage

For example, the green marked entry means that:

- The engine map used was produced out of the 1257.86 recorded kilometers driven by ‘Driver 1 (D1)’ and available in the learning database.
- The engine map with a 100rpm/20Nm resolution was selected.
- The four $\text{Timelines}_{[\text{torque}; \text{engine speed}]}$ were extracted out of the four ‘driver 1 (D1)’ test logs available in the Evaluation Database.
- Four fuel consumption predictions were computed using the four $\text{Timelines}_{[\text{torque}; \text{engine speed}]}$ as an input for the selected engine map.
- These predictions were then compared to the four real recorded consumptions and their deviation computed.
- The mean value of the four computed deviations was then calculated to be -1.64%.

Engine Map Resolution Observations and Analysis:

- For all the six drivers, the best results were observed with the higher resolution engine map, and in four of the six cases, the worst results were observed with the lowest resolution. Therefore, the general observed trend is that the higher the resolution, the better the results seem to be. The observed quality loss was around 0.5% between the highest and the lowest resolutions.

- The fuel prediction is generally lower than the recorded fuel consumption. These results may be related to the linear extrapolation approximation.

The worst results were observed for the second and the fourth drivers. This may be related to the low amount of data that was used: 842.19 recorded kilometers for Driver 2 and 1795.74 recorded kilometers for Driver 4. In the second case, 1121.52 kilometers were recorded on the highway, where the engine use is expected to be more monotonous than in the city.

Engine Map and Driver Influence:

To isolate the driver’s influence on the engine map, a similar abstract as the one presented in Table 10 has been computed. Unlike in the previous table, however, a global engine map that regroups all the 9370.02 recorded kilometers disregarding the driver was used.

9370 kilometers Engine Map					
	100rpm/20Nm	50rpm/10Nm	20rpm/5Nm	10rpm/2.5Nm	5rpm/1Nm
D1: 4 randomly selected lap logs (@63km)	-0.50	-0.47	-0.54	-0.45	-0.47
D2: 5 lap logs (@39km)	-2.86	-2.86	-2.82	-2.82	-2.78
D3: 4 randomly selected lap logs (@63km)	-0.46	-0.50	-0.53	-0.45	-0.49
D4: 6 lap logs (@39km)	-5.57	-5.52	-5.27	-4.98	-4.86
D5: 4 randomly selected lap logs (@63km)	0.02	-0.04	-0.03	-0.02	-0.01
D6: 4 randomly selected lap logs (@63km)	0.53	0.51	0.40	0.43	0.39

Table 11: Engine Map and Driver Influence on the Fuel Prediction Quality in Percentages

In this case, the observed results seems to be more homogeneous, the influence of the resolution being no longer important. The amount of data that was used to compute the engine maps could possibly explain this observation. To consolidate this supposition, the amount of data listed in the 35 engine maps was extracted and regrouped in the following table:

	100rpm/20Nm	50rpm/10Nm	20rpm/5Nm	10rpm/2.5Nm	5rpm/1Nm
D1 engine map	608	2124	7446	29369	97850
D2 engine map	535	1863	6375	25284	82192
D3 engine map	716	2369	7879	31205	111008
D4 engine map	682	2359	8296	35124	130571
D5 engine map	526	1815	6370	26327	99213
D6 engine map	563	2023	7348	31313	118513
9370 km engine map	816	2736	9427	40284	166781

Table 12: Number of Entries Found in the 35 Engine Maps

As expected, there are more entries in the 9370 km engine map than in the driver-related engine maps, therefore the case of fuel extrapolation should be reduced, and the saved values in the rarely used engine zones (displayed in ‘Figure 46’) consolidated. This may explain the better fuel prediction quality of the global engine map (listed as 9370km in the previous table).

Another observation made regarding the fuel prediction was that it is generally lower than the recorded fuel consumption. This effect might be explained by the observation made in the next paragraph.

Engine Map and Track Influence:

Comparing the results of Table 10 to the results of Table 11, it is apparent that the results computed out of the D1, D3, D5 and D6 Timelines_[torque; engine speed] got better when using the

global engine map, while the results computed out of the D2 and D4 Timelines_[torque, engine speed] got worse.

The data used for D2 and D4 was recorded on a different track than the one used to generate the engine map. It is possible that due to the effect of the ECU back regulation, the track has an influence on the driving style and therefore on the recorded fuel injection.

This supposition is consolidated by the observations made in the following figure:

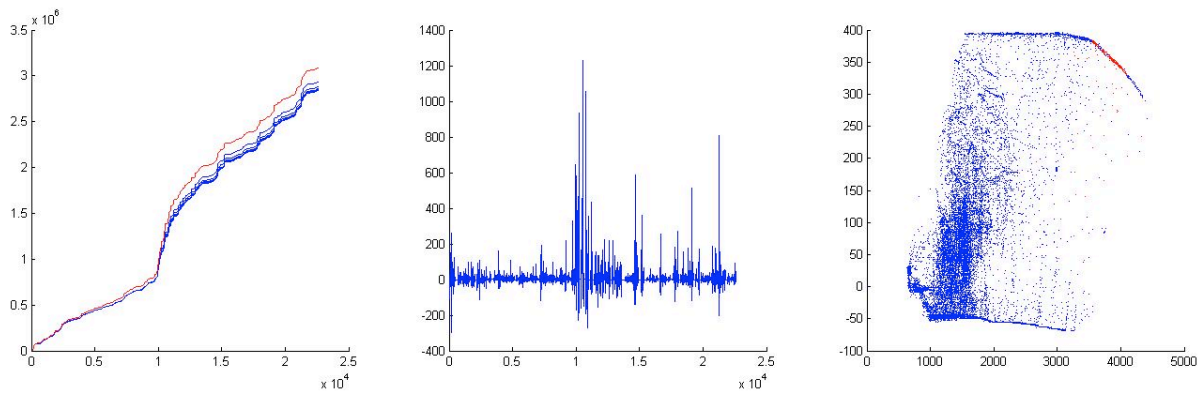


Figure 47: Origin of the Detected Errors Related to the Engine Map

Driver: D4

Engine map: Driver-related engine maps

The track log used was identified as the one with the highest deviation between prediction and recording.

Left Figure:

X-Axis: Time in 0.1sec

Y-Axis: Total of fuel

Red: Original fuel consumption

Blue: Five fuel predictions made using the five different engine map resolutions

Middle Figure:

X-Axis: Time in 0.1sec

Y-Axis: Deviation between original consumed fuel and prediction in µl/0.1sec

Right Figure:

X-Axis: Engine speed in rpm

Y-Axis: Engine torque in Nm

Blue: Engine zones used

Red: Engine zones with a deviation between original consumed fuel and prediction over 200 µl/0.1sec

According to the graphical representation of the worst fuel consumption prediction that was computed, the error origin seems to be very local. It was computed during an extreme engine use (maximum torque and maximum engine speed). One potential explanation is that this engine zone has a very few entries, and therefore, the quality may be low; on the other hand, the engine control unit may be responsible for the strong prediction error in this special case.

6.1.1.3 Lambda Sensor and the Engine Control Unit (ECU)⁷

The *Engine Control Unit* (ECU) is directly responsible for the amount of fuel injected into the engine. It is controlled by the engine load and influenced by the driver's pressure on the gas pedal. When the driver is accelerating and therefore pressing on the gas pedal, fuel is injected. After the controlled explosion in the engine, the exhaust gas is analyzed by the (one or more) lambda sensor to evaluate the combustion. This evaluation makes it possible to optimize the combustion by adapting the amount of fuel injected, therefore, the analysis results are sent to the ECU, which adapts the injected fuel amount. It means that the amount of fuel for a given

⁷ This description of the mode of operator of the lambda sensor is based on the Bosch technical brochure 'Lambdasonden richtig beurteilen und behandeln' [BoMKG06].

torque and engine rpm will vary according to how the driver uses the gas pedal before the ECU corrects it.

Therefore, for a short time lapse, there is a trace of driving style influence in the engine map. It also means that the quality is expected to become better the more that the driver-specific data of the second and fourth drivers are incorporated into the engine map, and the more data that is available in this extreme engine area that is rarely used.

6.1.2 Results – Simulation

The next level of prototype quality evaluation adds the vehicle simulation and the vehicle characteristics. These characteristics are used as simulation parameters to produce the input (out of gear information, driven speed, acceleration and slope) that is needed to use the engine map.

The evaluation procedure is similar to the one used for the engine map. The gear, driven speed, acceleration and slope over the time (Timeline_[Gear; Speed; Acc; Slope]) of the 27 evaluation database drives are converted into fuel injection timelines (Timeline_{Fuel}) using the simulation and some selected generated engine maps.

As depicted in ‘Figure 48’, the simulation itself uses the air resistance coefficient, the rolling resistance coefficient and the vehicle mass combined with speed, acceleration and slope to compute the needed torque. At the same time, the gear-specific ratio is used to compute the engine speed out of the gear and speed combination. At the end, the computed torque and engine speed variations over the time are used to find out the amount of fuel consumed every 0.1 seconds.

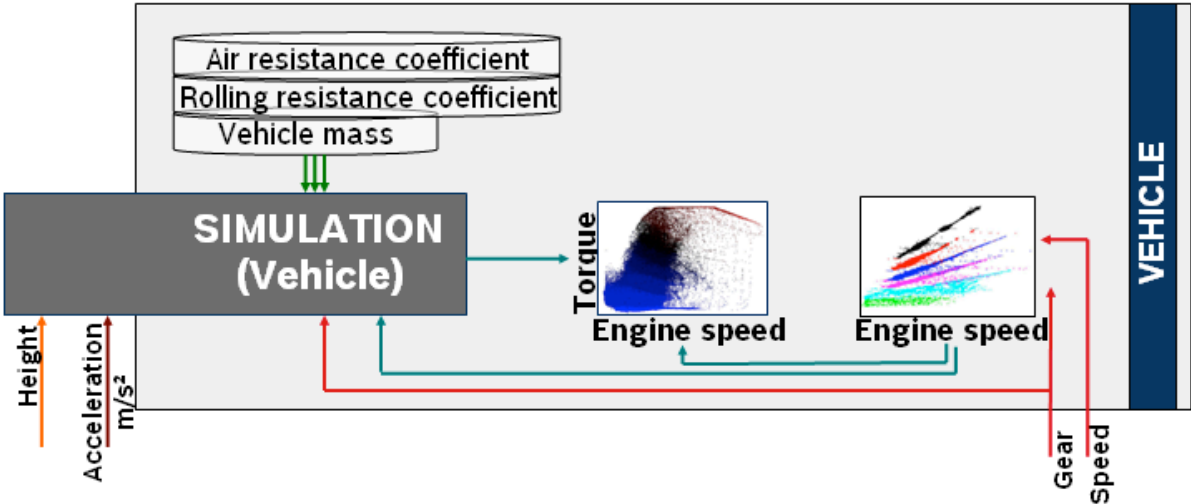


Figure 48: Description of the Input and Simulation Elements Being Involved

Prior to the simulation evaluation, the following decisions have been made:

Inputs:

While the gear information and the driven speed were available in a satisfying quality, as it has been previously established, that the quality of the height information, and therefore the slope, was insufficient (see Chapter 4.1). For this reason, and to estimate the quality loss in the case of ignoring the slope, the simulation is first tested without the slope information and the results later compared against the ones of similar tests using the computed slope.

The recorded acceleration (Chapter 4.2) brings a similar problem; therefore the simulation was tested with two acceleration versions. First, the original recorded acceleration was used, and then the acceleration smoothed using the driven speed information, which is provided from another sensor. The results were then compared.

Engine Map:

For simplification, and to allow a comparison between the results related to the different drivers, and because the quality was found out to be better in most cases (see Chapter 6.1.1.2), it was decided to use the global engine maps computed out of the 9370 kilometers for the evaluation. Beside that, due to the limited quality improvement observed compared to the time necessary for computing, the decision was made not to use the high-resolution engine map (5rpm/1Nm) anymore. Therefore, the following simulation tests have been done using the remaining four engine maps.

Vehicle Parameters:

The vehicle parameters (represented in Figure 48) needed to run the simulation are:

- The air resistance coefficient
- The rolling resistance coefficient
- The vehicle mass
- The gear specific ratio

The air resistance coefficient was calculated based on the BMW E91 official specification sheet (Annex B [BMW09]): with an air resistance coefficient = $0.29 \times 2.17 = 0.6293$.

The rolling resistance coefficient, which is unknown and can not be measured easily, was set to 0.011 because of the tire width (225mm) and the measurements made on similar tires in [Tuev02].

Because of the measurement instrumentation built in the vehicle rear trunk, the mass increased and had to be measured. With the help of an industrial balance, it was identified to be 1800kg (10kg steps).

The gear specific transmission ratio must be computed for each gear. According to the BMW E91 official specification sheet (Annex B [BMW09]):

- The axle ratio is 2.786
 - First gear ratio: 4.171
 - Second gear ratio: 2.340
 - Third gear ratio: 1.521
 - Fourth gear ratio: 1.143
 - Fifth gear ratio: 0.867
 - Sixth gear ratio: 0.691
-
- The tires are 225/45R 17 91W, which means:
 - 225 the tire width in millimeters
 - 45 the ratio of tire height/width, which means that the tire's height is 101.25 mm.
 - 17 stands for 17 inch rims = 43.18 cm.

The wheel (rim + tire) radius is: $\frac{43.18cm}{2} + 101.25mm = 0.31715m$

The wheel circumference is: $2 \times \pi \times Radius = 1.99271222m$

The relation between the engine speed and the vehicle speed is given by:

$$\frac{e_r}{60} \times \frac{1}{AxleRatio \times GearRatio} \times 2\pi Radius = speed$$

With e_r , the engine speed in rpms, and the vehicle speed in m/s. Therefore:

$$\text{The transmission ratio } \frac{speed}{e_r} = \frac{1}{60} \times \frac{1}{AxleRatio \times GearRatio} \times 2\pi Radius$$

This means that the:

- First gear transmission ratio is 0.00285806454
- Second gear transmission ratio is 0.00509443897

- Third gear transmission ratio is 0.00783759842
- Fourth gear transmission ratio is 0.01042956
- Fifth gear transmission ratio is 0.013749696
- Sixth gear transmission ratio is 0.01725179

The computed vehicle characteristics were then used to run the simulation in three distinct test runs to isolate the influence of slope information and to determine which one of the accelerations available should be used in the future:

- a first simulation test without slope and with the original acceleration (Chapter 6.1.2.1).
- a second simulation test with slope and the original acceleration (Chapter 6.1.2.2).
- a third simulation test with or without slope, depending on which one shows the best results, with the computed smoothed acceleration (Chapter 6.1.2.3).

The results were then compared and the decision was made as to which configuration should be retained for the future testing.

6.1.2.1 First Simulation Test

Because of the recorded height quality (see Chapter 4.1), and to determine how relevant the slope in the simulation is, the simulation was run with a slope equal to zero. In this special case, the input use for the simulation is a [gear; speed; acceleration] timeline for each one of the 27 test recordings that compose the evaluation database.

The mean deviation in percent between original recorded fuel consumption and the simulated consumption is presented in the following table:

Simulation Test Without Slope	9370 kilometers Engine Map			
	100rpm/20Nm	50rpm/10Nm	20rpm/5Nm	10rpm/2.5Nm
D1: 4 randomly selected lap logs (@63km)	-14.38%	-15.14%	-14.42%	-13.19%
D2: 5 lap logs (@39km)	-20.08%	-22.07%	-19.91%	-18.28%
D3: 4 randomly selected lap logs (@63km)	-10.48%	-11.05%	-10.84%	-10.43%
D4: 6 lap logs (@39km)	-24.04%	-26.20%	-24.49%	-22.10%
D5: 4 randomly selected lap logs (@63km)	-13.01%	-13.57%	-13.06%	-12.70%
D6: 4 randomly selected lap logs (@63km)	-11.07%	-11.83%	-11.09%	-10.45%

Table 13: Simulation Quality Results Without Slope Consideration

First of all, the simulation predictions are all way under the recorded consumptions. With an error rate of -10 to -25%, the simulation cannot be used with this special configuration to make fuel consumption predictions. So a second simulation test incorporating the slope was performed to clarify its responsibility in the unsatisfying first results, and see if a quality increase could then be reached.

6.1.2.2 Second Simulation Test⁸

The following tests have been performed with slope information extracted as described in Chapter 4.1 and with the original recorded acceleration. The input timeline is now a sequence of [gear; speed; acceleration; slope] combinations over time.

⁸ The following results are valid only for vehicle with an ICE (Internal Combustion Engine). In the case of Electric Vehicle, the slope influence might be different due to the recuperation possibilities integrated in the vehicle.

Simulation Test With Computed Slope	9370 kilometers Engine Map			
	100rpm/20Nm	50rpm/10Nm	20rpm/5Nm	10rpm/2.5Nm
D1: 4 randomly selected lap logs (@63km)	-11.64%	-12.34%	-12.23%	-11.81%
D2: 5 lap logs (@39km)	-13.11%	-15.29%	-13.17%	-11.39%
D3: 4 randomly selected lap logs (@63km)	-7.00%	-7.80%	-7.73%	-7.48%
D4: 6 lap logs (@39km)	-18.24%	-20.57%	-18.91%	-16.49%
D5: 4 randomly selected lap logs (@63km)	-8.91%	-9.72%	-9.37%	-9.18%
D6: 4 randomly selected lap logs (@63km)	-8.09%	-9.07%	-8.69%	-8.39%

Table 14: Simulation Quality Results With Computed Slope

Compared to the first test series, the error rate dropped a few percent, but remains unsatisfying high. Besides the simulation itself, the acceleration quality or the vehicle parameters could have been responsible for the error rate. For this reason, a third simulation test was done with the alternative acceleration smoothed using the vehicle speed information to evaluate its impact on the prediction quality. Because the slope information increases the quality of the simulation prediction, it was used for future predictions.

6.1.2.3 Third Simulation Test

This third test series was conducted using the computed slope and an acceleration that has been smoothed using the driven speed signal. Similar to the previous tests, the mean observed deviation between predictions and records for each driver has been formatted into a table.

Simulation Test with Slope and Computed Acceleration	9370 kilometers Engine Map			
	100rpm/20Nm	50rpm/10Nm	20rpm/5Nm	10rpm/2.5Nm
D1: 4 randomly selected lap logs (@63km)	-9.61%	-10.55%	-10.43%	-9.96%
D2: 5 lap logs (@39km)	-4.23%	-6.51%	-4.34%	-2.65%
D3: 4 randomly selected lap logs (@63km)	-7.06%	-8.00%	-7.97%	-7.64%
D4: 6 lap logs (@39km)	-12.66%	-15.06%	-13.32%	-10.93%
D5: 4 randomly selected lap logs (@63km)	-6.98%	-8.02%	-7.64%	-7.46%
D6: 4 randomly selected lap logs (@63km)	-4.61%	-5.93%	-5.55%	-5.12%

Table 15: Simulation Quality Results with Computed Slope and Acceleration Calculated out of the Speed Variations

The simulation prediction quality was increased again using the smoothed acceleration inputs instead of the original ones. Depending on the drivers, the quality increase was more or less remarkable, with a noticeable improvement in the case of the second driver. There is mainly one possible explanation for this observation: the acceleration input used previously came from the acceleration sensor built in the car. This sensor measures the effects of acceleration on the vehicle; therefore, there might be a little time shift between the acceleration signal and the other inputs used in the simulation. In addition, acceleration sensors are very sensitive. It might be possible that the values transcript showed some sensor overreactions. Smoothing the

acceleration recorded out of the sensor with the one computed out of the recorded speed of travel reduced the recorded overreactions and shortened the potential time shift.

Another observation is that the way the drivers accelerated may have influenced the quality improvements, explaining the discrepancies between the different drivers.

Because of these quality improvements, the decision was taken to run the further tests with the slope information and smoothed acceleration.

However, the vehicle simulation quality is still not satisfying. This might be due to the simulation itself, which uses equations to match the reality, or to the vehicle characteristics used as simulation parameters. Since one of the main goals of this work is to provide a self-learning solution with maximum reduced input, the decision was taken to learn the vehicle characteristics needed for the simulation (Chapter 6.1.3) and to later use them in combination with the simulation (Chapter 6.1.4) to make a last vehicle part estimation accuracy check.

6.1.3 Results of the Vehicle Parameters Estimation

The following subchapter regroups the main results and observations made while learning the vehicle parameters needed to run the simulation as explained in Chapter 5.2.

First, the results of the two transmission filters are compared and the quality of the transmission ratios computed are discussed, then the results of the air resistance coefficient, vehicle mass and rolling resistance coefficient approximations for different vehicle configurations are reviewed and discussed.

6.1.3.1 Transmission Filter Results

Two kind of possible filters were presented in Chapter 5.2. First a filter (Filter A) using various available sensors information and then a second filter (Filter B) using only the gas pedal signal. Both filters were implemented and their results are displayed and analyzed in this subchapter.

- Transmission ratio filter A uses the most available signals and was set to discard following entries:

$$t_{Gear-shift} - 1sec \leq \dots \leq t_{Gear-shift} + 1sec$$

$$Longitudinal_acceleration \leq -0.2m/s$$

$$Longitudinal_acceleration \geq 0.2m/s$$

$$Lateral_acceleration \leq -0.15m/s$$

$$Lateral_acceleration \geq 0.15m/s$$

$$10 < Gear \mid Gear \leq 0$$

$$Brake > 0$$

Using the filtered signal, a gear specific transmission ratio was computed for the six drivers of the Learning Database, and regrouped into the following table. The percentage of data filtered that could be used to compute those ratios is indicated as a driver-dependent mean value on the right.

	Gear 1	Gear 2	Gear 3	Gear 4	Gear 5	Gear 6	Data Used	Data Recorded	% Used
D1	0.0006	0.0049	0.0076	0.0101	0.0132	0.0167	93788	744010	12.6%
D2	0.0023	0.0047	0.0075	0.0101	0.0132	0.0167	48696	500693	9.7%
D3	0.0005	0.0050	0.0076	0.0101	0.0132	0.0166	125722	1021246	12.3%
D4	0.0018	0.0047	0.0075	0.0101	0.0132	0.0167	106231	829779	12.8%
D5	0.0003	0.0049	0.0076	0.0101	0.0132	0.0166	121754	1039129	11.7%
D6	0.0006	0.0049	0.0076	0.0101	0.0132	0.0166	105627	1082985	9.8%

Table 16: Gear Specific Transmission Ratio After the Use of Filter A

Two main observations can be made:

- The computed values for Gears 3, 4, 5 and 6 are identical (or almost identical) for all six drivers. The results for the Gear 2 are converging while the results for the Gear 1 are heterogeneous.

The heterogeneous results for Gear 1, and the little variations observed for Gear 2, may be due to the amount of data available to compute the approximations. In the case of Driver 2 for example, while there were up to 17,000 entries available to compute the ratios of the higher gears, less than 500 entries were used for Gear 2, and only 5 for Gear 1. The low amount of data available is partly due to the filtering as well as the frequency of the gear use. Strong acceleration and fast gear shifting, typical at low speeds, are discarded because of the noise.

- The percentage of data filtered is around 12% for four of the six drivers, and 10% for the remaining two.

Since the test track and the vehicle were identical for all the test drives, and the vehicle was equipped with an automatic gearbox, the differences observed in the amount of data filtered must be related to the driving style. The heavy use of the brake or a stronger typical acceleration may explain those differences. In fact, it was a combination of both that led to those results.

- The second transmission ratio filter (Filter B) was set to discard entries with a *GasPedal_pressure* > 0. Similar to Filter A, the results were condensed and formatted into the following table:

	Gear 1	Gear 2	Gear 3	Gear 4	Gear 5	Gear 6	Data Used	Data Recorded	% Used
D1	0.0001	0.0063	0.0088	0.0105	0.0136	0.0168	198607	744010	26.7%
D2	0.0001	0.0064	0.0085	0.0104	0.0136	0.0169	147404	500693	29.4%
D3	0.0001	0.0063	0.0087	0.0106	0.0136	0.0169	250034	1021246	24.5%
D4	0.0001	0.0063	0.0084	0.0105	0.0136	0.0169	215929	829779	26.0%
D5	0.0001	0.0063	0.0087	0.0105	0.0136	0.0168	251071	1039129	24.2%
D6	0.0001	0.0063	0.0088	0.0106	0.0137	0.0168	285699	1082985	26.4%

Table 17: Gear Specific Transmission Ratio after the use of Filter B

Compared to the results of Filter A, the gear specific transmission ratios seem to be more homogeneous in general, with little variations between the drivers throughout the gears.

Globally, the amount of data used for the approximations is more than two times higher than for Filter A, and the computed values are higher than in Table 16, except for the first gear. In this case, the vehicle idle may be responsible for the low values calculated. While the vehicle is not moving, the engine keeps rotating. Since the ratio is the direct connection between the speed of travel and, the engine rotations, it is then adulterated.

To see the quality of the filters, these results have been compared to the information available in the BMW E91 official specification sheet (in Annex B [BMW09]).

6.1.3.2 Transmission Ratio

	Gear 1	Gear 2	Gear 3	Gear 4	Gear 5	Gear 6
Gear specific transmission ratio	0.00286	0.00509	0.00784	0.010430	0.01375	0.01725
Mean gear specific transmission ratios (Filter alternative A)	0.0010	0.0048	0.0076	0.0101	0.0132	0.0166
Deviation from specification (A)	64.4%	5.0%	3.6%	3.4%	4.0%	3.5%
Mean gear specific transmission ratios (Filter alternative B)	0.0001	0.0063	0.0086	0.0105	0.0136	0.0169
Deviation from specification (B)	96.4%	-23.7%	-10.3%	-0.9%	1.1%	2.3%

Table 18: Gear Specific Transmission Ratio Compared to the Official BMW E91 Specification

The original and the computed mean gear specific transmission values over the six drivers for both filters have been regrouped into the previous table for more clarity.

The first line contains the ratios computed out of the official BMW E91 specification. The second and fourth lines respectively contain the approximations made with Filter A and Filter B. The third and fifth rows contain the deviation between approximation and official specifications in percent.

Starting with the results obtained with the application of Filter A, all the approximations are less than the official specification. The first gear has an error rate of 64% that may be related to the fact that only five entries were used to calculate it. The other gears accuracy varies between 3.5 and 5% under the official specification, which is acceptable for the purpose of this work.

The results of Filter B are less satisfying for the lower gears. The deviation for the first gear is even more than with Filter A, but this must be linked to the vehicle idle as explained before. The second and third gears have an important negative (the approximations are over the real values) error rate, which makes them not usable for the simulation, while the higher gear have a very low error rate. One possible explanation for the quality variation between Gears 2 and 3 and Gears 4, 5 and 6 may be that the filter is not considering the use of brake. Typically, the lower gears might get used at low speed in the city, where brakes are often used to regulate the vehicle speed, while coasting may be at higher speed (with higher gears).

The introduction of a brake signal analysis in Filter B would have led to a selection of almost the same data as Filter A, and was therefore abandoned.

In summary, Filter A seems to be more adapted to our purpose than Filter B because of the better reached quality in general. The deviation observed for Gear 1, even if noticeable, should have a limited impact on the simulations prediction quality because of the little use of this gear compared to the other ones.

This quality result related to the first gear can be better understood when displayed in the form of a comparison between the six gears. In the following Figure, Gear 1 is (almost) invisible at the bottom (because only 5 entries were used) while Gear 6 is visible at the top.

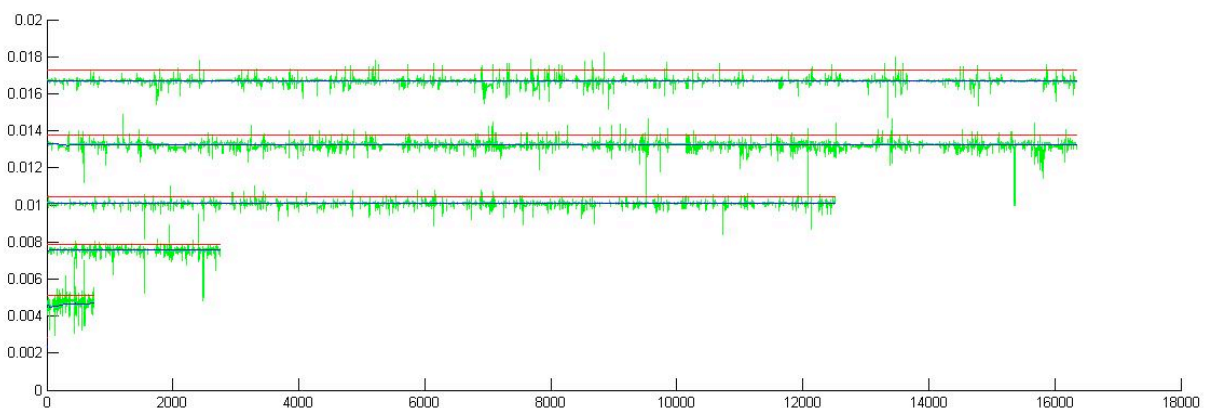


Figure 49: Evolution of the Gear Specific Transmission Ratios (Filter A)

Data used: Driver 2 Learning Database part (recorded: 500693 / used: 48696)

X-Axis: Number of data used (equal to 0.1 sec recorded)

Y-Axis: Transmission ratio

Green: Transmission ratios computed for each selected entries

Blue: Evolution of the mean transmission ratios over the time (computed out of the green inputs)

Red: BMW E91 official specification (Annex B [BMW09])

The green curves represent the recorded entries that have been used to calculate the gear specific transmission ratios. While the two higher ratios were computed out of more than 16.000 entries, the first gear had less than 5 available, and the second gear around 500. Beside

that, the noise is higher for the second gear than, for example, the fourth one. This may be related to the sensor used to determine the vehicle speed.

The following information that could explain this observation was collected during an interview of the Robert Bosch Car Multimedia GmbH Positioning Team in November 2012:

The vehicle speed is calculated based on the wheel rotation sensor. The accuracy depends on the number of emitters on the wheel. The more emitters there are, the better the speed accuracy. In the worst case, there is only one emitter on the wheel; the sensor is then able to count the number of wheel rotations (in our case a wheel circumference is almost 2 meters – see Chapter 6.1.2). Therefore, the accuracy will be around 2 meters. This has a lot more consequence on vehicle speed signal quality at low speed (few rotations / time) than it has for a fast moving vehicle.

Another possible explanation is that the vehicle may not have been calibrated with these wheels.

6.1.3.3 Torque Calculation

After investigating the potential error percentage related to the engine map, simulation and transmission ratio, the quality of the remaining vehicle characteristics used as simulation parameters must be analyzed.

As presented in Chapter 5.2.3.3, the vehicle parameters are learned using the torque value calculated from the simulation: $Torque_{Simulation}$. The simulation itself is made of a combination of various equations that describe the different influences on the fuel consumption. It uses a $Timeline_{[Gear; Speed; Acc; Slope]}$ produced by the driver simulation and the database description to compute a $Timeline_{[Torque; Engine Speed]}$ that will be converted into a $Timeline_{Fuel}$ with the help of the engine map. While the conversion from speed and gear to engine speed depends only on the gear specific transmission ratios and has a limited complexity, the conversion of gear, speed, slope and acceleration into a torque value is a far more complex calculation.

The comparison between original and computed torque showed some differences. Some of the most important differences could be linked to database inaccuracy (e.g. slope), or little time gaps between the selected gears. A 170 seconds example that contains some of the typical observed effects is displayed in the following figure.

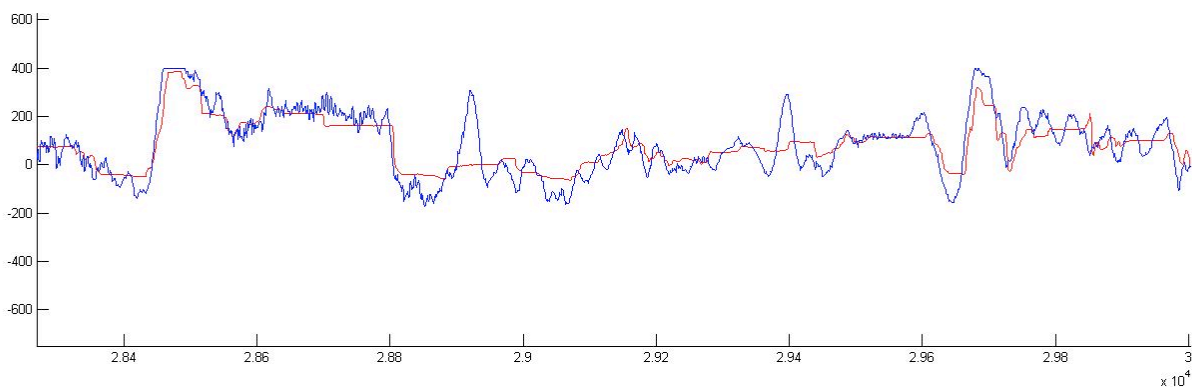


Figure 50: Torque Recorded Versus Torque Calculated Over Time

Data used: Driver 1 test track one

Observed time cycle: 170 seconds

X-Axis: Time in 0.1sec

Y-Axis: Torque in Nm

Red: Recorded torque available on CAN

Blue: Computed torque using the official BMW E91 specifications, a computed slope and acceleration.

The first general impression is that the torque signal found on the CAN bus ($Torque_{CAN}$) and the one calculated with the simulation ($Torque_{Simulation}$) global evolutions over the time are similar. This indicates that the observed prediction results so far may not be coincidental.

One of the main differences between the two curves is the smoothness of $Torque_{CAN}$ compared to $Torque_{Simulation}$. This is especially true between the timeline markers 2.86 and 2.88. The noise observed on $Torque_{Simulation}$ could be directly linked to the acceleration signal despite the signal cleaning done at first. In sum, such a noise should not have much influence on the fuel consumption prediction. More interesting is the fact that the test vehicle is not equipped with a torque sensor, which means that this value must have been computed. The algorithm used to compute it is unknown, but it commonly uses engine sensors to approximate it, and may be straightened. This would explain the ample differences around timeline marker 2.97.

To sum up, most of the differences between the two curves could be linked to database or input signal errors. With the increasing amount of sensors available in cars and the near future switch to the NDS database, those problems may be reduced or disappear in the future. On the other hand, the predictions were made using a behavior prediction, which may be far more imprecise than the vehicle sensors. Considering that $Torque_{CAN}$ is no recorded value, but a calculated one, it may also be subject to some errors. Because of all this imprecision in the data used by the simulation, the computed torque quality has been found out to be satisfying, and the tests of the vehicle characteristics learning have been conducted. The repercussions on the vehicle part simulation quality could only be tested in combination with the learned vehicle characteristics. This has been done in Chapter 6.1.4.

6.1.3.4 Remaining Vehicle Characteristics

The remaining components to be quality checked are the vehicle characteristics used as simulation parameters. Because those characteristics will be learned by the presented solution proposition, it is logical to quality check the learned vehicle characteristics rather than to make a judgment over the accuracy of the official ones. The learned characteristics are presented in the following chapters, and their accuracy measured against the values mentioned in the official specifications. After that, the simulation was run with the learned values and the quality of the computed results discussed.

Because the computed values are compared to the original ones, there is no need of a differentiation between learning and evaluation databases in this particular case; therefore, and to provide the maximum of discrete testing data, all the available recordings were used to learn the vehicle characteristics.

The transmission ratios and the engine map reached a satisfying minimum quality around 600km; therefore, the learned vehicle parameter quality reached after 600km is particularly interesting. For this reason, all the available recordings for testing was split into 14 inputs blocks, 13 of them being driver dependent, and 1 made of recordings of four different drivers. The input blocks regroup around 620km of data each; with one exception that has three times more (1790.5km) and contains additional information recorded on the highway while bringing the vehicle from Stuttgart to Hildesheim. This special block was planned to be use for the control of the values global evolution over a larger amount of driven kilometers.

6.1.3.4.1 Air Resistance Coefficient Estimation Over Time (With and Without Roof Box)

The observations made concerning the air resistance coefficient estimation are discussed first. These results were generated simultaneously with the vehicle mass and the rolling resistance, and influenced each other.

The values computed out of the 14 input blocks are regrouped in the following table:

Driver	Name	Air Resistance Coefficient	Kilometer Recordings Used (%)	Kilometer Recordings Total
D1	B1-1	0.626	5.1%	634.9 km
	B1-2	0.530	4.2%	633.6 km
D2	B2	0.704	5.0%	617.0 km
D3	B3-1	0.665	3.7%	589.1 km
	B3-2	0.666	4.8%	634.0 km
	B3-3	0.579	4.5%	634.3 km
D4	B4	0.467	4.5%	842.2 km
D5	B5-1	0.723	10.0%	1790.5 km
	B5-2	0.715	3.6%	632.0 km
	B5-3	0.628	4.2%	625.8 km
D6	B6-1	0.514	3.5%	625.5 km
	B6-2	0.578	5.1%	611.3 km
	B6-3	0.562	4.0%	877.6 km
D1-D3-D5-D6	B7	0.677	4.8%	617.6km
Mean		0.617	4.8%	

Table 19: Air Resistance Coefficient Approximations for each 14 Input Database Blocks

First row: Drivers involved in the recordings

Second row: The 14 input blocks designation

Third row: The computed values

Fourth row: The amount of the data that wasn't discarded by the filter (chapter 5.2.3.3)

Fifth row: The amount of recorded kilometers for each input block

Two main observations could be extracted out of the results:

- The percentage of kilometer recording used is very low and varies between 3.5-5% with only one exception.

The observed exception of 10% input data used was computed with the input block B5-1 that contains the highway recordings between Stuttgart and Hildesheim. These observations are directly related to the data dispatcher described in Chapter 5.2.3.3. Only values that match

100km/h \leq recorded speed

1° \leq recorded slope \leq 1°

0m/s² \leq recorded acceleration \leq 0.15 m/s²

are used to learn. Such values are mostly to be matched on the highway, which explains the 10% data use compared to the elsewhere observed 3.5-5% range. The range itself is due to driving behavior variations that could be partly due to traffic.

- At first sight, the computed values show a high variation between 0.467 (input block B4 / second lowest value is 0.514) and 0.723 (input block B5-1).

These variations can be put into perspective with the observations made in the Annex F: 'Vehicle Description used to Compute Forces'. According to the official BMW 3 Series specification sheets, the 3 Series air resistance coefficient varies according to the body style changes between 0.5616 and 0.6944.

Further on, the graphical representation of the 14 calculated air resistance coefficient variations over the driven distance helps to recognize what seems to be a general trend, and is not recognizable on the table form.

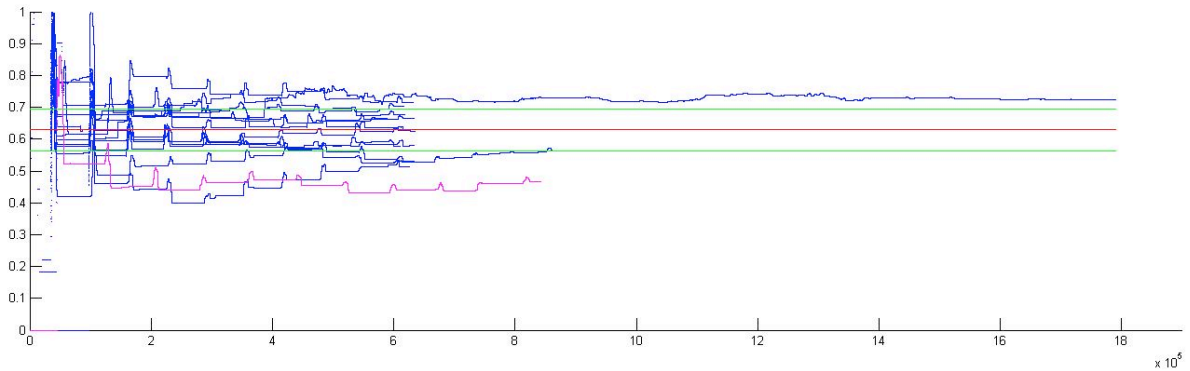


Figure 51: Evolution of the Air Resistance Coefficient over the Driven Kilometers (Specific)

Data used: 14

X-Axis: Distance in 10^5 m

Y-Axis: Air resistance coefficient

Red: Expected value of 0.6293

Green: Based on the Annex F ('Vehicle Description used to Compute Forces'), the 3 Series air resistance coefficient as a minimum of 0.5616 and a maximum of 0.6944.

Blue: Thirteen data blocks evolution over the distance

Magenta: Driver four data evolution (B4 - the worst result)

The 'steps' observed in the curves are related to the very periodic update of the values, when the vehicle is moving at higher speeds on the highway. All the recordings were made on the Hi01, Hi03 and Hi04 tracks (with the exception of B5); this explains the update synchronization between the curves.

With two exceptions, all the curves converge into the green delimited range that represent the extreme aerodynamic variations on the 3 Series, and therefore was defined as being an acceptable result.

- The first exception, colored in magenta, couldn't be explained in a reasonable amount of time, but seems to be related to an erroneous data which influenced the rolling resistance coefficient so badly, that its influence was visible on the air resistance coefficient and the vehicle mass (the learning of the vehicle characteristics is synchronous and not independent). The effects of this error should have disappeared over the driven kilometers as the vehicle mass and rolling resistance curves tendencies indicate (the analyzation of those two curves is presented in the following subchapters).

- The second exception is the 1790km curve. The input block B5-1 is not only made of a Stuttgart-Hildesheim highway drive, but also contains some test drives made around Hildesheim on the Hi01 circuit. This wouldn't have been a problem at all, if the vehicle characteristics hadn't changed over the time. As it was later found out, the highway drive was recorded with three people onboard, adding some weight to the vehicle. Since the Learning Component wasn't configured to 'forget' (this choice was made because of the limited amount of data available) the learning went wrong. In this case, the vehicle mass was initialized in 'empty' conditions, then, when the highway recordings were used, the increased resistance observed had to be dispatched on the 'for learning available' vehicle characteristic. Driving on the highway, the surrounding conditions are optimal for an over proportionally air resistance coefficient adaptation, which explains why the increased resistance was first attributed to the air resistance coefficient. This error would:

- have been corrected if the vehicle had been moving with this configuration (three passengers) on regional roads and inner-city condition to allow the learning system to adapt rolling resistance coefficient and vehicle mass as well.

- not have happened (or only for a limited time) if the learning system capability to 'forget' had been activated.

For the second time, to see the long term evolution of the vehicle parameter, and because they are not learned independently from each other, a sequence of input blocks was fed into the simulation and the result compared to the one computed out of the exact opposite sequence. The first sequence to be fed was defined [B5-1; B5-2; B5-3; B3-1; B3-2; B3-3; B1-1; B1-2; B6-1; B6-2; B7; B6-3; B2; B4], and the opposite one [B4; B2; B6-3; B7; B6-2; B6-1; B1-2; B1-1; B3-3; B3-2; B3-1; B5-3; B5-2; B5-1].

The values evolutions over the driven distance (in thousands of kilometers) are displayed in the following figure.

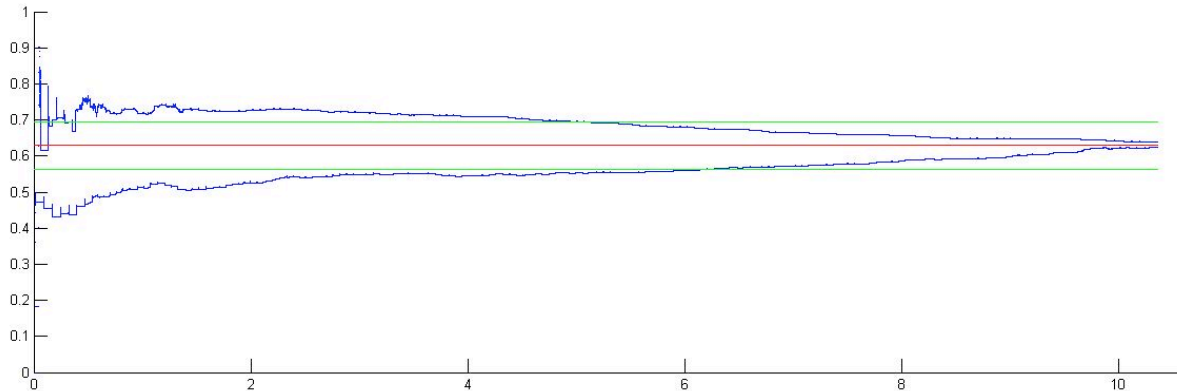


Figure 52: Evolution of the Air Resistance Coefficient over the Driven Kilometers (General)

Data used: All the 14 available data blocks in two opposite sequences

X-Axis: Distance in 10^6 m

Y-Axis: Air resistance coefficient

Red: Expected value of 0.6293

Green: Based on Annex F ('Vehicle Description used to Compute Forces'), the 3 Series air resistance coefficient is 0.5616 and the observed maximum is 0.6944.

Blue: The two sequences of data (first sequence on top)

The first sequence computation resulted in an air resistance coefficient of 0.6385, while the second sequence production was 0.6235. The system was not set to 'forget' and used all the available data to produce those results. For this reason, the evolution got smoother over the driven kilometers.

Since the air resistance coefficient computed out the official BMW specification is equal to 0.6293, and the influence of wind and minor aerodynamic changes (e.g. windows) couldn't be recorded, the reached quality is judged very satisfying.

Less satisfying is the driven distance needed to initialize the system, but there is some potential for a process optimization, if the learning is starting with presets, activating the short time learning ('forget' function) to make quicker adaptation possible, and optimizing the filter function of the dispatcher, using more vehicle sensors if available. The results presented here were made with a first implementation to demonstrate that the concept is valid, and not to make it as efficient as possible.

Now that it was proven, that the learning of the BMW E91 test vehicle air resistance coefficient is possible, at least a second test with another vehicle was needed to consolidate the results. Unfortunately, at this time, it wasn't possible to find data logs from another vehicle with the required sensor recordings quality. A backup solution was then proposed: the additional tests should be done with the available test vehicle and a modified aerodynamical configuration. For this purpose, the test vehicle was equipped with a roof box.

Roof Box Tests (The test set description is available in Annex C):

The roof box was chosen to be the widest that was available for rental in Hannover. It was a Thule Atlantis 900 with a roof rack and 90x46 cm dimensions. The air resistance coefficient is not published, and Thule couldn't communicate on this value over email⁹.

It is assumed that the rolling resistance didn't change much from the original value (only a small increase due to the additional weight) and it is therefore expected to be around 0.011 as mentioned in Chapter 6.1.2.

An air resistance increase is expected due to the roof box and rack. According to the official specifications, the roof box has a front surface equal to 0.414 m². The roof rack is approximated with 3 cm x 1.5 m = 0.045 m². Because the air resistance coefficient is unknown, this value had to be assumed. There are no reliable values in the literature and therefore it was decided to consider the very aerodynamic box and the rack, which is not aerodynamic (strong sharp edges), similar to a modern car with a drag coefficient of 0.3.

The 'roof box + roof rack + vehicle' air resistance coefficient multiplied with their respective front surface should be more or less about 0.7670.

The car (without driver, roof box and rack, but with the CAN recording equipment) weight was found out to be 1800kg on an industrial scale with a 10kg definition.

The vehicle was driven over 820.6 kilometers from different drivers in this configuration. The recordings were then used as input to learn the vehicle characteristics. Again, the original sequence and its inverse were tested, and the results have been formatted into the following table.

	Air Resistance Coefficient	Kilometer Recordings Used (%)	Vehicle Mass (kg)	Kilometer Recordings Used (%)	Rolling Resistance Coefficient	Kilometer Recordings Used (%)	Kilometer Recordings Total
Roof Box	0.7679	2.7%	1863.2kg	14.1%	0.0093	7.4%	820.6km
Roof Box Inverse	0.6828	2.7%	1845.5kg	14.1%	0.0132	7.4%	820.6km

Table 20: Air Resistance Coefficient Approximations for the Recorded Data Sequence and its Inverse

The percentage of data used to learn the air resistance coefficient is less important than in the standard vehicle configuration tests. The little changes made to the test track (because of road work – see differences between Hi01 and Hi02 in Annex B and C) should be partially responsible for this observation. On the other hand, the data filtering requires recordings at high speed to learn, and the recordings analysis showed that the average driven speed with the roof box was lower.

Even considering the possible imprecision of the simulation used to learn the vehicle characteristics, the learned vehicle mass quality is very satisfying.

Because the air resistance coefficient counteracts the roll resistance coefficient, and even though the two test runs were using the same data in a different sequence, they showed strong differences. This result can be explained by the little amount of data that was used to learn the air resistance coefficient; therefore, the two test sequences were extended using three and a half iterations of the original sequences: an “Original Sequence x 3.5” and an “Original

⁹ Date: June 22 2010, 10:40:24 HAE

From: Christoph.Gabler@thule.com

Object : AW: THULE CONTACT US FORM - General Comment

“Leider haben wir keine so detaillierten Angaben über unsere Boxen. Ich bedauere, Ihnen keinen positiven Bescheid geben zu können.”

Sequence Reverse x 3.5”. The evolution of the two extended sequence air resistance coefficient over 2872.1 kilometers is displayed in the following figure.

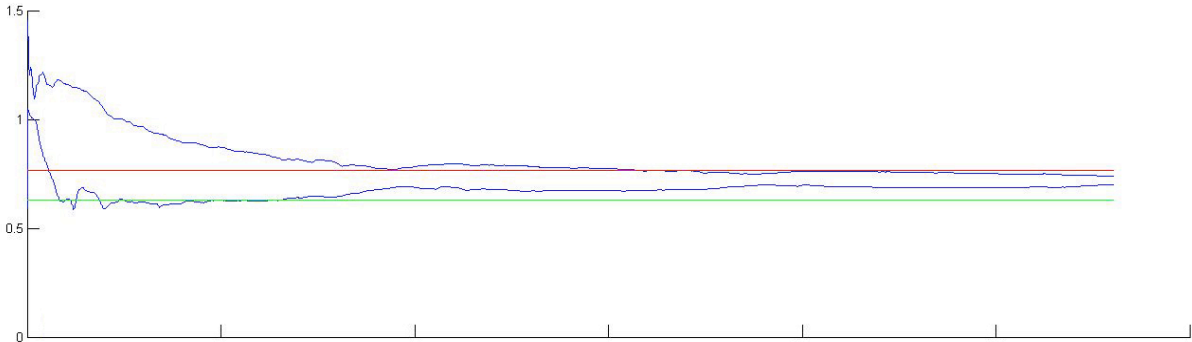


Figure 53: Evolution of the Air Resistance Coefficients over the Driven Kilometers (Roof Box)
Data used: All the roof box recording available used three times in a row
X-Axis: Distance from 0 to 2872.1km (3.5x820.6km)
Y-Axis: Air resistance coefficient
Red: The supposed air resistance coefficient of 0.7670
Green: Original air resistance coefficient (without roof box)
Blue: The two sequences of data

The result of the “Original Sequence x 3.5” computation was 0.7383, while the “Original Sequence Reversed x 3.5” computation was 0.6999. Mean value is 0.7191, which is superior to the air resistance coefficient without roof box (in green in the Figure), and may actually be right since the air resistance coefficient of the roof box is unknown (see Red in the figure above).

In summary, although only a little part of the recordings could be used to learn the vehicle air resistance coefficient, and despite the effect of wind and aerodynamic modifications that have an important impact and could not be documented, the values computed have a high quality matching the expectations. In case of the roof box tests, the value to match was unknown, but the learning results are very plausible since the aerodynamics of a roof box are assumed to be the same as a standard vehicle.

6.1.3.4.2 Vehicle Mass Estimation Over Time (With and Without an Additional 300kg)

This subchapter regroups the observation made concerning the vehicle mass estimation. These results were generated simultaneously with the air resistance and the rolling resistance coefficient, and influence each other.

The results computed out of the 14 previously detailed input blocks are regrouped in the following table:

Driver	Name	Vehicle Mass (kg)	Kilometer Recordings Used (%)	Kilometer Recordings Total
D1	B1-1	1734.2kg	13.2%	634.85km
	B1-2	1859.7kg	14.0%	633.60km
D2	B2	1843.0kg	14.1%	617.02km
D3	B3-1	1853.1kg	15.8%	589.12km
	B3-2	1705.5kg	14.1%	634.01km
	B3-3	1760.4kg	14.0%	634.30km
D4	B4	1612.4kg	14.5%	842.23km
D5	B5-1	1865.4kg	8.3%	1790.48km
	B5-2	1847.2kg	15.9%	632.04km
	B5-3	1802.6kg	15.3%	625.84km

D6	B6-1	1812.8kg	13.5%	625.49km
	B6-2	1827.0kg	13.6%	611.29km
	B6-3	1836.8kg	14.0%	877.57km
D1-D3-D5-D6	B7	1914.1kg	14.9%	617.56km
Mean		1805.3kg	13.9%	

Table 21: Vehicle Mass Approximations For Each of the 14 Databases

Compared to the air resistance coefficient results, and because of the filter specification, a more meaningful quantity of the recordings could be used to compute the vehicle mass (around 14%). Although the vehicle mass was measured to be 1800 kg on an industrial scale, the official BMW E91 specification mentions a 1675 kg weight for the automatic gearbox version. Adding the weight of some options (e.g. leather seats) and of the CAN bus recording setup, and supposing that the scale was +/-50 kg accurate, the vehicle mass could actually have been slightly under 1800 kg without a driver, and slightly over with a driver. Therefore, the measured mean value of 1805.3 kg is absolutely credible.

In reference to the air resistance coefficient results analysis, the value produced out of the B4 and B5-1 block must be considered separately from the others. The B4 block produced (again) the worst results for the same reasons that were mentioned in Chapter 6.2.3.4.1. While the quality of the value produced out of the B5-1 block is good enough, the percental amount of data used is lower than for the other blocks. This is due to the dispatcher selection to update the vehicle mass, which is defined as:

- Recorded speed $\leq 90\text{km/h}$
- $-0.2^\circ \leq \text{recorded slope} \leq 0.2^\circ$
- $0.2\text{m/s}^2 \leq \text{recorded acceleration}$
- $4 < \text{Gear}$

The recordings analysis showed that the time spent driving at speeds lower than 90km/h was proportionally less than it was for the test drives on the Hildesheim tracks.

The graphical representation of the 14 calculated vehicle mass variations over the driven distance helps to analyze the evolution of the values while learning and is displayed in the following figure.

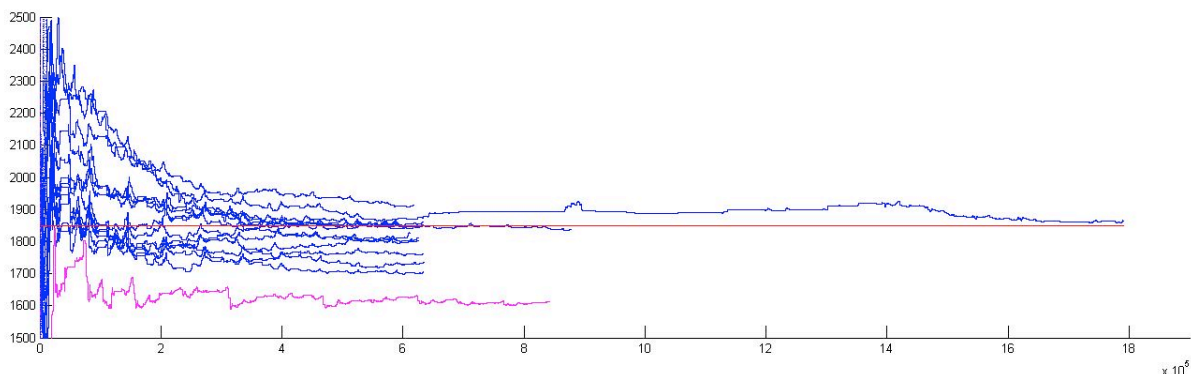


Figure 54: Evolution of the Vehicle Mass over the Driven Kilometers (Specific)

Data used: 14

X-Axis: Distance in 10^5m

Y-Axis: Vehicle mass in kg

Red: Expected value of 1850kg

Blue: Thirteen data blocks evolution over the distance

Magenta: Driver Four data evolution

First of all, the typical ‘steps’ that could be observed in the air resistance evolution curves (very punctual learning) are gone, indicating a more frequent learning update, which is confirmed by the percental use of the recording listed in the previous table. Then, the

evolution of the learned vehicle mass seems to downgrade over the time. To confirm or contradict this impression, an analysis over a longer distance is needed. For this reason, and similar to what has been done while investigating the air resistance coefficient learning, two sequences made out of all the 14 input blocks have been defined: [B5-1; B5-2; B5-3; B3-1; B3-2; B3-3; B1-1; B1-2; B6-1; B6-2; B7; B6-3; B2; B4], and the reverse one [B4; B2; B6-3; B7; B6-2; B6-1; B1-2; B1-1; B3-3; B3-2; B3-1; B5-3; B5-2; B5-1]. The learning results evolution over time is graphically represented in the following figure.

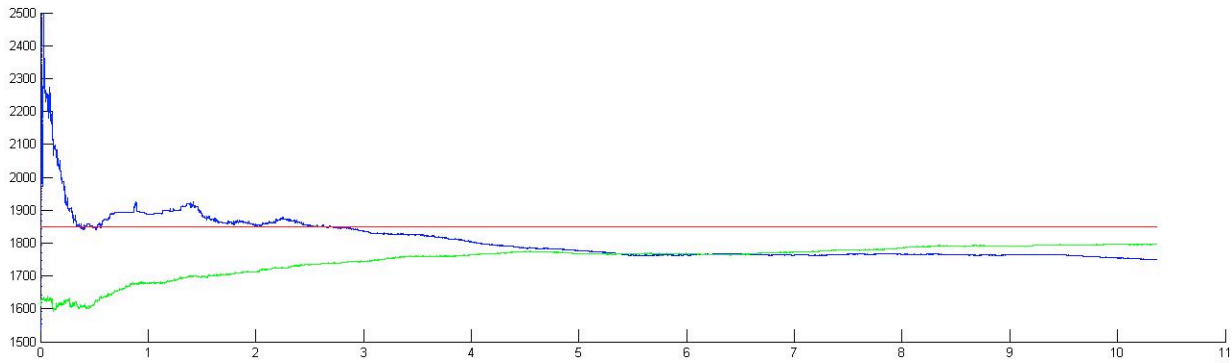


Figure 55: Evolution of the Vehicle Mass over the Driven Kilometers (General)

Data used: All the 14 available data blocks in two opposite sequences

X-Axis: Distance in 10^6 m

Y-Axis: Vehicle mass in kg

Red: Expected value of 1850kg

Blue: The first sequence of data

Green: The second (reverse) sequence of data

First of all, the previous downgrade impression over the distance can be refuted, because the reverse sequence resulting curve seems to keep increasing. These properties can be explained by the place of the recording blocks B4 and B5-1 (the two exceptions: data error and the Stuttgart-Hildesheim drive with 3 people on board) in the sequence. These are placed at the extremities of the sequences and therefore have an influence on the curves beginning and ending. This explanation is later confirmed with the analysis on the vehicle mass evolution during the ‘Roof Box’ tests and the ‘300 kg’ tests.

The vehicle mass was found out to be 1749.9 kg out of the first sequence, and 1796.1 kg out of the second sequence. Assuming that the learning system works right, these results would confirm the supposition made based on the official BMW E91 specification, which indicates a test vehicle mass that should be slightly under 1800 kg.

‘Roof Box’ and ‘300 kg’ tests (The test set description is available in Annex C):

Mounting a roof box on the test vehicle didn’t only influence the vehicle aerodynamic, but also added some weight. For this reason it is interesting to check if this limited weight increase was noticed, and in general, to confirm the vehicle mass learning ability with some new recordings. The results of the vehicle and roof box mass learning were over 3.5 times the recorded 820.6 kilometers (two sequence of recordings: chronological and reverse) and are displayed in the following figure:

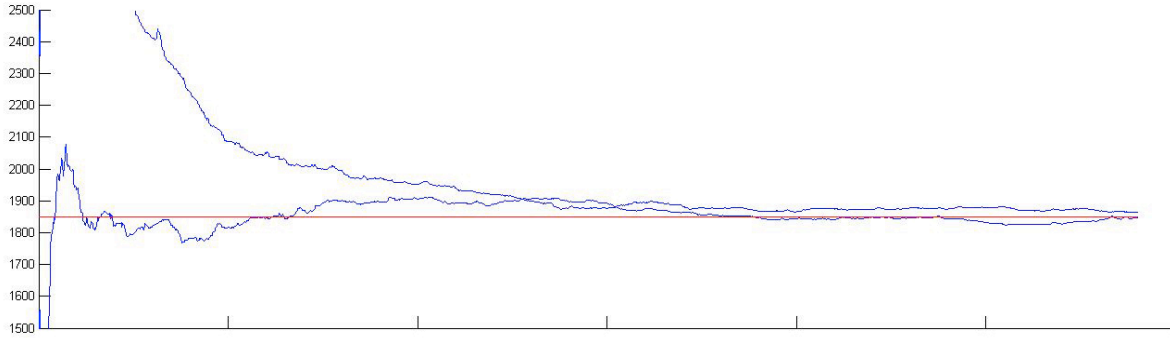


Figure 56: Evolution of the Vehicle Mass over the Driven Kilometers (With Roof Box)
Data used: All the available recordings with roof box
X-Axis: Distance from 0 to 2872km (3.5x820.6km)
Y-Axis: Vehicle mass in kg
Red: 1850kg (for comparison)
Blue: The two sequences of data (original and inverse)

The computed vehicle masses are 1863.2kg and 1845.5kg (Table 20: Air Resistance Coefficient Approximations for the Recorded Data Sequence and its Inverse), which is higher than the learned vehicle mass without roof box. The two curves also seem to convert and stabilize to these values. The observed mass difference between the learning with and without roof box can not just be attributed to the roof box and rack, because the drivers that drove the car during the Hi01 test drives couldn't be involved in the Hi02 test drives. Therefore, some weight variation should be related to the drivers' change.

Since there was only one vehicle available for tests, the main goal of the Hi02 test drives was to modify the test vehicle learned characteristics as much as possible to simulate new cars. Besides adding the largest roof box that could be found to modify the aerodynamics, it was planned to load 300kg sand on the backseat (as near as possible to the vehicle's center of gravity). In the second half of the test week, the vehicle was driven around the test track with a roof box and a 300kg load. The expected vehicle mass was 1800kg+roof box+driver+300kg=2200kg. A total of 642.3 kilometers was recorded with this configuration, then a chronological sequence and its reverse were used as inputs for the prototype. The results computed out of the two recording sequences are presented in the following table:

	Air Resistance Coefficient	Kilometer Recordings Used (%)	Vehicle Mass (kg)	Kilometer Recordings Used (%)	Roll Resistance Coefficient	Kilometer Recordings Used (%)	Kilometer Recordings Total
300kg	0.5996	3.5%	2293.5kg	12.8%	0.0094	8.6%	642.29km
300kg inverse	0.6170	3.5%	2284.3kg	12.8%	0.0089	8.6%	642.29km

Table 22: Vehicle Mass Approximations for the Recorded Data Sequence and its Inverse

Because of the heavy load, the test vehicle suspension was maximally compressed and the vehicle center of gravity lowered, reducing the air drag coefficient due to the underbody and spinning tire turbulence (the principle used in the AUDI adaptive air suspension and race cars). Therefore, the air resistance coefficient should have dropped a little in comparison to the one learned during the 'Roof Box' test.

The percentage data used to learn the vehicle air resistance coefficient remains constant while the coefficient itself dropped more than expected. It is balanced by a increase of the vehicle mass of around 85-95kg more than expected. This observation could have two possible origins:

- The learning values were initialized with zeros (worst case) and because of the little amount of data used to adapt the air resistance coefficient, it is possible that a longer test drive may have been needed to correct those values which directly influence the vehicle mass learning.
- The simulation involved in the learning process have a decreasing quality when it comes to learning the characteristics of extreme vehicle specifications, and a simulation adjustment according to the vehicle type (information available on CAN) could be needed.

The first supposition is not confirmed by the observation of the learned vehicle mass over the distance displayed in the following figure.

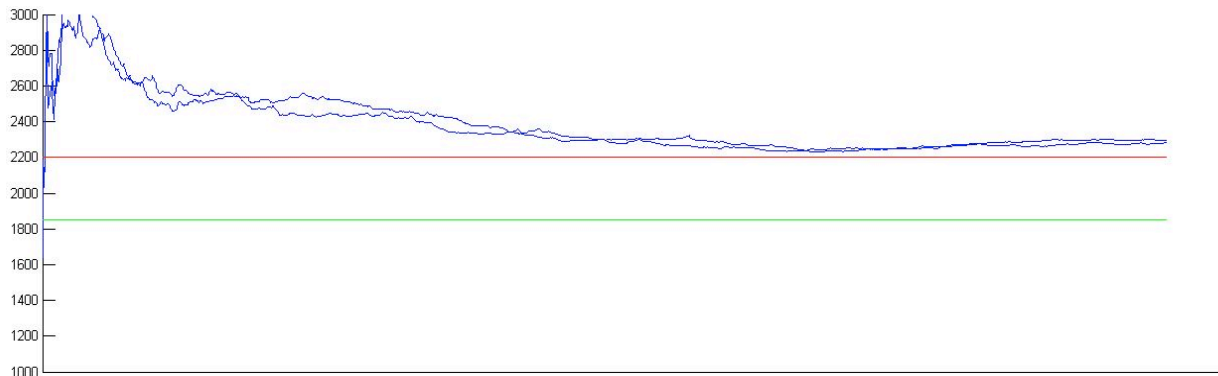


Figure 57: Evolution of the Vehicle Mass over the Driven Kilometers (300kg)
Data used: All of the ‘300kg Sand’ recordings available
X-Axis: Distance from 0 to 642.29km
Y-Axis: Vehicle mass in kg
Red: The supposed vehicle mass of 2200kg (1800kg + roof box + 300kg sand)
Green: 1850kg (for comparison)
Blue: The two sequences of data

It seems that the learned vehicle mass stabilized after half of the distance (320 kilometers) to the final value. For this reason, it is supposed that the simulation used in the learning process should be adapted to the vehicle type. The percentage repartition of rolling resistance and air resistance at low speed and the equation describing the rolling resistance could be adapted to a larger vehicle with larger tires at the prototype system initialization using the vehicle type description available on CAN bus.

However, if the vehicle characteristics are only used for fuel prediction, as it is the case in this work, the imprecision observed in this case should not have a noticeable influence on the fuel consumption prediction except for extreme situations (e.g. high slope). Therefore, the level of complexity was kept reduced and the further tests were made using the standard simulation as described in Chapter 5.

While the vehicle mass and the air resistance coefficient are being learned, there is a third vehicle characteristic, whose value has a direct influence on the air resistance coefficient, related to the tire friction on the ground that must be learned. The learning results of the rolling resistance are analyzed in the following chapter.

6.1.3.4.3 Rolling Resistance Coefficient Estimation Over Time

First, the results of the standard tests described in ‘Table 19’ and ‘Table 21’ are presented and discussed:

Driver	Name	Roll		
		Resistance Coefficient	Kilometer Recordings Used (%)	Kilometer Recordings Total
D1	B1-1	0.0085	4.6%	634.85 km
	B1-2	0.0103	6.8%	633.60 km
D2	B2	0.0068	3.6%	617.02 km
D3	B3-1	0.0088	6.4%	589.12 km
	B3-2	0.0102	6.5%	634.01 km
	B3-3	0.0102	4.8%	634.30 km
D4	B4	0.0161	8.9%	842.23 km
D5	B5-1	0.0081	3.4%	1790.48 km
	B5-2	0.0104	6.4%	632.04 km
	B5-3	0.0111	5.0%	625.84 km
D6	B6-1	0.0097	7.3%	625.49 km
	B6-2	0.0106	4.4%	611.29 km
	B6-3	0.0091	5.6%	877.57 km
D1-D3-D5-D6	B7	0.0061	4.5%	617.56km
Mean		0.0097	5.6%	

Table 23: Roll Resistance Coefficient Approximations For Each of the 14 Databases

The rolling resistance coefficient is adapted at speeds between 20km/h and 40 km/h, and positive acceleration smaller than 0.15 m/s². For this reason, the driver has an important influence on the amount of information that can be use to learn the coefficient. This explains the disparities in the percentage use of the recordings, with a maximum use at 8.9% for the recording block B4. This block contains the error that produced the erroneous air resistance coefficient and the erroneous vehicle mass in counter balance of the wrong rolling resistance coefficient. The graphical representation of the coefficients produced out of the 14 recording blocks emphasis this observation. The erroneous value computed out of B4 is marked in magenta as it was in ‘Figure 54’ and ‘Figure 51’.

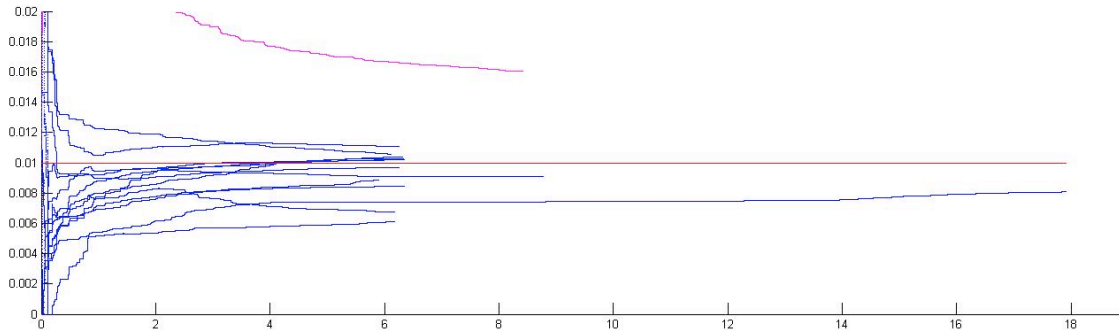


Figure 58: Evolution of the Roll Resistance Coefficient over the Driven Kilometers (Specific)

Data used: 14

X-Axis: Distance in 10⁵m

Y-Axis: Roll resistance coefficient

Red: Expected value of 0.0100

Blue: Thirteen data blocks evolution over the distance

Magenta: Driver Four data evolution

As was also the case for the air resistance coefficient and the vehicle mass, the values converge over the driven distance. While the mean value is equal to 0.0097, the median value of 0.00995 is more interesting due to the spikes. Although the rolling resistance coefficient of the tires mounted on the test vehicle remains unknown, this value places them between eco-efficient tires (0.008-0.009) and less efficient tires (0.012-0.013) according to the measurements made by TÜV in 2002 [Tuev02]. Regarding the test tire width, the rolling

resistance was expected to be around 0.011, but due to the efficiency evolution over the last 10 years, the value range of 0.0097-0.00995 is very plausible.

Air resistance and rolling resistance are almost impossible to isolate based on the available recordings analysis. Therefore, the extreme values of one of those coefficients have a direct influence on the other one. Three of the four highest computed air resistance coefficients (as seen in Table 19) used the recording blocks that led to the three lowest computed rolling resistance coefficients as input.

Similar to Figure 52 and Figure 55, the recordings were regrouped in two sequences. One is defined as [D5-1; D5-2; D5-3; D3-1; D3-2; D3-3; D1-1; D1-2; D6-1; D6-2; Mixed; D6-3; D2; D4] and the other as the inverse.

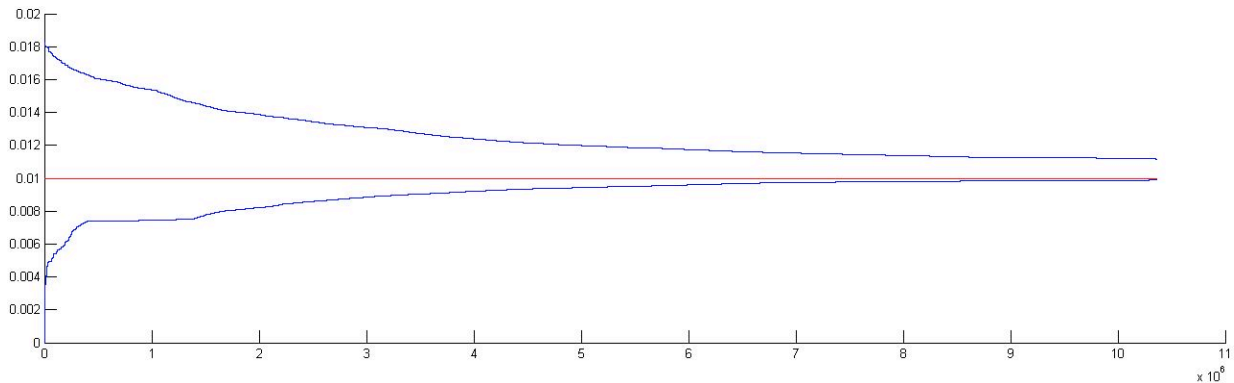


Figure 59: Evolution of the Roll Resistance Coefficient over the Driven Kilometers (General)

Data used: All the 14 available data blocks in two opposite sequences

X-Axis: Distance in 10⁶ m

Y-Axis: Roll resistance coefficient

Red: Expected value of 0.0100

Blue: The first sequence of data and its inverse

The two curves are converging, but the ‘learning without forgetting’ seems to dampen the evolution of the curves before they reach a unique value. The first recording sequence input into the learning prototype produced a 0.0099 rolling resistance coefficient, while the second sequence resulted in 0.011. The mean value of 0.0105 is still in the high probability true range as the previous computed median of 0.00995 was.

6.1.4 Prototype Quality Approximation: The Vehicle Part

As the learning results of the vehicle characteristics used as simulation parameters have been presented in Chapter 6.1.3, it is now possible to resume where Chapter 6.1.2 ended. The vehicle simulation accuracy check can now be performed using the learned vehicle characteristics. For the first test series, the driver specific mean learned values have been used. For example, in the case of the first driver (D1), the vehicle characteristics learned in the recording blocks B1-1 and B1-2 were used. The mean values of the computed characteristics were then used as parameters for the simulation and the tests were run in a similar configuration as the one presented in Chapter 6.1.2.3.

A second test run was made using the mean values computed out of all the recordings, disregarding the driver.

First Test: Driver-specific Vehicle Characteristics Learning:

Simulation With Driver Specific Learned Vehicle Characteristics					
	100rpm/20Nm	50rpm/10Nm	20rpm/5Nm	10rpm/2.5Nm	5rpm/1Nm
D1: 4 randomly selected lap logs (@63km)	-1.79%	-1.99%	-1.98%	-1.14%	-1.10%
D2: 5 lap logs (@39km)	-2.46%	-3.11%	-2.23%	-0.60%	0.14%
D3: 4 randomly selected lap logs (@63km)	-0.11%	0.01%	0.04%	0.91%	0.80%
D4: 6 lap logs (@39km)	-9.63%	-10.23%	-9.24%	-7.29%	-6.96%
D5: 4 randomly selected lap logs (@63km)	2.75%	3.25%	3.66%	5.06%	4.71%
D6: 4 randomly selected lap logs (@63km)	1.97%	1.64%	2.03%	2.89%	2.94%

Table 24: Simulation Quality Results with Learned Vehicle Characteristics (Driver Specific)

The first impression is that compared to the results obtained using the official BMW E91 specifications (see ‘Table 15’), the quality improved remarkably. In the special case of the results that uses the higher resolution engine map, the difference between the predictions and the recordings differ 1% or less in three of six cases. In only one case, the difference was over 5%.

The remarkable quality increase due to the use of learned vehicle characteristics instead of official BMW characteristics may have two reasons:

- The official BMW specification describes standard values for standard cars. The test vehicle was partly modified and had some extras built-ins (e.g. ‘M Packet’). Therefore the values did not match the reality anymore.
- The simulation used to make fuel consumption predictions is also used to learn the vehicle characteristics. It is therefore possible that the simulation inaccuracies are compensated by the learned vehicle characteristics. This would be especially apparent for extreme vehicle configuration or extreme situations (e.g. strong acceleration or slope).

The observations made during this work on the learned vehicle characteristics under different circumstances tend to indicate that the first explanation might be right.

Second Test: Driver Unspecific Vehicle Characteristic Learning:

Simulation With Mean Learned Vehicle Characteristics					
	100rpm/20Nm	50rpm/10Nm	20rpm/5Nm	10rpm/2.5Nm	5rpm/1Nm
D1: 4 randomly selected lap logs (@63km)	-0.19%	-0.38%	-0.38%	0.50%	0.54%
D2: 5 lap logs (@39km)	-1.52%	-2.09%	-1.19%	0.39%	1.11%
D3: 4 randomly selected lap logs (@63km)	0.07%	0.13%	0.18%	1.06%	0.95%
D4: 6 lap logs (@39km)	-9.10%	-9.64%	-8.76%	-6.60%	-6.09%
D5: 4 randomly selected lap logs (@63km)	-0.16%	0.34%	0.74%	2.19%	1.83%
D6: 4 randomly selected lap logs (@63km)	3.11%	2.78%	3.14%	4.02%	4.09%

Table 25: Simulation Quality Results with Learned Vehicle Characteristics (Mean Values)

For this second test series, the mean learned values disregarding the drivers were used. The air resistance coefficient was set 0.617, the vehicle mass 1805.3kg, and the rolling resistance coefficient 0.0097.

The uses of these mean values did little to influence the prediction results quality. Only the prediction quality for Drivers 5 and 6 showed noticeable improvement or decline. This is due to the driving style specificities that influenced the fuel injection and was discussed previously in Chapter 6.1.1.3.

Because of the little differences observed in the results, and to keep the simulation as simple as possible, it was decided to use the mean values of all the learned vehicle characteristics without driver consideration for the further tests.

One of the side products of this work was to provide a solution (as defined in the actual EcoRoute implementation) for how to activate the EcoRouting functionality even if the car manufacturer was not able to provide the needed consumption curves. The process of fuel consumption curve generation and the results quality analysis is presented in the following chapter.

6.1.5 Fuel Consumption Curves

The actual implementation of the EcoRoute uses consumption curves to determine the amount of fuel needed on a defined road segment at a constant driven speed. Those curves are vehicle dependent, with small driver-related variations due to the lambda sensor as explained in Chapter 6.1.1.3.

The very generalized curves were produced assuming that the slope is equal to zero, and the stabilization acceleration was lowered to 0.1m/s without regarding the driver or the situation. Then, the torque and the number of engine rotation per minute combinations at a 1km/h speed were calculated for each one of the six gears with the help of the simulation. Using the driver-specific engine maps, the amount of fuel needed in 0.1s was extracted and converted into an l/100km value. This operation was repeated for every 1km/h steps between 1 and 150km/h, resulting in six consumption curves (one for each gear) for each driver. The statistical repartition of the gear use over the speed was then used to calculate the speed dependent percentage of each curve included in the final merging. This operation was repeated for the six drivers, and the curves are displayed in the following figure.

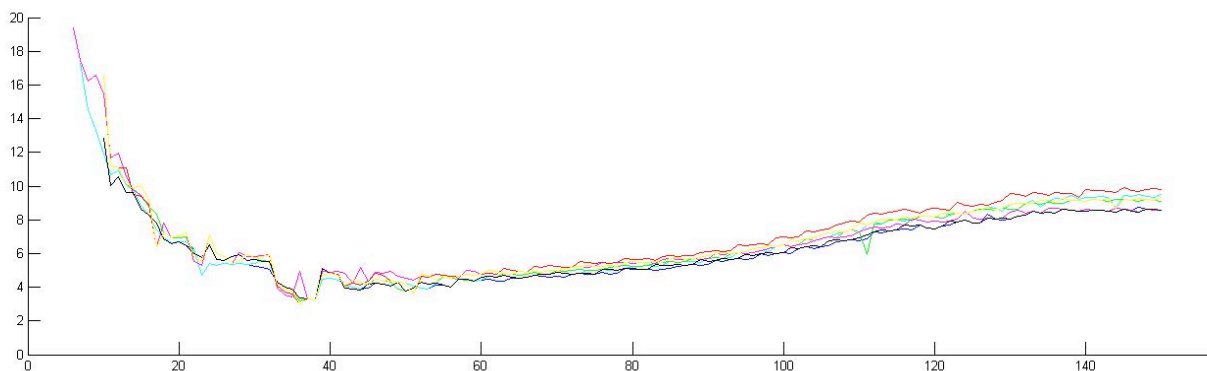


Figure 60: Driver-specific Consumption Curves

Data used: Learned vehicle characteristics and engine map with 25rpm/10Nm resolution

X-Axis: Speed in km/h

Y-Axis: Consumption in l/100km

Acceleration is set to 0.1m/s and slope is set to zero

The general aspect of the curve seems accurate, the only surprise being the gap between 35 and 40km/h. This can still be explained by the automatic gearbox setup that is configured for

an early gear change at 35 km/h. This would explain the observation though all the curves that use different driver-specific engine maps.

The first parts of the curves (1-50km/h) are less smooth than the second parts (50-150km/h). This may be due to the statistical gear use at lower speed, which has been mostly recorded in the city, while accelerating and decelerating because of traffic and situations (e.g. traffic light).

The driver differences are observable, for example the driver-specific consumption curve represented in red is always over the driver-specific consumption curve represented in blue (at least in the 50–150km/h confidence interval).

To judge the accuracy of the generated curves, it was decided to compare a generated mean consumption curve (one that uses the driver unspecific 9368km engine map) to a memorized consumption curve. However, memorizing a consumption curve is linked to some problems. The acceleration has a huge influence on the consumption and should therefore be filtered to dismiss the extreme cases. On the other side, due to the acceleration sensor's late and strong reaction, such a filter would have a limited effect. The slope should be considered as well, but considering that the records were made on a loop with a limited slope, and that the curve won't be used later except for comparison, it has been ignored.

The following figure displays the generated consumption curve (in black) and a memorized consumption curve (in red) that was recorded with accelerations between -0.1m/s^2 and 0.1m/s^2 .

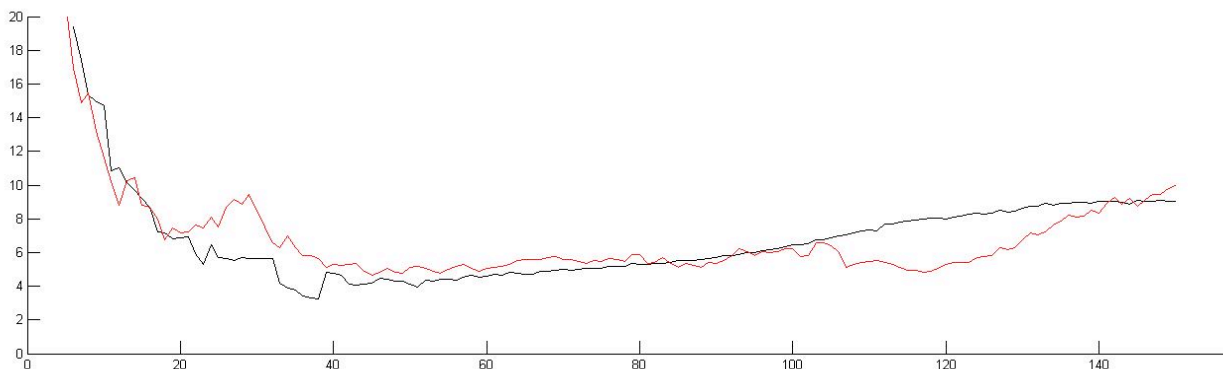


Figure 61: Memorized and Generated Consumption Curves

Data used:

- **Generated curve (black):** learned vehicle characteristics and engine map with 25rpm/10Nm resolution (mean of Figure 60)
- **Memorized curve (red):** all the data with $-0.1\text{m/s}^2 < \text{acceleration} < 0.1\text{m/s}^2$

X-Axis: Speed in km/h

Y-Axis: Consumption in l/100km

The two curves are similar in the low speed range, under 20km/h and 40-100 km/h, but show noticeable differences in the 20 to 40km/h range (where strong accelerations occurs in the city), which should be due to the acceleration sensor reaction time and the limited amount of data available in this speed range. The differences at high speed (over 100km/h) must be also linked to the acceleration sensor reaction time. In this case, and due to the high kinetic energy, a small deceleration is immediately responsible for a fuel injection shutoff. The fuel consumption is then 0l/100km, and for this reason, the memorized consumption curve is considerably lower than the generated one.

Therefore, the generated consumption curve seems to reach an acceptable quality to be used for the EcoRoute selection function, but not necessarily for a fuel consumption prediction that would be displayed to the user.

Compared to a memorized consumption curve, the generated curves are really adaptive and can be created for every slope, vehicle configuration, and even for speeds that haven't been driven so far, allowing an adapted fuel consumption prediction for almost every case.

6.2 Results – Driver Part

The implementation results of the driver part is presented in this chapter. The test track preparation for future prediction is explained, and the driving style that was learned and generated is analyzed. Finally, the quality of the fuel consumption prediction made using the simulation of driver and vehicle, with the learned driver and vehicle characteristics, is discussed.

6.2.1 Track Preparation

The track preparation is a four step procedure from extraction, over correction and finally preparation for input into the prototype simulation for fuel prediction. The four steps and their results are reviewed in this chapter.

6.2.1.1 First Step: Track Extraction out of the Navigation System Map Database

First of all, the test tracks used to learn and statistically represent the typical drivers driving styles were extracted as routes out of the navigation system database. To do so, a route log was generated at 10km/h (the slowest speed that could be configured in the software tooling program) in January 2013. In the route log lists, among other attributes that weren't used in this work, the following valid route segment attributes at one hertz:

- Time: the absolute time
- Long: longitudinal position
- Lat: latitude position
- Speed: driven speed (in this case: 10km/h)
- RoadClass: functional road class
- SpeedLimit: in km/h
- Slope: slope on segment

This method is a little different from extracting a route from the route calculation, and has a route segment length approximation error of 3.6 meters in the worst case since the route segment characteristics are updated every second at a speed of 10km/h.

It was not possible to access a route description extracted from the route calculation component at the time this study was done. Beside that, the segment length error of a maximum of 3.6 meters can be neglected when compared to the map digitalization quality that was observed while comparing the digital speed limit traffic signs position to their real positions (The speed limit traffic signs are one of the indicators used to split a route into segments).

While Drivers 1, 3, 5 and 6 drove on the Hi01 test track, Drivers 2 and 4 drove on Hi03 and Hi04 (see Annex B and Annex D). The test track Hi03 was very similar to the test track Hi01, and was only extended by two loops needed for a traffic sign recognition project. The data recordings linked to those two loops was of no particular interest for this work, and therefore was later dismissed to reduce the complexity and allow the use of one single test track log for Hi01 and Hi03.

The track log for Hi04 was generated separately.

6.2.1.2 Second Step: Database Logs Correction

The chronological list of attributes related to the test tracks must be reviewed for possible errors first. Since the route segment attributes are related to the navigation system map

database, this step should be similar for route logs extracted from the route calculation component.

Some attributes were not available continuously over the whole test track, for example, the slope information that is represented in the following figure.

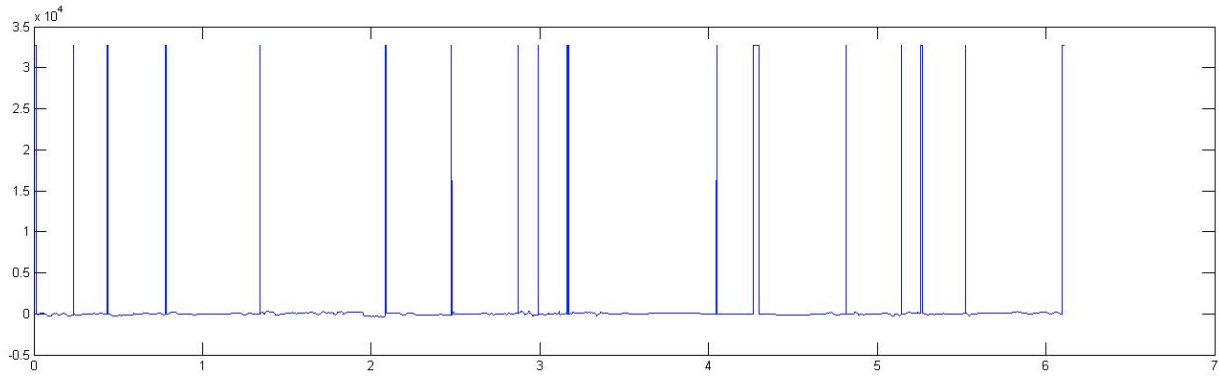


Figure 62: Hi01 Extracted Slope over the Distance

X-Axis: Distance in 10^4 meters
Y-Axis: Slope in degree

In the case of the slope, when not available, a default 16 bit signed integer (32767) was recorded. Those values were replaced with a 0.

The ‘SpeedLimit’ attribute identify a road segment without speed restriction with a ‘-1’ value. Since the typical driven speed is statistically represented as the difference to the speed limit, it is possible to keep the ‘-1’ value. But, because the simulation calculates accelerations and decelerations to the speed limit before correcting the stabilization parts, a realistic speed range value makes more sense. Therefore, and to prevent potential confusion with actual speed limits, a value over the maximal known speed limit of 130km/h was chosen, and the ‘-1’ entries replaced by ‘150’.

6.2.1.3 Third Step: Test Track Splitting into Situations and Phases

As explained in Chapter 5.3, the track must be split into situations and phases to make a driving style generation possible.

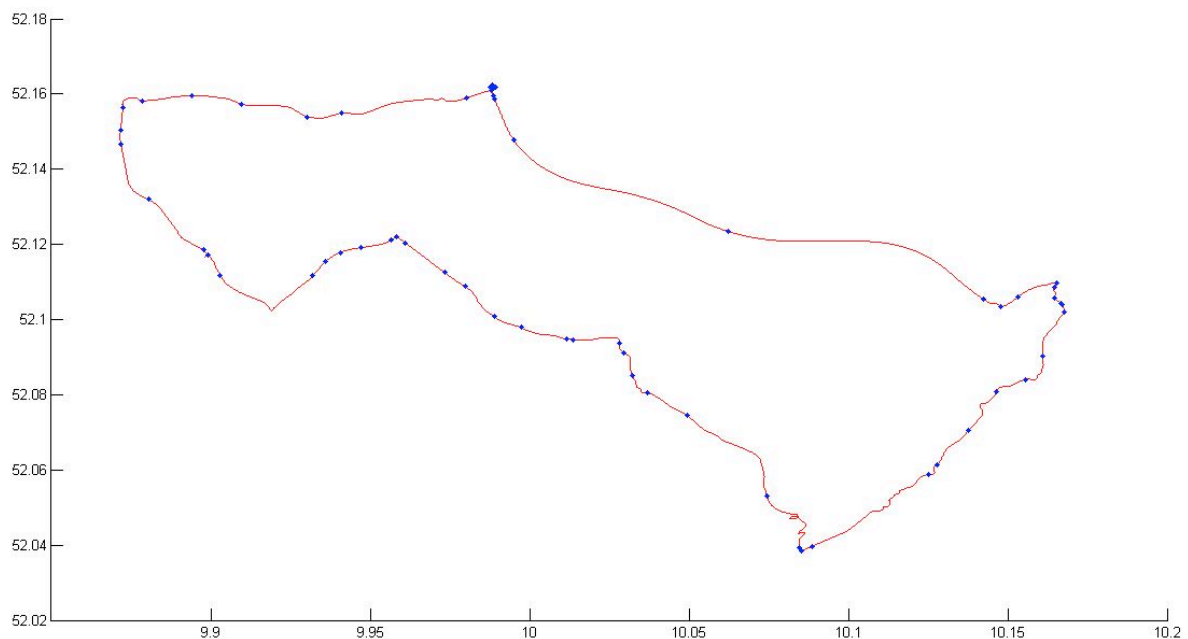


Figure 63: Hi01 GPS Coordinate Graphical Representation of the Situations

X-Axis: Latitude (WGS84)
Y-Axis: Longitude (WGS84)

The test track Hi01 was split into 60 situations, according to the navigation database route log speed limit, intersection and road type attributes as illustrated in the previous figure.

The track GPS coordinates were represented in red, while the situation markers are blue. The situations were defined based on the analysis of the route segment attributes and are not uniformly distributed over the track. On the highway part (North-East) few changes occurs, and therefore few situations are defined. On the other hand, in the cities (identifiable due to the higher concentration of situation markers) the road attributes change more often, and therefore, the driver has to adapt his driving behavior more often.

The same procedure was repeated for the Hi04 test track where 41 situations were identified.

6.2.1.4 Fourth Step: Chronological Attribute Variation Representation for Input into Simulation

In the last step, the route logs that were produced at 1Hz were converted into a simplified form: a list of phases delimited by the situations that were defined along the route. These phases were attributed a length, an average slope, a speed limit and a road type. The following figure (first line) displays, for example, the speed restriction attributed to each phase over the cumulated distance of the phases.

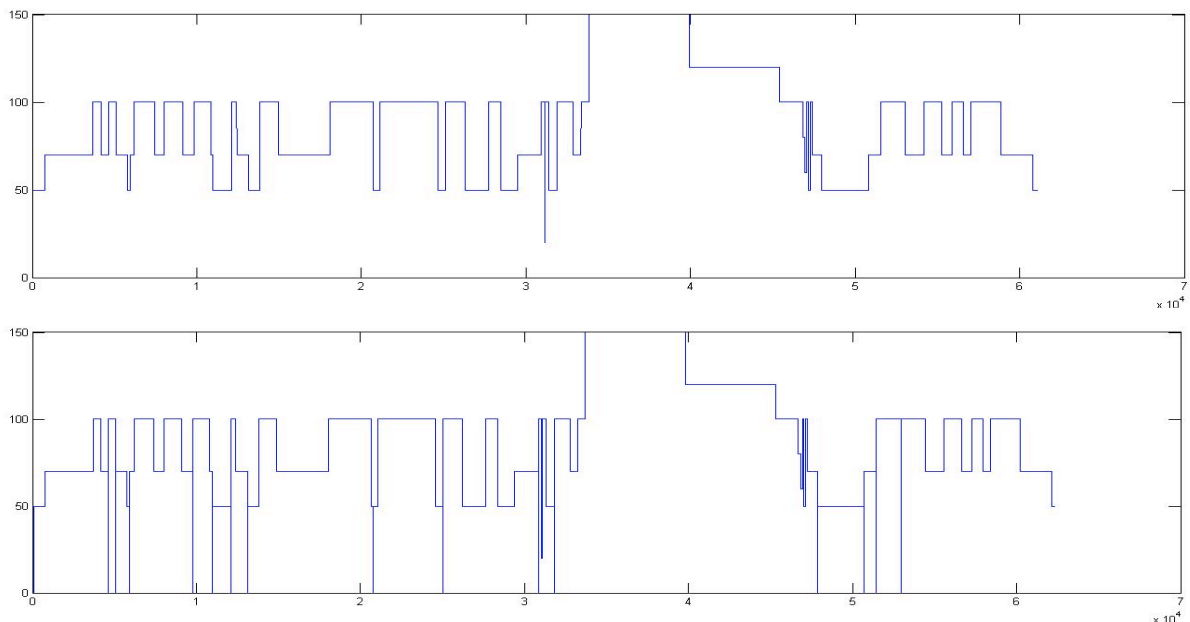


Figure 64: Hi01 Speed Restriction Phases over the Distance and Stops
X-Axis: Distance in 10^4 meters
Y-Axis: Speed restriction in km/h ('150' stands for unlimited)

During the simplification of the route log into a list of phases, stops were added following the rules presented in Chapter 5.3.3:

- Only the road types 'In City' and 'Outside City' were updated. Stops were not allowed on highways.
- In case the street name changed, it was supposed that a turn happened and inserted a stop.
- In the city, a stop was inserted for every intersection with a least 4 segments.

After the stop insertion process, the Hi01 track was assigned 17 stops (Figure 64– bottom graphic), and the Hi04 test track was assigned 9 stops.

The chronological list of phases and situations along the route could then be used as input to the prototype simulation to compute a fuel consumption prediction.

6.2.2 Driving Style Learning Results

For the first implementation, the learning of the driver characteristics was kept simple as explained in Chapter 5.3, and while it was intended to later add some complexity in order to raise the quality, the later analysis showed that this implementation was the most satisfying complexity to quality ratio that could be reached with the amount of test data available. Therefore, the driver's driving style learning presented was kept in this statistical-oriented form.

Because the Hi01 test track was later split into two halves (Chapter 6.2.4), the amount of recordings available for learning was strongly reduced. For this reason, the situation-dependent typical acceleration and deceleration curves that were generated, as explained in Chapter 5.3, were later merged together to one driver-specific acceleration curve and one driver-specific deceleration curve.

- The acceleration was defined as the maximum acceleration observed over the three curves (Figure 39) for each 1km/h speed interval, and the typical deceleration was computed in the same way.

- The typical driven speed was saved in form of an offset to the authorized speed limit, and extrapolated for speed restrictions that hadn't been encountered using the two offsets that had been memorized for the two next speed restrictions (e.g. saved offsets for 50km/h and 80km/h restrictions are proportionally used to figure the possible offset of a 70km/h restriction).

- The gear selection was saved in a statistical (speed dependent) form for each driver despite the fact that it was an automatic gearbox. As is observable in the following graphical representation of the statistical gear use over the speed, the driver's use of gas and brake pedals (e.g. kick-down) has an influence on the selected gears.

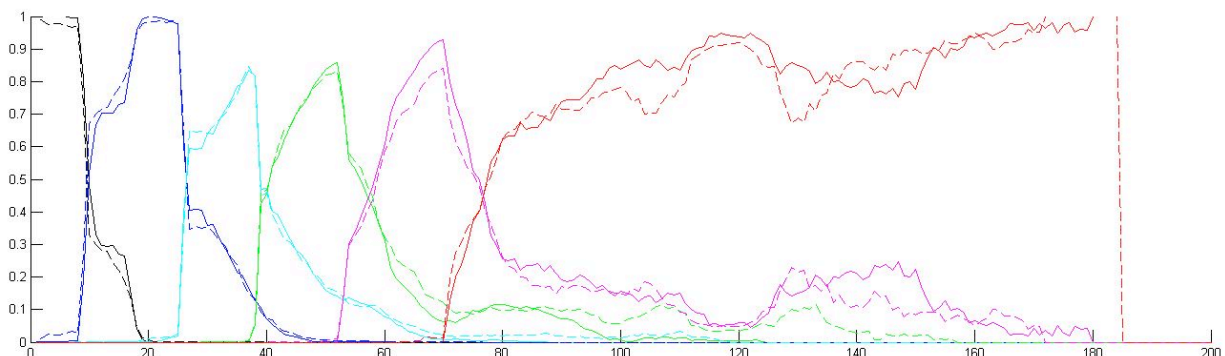


Figure 65: Statistical Repartition of the Used Gear over the Speed

X-Axis: Speed in km/h

Y-Axis: Gear use probability

Black: First gear

Blue: Second gear

Cyan: Third gear

Green: Fourth gear

Magenta: Fifth gear

Red: Sixth gear

Plain line: D2

Segmented line: D4

For example, the segmented line and the plain line represent the gear use repartition over the speed for two different drivers. Each color is linked to one of the six gears. In this particular example, Driver D4 (segmented line) uses the fourth gear more often than Driver D2 (plain line) while traveling at 70km/h.

6.2.3 Driving Style Prediction

Afterwards, the track description was extracted out of the navigation system map database and prepared, and the typical driver behaviors were learned or statistically represented. It was

then possible to compute a prognosticated driving behavior using the track description as described in Chapter 5.3.3.

The speed restriction frame was corrected using the driver-specific typically driven speed offsets (except for the 0km/h restriction), and then the typical accelerations and decelerations were generated. For example, the following graphic displays the typical acceleration generated after a ‘stop’ to 50km/h.

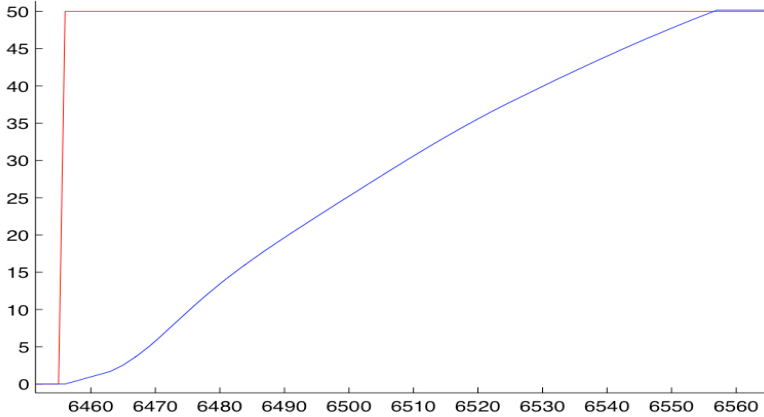


Figure 66: Typical Acceleration Computed From 0 to 50km/h

- X-Axis: Distance in meters**
- Y-Axis: Speed restriction in km/h (Starting from a ‘stop’)**
- Red: The defined restrictions**
- Blue: The generated speed over the distance**

The generated speed over the distance was converted into a 10Hz speed variation over time, and attributed with the slope information of the track input, the prognosticated acceleration, and the gear use probability.

This generated chronological sequence could then be used as an input to the prototype vehicle simulation for a fuel consumption prediction.

6.2.4 Prototype Quality Approximation: Adding the Driving Style

The following chapter regroups the presentation of the prototype quality testing strategy in the first part, and the analysis of the results that were computed in the second part.

6.2.4.1 Prototype Quality Testing Strategy and Hi01 Test Track Splitting into Two Halves

While there were recordings available for Driver 2 and Driver 4 on two distinct circuits - Hi03 (later shortened to Hi01) and Hi04 - Drivers 1, 3, 5 and 6 drove only on the test track Hi01. Because of limited scientific interest to learn and make predictions on one similar track, it was decided to split the test track Hi01 into two halves, one being used for learning and the second one for fuel prediction.

The split was done in the middle of the highway section (after the no speed restriction section), so that both halves contain city, outer-city and highway parts. The two parts are represented with two different colors in the following figure.

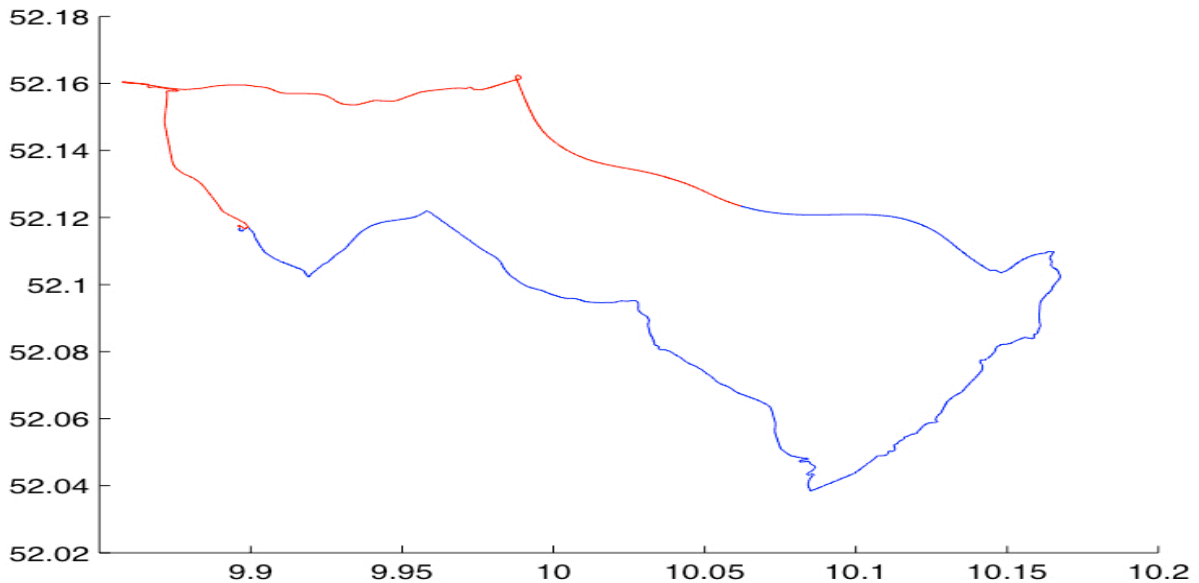


Figure 67: GPS Coordinate Representation of the Hi01 Test Track Splitting into Two Parts
X-Axis: Latitude (WGS84)
Y-Axis: Longitude (WGS84)
Blue: First section: Hi01-A
Red: Second section: Hi01-B

The first section of the Hi01 test track (in blue) was renamed Hi01-A and has a total length of approximately 40.1 kilometers. The second section of the Hi01 test track (in red) was renamed Hi01-B and has a total length of approximately 23.5 kilometers. The length indicated was provided by Google Maps (June 14, 2013) and could not be exactly measured because of little variations supposedly due to lane changes, GPS and wheel sensor inaccuracies, starts and stops of the log data, and wrong turns that were observed between the recordings.

6.2.4.2 Presentation and Analysis of the Prototype Fuel Consumption Prediction Results:

To isolate the driver style learning influence on the fuel consumption prediction, the vehicle part of the prototype was configured using the mean learned vehicle parameters (the vehicle characteristics used as simulation parameters have been presented in Chapter 6.1.3):

- Air resistance coefficient: 0.6167
- Vehicle mass: 1805.3kg
- Roll resistance coefficient: 0.0097
- Generator torque: 20.8776Nm
- Transmission ratios: 0.00102 / 0.00756 / 0.01007 / 0.01321 / 0.01665

The fuel consumption predictions were computed using driver-specific engine maps (the different kind of engine maps are explained in chapter 6.1.1.2).

First Prototype Quality Test Run (Drivers D1, D3, D5, D6):

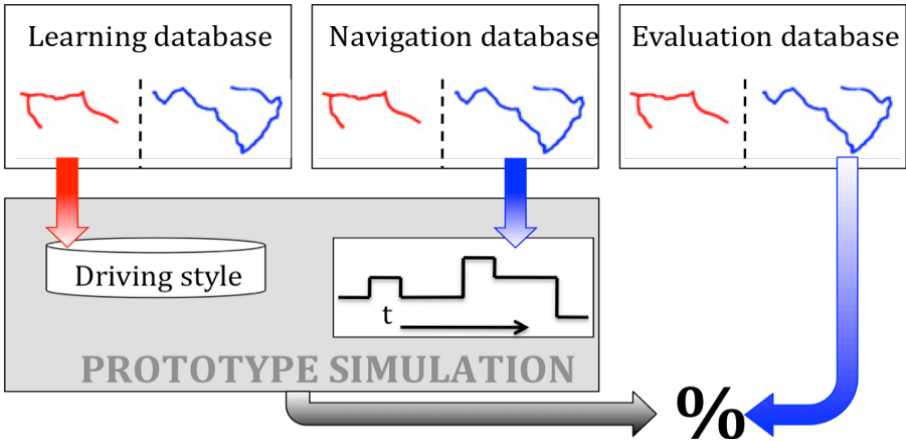


Figure 68: First Test Case Graphical Description
In red: Hi01-B track segment
In blue: Hi01-A track segment

The ‘Learning Database’ (definition in the Chapter 6 introduction) recordings made on Hi01-B were used to analyze the driving style (Figure 68 - left row). In the same time, a route log of the Hi01-A segment was extracted from the navigation system map database, and used as prototype simulation input (Figure 68 - middle row). Finally, the ‘Evaluation Database’ (Definition in Chapter 6 introduction – 4 laps per driver) recordings made on Hi01-A were used (Figure 68 - right row) to compare the predictions with recorded consumptions, and therefore make a judgment about the quality.

The following table regroups the recorded results (second table row / Figure 68 - right row), the computed fuel prediction (third table row / Figure 68 - black arrow), and the qualitative comparison in form of a percentage variation between the two values (fourth table row).

	Fuel Consumed	Fuel Prediction	Percentage Variation
D1	2.8101 liter	2.6515 liter	-5.64%
D3	2.7166 liter	2.8171 liter	+3.69%
D5	2.4966 liter	2.6319 liter	+5.42%
D6	2.8731 liter	2.6614 liter	-7.36%

Table 26: Hi01-A fuel Consumption Prediction (Drivers 1-3-5-6)

It was shown in Chapter 3.3 (page 34), that an error of 5% could be mostly attributed to the drivers. Adding error margin due to the vehicle parameters and surroundings changes, a constant margin of 5 to 10% error was defined as goal of this work. The best prediction with a 3.69% error is therefore very satisfying. The worst result obtained was a 7.36% error margin, which is still in the satisfying range of 5 to 10%. The average variation was found out to be 5.52%, which meets the best expectation.

Second Prototype Quality Test Run (Drivers D1, D3, D5, D6):

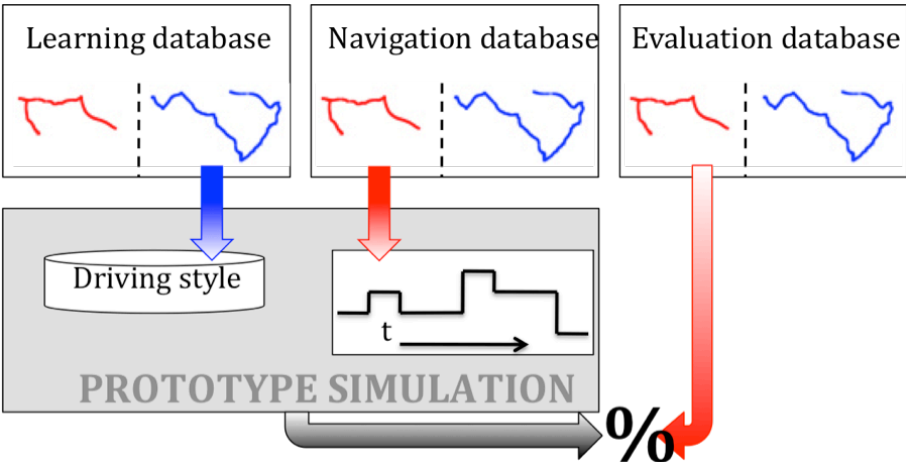


Figure 69: Second Test Case Graphical Description
In red: Hi01-B track segment
In blue: Hi01-A track segment

The second test was defined very similarly to the first one, but inverting the Hi01 track segments used. The driving style was now analyzed out of Hi01-A, while the prediction was computed for Hi01-B. Since the amount of data used to learn increased in comparison to the first test (Hi01-A segment length is 40.1 km while Hi01-B segment length is 23.5km), the quality of the learned driving style increased, and therefore the fuel prediction was more accurate.

	Fuel Consumed	Fuel Prediction	Percentage Variation
D1	1.4519 liter	1.4249 liter	-1.85%
D3	1.3899 liter	1.4075 liter	+1.26%
D5	1.5130 liter	1.3619 liter	-9.98%
D6	1.4149 liter	1.3494 liter	-4.63%

Table 27: Hi01-B Fuel Consumption Prediction (Drivers 1-3-5-6)

With two predictions out of four had an error margin less than 2%, the reached quality seems to be beyond every expectation, but the worst computed result of 9.98%, while still in the 5-10% goal quality range, counterbalances it. The lower quality attributed to Driver D5’s fuel consumption prediction may be related to the measured fuel consumption (in the second row). While D5 was found out to be the most economical driver on the Hi01-A track segment (Table 26: Hi01-A fuel Consumption Prediction (Drivers 1-3-5-6) second row), he used more fuel on the second track segment than the other drivers. Since the randomly selected recordings that form the evaluation database show no abnormalities, the driving style seems to have changed according to the surroundings. Hi01-B was mostly composed by a drive through the city of Hildesheim, where traffic could have had a more noticeable influence on the driving style than on Hi01-A.

Summing up, the average error observed was 4.43%, which is, as expected, better than the one observed during the first test, and even better than the set ideal goal of 5%.

Third Prototype Quality Test Run (Drivers D2, D4):

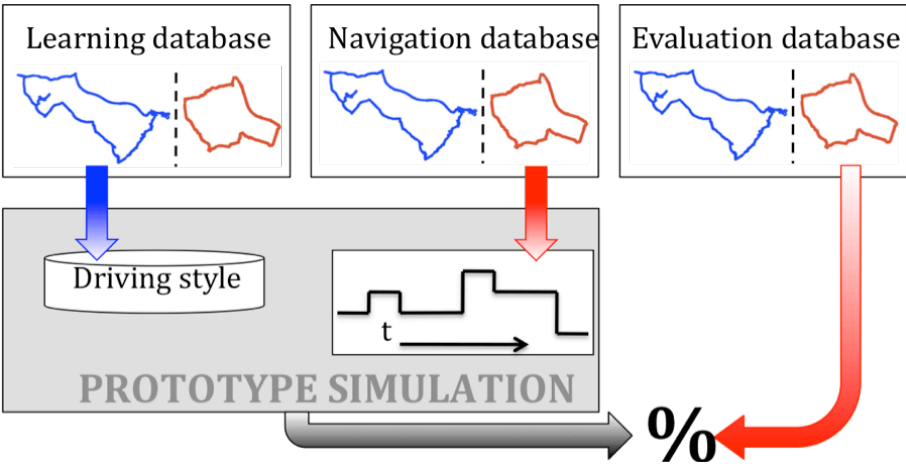


Figure 70: Third Test Case Graphical Description

In red: Hi04 track
 In blue: Hi03 track

While the first and second tests were investigating the recordings of Drivers 1, 3, 5 and 6, the third test was defined using the recordings of Drivers 2 and 4. In this test, recordings on two different tracks were available.

The typical driving behavior of Drivers 2 and 4 was learned using the whole Hi03 recordings, and the fuel prediction later computed using a Hi04 track description as an input.

	Fuel Consumed	Fuel Prediction	Percentage Variation
D2	2.6171 liter	2.5156 liter	-3.87%
D4	2.8269 liter	2.6448 liter	-6.44%

Table 28: Hi04 fuel Consumption Prediction (Drivers 2 & 4)

The results were both underestimating the fuel consumption. While there is no indication of this being a general trend (because only two drivers are considered), this could be due to the different surroundings or a coincidence.

The average error was 5.15%, which is again very satisfying, and the worst result of 6.44% variation is still in the expected 5 to 10% range.

A fourth test with a learning out of the Hi04 recordings for a prediction on the Hi03 track was not possible due to the very limited amount of data recorded on Hi04 (circa 200 kilometers for each driver).

6.3 Results Comparison with the State of the Art

The quality of the fuel consumption prediction computed out of the prototype has been found out to be around 5%, as seen in the previous chapter. This result seems to be very satisfying according to the driver-related variations observed during the analysis presented in Chapter 4.4.1, but a further comparison with the state of the art helps to get a feel for how good these results really are. This chapter regroups a quality analysis of three of the more likely-to-encounter fuel consumption predictions: onboard cluster prediction, actual EcoRoute implementation prediction and Google Maps prediction.

6.3.1 Comparison with Mean Consumption (Onboard Cluster)

One of the most common vehicle range predictions might be the one displayed in some cluster instruments. Beside the actual and some trip average fuel consumptions, an estimated ‘remaining driving range before empty fuel tank’ reading may be displayed.

The cluster informations were not recorded during the test drives, and therefore the computation must be done offline.

During the time lapse of this work, no available official documents that describe the algorithm used to make this prediction could be found. But since this option is available in the cluster instrument, and independent from the built-in of a navigation system, the algorithm might be using the following information:

- the level of remaining fuel
- the average fuel consumption over the last ‘X’ kilometers or hours. The value ‘X’ has to be chosen big enough to guarantee a smooth converging of the range prediction despite the variation of strong acceleration and deceleration.

The formula used should be: $range = \frac{fuel_remaining_ (liter)}{average_consumption_ (l/km)}$

By replacing the ‘range’ with the track length, the ‘fuel remaining (liter)’ becomes the fuel consumed on the track. The average consumption of driver D1, D3, D5 and D6 on Hi01-A and Hi01-B, and of D2 and D4 on Hi03 were calculated to compute a fuel prediction in the more likely way the cluster instrument should have done it. The results of the three test cases are regrouped the following table:

	Fuel Consumed	Fuel Prediction	Percentage Variation
First Test Case			
D1	2.8101 liter	2.4774 liter	-11.83%
D3	2.7166 liter	2.3717 liter	-12.69%
D5	2.4966 liter	2.5817 liter	+3.41%
D6	2.8731 liter	2.4143 liter	-15.96%
Second Test Case			
D1	1.4519 liter	1.6468 liter	+13.42%
D3	1.3899 liter	1.5920 liter	+14.54%
D5	1.5130 liter	1.4630 liter	-3.29%
D6	1.4149 liter	1.6837 liter	+19.00%
Third Test Case			
D2	2.6171 liter	2.1022 liter	-19.67%
D4	2.8269 liter	2.3295 liter	-17.59%

Table 29: Fuel Consumption Predictions out of Average Consumption Recorded

Surprisingly, the Driver D5 results are excellent, with a 3.29% and 3.41% error margin. This driver was found out to be the least economical driver during the second prototype quality test run (Table 27).

Less surprising are the results obtained for the other drivers with an average 15.59% error margin, and a worst case of almost 20%.

Even if the onboard cluster estimate is to be regarded with caution, the prototype fuel consumption prediction have produced more constant results of a greater quality, except in the case of Driver D5 which drove in a way that didn’t correspond to the general observed tendency.

6.3.2 Comparison with today’s EcoRoute

The actual (February 12 2013) implementation of the EcoRoute was used to record two route logs containing the amount of fuel needed on each road segment, and to switch between the

segments. These fuel amounts were then added to find out how much fuel in total was estimated to be used on these two tracks.

The route logs were described as follow:

Hi01 Test Track:

SW-Version: NAV_DI_SWNAVI_12_NT_x86_202SD_1301241139

Distance: 61.061 Km

Time needed: 01h02min51sec

Fuel consumption: 3.082045 liter

Hi04 Test Track:

SW-Version: NAV_DI_SWNAVI_12_NT_x86_202SD_1301241139

Distance: 39.685 Km

Time needed: 00h49min47sec

Fuel consumption: 2.227218 liter

The EcoRoute function uses fuel consumption curves for constant speed (as presented in chapter 6.1.5) and for acceleration. These curves are downloaded into the navigation system and adapted to the vehicle the system will be built-in. In this case, no BMW curves were available, and the system was run with adapted Ford S-Max Diesel consumption curves to approximate the test vehicle, which explains the differing consumption previsions.

The average consumption of a Ford S-Max 2.0 TDCI engine with 103 kW (140 PS) or 120 kW (163 PS), with Ford PowerShift automatic gearbox is indicated to be 6.0l/100km on the official Ford Germany Website¹⁰. Compared to the 6.5l/100km of the test vehicle (see Annex B - BMW E91 specification), this is a difference of circa 8%. Furthermore, the test vehicle increased mass and sport package could have been responsible for an increased difference, so that no real comparison is possible.

It is important to keep in mind, that the EcoRoute functionality main goal wasn't to provide a fuel consumption prediction to the driver, but to find the most economical route between two points, which may be perfectly done while underrating the global fuel consumption.

In the future EcoRoute implementation, such consumption curves will be learned, increasing the accuracy of the previsions. Summing up, while the approximation quality may rise, one remaining disadvantage of the EcoRoute compared to the prototype implementation, is the little degree of driving style and vehicle characteristics adaptation.

6.3.3 Comparison with Online Fuel Consumption Estimation

One of the best known website for route calculation and route guiding may be Google 'Maps' (<http://maps.google.com>). Unlike Microsoft's 'Bing' (<http://www.bing.com/maps>) or Apple's 'Maps' app (<http://www.apple.com/ios/maps>), Google provides an estimated fuel cost, which can be set to display fuel consumption estimation. The settings menu is represented in the following graphic, and allows choosing between different vehicle types, fuel types and to define a fuel price.

¹⁰ Access on June 23 2013: http://www.ford.de/Pkw-Modelle/FordS-MAX/Motoren_und_Getriebe

Estimated fuel cost ✕

Fuel cost estimates are based on the following information:

Vehicle type

Fuel type

Fuel price €/L

Figure 71: Google Maps Fuel Cost Estimation Settings (screenshot July 10 2013)

The vehicle type can be set to be ‘Compact’, ‘Standard’ or ‘High Consumption’, while the fuel type is ‘Gas’ or ‘Diesel’. Estimation for the Hi01-A track segment, Hi01-B track segment and Hi04 tracks were computed for all three kind of vehicle type. The fuel type ‘diesel’ was selected and the fuel price was set to be 1€/Liter to display the fuel consumption prediction without conversion.

	Hi01-A	Hi01-B	Hi04
‘Compact’	2.94 liters	1.63 liters	3.17 liters
‘Standard’	4.31 liters	2.36 liters	4.69 liters
‘High Consumption’	6.87 liters	3.69 liters	7.66 liters
Mean Measured Consumption	2.72 liters	1.44 liters	2.72 liters
Best Prognostic Variation (Compact)	+8%	+13%	+17%

Table 30: Google Maps Fuel Consumption Prediction (July 10 2013)

First of all, all the estimations were over the recorded fuel consumption. While a BMW E91 should be considered more like a ‘Standard’ than a ‘Compact’, the estimation results of ‘Compact’ were found out to be the best ones and therefore used to compute the percentage of error. The estimation errors were between 8 and 17%, depending on the route, and worse if the wrong kind of vehicle type had been selected.

The main disadvantage of online estimation is that, while there is a potential to run algorithms of high complexity due to the computing power, the information describing the vehicle and the driver are missing. As long as this information is still missing, the estimation quality will remain unsatisfying. Also, giving the user a choice between different vehicle types without any further explanation may lead to even bigger estimation errors as the one observed in this case.

7 Summary and Conclusion

The motivation behind this work was to provide a solution able to make a fuel consumption prediction. The solution had to be compatible with the navigation system in order to assist the future releases of EcoRouting and range prediction functionalities. EcoRouting rose out of the increasing traffic over the world, air pollution due to CO₂ rejection, and rising fuel prices. It is one of the technologies that contribute, and may increasingly contribute further, to a reduction of the fuel amount needed to reach a destination. The concept of EcoRouting is also relevant for electric vehicles since the electricity production is also responsible for air pollution.

The development of new solutions that support the navigation system has been made possible through increases in volume and quality to vehicle sensors as well as the increasingly better descriptions of the roads, predictions of weather and traffic, and the exponentially improved performances of the built-in hardware. The objective of this work was to explore these future possibilities and to seek to answer the following question:

Is it possible to make a fuel consumption prediction based only on learned and onboard available data, with a satisfying accuracy, and for a route that has never been driven before?

In addition to that, because this work was conducted within a core function development team instead of a research department, a more practical objective was added. The prototype solution was expected to be later compatible with the actual implementation of the EcoRouting functionality, and, as far as possible, to be used for Electric Vehicles as well.

To answer the main question, implicated subquestions were formulated, on which the layout of this work is based.

First, ‘What is responsible for fuel consumption?’. A bibliographic search on the multiple causes of fuel consumption and their importance was conducted. Some of the relevant findings could then be confirmed by the analysis of available test drive recordings. The findings were then classified according to their specificity to the vehicle and/or driver. Specific properties had to be learned to make it possible to compute a specific prediction.

In a second step, and because the system was expected to run onboard, the information available was analyzed and cross-referenced with the parameters involved in the fuel consumption. Meanwhile, the following questions were answered: ‘What could be recognized for an understanding of the situation while learning?’, and ‘What can be forecasted for a future prediction?’.

The solution had to include the elements with a significant influence on fuel consumption that could be approximated while learning, and later predicted.

The last question that had to be answered was regarding ‘reasonable’ and ‘expectable’ accuracies. The reasonable accuracy is defined as what a user would tolerate, while the expectable accuracy is defined as what the system can reach due to the multiple identified sources of variations and imprecision. Based on the analysis of measured travel time prediction deviations, and because the acceptance of the user was expected to be similar when it comes to fuel consumption, the reasonable accuracy was defined to be circa 10%. Assuming that the vehicle and surroundings are predictable, but the driver isn’t, the measured driver-related variation on fuel consumption was used to define the expected accuracy. The standard deviation of observed 5% was therefore used. For this reason, the goal of this work was to make a fuel consumption prediction with a deviation of less than 10%, ideally fewer than 5%. Finally, a concept was developed, implemented into Matlab, and tested with data recorded during three test drives.

The universally accepted Three-stage model as described by Durth, and extended by Donges, was used as the base of this work. It allowed a structured cataloging and analysis of the vehicle, driver and surroundings properties, and their interactions, that have a direct or indirect influence on fuel consumption. The relevance of every parameter has been questioned, and, if possible, measured on the available data recordings.

The vehicle part of the fuel consumption has been split into two categories: the vehicle internal energy conversion process, and the vehicle interaction with the surroundings. These two categories mix physics and mechanics, and are well-researched and documented in studies and books.

The driver part has been split into the driving style applied while executing the driving tasks, and the use of auxiliary energy consumers. The use of auxiliary energy consumers was outsourced, due to the weak connection to navigation and the high complexity, which would have required the definition of new test cases, the reconfiguration of the CAN bus recording system and the recording of additional test drives.

The driving style was segmented into the driving tasks. It was discovered that they were unequally researched over the years despite being all relevant. The driver impact on the fuel consumption was questioned and measured. It was found out that it is limited by the vehicle and the surroundings, and subject to 5 to 20% variation, sometimes even more in extreme situations.

Based on studies and observations made in the field of psychology and accident research, it was determined that the driver is highly influenced by the surrounding and his state of mind, which is unfortunately barely measurable.

A concept including a vehicle and driver simulation that needs the route description as an input was described. In addition to that, databases containing vehicle and driver properties that are required to run the simulation were set, and a learning component tightly coupled with the simulation was described. The learning component makes it possible to fill the properties databases while the vehicle is moving.

Despite the number of CAN recordings made during various projects in the past, almost none of them could be used for this work because the fuel injection value was rarely recorded. However, one set of recordings made in Stuttgart while testing the effects of an experimental ACC was used.

This dataset included the fuel injection information, but was missing the selected gear signal. As it was the only available database at the beginning of this work, a gear signal was generated, reasonably successfully, based on the engine rotation and the vehicle speed, and was used to set up the system while waiting for a reliable database. Because of the questionable scientific aspect of the dataset expansion, the results including the selected gear were not listed in this work. Due to the amount of drivers available, this database was mainly used to characterize the differences between economic drivers and the others.

Another vehicle used for the main analysis was acquired, modified and equipped with a CAN bus recording system during this work. The vehicle was equipped with modified brakes and steering, and used in multiple projects at the same time, so that the first usable recordings were available one and half years after the start of this work. Due to financial and time limitations, it remained the only vehicle available for commissioned recordings.

Three recording sessions were conducted:

The first recording session was used to test the learning and prediction functionalities on a defined route with four different drivers. The vehicle and the defined route were constant in order to limit the variations to the driver, weather or traffic related events.

During the second test session, the vehicle's aerodynamic and mass properties have been modified to match, and therefore simulate, other vehicles. A roof box was mounted on the

vehicle to increase the vehicle cross-section and alter the aerodynamic properties. During the second half of the recordings, the vehicle was loaded with 300 kilograms of sand on the back seats, since the trunk was being used for the recording instrumentation.

The last recording session took place on two routes. The main idea was to use the recordings made on one circuit to learn and predict the consumption on the second circuit. The prediction could then be compared with the recorded consumption. However, an accident immobilized the vehicle for three days, reducing the amount of usable recording from the initially planned four drivers to two.

Until the end of this work, only very few electric vehicle recording samples, recorded on three electric vehicles¹¹, could be used for testing. However, the amount of data was never sufficient for a non-questionable proof of concept, and the databases were not allowed for publication due to the prototype character of the vehicles used. Despite the fact that the system compatibility could not be proven during the work, further development based on the prototype described in this work has been conducted in order to provide a range prediction solution for EV in the project OpEneR. It is therefore expected, that the correct function will be confirmed in the future.

During the preparation phase of this work, calculations were made using the available database to validate or invalidate some observations and findings. Based on a total of 90 recordings using the same vehicle on the same route, it was found out that the amount of fuel consumed by a vehicle without start-stop technology while standing was responsible for an important part of the differences observed between the total amounts of fuel consumed during the trips.

An algorithm randomly combining sensor information and route characteristics was implemented to find out which driving actions and route characteristics were related to the fuel consumption. That way, it could be confirmed that the mean acceleration outside cities and the mean engine speed outside cities (because the selected gear information wasn't available it was supposed to be due to a late gear change to higher gear or high speeds) are important factors that explain fuel consumption differences between the recordings. Further, it was shown that the observations made in one city were not always applicable in another city.

High variations of the engine speed, which probably mean high acceleration and deceleration, as well as late gearshift and strong speed variations, were responsible for high fuel consumption. This was confirmed by the fact that the maximum recorded torque on a Highway or Expressway (strong acceleration and or highest speed) was also made responsible for the consumption differences observed.

However, despite confirming the observation found in several books and studies, the analysis considered only one vehicle and one route.

The analysis of the commissioned recording indicated that besides the driver, the observed fuel consumption variations amplitude seems to depend on the vehicle type, the route, the traffic conditions, and probably other non-recorded factors. The average difference measured between minimum and maximum consumed fuel was circa 20%. This gap was attributed to the driving style because route and vehicle remained constant, despite traffic, weather or other influences that could be responsible for it, because no extreme weather or traffic variations were observed during the recording. The standard deviation was found out to be around 5%, which was taken on as quality goal for this work.

The fact that all recordings show a similar consumption with a small degree of variation, and the observed resemblance in the speed variations over the driven distance, speaks for a limited 'degree of freedom' for the driver. It is reminiscent of the philosophical concepts of

¹¹ Volkswagen eGolf, Mitsubishi iMiev and Nissan Leaf

rationalism and determinism as defined by Spinoza, who suggests that everything, including human actions, must be explicable. The little unexplained variations could therefore be attributed to unidentified or unrecorded influencing factors.

On a more technical level, the concept of an engine map linking the fuel consumption to engine rotation speed and produced torque was proven to work, even at low resolution, because interpolation and extrapolation were made possible due to its pseudo-linear property. However, it was also shown, that most likely because of the fuel injection lambda regulation, the driver still left his mark. Furthermore, the engine map filling showed strong variations according to the driver type, and the way the engine was used.

The learning of the gear-dependent transmission ratio (relation between engine rotation and driven distance) could be computed in a satisfying quality for higher gears. Despite the fact that it wasn't used in the final implementation, the gear shifting logic of the automatic gearbox has been found out to be logically dependent on the engine rotation and the engine torque, and was later characterized.

Further important characteristics of the vehicle, including the tire rolling resistance coefficient, the air resistance coefficient and the vehicle mass, could be approximately computed. The learning procedure was not optimized, requiring circa 600 kilometer mixed road recordings to compute the coefficients and mass, but the values computed were judged to be very satisfying. Since the computed values are a side product, the optimization of the process was postponed to a later date. Changes in vehicle mass and aerodynamic property were also recognized.

While working on vehicle motion initiated by the driver, a solution to separate stabilization from acceleration and deceleration without using the database description of the route was proposed. Using it, it was then possible to match speed, acceleration and deceleration to situations defined based on the navigation database for a later use while computing a fuel consumption prediction.

Because the test routes were all loops, the level at start and destination was identical, putting into question the relevance of the slope resistance since it is a conservative force. For vehicles with an internal combustion engine, slope was proven to be relevant even if start and destination are on the same level.

Finally, the simulation was able to make fuel consumption predictions for three routes that weren't used to learn, and therefore 'never driven before' in the system's point of view, and a various amount of drivers. To make the prediction, only the route description extracted from the navigation database and the learned driver and vehicle characteristics were used. The deviation between recorded values and predictions was found out to be circa 5 percent in average, which meets the accuracy goal.

This work still suffers some limitations despite the fact that the goal set was reached, and an extensive research phase and tests made on the Stuttgart database have considerably reduced the potential amount of errors.

The limited amount of vehicles made it possible to test the engine map on only two diesel engines, no manual gearbox was tested, and aerodynamic and vehicle mass could only be artificially alternated. However, based on the mechanical and physical properties described in the books, the prototype system is expected to work on another standard vehicle without adaptation. Exotic components, for example, the CVT gearbox, may require some adaptation, but could still be incorporated into the system.

Of all the potential important influences on the fuel consumption, the use of auxiliaries, weather and traffic were put aside. The use of the auxiliaries was not identified as part of the navigation, and is therefore expected to be provided later by another system function component. Because the vehicle, route and conditions were identical or at least very similar during the recorded drives, the auxiliary energy use was replaced with a constant value.

Weather, traffic, and navigation system information in general was not recorded during the test drives. The recorded vehicle sensor information and GPS position was later matched to the route using the position coordinates. Therefore, weather or traffic consideration was not possible. However, the data used to verify the prototype system was always recorded over a one to two-week period, limiting the weather changes.

The lack of data recorded on a production car made it impossible to prove scientifically that the system is compatible with electric vehicles after small adaptation. A hybrid vehicle could then have been simulated as a two-engines system linked with a logical component.

The final version of the prototype was developed to support the actual EcoRouting implementation, and perhaps later even replace it. During the development, the compatibility with electric vehicles, that requires little adaptation of the vehicle part, was always considered. Besides the EcoRouting functionalities, electric vehicles can benefit from the combination of the electric horizon and the energy consumption prediction to display a vehicle range prediction in the map.

Besides these functionalities, the side results produced during the development of the fuel consumption prediction prototype can be used by other navigation system function components. For example, the driver characteristic and the vehicles maximum possible acceleration and deceleration for a given situation could be forwarded to the positioning component to support the prediction of the next plausible position.

Another technology that gains in importance besides EcoRouting, is EcoDriving. While EcoRouting concentrates on the optimal way, the focus of EcoDriving is on the driving tasks. Learned driver and vehicle characteristics are essential to understand: ‘what the driver can optimize’ and ‘how the vehicle can be driven in an optimal way in one precise situation’. Therefore, an EcoDriving functionality could use the collected information to make general recommendations to the driver, but also to make specific recommendations while driving, similar to the gear selection recommendation.

Last but not least, the learned information that provides a better understanding of the driver and the vehicle could be used by future *Advanced Driver Assistance Systems* (ADAS) if a way is found to confirm the accuracy of the learned characteristics.

While thinking about the future, and beyond replicating this work while overcoming limitations, new ideas emerged while doing this work.

The growth of the *Internet of Things*, the *Internet of Services* and the field of *Intelligent Transportation Systems* will revolutionize the world of transportation as we know it today. Experts agree that tomorrow's car will be connected, and at least partially self-controlled, if not automated.

In the Three-stage model, this means an increase of the information available to describe the surroundings, and a smaller influence of the driver. EcoRouting and EcoDriving could become EcoMoving: the optimal way to transport a person between two points. The solution could include a personal vehicle but also for example, public transportation or flights, and provide different options with approximated cost, ecological footprint and time of travel.

Taking the future state of information and transportation into consideration, the question formulated at the beginning of this work could be reformulated into:

Is it possible to make an ecological footprint, as well as cost and travel time prediction with a satisfying accuracy, that considers all the possible kind of transportation possibilities, while taking the personal preferences and needs of the user into account, for a start-destination combination that has never been traveled before?

References

- [Ahme99] K. Iftekhar Ahmed,
Modeling Drivers Acceleration and Lane Changing Behavior
Massachusetts Institute of Technology, pp 46-54, (1999)
- [All95] R.E. Allsop,
Reducing traffic injuries resulting from access and inappropriate speed
Brussels: European Transport Safety Council, ETSC, (1995)
- [App98] V. Appelt,
Sichtbare Radien als ein Kriterium zur Beurteilung der räumlichen Linienführung von einbahnigen Ausserortsstrassen,
Technische Universität Dresden Fakultät Verkehrswissenschaften, (1998)
- [Aral10] Aral,
Kraftstoffdaten 2010_06,
ARAL PDF Attached to email from Aral Service Center received on July 6 2010 04:54:04
HAE (2010)
- [ArSu10] Aral,
Technisches Produktdatenblatt Aral SuperPlus98, Rev.3.4,
29.04.2010, Aral-Forschung, GFT MS-EU, 44789 Bochum, (2010)
- [ArUl10] Aral,
Technisches Produktdatenblatt Aral Ultimate 102, Rev.1.1,
29.04.2010, Aral-Forschung, GFT MS-EU, 44789 Bochum, (2010)
- [BAFU06] Bundesamt für Umwelt BAFU, Rapp Trans AG, Zürich INFRAS, Bern EMPA,
Dübendorf IMA, Hochschule Rapperswil,
*Studie zur Erhebung des Fahrverhaltens von Personenwagen in der Schweiz,
Luftschadstoffemissionen des Strassenverkehrs - Folgearbeiten zum BUWAL-Bericht SRU
Nr. 255.*
Arbeitsunterlage 37 April 2006, pp 23-24, (2006)
- [Baka03] J.E. Bakaba,
*Ableitung vereinfachter Modellansätze zur Geschwindigkeitsprognose auf
Außerortsstraßen auf der Grundlage der verfügbaren Variablen aus der Straßendatenbank,*
TU, Lehrstuhl Gestaltung von Straßenverkehrsanlagen, (2003)
- [BaKo11] T. Baer, R. Kohlhaas, J. M. Zoellner, K.-U. Scholl,
Anticipatory Driving Assistance for Energy Efficient Driving,
2011 IEEE Forum on Integrated and Sustainable Transportation, (2011)
- [BaMa90] J. Baxter, A. Manstead, S. Stradling, K. Campbell, T. Reason, D. Parker,
Social facilitation and driver behaviour.
British Journal of Psychology, pp 81/351–360, (1990)
- [Bart95] G. Bartl,
Die Psychophysiologie des Schnellfahrens,
Kleine Fachbuchreihe des KfV Band 31, Kuratorium für Verkehrssicherheit, Wien, (1995)

[BaRu10] G. Baumann, P. Rumbolz, A. Piegsa, M. Grimm, H.-C. Reuss,
Analysis of driver's influence on energy consumption of conventional and hybrid electric vehicles using real-world road tests and interactive driving simulation,
VDI SIMVEC (2010)

[Bass08] R. van Basshuysen,
Ottomotoren mit Direkteinspritzung. Verfahren, Systeme, Entwicklung, Potenzial,
pp 189-204/362/357/368, (2008)
ISBN: 978-3-658-01407-0

[BeGl94] L. Beilinson, A. Glad, L. Larsen, L. Åberg,
Attitudes to driving speeds,
Proceedings of conference paper presented in Israel, (1994)

[BeWe07] H. Berndt, S. Wender, K. Dietmayer,
Driver Braking Behavior during Intersection Approaches and Implications for Warning Strategies for Driver Assistant Systems,
2007 IEEE Intelligent Vehicles Symposium, pp 246, (2007)

[BiWa11] C. Bingham, C. Walsh, S. Carroll,
Impact of driving characteristics on electric vehicle energy consumption and range,
IET Intelligent Transport Systems (2011)

[BoBa10] K. Boriboonsomsin, M. Barth, W. Zhu, A. Vu,
ECO-Routing Navigation System based on Multi-Source Historical and Real-Time Traffic Information,
IEEE 2010 Workshop on Emergent Cooperative Technologies in Intelligent Transportation Systems, (2010)

[Bohl80] W. Bohl,
Technische Strömungslehre,
Vogel Verlag, pp 49, (1980)

[BoMKG06] Robert Bosch GmbH (AA/MKG2),
Lambdasonden richtig beurteilen und behandeln,
(2006)

[Bosc02] Robert Bosch GmbH,
Kraftfahrtechnisches Taschenbuch. 24. Auflage,
Vieweg Verlag, Braunschweig/Wiesbaden, (2002)

[Bosc95] Robert Bosch GmbH,
Kraftfahrtechnisches Taschenbuch, 22. Auflage,
Düsseldorf: VDI Verlag, (1995)

[Bosch10] Robert Bosch GmbH (J. Siedler),
Verbrauchsoptimiert zum Ziel: ECO2-Navigation von Bosch - Routenempfehlung wird energieeffizient ermittelt,
PI 6801 CM Si Presse-Information, (2010)

- [BrGi10] A. Bresges, E. Gizewski,
Routine bringt Autofahrer in Gefahr,
Köln/Essen 17.02.2010, <http://presstext.com/news/100217018/routine-bringt-autofahrer-in-gefahr/>, Access: 18.08.2010
- [Brid10] Bridgestone Deutschland GmbH (S. Grimm), Email interview from June 18 (2010)
- [Buck92] M. Buck,
Geschwindigkeitsverhalten auf einbahnigen Außerortsstraßen in Abhängigkeit von baulichen, betrieblichen und verkehrlichen Randbedingungen,
Forschung Straßenbau und Straßenverkehrstechnik, Heft 621, (1992)
- [BuVe10] Bundesministerium für Verkehr, Bau und Stadtentwicklung,
Verkehr in Zahlen 2009/2010,
(2010)
- [Cacc07] C. Cacciabue,
Modelling Driver Behaviour in Automotive Environments: Critical Issues in Driver Interactions with Intelligent Transport Systems,
Springer Verlag London, (2007)
ISBN-10: 1-84628-617-4
- [CaGa10] L. Canoira, J. G. Galeán, R. Alcántara, M. Lapuerta, R. García-Contrerasb,
Fatty acid methyl esters (FAMES) from castor oil: Production process assessment and synergistic effects in its properties,
Renewable Energy vol.35 Issue 1, pp 208-217, (2010)
- [CaLu87] S.M. Casey, A.K. Lund,
Three field studies of driver speed adaptation,
Human Factors, Vol29, No.5, (1987)
- [CoAb93] T. Connolly, L. Åberg,
Some contagion model of speeding. Accident Analysis and Prevention,
pp 25/57–66, (1993)
- [Coms95] Comsis Corporation, The Johns Hopkins University (Baltimore, Maryland),
Understanding youthful risk taking and driving interim report,
Contract No. DTNH22-93-C-05182, (1995)
- [CoSi92] C. Corbett, F. Simon,
Decisions to break or adhere to the rules of the road, viewed from the rational choice perspective,
British Journal of Criminology, pp 4/32/537–549, (1992)
- [Damb10] M. Dambier,
Adaptive Information Flow Control, Recognition and Prediction of Factors Contributing to Driver's Stress,
Der andere Verlag, pp 76-79, (2010)
ISBN: 978-3-86247-042-6
- [DATG11] Deutsche Automobil Treuhand GmbH,

Leitfaden zu Kraftstoffverbrauch und CO₂ Emissionen aller neuen Personenkraftwagenmodelle die in Deutschland zum Verkauf angeboten werden,
(2011)

[Dent80] G. Denton,
The influence of visual pattern on perceived speed,
Perception vol 9, pp 393 – 402, (1980)

[Dhao11] I. Ben Dhaou,
Fuel Estimation Model for ECO-Driving and ECO-Routing,
College of Engineering, Al Jouf University, Kingdom of Saudi Arabia, 2011 IEEE Intelligent Vehicles Symposium, (2011)

[Diet65] K. Dietrich,
Dauergeschwindigkeiten von Personenwagen auf Steigungen,
Institut für Orts-, Regional- und Landesplanung an der ETH Zürich, (1965)

[Dill73] J. Dilling,
Fahrverhalten von Kraftfahrzeugen auf kurvigen Strecken, in Straßenbau und Verkehrstechnik,
Heft 151, (1973)

[DoJu12] B. Dornieden, L. Junge, P. Pascheka,
Vorausschauende energieeffiziente Fahrzeuglängsregelung,
ATZ 03/2012, pp 231, 2012, (2012)

[Dong78] E. Donges,
Ein regelungstechnisches Zwei-Ebenen-Modell des menschlichen Lenkverhaltens im Kraftfahrzeug,
Zeitschrift für Verkehrssicherheit, 24, pp 98-112, (1978)

[Dong82] E. Donges,
Aspekte der Aktiven Sicherheit bei der Führung von Personenkraftwagen,
Automobil- Industrie, pp 183–190, (1982)

[Dong09] E. Donges, H. Winner, S. Hakuli, G. Wolf,
Handbuch Fahrerassistenzsysteme, Grundlagen, Komponenten und Systeme für aktive Sicherheit und Komfort,
Vieweg+Teubner GWV Fachverlage GmbH, Wiesbaden (2009)
ISBN 978-3-8348-0287-3

[Dorr03] C. Dorrer,
Effizienzbestimmung von Fahrweisen und Fahrerassistenz zur Reduzierung des Kraftstoffverbrauchs unter Nutzung telematischer Informationen,
Dissertation am Institut für Verbrennungsmotoren und Kraftfahrwesen der Universität Stuttgart, Schriftenreihe des Instituts für Verbrennungsmotoren und Kraftfahrwesen der Universität Stuttgart, Band 24, (2003)

[DuBi83] W. Durth, B. Biedermann, B. Vieth,
Einflüsse der Erhöhung der Geschwindigkeiten und Beschleunigungen von Fahrzeugen auf die Entwurfsgeschwindigkeit,

Forschung Straßenbau und Straßenverkehrstechnik Heft 385, Bonn-Bad Godesberg (1983)

[DuLi93] W. Durth, C. Lippold,
Anpassung der Entwurfsrichtlinien für die Linienführung (RAS-L-1 1984) an neuere Entwurfsrichtlinien,
Forschungsauftrag G.2.2/91 des BMV, (1993)

[Durt68] W. Durth,
Die Straße als Führungsgröße eines Regelkreises,
International Automotive congress (FISITA), Barcelona, (1968)

[Durt72] W. Durth,
Ein Beitrag zur Erweiterung des Modells für Fahrer, Fahrzeug und Straße in der Straßenplanung,
Dissertation an der Technischen Hochschule Darmstadt, (1972)

[Durt74] W. Durth,
Ein Beitrag zur Erweiterung des Modells für Fahrer, Fahrzeug und Straße in der Straßenplanung, in Straßenbau und Verkehrstechnik,
Heft 163, (1974)

[Dvr02] Deutsche Verkehrsrat,
Stress im Straßenverkehr,
DVR-Report 4/2002, (2002)

[Eber06] D. Ebersbach,
Entwurfstechnische Grundlagen für ein Fahrerassistenzsystem zur Unterstützung des Fahrers bei der Wahl seiner Geschwindigkeit,
Fakultät Verkehrswissenschaften "Friedrich List" der Technischen Universität Dresden, pp 61-78, (2006)

[ECERE39] *Regulation No 39 of the Economic Commission for Europe of the United Nations (UN/ECE), Uniform provisions concerning the approval of vehicles with regard to the speedometer equipment including its installation,*
L 120/40, Official Journal of the European Union, (2010)

[ECEWP29] Economic Commission for Europe, Inland Transport Committee, World Forum for Harmonization of Vehicle Regulations,
Consolidated Resolution on the Construction of Vehicles (R.E.3),
ECE/TRANS/WP.29/78/Rev.2

[EiKI08] H. Eichlseder, M. Klütting W. F. Piock,
Der Fahrzeugantrieb: Grundlagen und Technologien des Ottomotors,
2008 Springer-Verlag/Wien, pp 14/26/161-165 (2008)
ISBN 978-3-211-25774-6

[EiSu10] N. Eikelenberg, J. Subbian, R. Blanco, D.Sanchez, L. Andreone, S. Damiani, E. Balocco, E.-P. Neukirchner, L. Bersiner,
SP3 ecoSmartDriving Use Cases & System Requirements, in Figure, On-trip Primary driving task related inefficiencies',
pp 24, (2010)

- [Ekos05] EKOS Research Associates,
Driver attitude to speed and speed management: A quantitative and qualitative study - Final report,
Transport Canada, Report no. TP 14756 E, (2005)
- [EiSt03] D. Ellinghaus, J. Steinbrecher,
Fahren auf Landstraßen Traum oder Albtraum? Untersuchung zum Fahrverhalten und Fahrvergnügen von Pkw-Fahrern auf Landstraßen,
Im Auftrag der Continental AG, Hannover, Köln/Hannover (2003)
- [Elli06] B.J. Elliot,
Updating the Victorian driver's perspective - Wipe off 5 campaign: A situation analysis,
Transport Accident Commission, Australia, (2006)
- [EnGr08] I. Engström, N.P. Gregersen, K. Granstöm, A. Nyberg,
Young drivers - reduced crash risk with passengers in the vehicle,
Accident Analysis and Prevention. (2008)
- [ErBr06] E. Ericsson, H. Larsson, K. Brundell-Freij,
Optimizing route choice for lowest fuel consumption Potential effects of a new driver support tool.
Transportation Research Part C: Emerging Technologies, Bd. 14, pp 369–383, (2006)
- [EU661/2009] *Regulation (EC) No 661/2009 of the European parliament and of the council of 13 July 2009 concerning type-approval requirements for the general safety of motor vehicles, their trailers and systems, components and separate technical units intended therefore,*
EN 31.7.2009, Official Journal of the European Union, L 200/1 (2009)
- [EwEb09] U. Ewert, P. Eberling,
bfu-Report 61: Sicherheit auf Ausserortsstrassen,
bfu - Beratungsstelle für Unfallverhütung, Bern, (2009)
- [FEdS10] Fiat,
Fiat Eco-drive Studie - Daten und Fakten zu Eco:drive,
(2010)
- [FFG07] J. Franco, M. Franchek, K. Grigoriadis,
Real-time brake torque estimation for internal combustion engines,
Mechanical Systems and Signal Processing 22, pp 338–361, (2007)
- [Fial06] E. Fiala,
Mensch und Fahrzeug, Fahrzeugführung und sanfte Technik,
Vieweg ATZ/MTZ-Fachbuch, pp 48-53/224, (2006)
ISBN: 978-3-8348-0016-9
- [Fiat10] Fiat,
Daten und Fakten zu ECO:DRIVE - Die Stärken und Herausforderungen von eco:Drive, basierend auf der ersten Studie mit echten Fahrtdaten,
full report, (2010)

[FiCa10] K. Fitzpatrick, P. J. Carlson, M. D. Wooldridge, M. A. Brewer,
Project 0-1769: Identify Design Factors That Affect Driver Speed and Behavior,
Project Summary Report 1769-S, Texas Transportation institute / the texas A&M University
System, (2000)

[FiRu91] B. Fildes, G. Rumbold, A. Leening,
Speed behaviour and drivers' attitudes to speeding.
Monash University Accident Research Centre, (1991)

[FKAa09] Forschungsgesellschaft Kraftfahrwesen mbH Aachen,
Kraftstoffverbrauchsminderung durch vorausschauende Fahrweise,
Projektnummer 87400, (2009)

[Ford12] thempgmarathon.co.uk,
Ford Fiesta goes over a "ton" in epic MPG Marathon
Source: <http://www.thempgmarathon.co.uk/latest-news/news-archive/ford-fiesta-goes-over-a-ton-in-epic-mpg-marathon/>, Stand: 8th October (2012)

[GJPY11] Min Goo Lee, Kyung Kwon Jung, Yong Kuk Park, Jun Jae Yoo,
Effect of In-Vehicle Parameters on the Vehicle Fuel Economy,
U-embedded Convergence Research Center, Korea Electronics Technology Institute,
Seongnam-si, Gyeonggi-do, Korea, AST 2011, Springer-Verlag Berlin Heidelberg, pp 132–
142, (2011)

[Goll05] R. Golloch,
**Downsizing bei Verbrennungsmotoren: Ein wirkungsvolles Konzept zur
Kraftstoffverbrauchssenkung,**
Springer-Verlag Berlin Heidelberg, pp 3-66 (2005)
ISBN: 978-3-540-23883-6

[GrAn09] K.-H. Grote, E. K. Antonsson,
Internal combustion engines,
Springer Handbook of Mechanical Engineering, pp 915, Springer, (2009)
ISBN-13: 978-3540491316

[GuSc05] L. Guzzella, A. Sciarretta,
Vehicle Propulsion Systems: Introduction to Modeling and Optimization,
pp 15-27, (2005)
ISBN: 978-3-540-25195-8

[Hake07] K.-L. Haken,
Grundlagen der Kraftfahrzeugtechnik,
Carl Hanser Verlag, pp 146-157, (2007)
ISBN 978-3-44622-812-2

[Haur06] R. Hauri-Bionda,
Fahrfähigkeit – Grundlagen der Rechtsmedizin,
Institut für Rechtsmedizin, Universität Zürich, (2006)

[Hawk88] R. Hawkins,

Verkehrsverhalten auf Autobahnen unter Bedingungen eingeschränkter Sicht,
Zeitschrift für Verkehrssicherheit, vol. 34, Nr: 2/, pp 74-79, (1988)

[HeAk11] H.-R. Hein, K. Akutagawa, H. Heguri, N. Yamagishi,
Reifen Ecopia mit niedrigem Rollwiderstand für eine bessere Umweltverträglichkeit,
ATZ 06/2011, pp 488, (2011)

[Heise11] Heise computer magazine,
OBD2-Echtzeitdaten versprechen einigen Zusatznutzen für mobile Navis,
Source: <http://www.heise.de/autos/artikel/Der-OBD2-Adapter-Garmin-ecoRoute-HD-im-Test-1191004.html?view=print> accessed in February (2011)

[Hess93] S. Hesse,
Suchtprävention in der Schule,
Leske & Budrich, (1993)
ISBN 978-3810011510

[HiKn89] H. Hiersche, S. Knepper, H. Messmer, A. Nikpour, G. Euler, J. Lang, D. Jakobi, G. Retzla, R. Plahak,
Bewertung des Fahrverhaltens auf nassen Fahrbahnen unter Einsatz der konduktometrischen Meßsonde,
Forschung Straßenbau und Verkehrstechnik Heft 575, Bundesministerium für Verkehr, Abteilung Straßenbau, (1989)

[Hoff84] G. Hoffmann,
Witterungsbedingte Veränderungen der Verkehrssicherheit und des Verkehrsablaufs auf innerstädtischen Autobahnen und Hauptverkehrsstraßen,
Bundesminister für Verkehr, Abt. Straßenbau, Bonn, Bad Godesberg (1984)

[HuBa11] T. Hüsemann, C. Bachmann, S. Winter, D. Henrichmüller,
Mobile Prüfstandstechnik zur Messung von Reifen-Fahrbahn- Reibwerten,
ATZ 06/2011, pp 504, (2011)

[Huch05] W.-H. Hucho,
Aerodynamik des Automobils: Strömungsmechanik, Wärmetechnik, Fahrdynamik, Komfort. 5. Auflage.
Friedr. Vieweg & Sohn Verlag/GWV Fachverlage GmbH, Wiesbaden, (2005)

[Huch98] W. H. Hucho,
Aerodynamics of road vehicles,
SAE Publishing Warrendale PA, (1998)

[IsOn10] N. Ishikawa, K. Onda, K. Watanabe, K. Kobayashi, Y. Kurihara,
Mobile phone application for ecodriving,
SICE Annual Conference, (2010)

[Jaza08] R. N. Jazar,
Vehicle Dynamics: Theory and Application,
2008 Springer Science+Business Media, LLC, pp 95-163 (2008)
ISBN: 978-0-387-74243-4

- [JoFa99] H. Johansson, J. Farnlund, C. Engstrom,
Impact of Ecodriving on emissions and fuel consumption, a pre-study,
Swedish National Road Administration, (1999)
- [KalStutt04] R. Kleinbauer,
Kalman filtering implementation with matlab,
Institute of Geodesy, Universität Stuttgart, Helsinki, (2004)
- [KaMa11] J. Kang, T. Ma, F. Ma, J. Huang,
Link-based Emission Model for Eco Routing,
State Key Laboratory of Software Development Environment Beihang University, Beijing,
China, 11th International Conference on ITS Telecommunications, (2011)
- [KeuG07] Kommission der europäischen Gemeinschaften,
Ergebnisse der Überprüfung der Strategie der Gemeinschaft zur Minderung der CO₂-Emissionen von Personenkraftwagen und leichten Nutzfahrzeugen,
(2007)
- [Kimu93] I. Kimura,
The relationship between drivers' attitude toward speeding and their speeding behaviour in hypothetical situations.
Hiroshima Forum for Psychology, pp 15/51–60, (1993)
- [Knep92] S. Knepper,
Untersuchung des Geschwindigkeits- und Abstandsverhaltens auf nasser bzw. trockener Fahrbahn unter Berücksichtigung der Lichtverhältnisse sowie der Wochentage,
TU Karlsruhe, (1992)
- [KöBo79] Köppel, H. Bock,
Fahrgeschwindigkeit in Abhängigkeit von der Kurvigkeit,
Forschung Straßenbau und Straßenverkehrstechnik, Heft 269, (1979)
- [Köhl09] S. Köhler,
Erkennung des Fahrertyps zur Verbesserung der Detektion von Fahrerablenkung,
Institut für Technik der Informationsverarbeitung (ITIV) Universität Karlsruhe, pp 9, (2009)
- [Lamm73] R. Lamm,
Fahrdynamik und Streckencharakteristik, Ein Beitrag zum Entwurf von Straßen unter besonderer Berücksichtigung der Geschwindigkeit,
Institut für Straßenbau und Eisenbahnwesen, Universität Karlsruhe, Heft 11, (1973)
- [Lee05] J. Lee,
Rotating Inertia Impact on Propulsion and Regenerative Braking for Electric Motor Driven Vehicles,
Virginia Polytechnic Institute and State University, pp 16, (2005)
- [LeKw12] C. Lee, J. Kwon, Y. Lee, J. Park,
Optimiertes Klimaanlage System für erhöhte Reichweite von Elektrofahrzeugen,
ATZ 06/2012, pp 489, (2012)
- [Lipp94] D. Lipphard,

Geschwindigkeiten in den neuen Bundesländern,
Zeitschrift für Verkehrssicherheit, Bd. 40, pp 151-154, (1994)

[Lipp97] C. Lippold,
Weiterentwicklung ausgewählter Entwurfsgrundlagen von Landstraßen,
Dissertation TU Darmstadt, (1997)

[Luna09] M. Lunanova,
Optimierung von Nebenaggregaten: Maßnahmen zur Senkung der CO2-Emission von Kraftfahrzeugen,
Vieweg +Teubner | GWV Fachverlage GmbH, Wiesbaden, pp 7-91, (2009)
ISBN 978-3-8348-0730-4

[MeGe75] V. Meewes, U. Gerz,
Zur Beschreibung des Verkehrsablaufs auf Straßen mit und ohne Richtungstrennung,
Forschungsbericht des Landes NRW, (1975)

[Mich03] Michelin,
Le pneu: résistance au roulement et basse consommation,
Société de Technologie Michelin 23, rue Breschet, 63000 Clermont-Ferrand, pp 53-115,
(2003)

[Mich10] D. Hallez-Goazard (Michelin Europe), Email interview from June 18 (2010)

[MiWa04] M. Mitschke, H. Wallentowitz,
Dynamik der Kraftfahrzeuge,
Springer Verlag, (2004)
ISBN 3-540-42011-8

[MiZi03] P. Mitchell-Taverner, L. Zipparo, J. Goldsworthy,
Survey on speeding and enforcement,
Australian Transport Safety Bureau, Report no. CR 214a, (2003)

[MuSh80] B.J. Mustyn, D. Sheppard,
A National Survey of Driver' Attitudes and Knowledge About Speed Limits.
SR 548, Transport and Road Research Laboratory, Crowthorne, England, (1980)

[NaBe07] H. Naunheimer, B. Bertsche,
Fahrzeuggetriebe, Grundlagen, Auswahl, Auslegung und Konstruktion,
Springer Verlag Berlin Heidelberg, pp 67/78/ (2007)
ISBN: 978-3-540-30625-2

[NavGreen10] Navteq,
Navteq Green Streets White Paper,
pp 3-4, (2010)

[NavRDF10] Navteq,
Relational Database Format (RDF) Reference Guide, Version 2.2,
Q2 (2010)

[Navt08] Navteq,

Data product release notes: NAVTEQ Traffic Patterns Europe v2.0,
pp 5, (2008)
EUPD08400TRFVAR, 2008.4

[NoHu09] K. Norman, S. Huff, B. West,
Effect of intake air filter condition on vehicle fuel economy,
Oak ridge national laboratory for the U.S. department of energy, pp 25, (2009)

[Oecd07] OECD Publishing,
La Gestion de La Vitesse,
European Conference of Ministers of Transport (2007)
ISBN 978-9282103791

[Orci05] ORC International,
Lancashire Partnership for Road Safety: Public opinion survey,
(2005)

[ÖrRü09] S. Öri, U. Rügheimer, M. Blazevski, T. Söllner,
Effizienz-Technologien von A bis Z,
Audi AG Kommunikation Produkt, pp 49-74, (2009)

[Rajp05] R. K. Rajput,
Elements of Mechanical Engineering,
Firewall Media, pp 248 – Introduction to mechanical engineering, (2005)
ISBN: 8170086361

[RaMa08] H.-P. Rabl, I. Makarenko,
Spritsparendes Autofahren,
Combustion Engines & Emission Control Laboratory University of Applied Sciences
Regensburg, pp 27-29/42, (2008)

[Rasm83] J. Rasmussen,
Skills, Rules and Knowledge; Signals, Signs and Symbols and other Distinctions in Human Performance Models.
IEEE Trans. on Systems, Man and Cybernetics, Vol. SMC 13, No. 3, pp 257–266, (1983)

[Reic98] G. Reichart,
Potentials of BMW Driver Assistance to Improve Fuel Economy,
Fisita 1998 World Automotive Congress, Paris (1998)

[RuBa11] P. Rumbolz, G. Baumann, H.-C. Reuss,
Messung der fahrzeuginternen Leistungsflüsse im Realverkehr,
ATZ 05I2011, pp 417, (2011)

[Saf03] M. J. Safoutin,
Virtual Car 4.0: Virtual Prototyping and Rapid Prototyping in Engineering Design,
Instructor of ENGR 100 at the University of Washington, 2003 (Link: <http://www.virtual-car.org/wheels/parameters.html>, Stand: 23 September 2010)

[SaKu01] K. Samper, K.-P. Kuhn,
Reduktion des Kraftstoffverbrauchs durch ein vorausschauendes Assistenzsystem,

VDI-Berichte Nr. 1613, Der Fahrer im 21. Jahrhundert, VDI-Verlag, Düsseldorf, (2001)

[Sand04] D. Sandkühler,
Identification of traffic situation: Development and application in driver assistance systems,
Aachener Kolloquium Fahrzeug- und Motorentechnik 2004, pp 5-6, (2004)

[Sch176] H.G. Schlichter,
Streckencharakteristik: Eine analytische Betrachtung,
Straße und Autobahn, Heft 2, (1976)

[Schr10] R. Schroth (Bosch SG/EGE3), Email interview from October 25 (2010)

[ScTh07] M. Schmidt, H. Theuerkauf,
Elektrische Energiemanagementstrategien zur CO₂-Reduktion– Technische Voraussetzungen und Auswirkungen auf das Bordnetz, Dokumentation: CO₂ – Die Herausforderung fuer unsere Zukunft,
ATZ/MTZ-Konferenz – Energie 2007, pp 68, (2007)

[ShAl01] B. A. Shannak, M. Alhasan,
Effect of atmospheric altitude on engine performance,
Forschung im Ingenieurwesen 67 (2002), pp 157–160, Springer-Verlag, (2002)
DOI 10.1007/s10010-002-0087-y

[ShKn85] D. Shinar, J. McKnight,
The effects of enforcement and public information on compliance.
Evans, L. & Schwing, R. (Eds). Human behaviour and traffic safety. pp 385-415, Plenum:
New York, (1985)

[Shop06] J.T. Shope,
Influences on youthful driving behavior and their potential for guiding interventions to reduce crashes,
Injury Prevention. 2006, 12 (Suppl 1): i9–i14, (2006)

[ShSt86] D. Shinar, J. Stiebel,
The Effectiveness of Stationary Versus Moving Police Vehicle on Compliance with Speed Limit.
Human Factors, Vol. 28, (1986)

[Soso01] A. Sosouhmihen,
Entwicklung eines Rahmenkonzeptes zur Bewertung der Linienführung von Außerortsstraßen nach der Zielfunktion Fahrsicherheit,
Technische Universität Dresden, Fakultät Verkehrswissenschaften, (2001)

[SpBe98] P. Spacek, I. Belopitov,
Geschwindigkeit in Kurven,
Forschungsauftrag Nr. 01/96 des Eidgenössischen Verkehrs- und Energiewirtschaftsdepartments (UVEK), (1998)

[Spic12] U. Spicher,
Analyse der effizienz zukünftiger Antriebssysteme für die individuelle Mobilität,

MTZ 02/2012, pp 98-105, (2012)

[StRa04] R. Stenschke, A. Rauterberg-Wulff,
Umwelteigenschaften von Reifen – Stand der Gesetzgebung,
Umweltbundesamt, pp 4-5, 12-15, (2004)

[TeAt08] Tele Atlas,
Speed Profiles: Intelligent data for optimal routing, version 2008.10
User guide, pp 16, (2008)

[Thom94] J. Thoma,
Geschwindigkeitsverhalten und Risiken bei verschiedenen Straßenzuständen, Wochentagen und Jahreszeiten,
Zeitschrift für Verkehrssicherheit, Bd. 40, pp 7-11, (1994)

[ToCh09] F. Töpler, F. Christen, A. Benmimoun, S. Gies,
Kraftstoffverbrauchsminderung durch vorausschauende Fahrweise,
Projekt 87400, Forschungsgesellschaft Kraftfahrwesen mbH Aachen – Geschäftsbereich Fahrerassistenz, März (2009)

[Trap74] K. Trapp, F. Oellers,
Streckencharakteristik und Fahrverhalten auf zweispurigen Landstraßen,
Straßenbau und Straßenverkehrstechnik, Forschungsberichte, Bundesministeriums und der Forschungsgesellschaft für das Straßenwesen e.V., Heft 176, (1974)

[TrKe10] M. Treiber, A. Kesting,
Verkehrsdynamik und simulation Daten, Modelle und Anwendungen der Verkehrsflussdynamik,
Springer Heidelberg Dordrecht London New York, pp 25-36 / 278, (2010)
ISBN 978-3-642-05227-9

[Trze10] M. Trzesniowski,
Rennwagentechnik: Grundlagen, Konstruktion, Komponenten, Systeme,
Vieweg+Teubner Verlag | GWV Fachverlage GmbH, Wiesbaden, pp 185-225, (2010)
ISBN: 978-3-8348-0857-8

[Tuev02] W. Reithmaier, T. Salzinger,
Ermittlung des aktuellen Standes der Technik im Hinblick auf Abrollgeräusch, Rollwiderstand sowie Sicherheitseigenschaften moderner Pkw-Reifen,
Umweltforschungsplan des Bundesministers für Umwelt, Naturschutz und Reaktorsicherheit, Forschungsbericht 201 54 112, (2002)

[täv04] TÜV automotive GmbH,
TÜV Reifen/Räder-Test-Center automotive - Pkw Reifen-Test der TÜV automotive GmbH,
Umweltbundesamt, (2004)

[Vaux11] J. Hawkins (Press Officer, Vauxhall Product, CV & Fleet),
Vauxhall wins mpg marathon in 6.2 litre V8,
Source:
http://media.vauxhall.co.uk/media/gb/en/vauxhall/news.detail.html/content/Pages/news/gb/en/2011/VAUXHALL/10_10_vauxhall_wins_MPG_marathon.html, Stand: 2011-10-10

[VIKe00] I. De Vlieger, D. De Keukeleere, J.G. Kretzschmar,
Environmental effects of driving behaviour and congestion related to passenger cars,
Flemish Institute for Technological Research (Vito), 200 Boeretang, 2400 Mol, Belgium,
Atmospheric Environment 34 (2000) 4649-4655, (2000)

[VoDo01] M. van der Voort, M. S. Dougherty, M. van Maarseveen,
A prototype fuel-efficiency support tool.
Transportation Research Part C: Emerging Technologies, pp 279–296, (2001)

[Volk08] Volkswagen AG,
Das DSG-Doppelkupplungsgetriebe Umweltprädikat,
Konzernforschung Umwelt-Produkt, Wolfsburg Stand: Oktober (2008)
Artikelnummer: 815.1245.12.01

[VoLo01] M. Vollrath, R. Löbmann, H.-P. Krüger, H. Schöch, T. Widera, M. Mettke,
Fahrten unter Drogeneinfluss - Einflussfaktoren und Gefährdungspotenzial,
Berichte der Bundesanstalt für Straßenwesen, 2001, Reihe Mensch und Sicherheit (Heft
M132). Bremerhaven: Wirtschaftsverlag NW, (2001)

[VrMa10] J. Vreeswijk, M. Mahmood, B. van Arem,
*Energy efficient traffic management and control - The eCoMove approach and expected
benefits*, pp 3, (2010)

[VWir10] Volkswagen,
Glossar: “Wirkungsgrad”, Website: <http://www.volkswagen.de>
Accessed: 25.05.2010

[Walsh10] S. Walsh,
NAVTEQ Maps for Advanced Routing, pp 25, (2010)

[WaRo94] D. De Waard, T. Rooijers,
*An experimental study to evaluate the effectiveness of different methods and intensities of
law enforcement on driving speed motorways*.
Accident Analysis and Prevention, pp 6/26/751–765, (1994)

[YiLe95] Y. Yinon, E. Levian,
Presence of other drivers as a determinant of traffic violations.
The Journal of Social Psychology, pp 3/135/299–304, (1995)

[Zaid92] D. Zaidel,
A modelling perspective on the culture of driving.
Accident Analysis and Prevention, 24, pp 585–597, (1992)

[Zerv11] E. Zervas,
Impact of altitude on fuel consumption of a gasoline passenger car,
Fuel Volume 90, Issue 6, June 2011, pp 2340-2342, (2011)

ANNEX A: The Stuttgart Bosch-FKFS Dataset

A1. Test Track Presentation:

The track is referred to as ‘ST01’

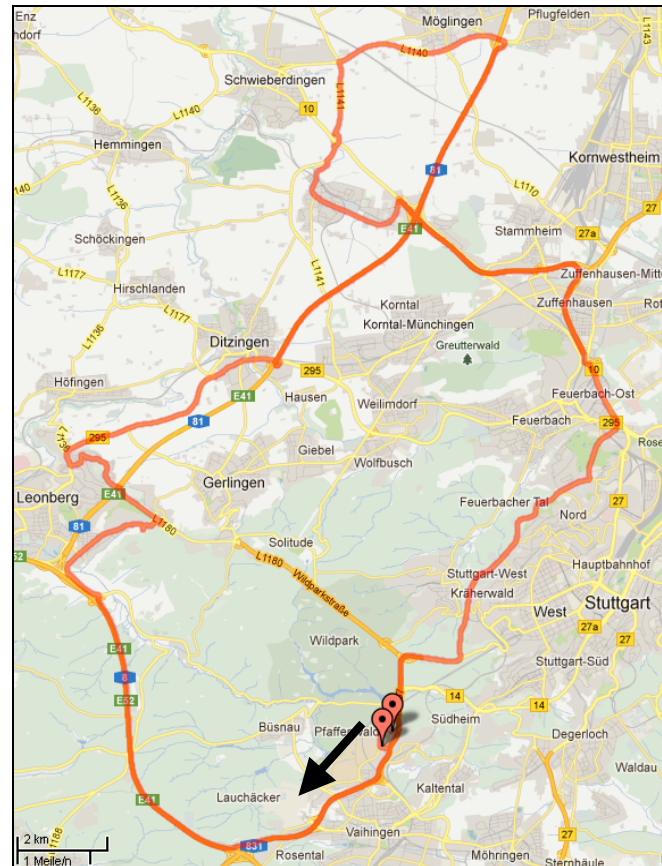


Figure 72: The Bosch-FKFS Track
Map data @2013 GeoBasis-DE/BKG(@2009) Google

Track length: The total length is around 63 kilometers (with some variations due to the chosen lanes).

Start / End: FKFS / Pfaffenwaldring 12 / Stuttgart / Germany

Travel direction: Heading south-west to the A8, then Leonberg, Ditzingen, A81 heading north, Schwieberdingen, Feuerbach and back FKFS.

Road type repartition: The track was designed by the FKFS (Forschungsinstitut für Kraftfahrwesen und Fahrzeugmotoren Stuttgart) to represent the yearly average road distribution in Germany [Reuss09]:
~ 25.9 % inner city ~ 26.5 % outer city (except highway) ~ 47.6 % on highway

Slope: slope is considered to be average according to the Stuttgart region. The altitude variation observed over the full distance is represented in the following figure:

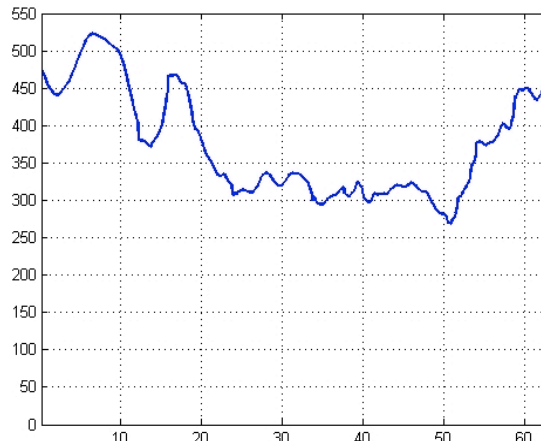


Figure 73: Altitude Variation Along the Bosch-FKFS track [Reuss09]
Y-Axis: Altitude in meter
X-Axis: Distance in kilometers

A2. Drivers

Thirty drivers were selected out of a driver database in an attempt to represent all the main age groups and reach a balanced sex repartition. The repartition was as indicated in the following table:

Age	<30	30-40	40-50	50-60	>60	Total
Women	3	2	3	3	1	12
Men	4	4	3	3	4	18
Total	7	6	6	6	5	30

Table 31: Distribution of the Drivers over Age and Sex [Reuss09]

A3. Date

The dataset was recorded between 05 November 2008 and 16 January 2009. Every one of the thirty drivers had to drive around the test track three times:

- The first drive was to acclimate to the car
- The second drive was with the use of a regular built-in ACC system on the highway
- The third drive was with the use of an experimental ACC system on the highway

The three drives were not recorded on the same day.

A4. Vehicle Specification

Brand & model: BMW 530d E60 (2005-2007) Sedan

Engine & Gearbox: V6 diesel with 500Nm of torque at 2000-2750rpm and a 6 Speed Automatic Gearbox

Specifications: further specification can be found in the BMW E60 official specification sheet [BMW06]

Modifications:

- Brake system ESP Premium (ESP8)
- CLAUS-BOX for communication between ACC-CAN and Vehicle-CAN
- USB Videocamera
- THALES DG 14 GPS sensor
- Hardware for CAN and GPS recording during the tests

A5. Recorded Signals

Vehicle-CAN and ACC-Signal (10Hz)

- Driven distance in miles
- Fuel injected in $\mu\text{l}/0.1\text{s}$
- Longitudinal acceleration in m/s^2
- Lateral acceleration in m/s^2
- Yaw
- Vehicle speed in $\text{cm}/0.1\text{s}$
- Wheel angle
- Steering wheel
- Torque in Nm
- Engine speed in rotation/minute

GPS (1Hz)

- Longitude
- Latitude
- Altitude
- Speed in m/s
- Number of recognized satellite
- Number of used satellite for position

Additional ACC (10Hz)

Some additional ACC signals were recorded, but they are not relevant for this work.

A6. Track Segmentation According to the Video Recordings

Segment number	Lanes	Speed limit	Inner-city	Outer-city	Highway	RAMP	Road works	Ends with a traffic light	Functional road class	Road name	Left turn	Right turn	Exit
1	1	50	X						5				
2	1	50	X						5		X		
3	1	50	X				X		3-4	Universitätsstraße		X	
4	1	80		X		X			RAMP	From Universitätstrasse to B14			X
5	2	80		X					2	B14			
6	3	80		X					2	B14			
7	1	80		X			X		2	B14			
8	3	100		X	X				2	A831/B14			
9	1	100		X	X	X			RAMP	A831 / B14 to A81			X
10	3	100		X	X	X			RAMP	A831 / B14 to A81			X
11	3	100		X	X				1	A81			
12	4	100		X	X				1	A81			
13	2	100		X	X		X		RAMP	A81	X		X
14	2	100		X					3-4	L1187			
15	1	70		X					3-4	L1187/Neue Ramtelstraße			
16	1	100		X					3-4	L1187/Neue Ramtelstraße			
17	1	50	X				X		3-4	L1187/Neue Ramtelstraße			
18	1	50	X				X		3-4	L1187/Neue Ramtelstraße			
19	1	50	X				X		3-4	L1141/Neue Ramtelstraße			
20	1	100		X					3-4	L1141/Neue Ramtelstraße			
21	1	50		X			X		3-4	L1141/Neue Ramtelstraße	X		
22	1	100		X					3-4	Stuttgarterstrasse			
23	1	70		X					3-4	Stuttgarterstrasse			
24	R.	30	X				X		3-4	Stuttgarterstrasse			
25	1	50	X						3-4	Stuttgarterstrasse			
26	1	30	X				X	X	3-4	Stuttgarterstrasse			
27	1	30	X				X		3-4	Stuttgarterstrasse			
28	1	30	X				X	X	3-4	Stuttgarterstrasse			

Segment number	Lanes	Speed limit	Inner-city	Outer-city	Highway	RAMP	Road works	Ends with a traffic light	Functional road class	Road name	Left turn	Right turn	Exit
29	1	30	X				X		3-4	Stuttgarterstrasse			
30	1	50	X					X	3-4	Stuttgarterstrasse		X	
31	1	50	X						3-4	Feuerbacherstrasse			
32	1	50	X					X	3-4	Feuerbacherstrasse			
33	1	80		X					3-4	Feuerbacherstrasse			
34	1	60		X					3-4	Feuerbacherstrasse			
35	1	80		X					3-4	Feuerbacherstrasse /Calwererstrasse			
36	1	40		X				X	3-4	Feuerbacherstrasse /Calwererstrasse		X	
37	1	100		X				X	3-4	Siemensstrasse			
38	1	50	X					X	3-4	Siemensstrasse			
39	1	50	X					X	3-4	Siemensstrasse			
40	1	50	X					X	3-4	Siemensstrasse			
41	2	50		X				X	3-4	Siemensstrasse			
42	2	60		X				X	3-4	Siemensstrasse			
43	2	60		X				X	3-4	Weilimdorferstrasse		X	
44	1	100		X		X			RAMP	Weilimdorferstrasse -> A81			
45	3	999		X	X				1	A81			
46	3	120		X	X				1	A81			
47	2	100		X	X			X	RAMP	Exit A81	X		X
48	2	60		X				X	3-4	Schwieberdingerstrasse			
49	2	60		X				X	3-4	Schwieberdingerstrasse			
50	2	60		X					3-4	Schwieberdingerstrasse			
51	1	70		X				X	3-4	Schwieberdingerstrasse			
52	1	70		X					3-4	Umgehungsstrasse(L1140)			
53	1	100		X					3-4	Umgehungsstrasse(L1140)			
54	1	70		X				X	3-4	Umgehungsstrasse(L1140)	X		
55	1	100		X					3-4	L1141			
56	1	80		X					3-4	L1141			
57	R.	50		X					3-4	L1141			
58	1	50		X				X	3-4	L1141			
59	1	50		X					3-4	L1141			
60	R.	50		X					3-4	L1141			
61	1	70		X				X	3-4	L1141			
62	1	70		X					3-4	Markgröningerstrasse			
63	1	70		X					3-4	Markgröningerstrasse			
64	1	50	X					Bahngleis	3-4	Markgröningerstrasse			
65	1	50	X					X	3-4	Stuttgarterstrasse			
66	1	50	X					X	3-4	Stuttgarterstrasse			
67	1	50	X					X	3-4	Stuttgarterstrasse			
68	1	50	X					Bahngleis	3-4	Stuttgarterstrasse			
69	1	50		X					3-4	Stuttgarterstrasse			
70	1	70		X					3-4	Stuttgarterstrasse			
71	1	100		X					3-4	Stuttgarterstrasse			
72	1	70		X					3-4	Stuttgarterstrasse			
73	1	50	X					X	3-4	Stuttgarterstrasse			
74	1	100		X		X			RAMP	RAMP on B10			
75	2	100		X					2	B10			

Segment number	Lanes	Speed limit	Inner-city	Outer-city	Highway	RAMP	Road works	Ends with a traffic light	Functional road class	Road name	Left turn	Right turn	Exit
76	2	80		X					2	B10			
77	2	50		X					2	B10			
78	2	80		X					2	B10			
79	3	80		X					2	B10 / B27			
80	2	60		X					2	B10 / B27			
81	2	60		X			X		2	B10 / B27		X	
82	2	50	X				X		2	B10 / B27			
83	2	50	X			X	X		2	B10 / B27			
84	2	50	X			X	X		2	B10 / B27			
85	2	50	X			X	X		2	B10 / B27			
86	2	50	X						RAMP	B10 / B27			X
87	2	50	X				X		RAMP	B10 / B27			X
88	1	50	X				X		3-4	Stresemannstrasse			
89	1	50	X				X		3-4	Stresemannstrasse			
90	1	50	X				X		3-4	Stresemannstrasse			
91	1	50	X				X		3-4	Stresemannstrasse			
92	2	50	X						3-4	Stresemannstrasse			
93	2	50	X						3-4	Stresemannstrasse			
94	2	50	X				X		3-4	Stresemannstrasse			
95	2	50	X				X		3-4	Am Kochenhof			
96	2	50	X				X		3-4	Am Kochenhof			
97	2	50	X				X		3-4	Am Kochenhof			
98	2	50	X				X		3-4	Am Kochenhof			
99	2	50	X				X		3-4	Am Kochenhof			
100	2	50		X					3-4	Am Kochenhof			
101	1	50		X					3-4	L1187			
102	2	50		X					3-4	L1187			
103	1	50	X				X		3-4	Am Krähenwald			
104	1	50	X				X		3-4	Am Krähenwald			
105	1	50	X				X		3-4	Am Krähenwald			
106	1	50	X				X		3-4	Am Krähenwald			
107	1	50	X						3-4	Am Krähenwald			
108	2	60		X			X		3-4	Geißeichstrasse			
109	2	80		X					2	B14			
110	3	80		X					2	B14			
111	2	80		X					RAMP				X
112	1	50	X						RAMP				
113	1	30	X			X			5	Universitätsstrasse			
114	1	50	X						5	Universitätsstrasse		X	
115	1	50	X						5	Pfaffenring			

References:

[Reuss09] Prof. Dr. Ing. H.C. Reuss, ‘Quantifizierung des Einflusses von ACC auf die CO2-Emissionen im kundenrelevanten Fahrbetrieb’, Abschlussbericht der Forschungsinstitut für Kraftfahrwesen und Fahrzeugmotoren Stuttgart, 24.07.2009

[BMW06] BMW Presse, Technische daten BMW 5er Limousine (520d, 525d, 530d, 535d), version 06/2006, valid from 03/2005

ANNEX B: The Hildesheim 'Original' Dataset

B1. Test Track Presentation:

The track is referred to as 'Hi01'

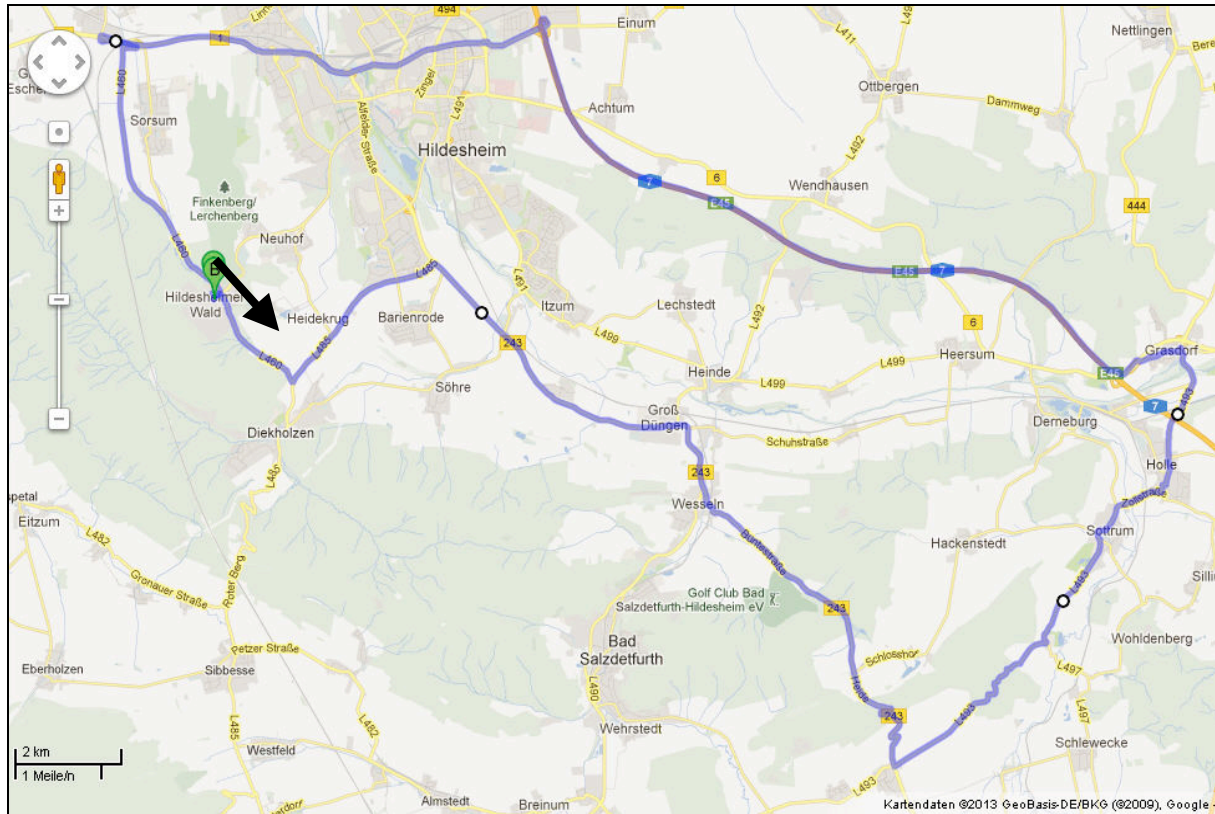


Figure 74: The 'Hi01' Track
Map data @2013 GeoBasis-DE/BKG(@2009) Google

Track length: The total length is around 62 kilometers (with some variations due to the chosen lanes).

Start / End: Robert Bosch Car Multimedia GmbH / Robert-Bosch-Straße 200 / 31139 Hildesheim / Germany

Travel direction: Heading south-east to Diekholzen, Wesseln, Sotrum, A7 to Hannover, B1

Road type repartition: The track was designed by the Robert Bosch Car Multimedia GmbH to test a speed sign recognition system. The road type repartition is:

- ~ 27.3 % inner city
- ~ 51.9 % outer city (Highway excluded)
- ~ 20.8 % on highway and expressway

Slope: slope is considered to be low according to the Hildesheim region. The altitude variation observed over the full distance is represented in the following figure:

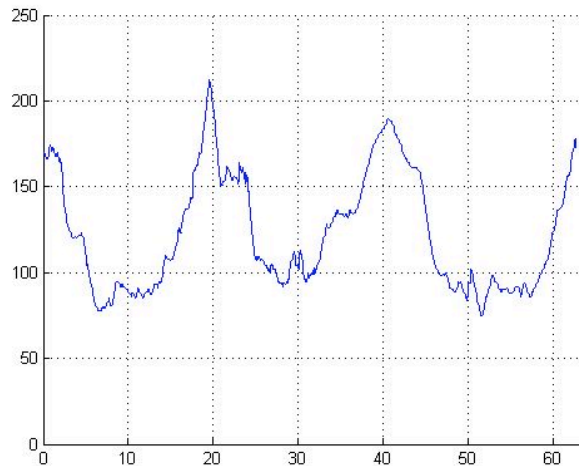


**Figure 75: Altitude Variation Along the Hi01 Track
(With original interferences)**

Y-Axis: Altitude in meter
X-Axis: Distance in kilometer

B2. Drivers

Four drivers were hired to drive the car for two weeks. While the Stuttgart database ST01 (30 drivers x 3 laps) focuses on the differences between the drivers, only a few drivers had to drive a lot (around 30 laps) to make it possible to analyze their driving style.

B3. Date

This dataset was recorded between 05 September 2011 and 16 September 2011. A day was starting at 5:00AM or 09:00AM and ending at 10:00PM. During a time slot, a driver was able to drive 3 or 4 laps. The schedule is listed in the following table:

	05:00AM to 09:00AM	09:00AM to 01:00PM	01:00PM to 06:00PM	06:00PM to 10:00PM
05.09.2011		R	V	K
06.09.2011		B	V	K
07.09.2011		B	R	K
08.09.2011		V	B	R
09.09.2011		R	V	K
12.09.2011		V	K	R
13.09.2011	B	V	R	K
14.09.2011	R	B	V	K
15.09.2011	V	K	B	R
16.09.2011	V	B	R	K

Table 32: Driver repartition over the two weeks

During the two weeks:

- Driver R. was able to record 32 laps
- Driver V. was able to record 35 laps
- Driver K. was able to record 33 laps
- Driver B. was able to record 24 laps

B4. Vehicle Specification

Brand & model: BMW 325d E91 (2008-2012) Touring

Engine & Gearbox: V6 diesel with maximum 400Nm of torque and a 6 Speed Automatic Gearbox

Specifications: further details are available on the BMW E91 official specification sheet [BMW09]

Modifications:

- Brake system and steering were upgraded by Robert Bosch GmbH for internal prototypical use. Because these changes have no strong influence on the driving style, they were not relevant for this work.
 - Ford MFD Navigation system with prototypical software for lap logging
 - External GPS sensor
 - Hardware for communication with the CAN
- The whole vehicle weighed 1800kg.

B5. Recorded Signals

Vehicle-CAN Signal (10Hz)

- Speed in cm/s
- Yaw rate
- Longitudinal acceleration in m/s^2
- Lateral acceleration in m/s^2
- Steering wheel angle
- Steering wheel rate
- Gear box position
- Gear box converter clutch
- Gear box sport mode
- Gear box clutch switch
- Brake pedal pressed
- Brake ESP state
- Brake handbrake
- Brake pressure
- Engine speed in rpm
- Acceleration pedal pressure
- Wheel momentum in Nm
- Engine torque in Nm
- Fuel shutoff
- Temperature engine
- Temperature oil
- Fuel injected volume in $\mu l/0.1s$.
- ACC state
- ACC set speed
- ACC locked lead car
- ACC LLC speed

GPS (1Hz)

- Longitude
- Latitude
- Altitude
- Speed in m/s

References:

[BMW09] BMW Presse, Technische daten BMW 3er Touring (325d, 330d, 335d), version 01/2009, valid from 03/2009

ANNEX C: The Hildesheim ‘Mass & Air’ Dataset

C1. Test Track Presentation:

The track is referred to as ‘Hi02’

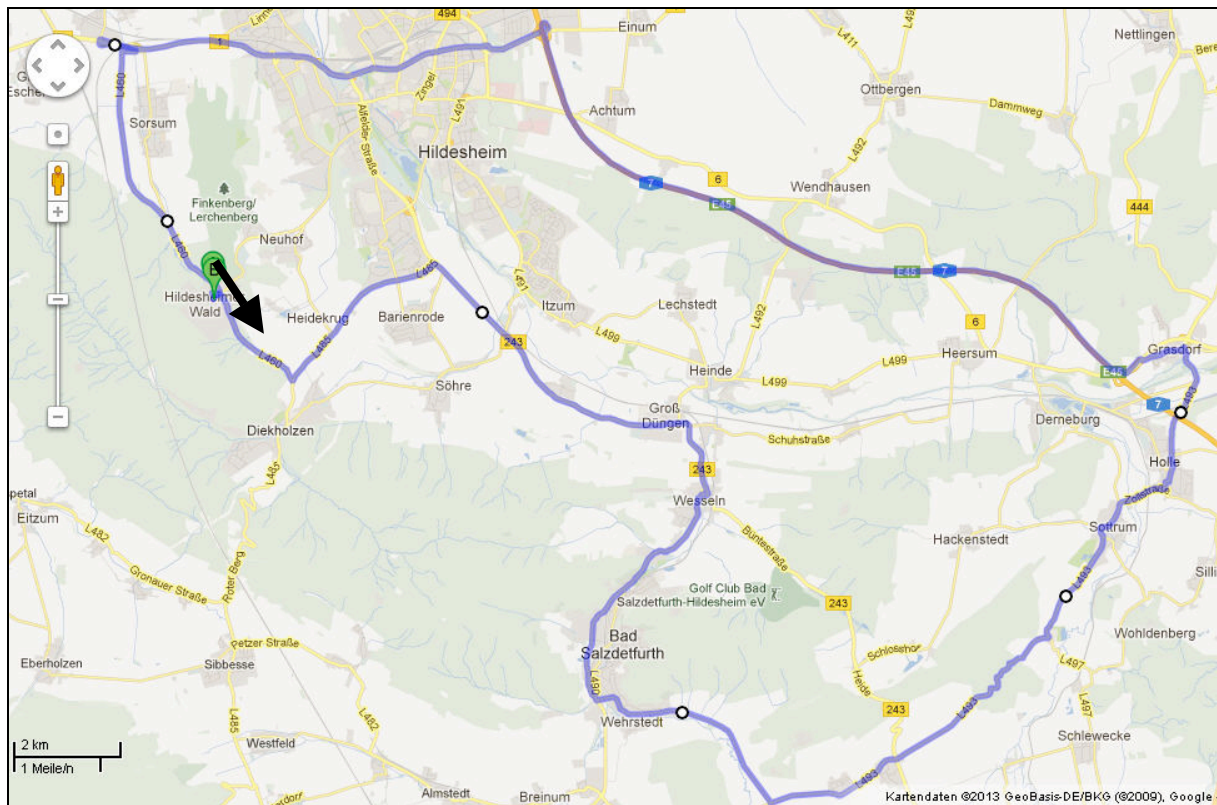


Figure 76: The ‘Hi02’ Track
Map data @2013 GeoBasis-DE/BKG (@2009) Google

Track length: The total length is around 66.5 kilometers (with some variations due to the chosen lanes). The track is almost identical to the HI01 track, with a deviation starting in Wesseln due to road work.

Start / End: Robert Bosch Car Multimedia GmbH / Robert-Bosch-Straße 200 / 31139 Hildesheim / Germany

Travel direction: Heading south-east to Diekholzen, Wesseln, Bad Salzdetfurth, Sottrum, A7 to Hannover, B1

Slope: the altitude variations are comparable to the one observed in Hi01.

C2. Drivers

While the ST01 and Hi01 databases were used to learn about drivers and driving styles, the objective in this case was to modify the car properties to test the system prototype ability to adapt. To reduce the driver influence on the system behavior, attention was paid to increase the number of different drivers. After one week, a total of eight drivers had driven the car and 23 laps were recorded. Additionally, the trips to get and bring the roof box back to Hannover were recorded on the highway (A7).

C3. Date

The dataset was recorded between 07 May 2012 and 11 May 2012. The schedule is described in the following table:

	07.05.2012	08.05.2012	09.05.2012	10.05.2012	11.05.2012
06:00AM-07:00AM		MA			
07:00AM-08:00AM				MA	
08:00AM-09:00AM	Get the roof box	GA x2	VA x2	RB x2	PW
09:00AM-10:00AM					MA
10:00AM-11:00AM					
11:00AM-12:00AM		MA x2			
12:00AM-01:00PM					
01:00PM-02:00PM	BW		+ 300kg sand	EA	
02:00PM-03:00PM	MA x3				Bring the sand and roof box back
03:00PM-04:00PM		MA			
04:00PM-05:00PM			MA x2	EP x2	
05:00PM-06:00PM					
06:00PM-07:00PM			BW		
07:00PM-08:00PM					
08:00PM-09:00PM					

Table 33: Driver Repartition Over the Week

During the week, the car was driven with a roof box, and starting Wednesday midday to Friday midday, the car was additionally loaded with 300kg of sand.

C4. Vehicle specification

Brand & Model: BMW 325d E91 (2008-2012) Touring: this is the same car as in the Hi01 database.

Engine & Gearbox: V6 diesel with maximum 400Nm of torque and a 6 Speed automatic gearbox

After the system was proven to run on the E91, it was important to test it on other cars. However, the budget and time to equip them with the whole CAN recording system was insufficient. An alternative solution was to modify the cars' characteristics to be similar to other car models. It was decided to implement this option and to modify the aerodynamic and the vehicle mass.

Configuration A: With a Roof Box:

The roof box was the biggest available for rental in Hannover. It was a Thule Atlantis 900 with roof rack. The dimensions were 90x46 cm, and the air resistance coefficient was unknown (Thule refused to communicate on this value).

- It is assumed that the rolling resistance didn't change much from the original value (small increase due to the weight) and be equal to: 0.011.

- According to the official specifications, the roof box has a front surface equal to 0.414 m². The roof rack is approximated with 3 cm x 1.5 m = 0.045 m². Because the air resistance coefficient is unknown, this value had to be assumed. No reliable values could be found in the literature, it was therefore considered that the aerodynamic box and the rack (with strong edges) have modern passenger car properties, and the air resistance coefficient was assumed to be 0.3.

The 'roof box + roof rack + vehicle' air resistance coefficient multiplied with their respective front surface should be equal to 0.7670.

- The roof box and rack mass, the whole CAN recording equipment mass and the mass of a driver had to be added to the original vehicle mass. The car (without driver and roof box and rack, but with the CAN recording equipment weighed 1800kg – this value has been measured on a over-dimensioned balance at the Bosch Car Multimedia facility).

The car characteristics are considered to be similar to a BMW X1 xDrive 28i with some passengers:

	BMW X1 xDrive 28i 2009	BMW 325d Touring 2009
Weight, to EU in kg	1685	1800
Air resistance coefficient * front surface in m ²	0.33 * 2.34 = 0.7722	0.7670 (with roof box & rack)
Tires	225/50 R17 94H	225/45 R17 91W RSC

Table 34: BMW Official Specification Sheet Comparison [BMW09X] [BMW09]

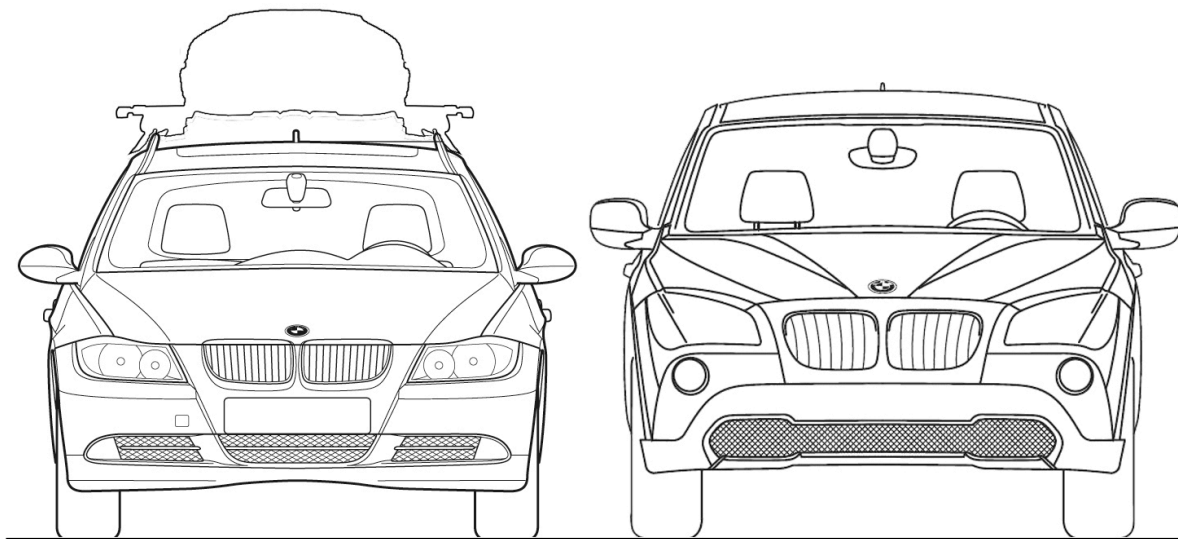


Figure 77: Modified BMW E91 (With Roof Box and Rack) and BMW X1 Blueprints [CarBP12]

Configuration B: With a roof box and 300kg of sand:

The roof box remains the same, but 300kg of sand was transported on the passenger seat row, the trunk being used to record the CAN signals.

- It is assumed that the rolling resistance increased due to the weight.

- The air resistance increases due to the roof box and rack.

- The weight wasn't measured but assumed to be 2100kg. The sand was packed in 25kg bags and was assumed to be an accurate 300kg.

The car characteristics were considered to be similar to a BMW 750i (2009):

	BMW 750i 2009	BMW 325d Touring 2009
Weight, to EU in kg	2105	2100 (Automatic Gearbox)
Air resistance coefficient * front surface in m ²	0.31 *2.41= 0.7471	0.7670 (with roof box & rack)
Tires	245/50 R18 100Y RSC	225/45 R17 91W RSC

Table 35: BMW Official Specification Sheet Comparison [BMW097] [BMW09]

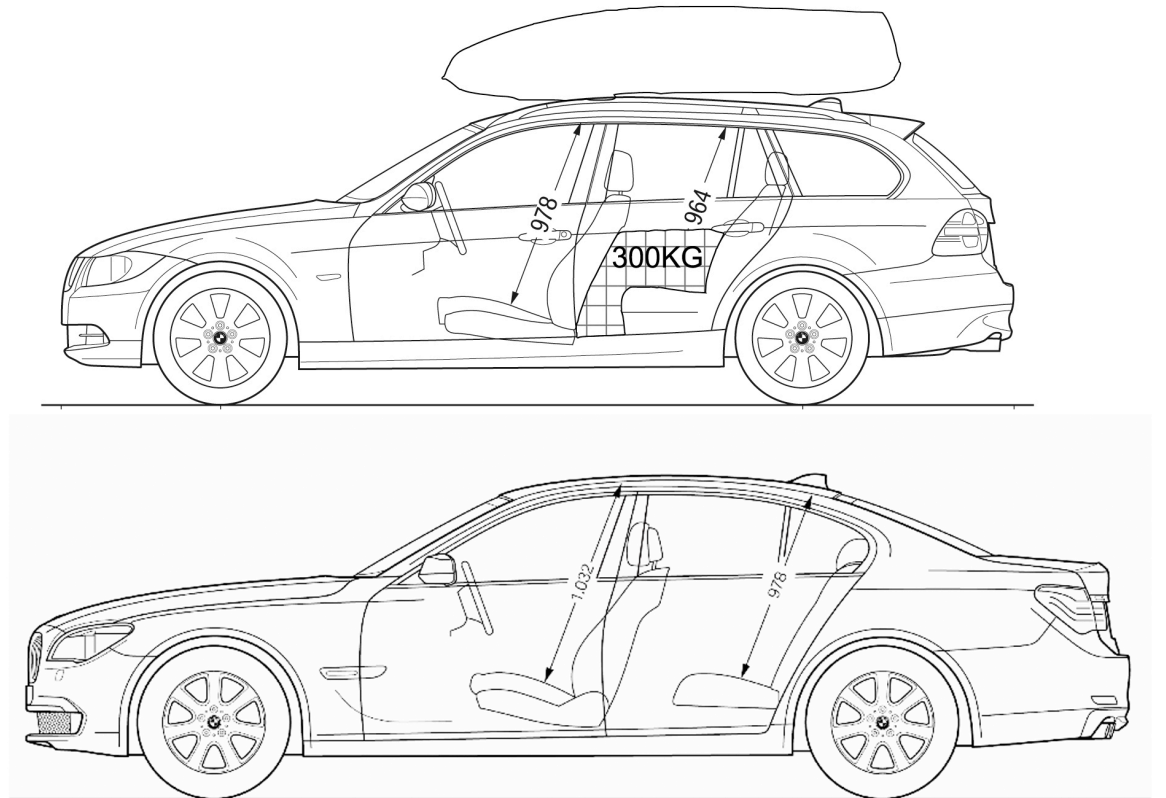


Figure 78: Modified BMW E91 and BMW 750i Blueprints [CarBP12]

C5. Recorded Signals

The recorded signals were identical to the one in the Hi01 database, however, some minor changes occurred in the log file specification and the Matlab scripts had to be adapted.

References:

[BMW09] BMW Presse, Technische daten BMW 3er Touring (325d, 330d, 335d), version 01/2009, valid from 03/2009

[BMW09X] BMW Media Information, Specifications BMW X1 (X1 xDrive28i), 07/2009, valid from 09/2009

[BMW097] BMW Media Information, Specifications BMW 7 Series Saloon (750i xDrive), 07/2009

[CarBP12] Blue prints downloaded from 'carblueprints.info', version from 11.12.2012

ANNEX D: The Hildesheim ‘Double Loop’ Dataset

D1. Test Tracks Presentation:

This dataset was recorded on two different tracks. The objective was to use the characteristics learned on one track to make a fuel consumption prediction on the other track.

The first track is referred to as ‘**Hi03**’

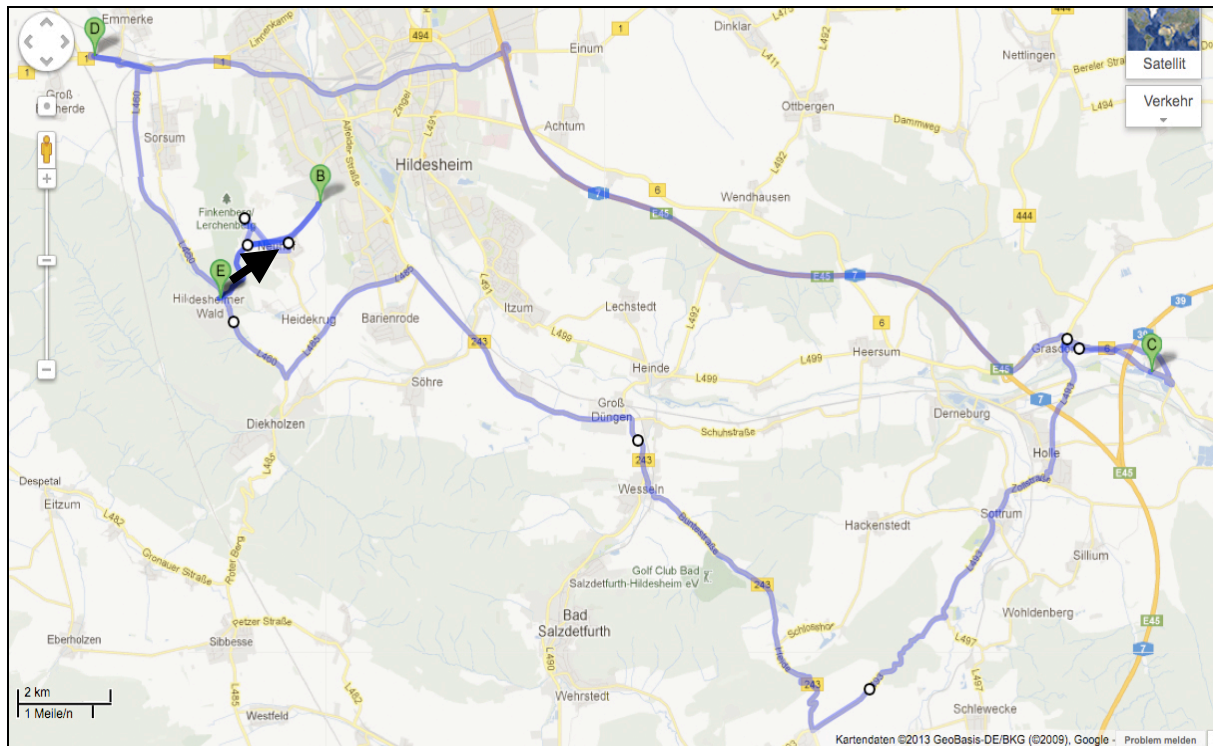


Figure 79: The 'Hi03' Track
Map data @2013 GeoBasis-DE/BKG(©2009) Google

Track Length: The total length is circa 78 kilometers (with some variations due to the chosen lanes). The track is based on the Hi01 track, with two deviations to collect new speed signs.

Start / End: Robert Bosch Car Multimedia GmbH / Robert-Bosch-Straße 200 / 31139 Hildesheim / Germany

Travel direction: Heading northeast to Trockener Kamp.

Slope: the altitude variations are similar to Hi01

The second track is referred to as ‘**Hi04**’

Track length: The total length is circa 39 kilometers (with some variations due to the chosen lanes).

Start / End: Robert Bosch Car Multimedia GmbH / Robert-Bosch-Straße 200 / 31139 Hildesheim / Germany

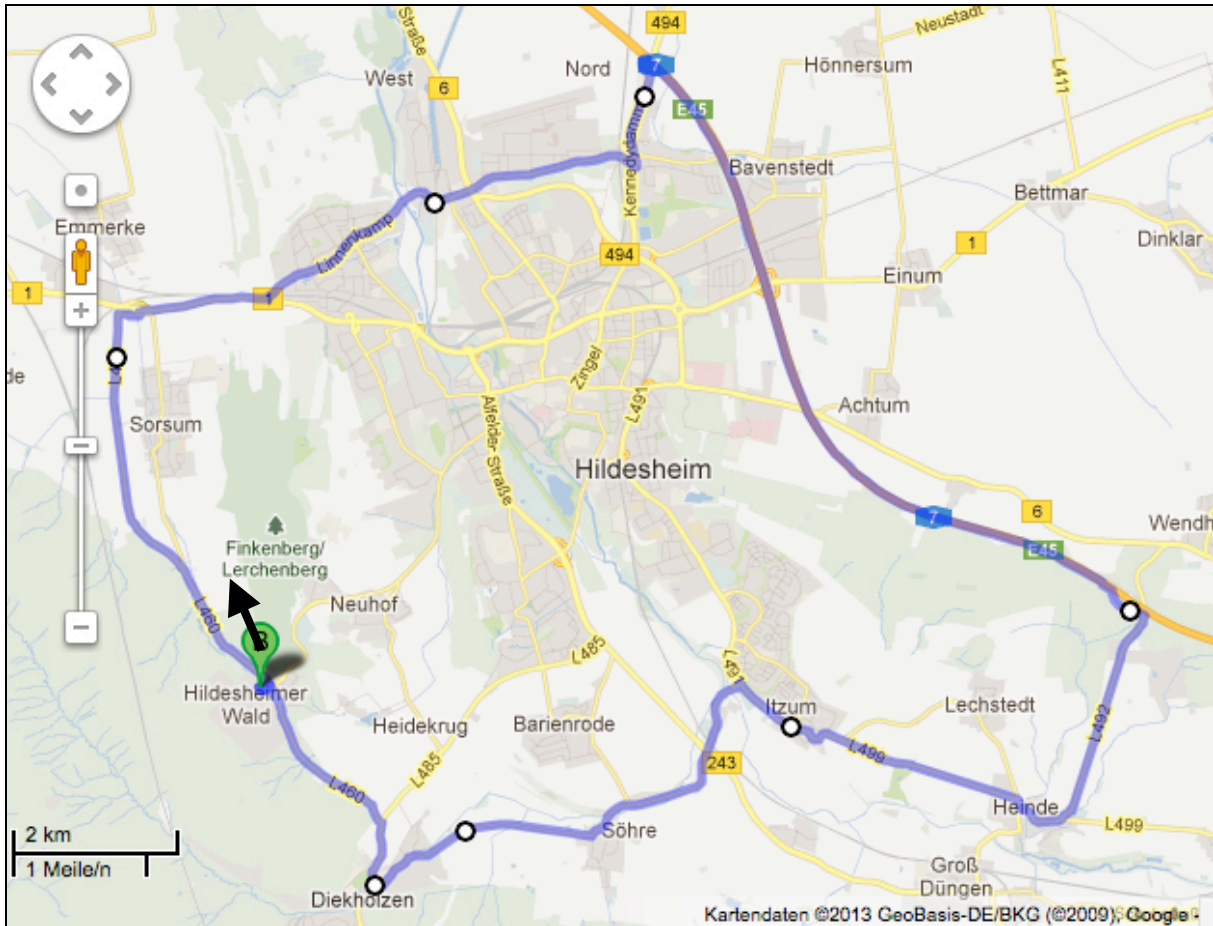


Figure 80: The 'Hi04' Track
 Map data @2013 GeoBasis-DE/BKG(@2009) Google

Travel direction: Heading northwest to B1. Some roads were used in H01, H02 and H03, but the travel direction is the opposite.

Slope: the altitude variations are low according to the Hildesheim region

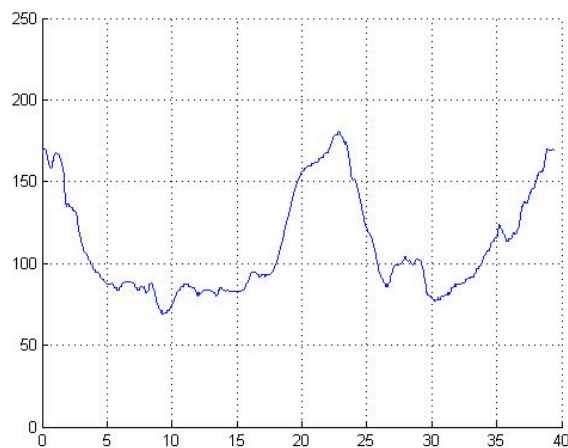


Figure 81: Altitude Variation Along the Hi04 Track
 (With interferences, according to the GPS logs)
Y-Axis: Altitude in meter
X-Axis: Distance in kilometer

D2. Drivers

The vehicle should have been available for 2 weeks, but it had to be reconfigured three days, and was immobilized for 4 additional days for reparations. In addition to that, the driver availability was reduced because of project stress. At the end they were only two drivers who had driven enough to make a driving style analysis possible.

The first driver is a male aged 30-35 (referred to as D1) and second driver is a woman aged 25-30 (referred to as D2).

D3. Date

The dataset was recorded between 28 August 2012 and 10 September 2012. Considering only the two relevant drivers, the repartition was according following tables. Additional, the vehicle was driven by one of the driver over the weekend more than 1000km on the highway.

Driver schedule HI03:

	28.08	29.08	30.08	03.09	04.09	05.09
08:00AM-09:30AM		D1	D2	D1	D2	
10:00AM-11:30AM		D1	D2	D1	D2	
12:30AM-02:00PM		D2		D2	D1	D2
02:00PM-03:30PM	D1	D2		D2	D1	D2
03:30PM-05:00PM			D1			
05:00PM-06:30PM			D1			

Table 36: Driver Repartition For the Test Drives on HI03

The vehicle was then unavailable from 06 September 2012 to 09 September 2012 for reparations.

Driver schedule HI04:

10.09.2012	07:00AM-07:45AM	07:45AM-08:30AM	08:30AM-09:15AM	09:15AM-10:00AM	10:00AM-10:45AM	10:45AM-11:30AM	12:30AM-01:30PM	01:30PM-02:00PM	02:00PM-03:45PM	03:00PM-03:45PM	03:45PM-04:00PM
	D1	D1	D1	D1	D2	D2	D2	D2	D2	D1	D1

Table 37: Driver Repartition For the Test Drives on HI04

D4. Vehicle specification

Brand & model: BMW 325d E91 (2008-2012) Touring: this is the same car as in Hi01.

D5. Recorded signals

The recorded signals were identical to the Hildesheim ‘original’ database.

ANNEX E: Analysis of the Driving Style and the Database Characteristics that Influences the Fuel Consumption

The following analysis is based on the Stuttgart ST01 recordings.

E1. Recorded Sensor Information

- Duration in seconds
- Fuel consumed in μl
- Fuel consumed over time in $\mu\text{l}/0.1\text{s}$.
- Actual driven speed in m/s
- Number of Stops
- Duration of Stops in seconds
- Number of braking maneuvers
- Duration of braking maneuvers in seconds
- Braking intensity from 0 to 12000
- Speed variations caused by operating the brakes in m/s
- Number of accelerations
- Duration of accelerations in seconds
- Acceleration intensity from 0 to 100
- Speed variations caused by operating the gas pedal in m/s
- Number of engine brakings
- Duration of engine brakings in seconds
- Side slip
- Velocity in m/s^2
- Steering wheel
- Yaw
- Engine speed in rpm
- Engine torque in Nm
- Driven distance in meters
- Actual speed compared to speed limit in m/s

E2. Description of the Database Situations That Were Defined

- Inner city
- Outer city (Highway excluded)
- Highway
- Road work
- Route segment ends with a traffic light
- Functional road class 1 according to Nokia-Navteq
- Functional road class 2 according to Nokia-Navteq
- Functional road class 4 according to Nokia-Navteq
- Functional road class 5 according to Nokia-Navteq
- Functional road class 8 (ramp to highway)
- Functional road class 9 (ramp from highway)
- Number of lanes=0 (unknown)
- Number of lanes=1
- Number of lanes=2
- Number of lanes=3
- Number of lanes=4
- Speed restriction = 30 km/h
- Speed restriction = 40 km/h
- Speed restriction = 50 km/h
- Speed restriction = 60 km/h
- Speed restriction = 70 km/h
- Speed restriction = 80 km/h
- Speed restriction = 100 km/h
- Speed restriction = 120 km/h
- No speed restriction

- Driven speed is between:
0-20km/h 0-30km/h 0-40km/h 0-50km/h

0-60km/h	40-50km/h	40-60km/h	50-100km/h
0-70km/h	50-60km/h	60-80km/h	100-150km/h
0-80km/h	60-70km/h	80-100km/h	Over 80km/h
0-90km/h	70-80km/h	100-120km/h	Over 90km/h
0-100km/h	80-90km/h	120-140km/h	Over 100km/h
0-110km/h	90-100km/h	30-60km/h	Over 110km/h
0-120km/h	100-110km/h	60-90km/h	Over 120km/h
10-20km/h	110-120km/h	90-120km/h	
20-30km/h	120-130km/h	40-80km/h	
30-40km/h	20-40km/h	80-120km/h	

- Drives through 'Leonberg 'east
- Drives through 'Leonberg 'north
- Drives through 'Ditzingen'
- Drives through 'Möglingen'
- Drives through 'Münchingen'
- Drives through 'Zuffenhausen'
- Drives through 'Feuerbach'
- Drives through 'Stuttgart-West'

- Drives on 'A831/B14'
- Drives on 'A81'
- Drives on 'L1187/Neue Ramtelstraße'
- Drives on 'Stuttgarterstrasse'
- Drives on 'Feuerbacherstrasse / Calwererstrasse'
- Drives on 'Siemensstrasse'
- Drives on 'Weilimdorferstrasse'
- Drives on 'A81'
- Drives on 'Schwieberdingerstrasse'
- Drives on 'Umgehungsstrasse(L1140)'

- Drives on 'L1141'
- Drives on 'Markgröningerstrasse'
- Drives on 'Stuttgarterstrasse'
- Drives on 'B10 / B27'
- Drives on 'Stresemannstrasse'
- Drives on 'Am Kochenhof'
- Drives on 'L1187'
- Drives on 'Am Krähenwald'
- Drives on 'Geißeichstrasse'
- Drives on 'B14'

- Drives over speed restriction
- Vehicle is not moving
- Vehicle is moving
- Acceleration (pressing gas pedal)
- Braking maneuver (pressing on brake pedal)
- Engine brake
- Driving without ACC
- ACC activated
- Prototype ACC activated

E3. Evaluation and Possible Error

To make a decision about the relevance of the driving style and to find out which database characteristics are relevant to make a fuel consumption prediction, the available sensor information (Chapter E1) and database information (Chapter E2) have been observed for a selection of database properties combinations.

For each combination in the form '**Sensor * Database property * Database property**',

- Sum
- Mean value
- Standard deviation
- Mean value + standard deviation
- Mean value + mean absolute deviation
- Mean absolute deviation

- Maximum
have been calculated.

- Minimum

However, not all combinations are relevant, (e.g. ‘Vehicle is not moving’ & ‘Vehicle is moving’), therefore, 69126 combinations (called ‘filters’) have been specified.

For each combination, the 90 (30 drivers x 3 laps) results out of the 90 recorded CAN files (CAN_{REC}) have been sorted and compared to two reference lists:

- The 90 CAN_{REC} ordered by the total fuel consumed during the trip.
- The 90 CAN_{REC} ordered by the total fuel consumed during the trip when the car was moving.

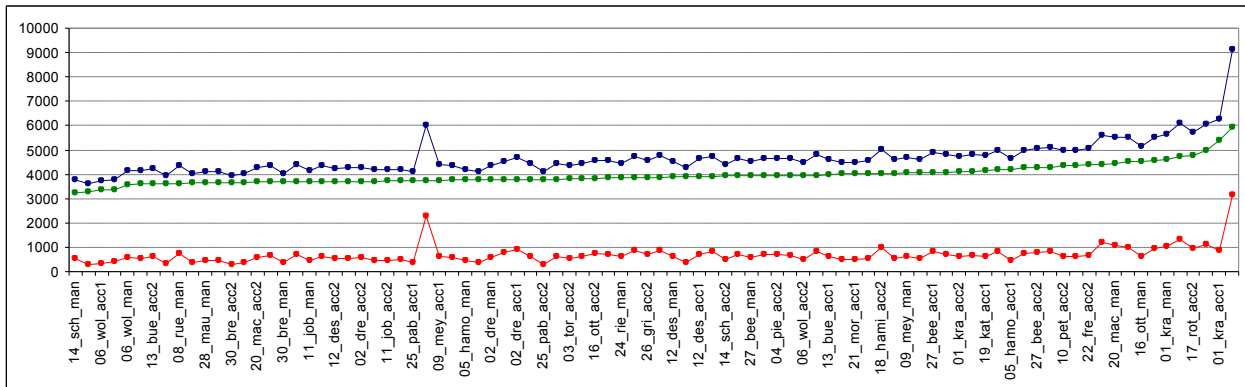


Figure 82: 90 CAN_{REC} sorted by their total fuel consumption while the vehicle was moving

In red: total fuel consumed while the vehicle was not moving
In green: total fuel consumed while the vehicle was moving
In blue: total fuel consumed

Finding n^o1: The total amount of fuel consumed is very dependent from the amount of fuel consumed while the vehicle wasn't moving.

Therefore, traffic lights and traffic jam may be a very important factor in the fuel consumption prediction. It is important to note that the test vehicle wasn't equipped with start/stop system.

To compare the 69126 resulting lists to the two references (Green and Blue in Figure 82), it is not sufficient to compare their respective sequence. While it is important to place the CAN_{REC} with the highest and lowest consumption at the right place in the sequence, the average CAN_{REC} has a similar gas consumption and their place in the sequence should have less impact on the final evaluation.

To do so, a power P is associated to each CAN_{REC}. This power is equal to the positive difference between the recorded fuel consumption of each CAN_{REC} and the average consumption over the 90 CAN_{REC}.

$$P = | \text{Recorded fuel consumption} - \text{Average consumption over 90 lap logs} |$$

It is now possible to compare the sequences of the 69126 generated lists with the two references. First, the distance D between the place of each element in the observed list and its place in the reference list is been calculated. For each one of the 90 elements, the distance is then multiplied with its related power P. Considering the whole sequence, the 90 results are then summed up and form an Index I linked to the respective filter.

$$I = \sum_{k=1}^{90} P_k \cdot D_k$$

The minimum of zero is expected for lists that have the exact same sequence as the reference. The maximum value is reached when a list has the exact opposite sequence, and is therefore also a good indicator.

Erroneous results are only possible if some of the CAN_{REC} have the same fuel consumption (which is not the case), or if identical results for a minimum of two CAN_{REC} are computed. In this case, there is more than one sequence possible for the resulting list, and due to the relevance of the sequence in the evaluation, the calculated index may vary a little. However, because the available sensor data has a high degree of precision, identical results should be an exception, and, for this reason, the method should be precise enough to find out which driving characteristics (and maybe database characteristics) are responsible for fuel consumption.

E4. Results

The following figures show the distribution of the 69126 calculated indexes with:

- Fuel consumed during the whole trip as a reference on the left
- Fuel consumed when the vehicle was moving as a reference on the right.

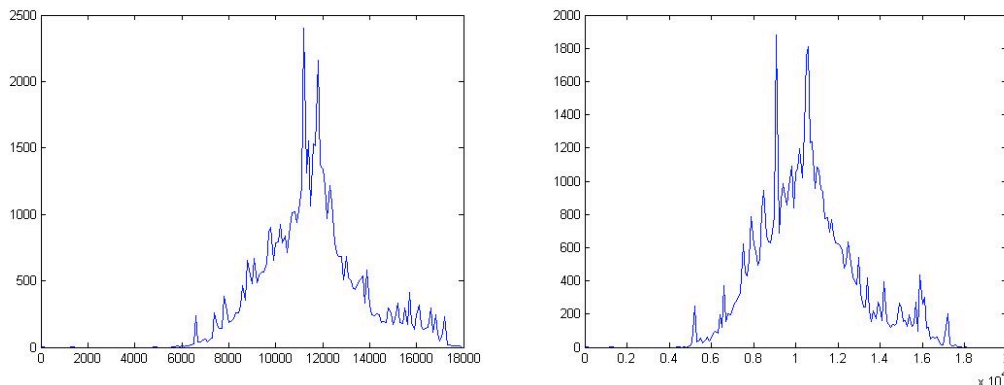


Figure 83: repartition of the calculated indexes

X-Axis: calculated index value

Y-Axis: number of indexes with the same rounded value

The two sequences of indexes have almost the characteristics of a Gaussian distribution. As mentioned before, the observed combinations of sensor data and database situation of the indexes that forms the peak of the distribution are not related to the fuel consumption.

Relevant are the smallest indexes (Left figure: 0 to 6000, Right figure: 0 to 5120), and the highest indexes (Left figure: 17580 to 17919, Right figure: 17297 to 18129).

E4.1 Indexes were generated while comparing to the ‘total fuel consumed’ sequence:

Index	Category 1	Database 1	Database 2	Math.
0	Consumed fuel			
64	Consumed fuel	City1		
91	Consumed fuel	Lanes=0		
91	Consumed fuel	Lanes=0	City1	
1343	Consumed fuel	City3		
1351	Consumed fuel	Lanes=0	City3	
4847	Acceleration intensity	Lanes=2		Mean
4903	Acceleration intensity	Lanes=2		Std
5645	Engine speed	City3		Mean
5650	Engine speed	Lanes=0	City3	Mean
5652	Engine speed	Outer-City		Std

5778	Engine speed	Outer-City	City3	Std
5780	Engine speed	0-110km/h		Mean
5793	Engine speed	Lanes=0		Mean
5793	Engine speed	Lanes=0	City1	Mean
5795	Engine speed			Mean
5799	Engine speed	Lanes=0	0-110km/h	Mean
5812	Engine speed	City1		Mean
5812	Engine speed	0-90km/h		Mean
5820	Engine speed	0-100km/h		Mean
5821	Engine speed	Lanes=0	0-90km/h	Mean
5835	Engine speed	Lanes=0	0-100km/h	Mean
5882	Engine speed	Lanes=0	0-120km/h	Mean
5882	Engine speed	0-120km/h		Mean
5903	Consumed fuel	0-110km/h		
5911	Consumed fuel	0-120km/h		
5928	Acceleration intensity	Lanes=2		Mad
5978	Engine speed	Outer-City	0-120km/h	Std
5989	Acceleration intensity	Outer-City		Mean
5989	Engine speed	Outer-City	0-110km/h	Std
5991	Speed variations because of braking manoeuvre			Max
5991	Speed variations because of braking manoeuvre	Lanes=0		Max
5993	Consumed fuel	Lanes=0		
17584	Torque	Lanes=3	City1	Max
17613	alpSideSlip	Limit = 70	60-70km/h	Max
17621	alpSideSlip	Traffic light	60-70km/h	Max
17624	alpSideSlip	Traffic light	60-80km/h	Max
17655	Yaw	Limit = 80	0-90km/h	Summe
17662	Yaw	Limit = 80	0-80km/h	Summe
17669	alpSideSlip	Limit = 60	40-80km/h	Max
17670	alpSideSlip	Highway	City6	Max
17670	alpSideSlip	Limit = 100	City6	Max
17671	alpSideSlip	Lanes=3	City1	Max
17677	alpSideSlip	Limit = 80	80-90km/h	Max
17685	Yaw	Limit = 80	40-80km/h	Summe
17688	alpSideSlip	Of Highway	0-50km/h	Max
17693	alpSideSlip	Of highway	40-50km/h	Max
17694	alpSideSlip	Traffic light	80-120km/h	Max
17694	alpSideSlip	Traffic light	80km/h++	Max
17712	alpSideSlip	Lanes=2	80-100km/h	Max
17763	alpSideSlip	FRC2	80-120km/h	Max
17763	alpSideSlip	FRC2	80km/h++	Max
17763	alpSideSlip	FRC2	City1	Max
17763	alpSideSlip	Lanes=2	80-120km/h	Max
17763	alpSideSlip	Lanes=2	80km/h++	Max
17763	alpSideSlip	Limit = 80	80-120km/h	Max
17763	alpSideSlip	Limit = 80	80km/h++	Max
17763	alpSideSlip	Limit = 80	City1	Max
17764	alpSideSlip	Outer-City	50-60km/h	Max
17764	alpSideSlip	Limit = 70	0-70km/h	Max
17764	alpSideSlip	Limit = 100	40-60km/h	Max
17835	alpSideSlip	Lanes=2	50-60km/h	Max
17919	alpSideSlip	FRC2	80-100km/h	Max

17919	alpSideSlip	Limit = 80	80-100km/h	Max
-------	-------------	------------	------------	-----

Table 38: Indexes generated while comparing the sequence to the total fuel consumed sequence

The control sequence has an index equal to zero as expected (because it is a perfect match). Because of the numerous concordant database categories, some filters describe the same situation. For example:

17763	alpSideSlip	FRC2	80-120km/h	Max
17763	alpSideSlip	FRC2	80km/h++	Max
17763	alpSideSlip	FRC2	City1	Max
17763	alpSideSlip	Lanes=2	80-120km/h	Max
17763	alpSideSlip	Lanes=2	80km/h++	Max
17763	alpSideSlip	Limit = 80	80-120km/h	Max
17763	alpSideSlip	Limit = 80	80km/h++	Max
17763	alpSideSlip	Limit = 80	City1	Max

All describe a situation where the car was moving on a functional road class 2 road with two lanes at a speed between 80 and 120 km/h although the speed restriction was 80km/h. As expected, the indexes are identical.

According to the results, it is assumable that following filters are very relevant for the differences between the observed fuel consumption of different trips or drivers:

- Mean acceleration outside cities
- Mean engine speed outside cities (because the selected gear information wasn't available it is supposed to be related to late gear change to higher gear or high speeds).
- City is not like city: the first and third cities seem to have more influence on fuel consumption than the other ones. However, the city description is not precise enough to explain the results.
- High variations of the engine speed: is possibly linked to high acceleration and decelerations, late gearshift and strong speed variations.
- Strong speed variations because of braking maneuver
- Amount of fuel consumed in the cities
- Maximum side slip and yaw sum both while the car was moving on a functional road class 2 road with two lanes at a speed between 80 and 120 km/h although the speed restriction was 80km/h describes the same situation. The section being described here is a low visibility road section with tight curves. The road curvature information was only visible on the recorded video and not available in the recorded navigation database. Therefore it couldn't be used as a criterion for analyzing the driving behavior.
- Maximum recorded torque on Highway or Expressway. It means highest acceleration and or highest speed.

Finding n°2: Accelerations, decelerations, selected gear and the chosen speeds of travel have an impact on the fuel consumption. 'Sports' drivers with high acceleration, strong braking, strong speed variations, high speed of travel, high side slip and yaw tend to consume more fuel.

E4.2 Indexes were generated while comparing to the 'total fuel consumed while the vehicle was moving' sequence:

Index	Category 1	Database 1	Database 2	Math.
0	Consumed fuel			
112	Consumed fuel	City1		
1208	Consumed fuel	Lanes=0		
1227	Consumed fuel	Lanes=0	City1	
1258	Consumed fuel	City3		

1258	Consumed fuel	Lanes=0	City3	
4388	Acceleration intensity	Lanes=2		Mean
4493	Acceleration intensity	Lanes=2		Std
4710	Engine speed	City3		Mean
4854	Engine speed	Lanes=0	City3	Mean
4855	Engine speed	Outer-City		Std
4867	Engine speed	Inner-City	City3	Std
4905	Engine speed	0-110km/h		Mean
4948	Engine speed	Lanes=0		Mean
5004	Engine speed	Lanes=0	City1	Mean
5008	Engine speed			Mean
5027	Engine speed	Lanes=0	0-110km/h	Mean
5043	Engine speed	City1		Mean
5045	Engine speed	0-90km/h		Mean
5047	Engine speed	0-100km/h		Mean
5047	Engine speed	Lanes=0	0-90km/h	Mean
5050	Engine speed	Lanes=0	0-100km/h	Mean
5066	Engine speed	Lanes=0	0-120km/h	Mean
5068	Engine speed	0-120km/h		Mean
5070	Consumed fuel	0-110km/h		
5106	Consumed fuel	0-120km/h		
5106	Acceleration intensity	Lanes=2		Mad
5106	Engine speed	Outer-City	0-120km/h	Std
5106	Acceleration intensity	Outer-City		Mean
5106	Engine speed	Outer-City	0-110km/h	Std
5106	Speed variations because of braking manoeuvre			Max
5106	Speed variations because of braking manoeuvre	Lanes=0		Max
5106	Consumed fuel	Lanes=0	0-120km/h	
5107	Consumed fuel	Lanes=0	0-110km/h	
5107	Acceleration intensity	FRC4		Mean+Mad
5108	Engine speed	Outer-City	City3	Mean
5111	Acceleration intensity	Lanes=2		Mean+Std
5118	Acceleration intensity	FRC2		Std
17297	Speed	20-30km/h		Mean+Std
17300	Speed	Lanes=0	20-30km/h	Mean+Std
17313	alpSideSlip	Limit = 100	City5	Max
17314	alpWheel	Limit = 80	0-90km/h	Summe
17332	Speed	Lanes=0	20-30km/h	Mad
17349	Speed	20-30km/h		Mad
17379	Torque	Lanes=3	City1	Max
17392	alpSideSlip	Limit = 70	60-70km/h	Max
17392	alpSideSlip	Traffic light	60-70km/h	Max
17397	alpSideSlip	Traffic light	60-80km/h	Max
17433	yaw	Limit = 80	0-90km/h	Summe
17439	yaw	Limit = 80	0-80km/h	Summe
17455	alpSideSlip	Limit = 60	40-80km/h	Max
17481	alpSideSlip	Highway	City6	Max
17506	alpSideSlip	Limit = 100	City6	Max
17540	alpSideSlip	Lanes=3	City1	Max
17543	alpSideSlip	Limit = 80	80-90km/h	Max
17543	yaw	Limit = 80	40-80km/h	Summe
17546	alpSideSlip	Of Highway	0-50km/h	Max

17626	alpSideSlip	Of Highway	40-50km/h	Max
17643	alpSideSlip	Traffic light	80-120km/h	Max
17643	alpSideSlip	Traffic light	80km/h++	Max
17643	alpSideSlip	Lanes=2	80-100km/h	Max
17643	alpSideSlip	FRC2	80-120km/h	Max
17643	alpSideSlip	FRC2	80km/h++	Max
17643	alpSideSlip	FRC2	City1	Max
17643	alpSideSlip	Lanes=2	80-120km/h	Max
17643	alpSideSlip	Lanes=2	80km/h++	Max
17644	alpSideSlip	Limit = 80	80-120km/h	Max
17644	alpSideSlip	Limit = 80	80km/h++	Max
17644	alpSideSlip	Limit = 80	City1	Max
17659	alpSideSlip	Outer-City	50-60km/h	Max
17666	alpSideSlip	Limit = 70	0-70km/h	Max
17666	alpSideSlip	Limit = 100	40-60km/h	Max
17717	alpSideSlip	Lanes=2	50-60km/h	Max
17762	alpSideSlip	FRC2	80-100km/h	Max
18129	alpSideSlip	Limit = 80	80-100km/h	Max

Table 39: Generated Indexes While Comparing to the ‘Total Fuel Consumed While the Vehicle was Moving’ Sequence

Similar to the first comparison, it seems that the fuel consumed in the first and third city on was very relevant. Based on the video evaluation, it is assumed that the amount of traffic lights (provoking acceleration and strong decelerations) may be responsible for it.

The acceleration outside the city (late shift to upper gear and or high speed) and the braking inside and outside the city are also confirmed to be relevant.

ANNEX F: Vehicle Database Used to Compute the Forces that Influence a Moving Vehicle Depending on the Speed of Travel

The table is filled with data collected from official BMW Group Press technical vehicle specifications. It lists 188 vehicles that have been described in 98 BMW technical specification press releases. The list lists from small cars to SUVs, and represents almost all the BMW vehicles available for sale in early 2012. It was assumed to have a sufficient representative distribution.

Note: BMW is one of the very few brands that communicate on the vehicle aerodynamical properties.

Brand	Modell	Version	Valid from	cw	A (m ²)	cw.A	Max Torque (Nm)	Vehicle mass (kg)	Front tire wide (mm)
BMW	116d	5door	9.2011	0,30	2,14	0,642	260	1385	195
BMW	118d	5door	9.2011	0,30	2,14	0,642	320	1395	195
BMW	120d	5door	9.2011	0,31	2,14	0,6634	380	1420	205
BMW	116i	5door	9.2011	0,31	2,14	0,6634	220	1365	195
BMW	118i	5door	9.2011	0,32	2,14	0,6848	250	1370	195
BMW	118d	Convertible	3.2011	0,33	2,10	0,693	300	1560	195
BMW	120d	Convertible	3.2011	0,33	2,10	0,693	350	1580	195
BMW	123d	Convertible	3.2011	0,34	2,10	0,714	400	1615	205
BMW	118i	Convertible	3.2011	0,33	2,10	0,693	190	1495	195
BMW	120i	Convertible	3.2011	0,34	2,10	0,714	210	1505	205
BMW	125i	Convertible	3.2011	0,34	2,10	0,714	270	1585	205
BMW	135i	Convertible	3.2011	0,34	2,10	0,714	400	1665	205
BMW	118d	Coupé	3.2011	0,30	2,11	0,633	300	1395	195
BMW	120d	Coupé	3.2011	0,31	2,11	0,6541	350	1450	205
BMW	123d	Coupé	3.2011	0,31	2,11	0,6541	400	1495	205
BMW	120i	Coupé	3.2011	0,30	2,10	0,63	210	1375	205
BMW	125i	Coupé	3.2011	0,30	2,10	0,63	270	1480	205
BMW	135i	Coupé	3.2011	0,33	2,10	0,693	400	1530	215
BMW	316d	Limousine	09.2009	0,27	2,17	0,5859	260	1475	205
BMW	318d	Limousine	09.2009	0,27	2,17	0,5859	300	1505	205
BMW	320d	Limousine	09.2009	0,27	2,17	0,5859	350	1505	205
BMW	325d	Sedan	09.2009	0,28	2,17	0,6076	400	1600	225
BMW	330d	Sedan	09.2009	0,28	2,17	0,6076	520	1610	225
BMW	335d	Sedan	09.2009	0,30	2,17	0,651	580	1625	225
BMW	318i	Sedan	09.2009	0,26	2,17	0,5642	190	1435	205
BMW	320i	Sedan	09.2009	0,26	2,17	0,5642	210	1445	205
BMW	325i	Sedan	09.2009	0,27	2,17	0,5859	270	1505	205
BMW	330i	Sedan	09.2009	0,27	2,17	0,5859	320	1550	225
BMW	335i	Sedan	09.2009	0,30	2,17	0,651	400	1610	225
BMW	320d	Sedan xDrive	09.2009	0,30	2,17	0,651	350	1600	205
BMW	330d	Sedan xDrive	09.2009	0,30	2,17	0,651	520	1710	225
BMW	325i	Sedan xDrive	09.2009	0,30	2,17	0,651	270	1605	225
BMW	330i	Sedan xDrive	09.2009	0,31	2,17	0,6727	320	1640	225
BMW	335i	Sedan xDrive	09.2009	0,32	2,17	0,6944	400	1710	225

BMW	318d	Touring	09.2009	0,27	2,17	0,5859	300	1580	205
BMW	320d	Touring	09.2009	0,28	2,17	0,6076	350	1580	205
BMW	325d	Touring	09.2009	0,29	2,17	0,6293	400	1665	225
BMW	330d	Touring	09.2009	0,29	2,17	0,6293	520	1675	225
BMW	335d	Touring	09.2009	0,31	2,17	0,6727	580	1720	225
BMW	318i	Touring	09.2009	0,27	2,17	0,5859	190	1505	205
BMW	320i	Touring	09.2009	0,27	2,17	0,5859	210	1505	205
BMW	325i	Touring	09.2009	0,28	2,17	0,6076	270	1585	205
BMW	330i	Touring	09.2009	0,29	2,17	0,6293	320	1615	225
BMW	335i	Touring	09.2009	0,31	2,17	0,6727	400	1690	225
BMW	320d	Touring ED	09.2009	0,27	2,17	0,5859	380	1580	205
BMW	320d	Coupé	09.2009	0,28	2,08	0,5824	350	1505	225
BMW	325d	Coupé	09.2009	0,28	2,08	0,5824	400	1590	225
BMW	330d	Coupé	09.2009	0,28	2,08	0,5824	520	1600	225
BMW	335d	Coupé	09.2009	0,30	2,08	0,624	580	1645	225
BMW	320d	Convertible	09.2009	0,28	2,08	0,5824	350	1730	225
BMW	325d	Convertible	09.2009	0,28	2,08	0,5824	400	1815	225
BMW	330d	Convertible	09.2009	0,28	2,08	0,5824	520	1825	225
BMW	320i	Convertible	09.2009	0,27	2,08	0,5616	210	1670	225
BMW	325i	Convertible	09.2009	0,28	2,08	0,5824	270	1730	225
BMW	330i	Convertible	09.2009	0,28	2,08	0,5824	320	1780	225
BMW	335i	Convertible	09.2009	0,31	2,08	0,6448	400	1810	225
BMW	530d	GT	10.2011	0,30	2,57	0,771	540	2035	245
BMW	535d	GT	10.2011	0,31	2,57	0,7967	600	2045	245
BMW	530d	GT xDrive	10.2011	0,30	2,57	0,771	540	2090	245
BMW	535d	GT xDrive	10.2011	0,31	2,57	0,7967	600	2110	245
BMW	535i	GT	10.2011	0,31	2,57	0,7967	400	2015	245
BMW	550i	GT	10.2011	0,32	2,57	0,8224	600	2135	245
BMW	535i	GT xDrive	10.2011	0,31	2,57	0,7967	400	2070	245
BMW	550i	GT xDrive	10.2011	0,32	2,57	0,8224	600	2205	245
BMW	520d	Sedan	9.2011	0,28	2,35	0,658	380	1695	225
BMW	525d	Sedan	9.2011	0,28	2,35	0,658	450	1720	225
BMW	530d	Sedan	9.2011	0,28	2,35	0,658	540	1760	225
BMW	535d	Sedan	9.2011	0,28	2,35	0,658	630	1800	225
BMW	525d	Sedan xDrive	9.2011	0,29	2,35	0,6815	450	1795	225
BMW	530d	Sedan xDrive	9.2011	0,29	2,35	0,6815	560	1865	225
BMW	535d	Sedan xDrive	9.2011	0,29	2,35	0,6815	630	1870	225
BMW	520d	Sedan ED	9.2011	0,27	2,35	0,6345	380	1695	225
BMW	520i	Sedan	9.2011	0,29	2,35	0,6815	270	1670	225
BMW	528i	Sedan	9.2011	0,29	2,35	0,6815	350	1685	225
BMW	530i	Sedan	9.2011	0,28	2,35	0,658	310	1710	225
BMW	535i	Sedan	9.2011	0,29	2,35	0,6815	400	1760	225
BMW	550i	Sedan	9.2011	0,30	2,35	0,705	600	1905	245
BMW	528i	Sedan xDrive	9.2011	0,29	2,35	0,6815	350	1780	225
BMW	535i	Sedan xDrive	9.2011	0,29	2,35	0,6815	400	1840	225
BMW	550i	Sedan xDrive	9.2011	0,31	2,35	0,7285	600	1975	245
BMW	5er ActiveHybrid	ActiveHybrid	10.2011	0,28	2,35	0,658	450	1925	225
BMW	520d	Touring	9.2011	0,31	2,35	0,7285	380	1785	225
BMW	525d	Touring	9.2011	0,31	2,35	0,7285	450	1820	225
BMW	530d	Touring	9.2011	0,31	2,35	0,7285	540	1860	225
BMW	535d	Touring	9.2011	0,31	2,35	0,7285	630	1900	225
BMW	520i	Touring	9.2011	0,32	2,35	0,752	270	1780	225

BMW	528i	Touring	9.2011	0,32	2,35	0,752	350	1790	225
BMW	530i	Touring	9.2011	0,31	2,35	0,7285	310	1800	225
BMW	535i	Touring	9.2011	0,32	2,35	0,752	400	1840	225
BMW	550i	Touring	9.2011	0,33	2,35	0,7755	600	1975	245
BMW	525d	Touring xDrive	9.2011	0,32	2,35	0,752	450	1895	225
BMW	530d	Touring xDrive	9.2011	0,32	2,35	0,752	560	1940	225
BMW	535d	Touring xDrive	9.2011	0,32	2,35	0,752	630	1970	225
BMW	528i	Touring xDrive	9.2011	0,32	2,35	0,752	350	1880	225
BMW	535i	Touring xDrive	9.2011	0,32	2,35	0,752	400	1915	225
BMW	M5	M5	10.2011	0,33	2,40	0,792	680	1945	265
BMW	530i	Touring	9.2009	0,29	2,26	0,6554	320	1695	225
BMW	550i	Touring	9.2009	0,29	2,26	0,6554	490	1835	225
BMW	520i	Sedan	9.2009	0,27	2,26	0,6102	210	1535	225
BMW	523i	Sedan	9.2009	0,27	2,26	0,6102	240	1575	225
BMW	525i	Sedan	9.2009	0,27	2,26	0,6102	270	1585	225
BMW	530i	Sedan	9.2009	0,27	2,26	0,6102	320	1605	225
BMW	540i	Sedan	9.2009	0,28	2,26	0,6328	390	1725	225
BMW	550i	Sedan	9.2009	0,28	2,26	0,6328	490	1735	225
BMW	525d	Sedan	9.2009	0,27	2,26	0,6102	400	1655	225
BMW	530d	Sedan	9.2009	0,28	2,26	0,6328	500	1655	225
BMW	535d	Sedan	9.2009	0,27	2,26	0,6102	580	1735	225
BMW	525d	Sedan xDrive	9.2009	0,29	2,28	0,6612	400	1745	225
BMW	530d	Sedan xDrive	9.2009	0,29	2,28	0,6612	500	1760	225
BMW	525i	Sedan xDrive	9.2009	0,29	2,28	0,6612	270	1700	225
BMW	530i	Sedan xDrive	9.2009	0,29	2,28	0,6612	320	1710	225
BMW	630i	Coupé	9.2009	0,30	2,15	0,645	320	1605	245
BMW	650i	Coupé	9.2009	0,30	2,15	0,645	490	1725	245
BMW	635d	Coupé	9.2009	0,30	2,15	0,645	580	1725	245
BMW	640i	Convertible	3.2011	0,31	2,23	0,6913	450	1915	225
BMW	650i	Convertible	3.2011	0,32	2,23	0,7136	600	2015	245
BMW	640d	Coupé	9.2011	0,29	2,23	0,6467	630	1790	225
BMW	640i	Coupé	9.2011	0,30	2,23	0,669	450	1735	225
BMW	650i	Coupé	9.2011	0,31	2,23	0,6913	600	1845	245
BMW	650i	Coupé xDrive	9.2011	0,32	2,23	0,7136	600	1920	245
BMW	730d	Sedan	7.2009	0,29	2,41	0,6989	540	1940	245
BMW	740d	Sedan	7.2009	0,30	2,41	0,723	600	1950	245
BMW	730Ld	Sedan	7.2009	0,29	2,41	0,6989	540	1975	245
BMW	740i	Sedan	9.2009	0,30	2,41	0,723	450	1860	245
BMW	750i	Sedan	9.2009	0,31	2,41	0,7471	600	1945	245
BMW	760i	Sedan	9.2009	0,32	2,41	0,7712	750	2105	245
BMW	740Li	Sedan	9.2009	0,30	2,41	0,723	450	1970	245
BMW	750Li	Sedan	9.2009	0,31	2,41	0,7471	600	2055	245
BMW	760Li	Sedan	9.2009	0,32	2,41	0,7712	750	2250	245
BMW	750i	Sedan xDrive	7.2009	0,31	2,41	0,7471	600	2105	245
BMW	750Li	Sedan xDrive	7.2009	0,31	2,41	0,7471	600	2060	245
BMW	X1 18d	sDrive	9.2009	0,32	2,34	0,7488	320	1545	225
BMW	X1 18d	xDrive	9.2009	0,32	2,34	0,7488	320	1615	225
BMW	X1 20d	sDrive	9.2009	0,32	2,34	0,7488	350	1565	225
BMW	X1 20d	xDrive	9.2009	0,33	2,34	0,7722	350	1650	225
BMW	X1 23d	xDrive	9.2009	0,33	2,34	0,7722	400	1670	225
BMW	X1 28i	xDrive	9.2009	0,33	2,34	0,7722	310	1685	225
BMW	X1 18d	sDrive	9.2011	0,32	2,34	0,7488	320	1545	225

BMW	X1 18d	xDrive	9.2011	0,33	2,34	0,7722	350	1565	225
BMW	X1 20d	sDrive ED	9.2011	0,32	2,34	0,7488	380	1565	225
BMW	X1 18i	sDrive	9.2011	0,32	2,34	0,7488	200	1505	225
BMW	X1 20i	sDrive	9.2011	0,33	2,34	0,7722	270	1560	225
BMW	X1 20i	xDrive	9.2011	0,34	2,34	0,7956	270	1650	225
BMW	X1 28i	xDrive	9.2011	0,34	2,34	0,7956	350	1655	225
BMW	X3 20d	xDrive	9.2011	0,34	2,65	0,901	380	1790	225
BMW	X3 30d	xDrive	9.2011	0,34	2,65	0,901	560	1875	225
BMW	X3 35d	xDrive	9.2011	0,35	2,65	0,9275	630	1925	245
BMW	X3 20i	xDrive	9.2011	0,34	2,65	0,901	270	1770	225
BMW	X3 28i	xDrive	9.2011	0,34	2,65	0,901	310	1820	225
BMW	X3 35i	xDrive	9.2011	0,35	2,65	0,9275	400	1880	245
BMW	X5 30d	xDrive	9.2009	0,34	2,87	0,9758	520	2150	255
BMW	X5 35d	xDrive	9.2009	0,34	2,87	0,9758	580	2185	255
BMW	X5 30i	xDrive	9.2009	0,33	2,87	0,9471	315	2075	255
BMW	X5 48i	xDrive	9.2009	0,35	2,87	1,0045	475	2180	255
BMW	X5 30d	xDrive	9.2011	0,34	2,87	0,9758	540	2150	255
BMW	X5 40d	xDrive	9.2011	0,34	2,87	0,9758	600	2185	255
BMW	X5 35i	xDrive	9.2011	0,33	2,87	0,9471	400	2145	255
BMW	X5 50i	xDrive	9.2011	0,35	2,87	1,0045	600	2265	255
BMW	X5 M	M	9.2011	0,38	2,90	1,102	680	2380	275
BMW	X6 ActiveHybrid	ActiveHybrid	9.2011	0,36	2,82	1,0152	600	2525	255
BMW	X6 30d	xDrive	9.2011	0,33	2,82	0,9306	540	2150	255
BMW	X6 40d	xDrive	9.2011	0,34	2,82	0,9588	600	2185	255
BMW	X6 35i	xDrive	9.2011	0,34	2,82	0,9588	400	2145	255
BMW	X6 50i	xDrive	9.2011	0,36	2,82	1,0152	600	2265	255
BMW	X6 M	M	10.2011	0,38	2,85	1,083	680	2380	275
BMW	Z4 20i	sDrive	9.2011	0,34	1,96	0,6664	270	1470	225
BMW	Z4 28i	sDrive	9.2011	0,34	1,96	0,6664	350	1475	225
BMW	Z4 35i	sDrive	9.2011	0,35	1,96	0,686	400	1580	255
BMW	Z4 35is	sDrive	9.2011	0,35	1,96	0,686	450	1600	255
MINI	Cooper D	Convertible	2.2011	0,35	2,01	0,7035	270	1275	175
MINI	Cooper D	Convertible (A)	2.2011	0,35	2,01	0,7035	270	1300	175
MINI	Cooper D	Clubman	2.2011	0,32	2,02	0,6464	270	1260	175
MINI	Cooper D	Clubman (A)	2.2011	0,32	2,02	0,6464	270	1290	175
MINI	Cooper D	Countryman	2.2011	0,35	2,36	0,826	270	1385	205
MINI	Cooper D	Countryman (A)	2.2011	0,35	2,36	0,826	270	1410	205
MINI	Cooper D	Countryman ALL4	2.2011	0,35	2,36	0,826	270	1455	205
MINI	Cooper D	Countryman ALL4 (A)	2.2011	0,35	2,36	0,826	270	1480	205
MINI	Cooper SD	Sedan	3.2011	0,36	2,01	0,7236	270	1165	175
MINI	Cooper SD	Sedan (A)	3.2011	0,36	2,01	0,7236	270	1195	175
MINI	Cooper SD	Clubman	3.2011	0,34	2,04	0,6936	305	1310	195
MINI	Cooper SD	Clubman (A)	3.2011	0,34	2,04	0,6936	305	1330	195
MINI	Cooper SD	Convertible	3.2011	0,37	2,02	0,7474	305	1325	195
MINI	Cooper SD	Convertible (A)	3.2011	0,37	2,02	0,7474	305	1340	195
MINI	Cooper SD	Countryman	3.2011	0,35	2,36	0,826	305	1790	205
MINI	Cooper SD	Countryman (A)	3.2011	0,35	2,36	0,826	305	1815	205
MINI	Cooper SD	Countryman ALL4	3.2011	0,35	2,36	0,826	305	1470	205

MINI	Cooper SD	Countryman ALL4 (A)	3.2011	0,35	2,36	0,826	305	1495	205
------	-----------	------------------------	--------	------	------	-------	-----	------	-----

Table 40: Characteristics of 188 BMW and MINI